INVESTIGATING THE CAPACITY AND STIFFNESS OF JOINTS USED IN GYPSUM WALLBOARD SHEATHED LIGHT-FRAME WOOD SHEARWALLS

By

Alexandre Lafontaine

Thesis Submitted to the

Faculty of Graduate and Postdoctoral Studies

in partial fulfillment of the requirements for the degree of

Master of Applied Science

in Civil Engineering

Under the auspices of the Ottawa-Carleton Institute for Civil Engineering

uOttawa

Department of Civil Engineering

University of Ottawa

September 2015

ABSTRACT

The provisions to determine the deflection of gypsum wallboard (GWB) sheathed shearwalls available in the Canadian and American standards are limited to nailed shearwalls and are rudimentary compared to the wood based sheathing equations. There is currently no fastener slip model for the GWB sheathed shearwalls that are fastened with GWB screws. A main goal of this study is to improve the existing equations for nailed GWB sheathed shearwalls and develop a suitable analytical expression that can be used for GWB fastened with screws. In total, 270 GWB sheathed joints were subjected to reversed cyclic loading with variations including GWB type, thickness, fastener type, fastener size and manufacturers. The power model type is used to develop the fastener slip equations for nails and screws, which have GWB density and fastener diameter as equation inputs. The accuracy of the developed model is then validated by comparing the tested full-scale GWB sheathed shearwall deflection to the deflection calculated using the newly proposed fastener slip models. The proposed equation is a significant improvement to the existing code provisions. Component testing was performed on the fasteners (center point bending test) and the GWB (dowel bearing test). The results of these tests were used to determine the joint capacity based on the European Yield Model. It was also found that the shearwall capacity could be predicted by considering the joint level capacity while accounting for the number of joints at a panel edge. The joint level and full-scale experimental results are also validated with the use of an analysis program (SAPWood) to model the joint level hysteresis as a hysteretic spring with 10 model fitting parameters. The developed joint level hysteretic model was then used to represent the fasteners connecting the sheathing panels to the lumber framing in the construction of the full-scale shearwall model.

ACKNOWLEDGEMENTS

I would like to thank Dr. Hassan Aoude and Dr. Jeffery Erochko for reviewing my thesis.

I would also like to thank my supervisor Dr. Ghasan Doudak for his patience, guidance and invaluable help.

The experimental portion of the study would not have been possible without the help of the laboratory technician staff at the University of Ottawa and the University of New Brunswick. A special thanks to Dean McCarthy, Madelyn Pos and Daniel Lacroix for their help and dedication towards the completion of this project.

Finally I would like to thank my girlfriend Gabrièle for her support, patience and motivation throughout the entirety of this study.

TABLE OF CONTENTS

LIST OF TABLES

LIST OF FIGURES

1. INTRODUCTION

1.1 Background

The current research project deals with the behaviour of gypsum wallboard (GWB) panels in the context of light-frame wood constructions. GWB may be designed specifically to resist lateral loads (i.e. as a shearwall), used as a non-structural element but be designed to enhance the fire performance of wood frame structural elements, or finally as interior finishing that is typically completely ignored by designers. The need to investigate this material and understand its behaviour is further explained in section 1.2 of this chapter. The following sections provide a general understanding of the material composition and how GWB panels are used in light-frame wood construction.

1.1.1 Gypsum as a Material

Gypsum is a non-toxic sulphate mineral known as "calcium sulphate dihydrate", which consists of calcium, sulphur bound to oxygen, and water. There exist two types of gypsum: Natural and Flue-Gas Desulfurization (FGD). Natural gypsum is present where sedimentary rocks form. It is estimated that about 21 pounds of chemically combined water exist in one hundred pounds of gypsum rock. The process of transforming gypsum rock into powder includes mining, crushing and grinding of the rock. The powder then undergoes a process called calcining, where it is heated to approximately 350 degrees Fahrenheit. This process is known to remove three-quarters of the chemically combined water. As a result, the calcined gypsum develops into the base for what is used in GWB panels (Gypsum Association, 2015). For more than 30 years, FGD gypsum has been used to manufacture GWB. As desulfurization of flue gas from the stacks of fossil-fuelled power plants takes place, the smoke emissions can be purified into a hard substance and then transformed into gypsum. Figure 1 displays the raw gypsum material prior to wallboard fabrication (Gypsum Association, 2015).

Figure 1: Gypsum Material (Gypsum Association, 2015)

1.1.2 Gypsum Wallboard

Gypsum wallboard (GWB) is the technical product name referring to a board composed of gypsum core and paper facing; a product commonly referred to as drywall. It is one of the primary building materials used in the construction of walls, ceilings, and partitions in various construction types. Figure 2 shows the fabricated type-X GWB (Gypsum Association, 2015).

Figure 2: Gypsum Wallboard

The Gypsum Association ensures that its members manufacture GWB that meet or exceed any of the requirements found in the ASTM 1396: Standard Specification for Gypsum Board (ASTM, 2013). The three Canadian members of the Gypsum Association are CGC, CertainTeed Gypsum Canada Inc and Georgia-Pacific Gypsum LLC. To ensure that the variability that exists in construction is fully represented in the results obtained from the current study, products from all three manufacturers were tested.

One primary advantage of gypsum when used in combination with other materials such as plywood, hardboard, and fiberboard is its resistance to fire. GWB can be divided into “regular” gypsum and type-X gypsum wallboards. In this document “regular” GWB refers to any GWB panel that is sold as finishing material to cover interior walls that does not hold the type-X designation, yet conforms to ASTM 1396 (ASTM, 2013). Due to the presence of gypsum in its core, regular GWB inherently also possess fire resistance properties. Type-X gypsum boards are further modified in order to increase their fire resistance by including special core additives. In addition to some additives, type-X has a glass fiber reinforced gypsum core. The fibers reduce the extent and severity of cracks in the board when exposed to flame and heat, thus increasing the time it performs without failure (AWC, 1983). The fibers can be seen in Figure 3.

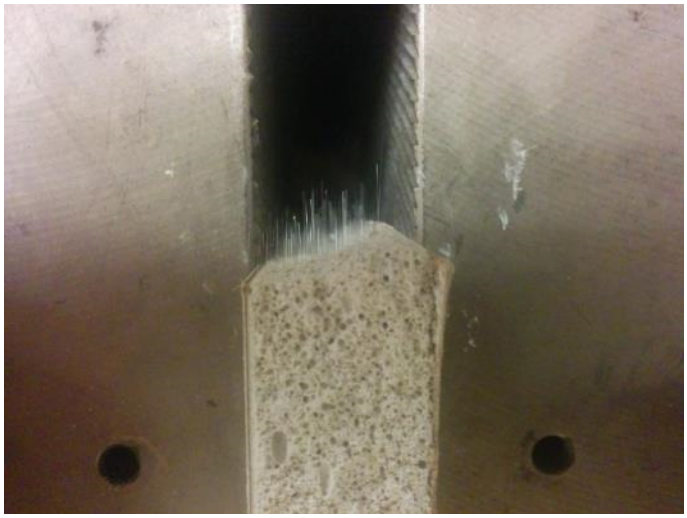

Figure 3: Typical Type-X GWB Fibers

1.1.3 Light-Frame Wood Construction

Light-frame wood construction is the most prevalent construction type in North America due to the availability of the construction material and the ease of construction. The ability to construct wood structures with minimal specialized equipment and training to workers has a great advantage in terms of construction time and total cost.

The main structural form employed in light-frame wood construction is platform framing. The basic construction characteristics of platform construction are that walls only extend one storey and each floor acts as a platform surface for the construction of the storey above. Balloon framing is another type of structural form used for light-frame wood construction and it consists of exterior walls that extend through the entire height of the structure. Floors are tied to the side of exterior walls at each storey. Figure 4 is a simple representation of the two construction types.

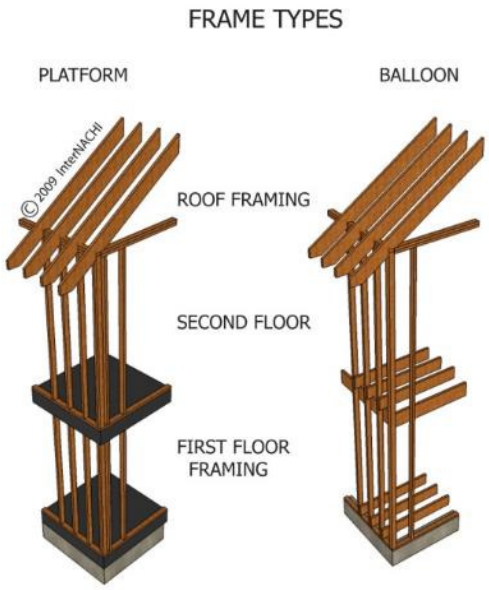

Figure 4: Platform Framing vs Balloon Framing (Insight Home Services, 2013)

Light-frame construction consists of stud walls to resist gravity loads, while shearwalls and diaphragms work jointly to resist lateral loads such as wind and earthquake. The two most common fasteners used in light-frame construction are nails and screws. Nails are smooth shanked ductile fasteners, while screws consist of hardened steel which may result in a higher capacity but brittle behaviour. The shape of the screws provides better withdrawal capacity than what can be obtained using nails. It is important to note that the behavior may be different when the fastener is part of a joint or subsystem, like walls or floors. This issue will be explored further in the current study.

Lumber framing members are used as part of stud walls, floor joists and roof trusses. Lumber used in light-frame construction has a rectangular cross-section and varies in size depending on its use. The typical size used for structural light-frame walls is 38 x 140 mm, but this size could be increased for taller walls or when used in balloon framing construction. The lumber is typically visually graded according to the NLGA Standard Grading Rules for Canadian Lumber (CSA-O86, 2010), which for structural light framing includes Select Structural, No.1, No.2 and No.3. In order to properly define the lumber member, the species of wood is also required. The species is an important characteristic since the density of the wood varies with each species type and could have a direct impact on the capacity of the member. The density of the wood is especially important for connection capacity since the embedding strength of a member is a function of the member density. The four main species groups are Douglas Fir-Larch (D Fir-L), Hem-Fir, Spruce-Pine-Fir (S-P-F) and Northern Species (North Species). The D. Fir-L and Hem-Fir are commonly found in western part of Canada, while S-P-F is more common in eastern Canada. Northern Species group is a grouping of

all other Canadian species. The following table lists the oven-dry relative densities of each lumber group and their associated species, given by the CSA-O86 Standard (CSA, 2009). It is important to note that the table provides mean values for design purposes and that there may be some variability associated with the values.

Table 1: Lumber Species Characteristics (Reproduced from CSA-O86)

Species Combinations	Stamp Identification	Species included	Mean Oven Dry Relative Density
Douglas Fir-Larch	D Fir-L (N)	Douglas fir, western larch	0.49
Hem-Fir	Hem-Fir (N)	Pacific coast hemlock, amabilis fir	0.46
Spruce-Pine-Fir	S-P-F	Spruce (all except Sitka spruce), Jack pine, lodgepole pine, balsam fir, alpine fir	0.42
Northern Species	North Species	Any Canadian species graded in accordance with the NLGA rules	0.35

In addition to using GWB as a sheathing material floors and walls are typically sheathed with oriented strand board (OSB) or plywood (Figure 5), to resist gravity and lateral loads.

a) OSB **b) Plywood**

Figure 5: Wood Based Sheathing

The OSB product is an engineered wood product and is made of less valuable, fast growing wood species. The strands on the outer faces of the OSB panel are oriented along the long axis which makes it stronger along this axis and the inner layers are oriented perpendicular to the long axis or randomly.

The typical sheathed wood shearwall consists of a bottom lumber plate, two top plates, two end vertical studs on each end and intermediate vertical studs spaced evenly. All of the lumber is fastened with smooth shank wood nails. Sheathing is fastened to the wood frame, providing the shear resistance of the wall. The shearwall essentially acts as a cantilever where the span of the cantilever is the height of the wall and the depth is the length of the wall. Since in the case of a typical shearwall, the depth to height ratio is quite large, shear deformation replaces bending as the significant action.

1.2 Research Needs and Contribution

1.2.1 Stiffness estimation of light-frame wood shearwalls

Knowledge about the stiffness of light-frame wood shearwalls is very important for the purpose of load distribution, building period estimation and drift calculations. Wood frame construction can be designed with only wood-based shear walls resisting the earthquake effects or with both wood-based and GWB shear walls considered as part of the LLRS. There is typically a large presence of GWB walls in wood-frame structures and the design engineer is required to evaluate whether or not to take the GWB shear strength and stiffness into consideration. Even if GWB is deemed "non-structural" by the design engineer, its contribution to the estimation of the wall stiffness may still be significant. According to the National Building Code of Canada (NBCC, 2010), stiff elements that are not considered part of the LLRS shall be separated from all structural elements of the building so that no interaction takes place as the building undergoes deflections due to earthquake effects (NBCC, 2010). However, if such separation is not feasible, the stiffness imparted to the structure from elements that are not part of the LLRS shall be accounted for in calculating the period of the structure for determining the lateral forces if the added stiffness decreases the fundamental lateral period by more than 15% (NBCC, 2010).

In typical light-frame wall construction the GWB panels are fastened directly to walls. GWB have therefore a significant influence on the building period and overall response of wood frame structures. The underestimation of stiffness can also lead to an unrealistic load distribution, and to an overestimation of the building period, which in turn leads to an underestimation of the base shear. Currently, no reliable method is available to help estimate the stiffness contribution of walls with GWB, whether the GWB panels are intentionally considered to contribute to the strength of the LLRS or simply used as finishing material.

1.2.2 Ductility estimates of shearwalls including GWB

A structural system is deemed ductile if it can undergo displacement in the inelastic range without significant loss of strength. A ductile structure is necessary when dealing with earthquake loads. The ductility of the structure allows it to dissipate energy and permits the designer to reduce the earthquake base

shear force. The effect of ductility can be visualized through the equal displacement principle, as shown in Figure 7. The principle shown is that for a system with ductility, the force is reduced for the same displacement.

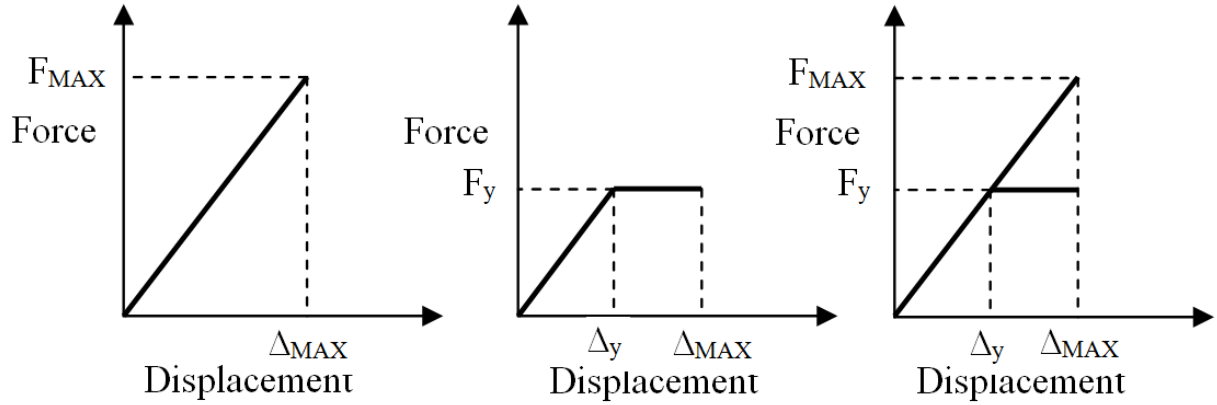

Figure 6: Equal Displacement Principle

Structures subjected to the same ground motions and with that same period have approximately the same peak displacements, independent of the response type. The difference occurs in the applied force, which is reduced by a given ductility factor. The NBCC lists values for ductility factors for different LLRS (NBCC, 2010).

Wood members that are subjected to crushing parallel or perpendicular to grain exhibit non-linear behavior and can be a good source for a "one time" energy dissipater. Once cyclic loading is introduced, the behavior is not effective since the crushed wood is not able to recover and recreate the energy dissipation. The source of the ductility and energy dissipation in wood frame structures is the joint between the sheathing material and the wood frame shearwall. The energy dissipation is a combination of crushing of the wood member, yielding of the fastener and crushing of the sheathing panel.

The shear strength contribution of GWB can sometimes be ignored for seismic considerations, in order to utilize a more favorable ductility reduction factor. The ductility reduction factor is taken as 3.0 for light-frame wood shearwalls with wood based structural panels while the ductility factor is 2.0 when taking into account the shear strength contribution of the GWB. The ductility reduction factor is used to reduce the seismic force; therefore the magnitude of the shear strength contribution of the GWB walls is required to be at least 50% of the seismic force in order to make it worth considering the strength of the GWB walls.

1.2.3 Research Contribution

A load-deflection model is required to accurately represent the response of wood frame shearwalls sheathed with GWB. Developing a joint level load-deflection model is essential to obtain an accurate shearwall deflection model.

The Canadian and American wood design codes currently have provisions to determine the deflection of shearwalls sheathed with wood-based panels (plywood and OSB). The provisions to determine the deflection of GWB sheathed shearwalls available in these standards are limited to nailed shearwalls and are rudimentary compared to the wood based sheathing equations. There is currently no fastener slip model for the GWB sheathed shearwalls that are fastened with GWB screws. The current study attempts to improve the existing equations for nailed GWB sheathed shearwalls and develop a suitable analytical expression that can be used for GWB fastened with screws.

1.3 Objectives

The overall goal of the current research project is to establish a better understanding of the behaviour of GWB sheathed walls used in light-frame wood structures. More specifically, the project's objectives are to:

1) Develop a model capable of describing the non-linear response at the joint level of nailed and screwed GWB panels to stud framing members.

2) Investigate the effects of the variation of construction materials from different manufacturers of GWB as well as metal fasteners on the behaviour of the connection joint

3) Investigate whether the behaviour of shearwalls can be predicted through the use of components inputs obtained from testing.

4) Validate numerical models using full-scale GWB shearwalls

1.4 Methodology

The methodology followed in this research project is presented in the following steps:

- It has been established that for wood frame shearwalls, the non-linearity stems from the joint level sheathing to lumber connection. Therefore, joint level tests on fasteners typically used to attach GWB panels to wall framing are conducted. Construction parameters such as using products from different manufacturers, fastener size and type, and density of lumber and GWB were investigated.

The assumption is that findings from these joint level tests can provide a good indication of the effects the parameter will have in the subsystem level shearwalls.

- Embedment strength tests are done on the GWB panels using the fasteners from the joint level tests as well as two dowels with different diameter sizes. Fastener center point bending test was also performed to obtain the bending yield strength of the steel connectors. These parameters would help establish analytical expressions to describe the joint behaviour. The results of the material inputs (connector yield strength and GWB embedment strength) are used as inputs in the yielding equation, which is compared to the mean value obtained from the tested yield capacities of each joint test group.
- Ultimately, it is the behaviour of the wall that is of interest. Therefore, full-scale monotonic and cyclic tests are performed in order to test some of the parameters that may affect the shearwall load-deflection response at real scale and that cannot be tested at joint level. This includes fastener edge/end distance as well as fastener spacing. Another objective of testing the full scale walls is to investigate whether a link can be established between joint level and wall level stiffness and capacity. The full scale tests will also serve as validation for the modelling work.
- Curve fitting performed on the joint level data is used to develop a fastener level load-slip equation capable of describing the joint response. The trends observed in the curve fitting parameters are used to develop the fastener slip equations with material characteristics as input. Analysis is performed using the SAPWood software with the objective to model the joint as a hysteretic spring and use the fastener model to construct a shearwall model. The shearwall model is subject to the same reversed cyclic loading protocol used during testing. The hystereses resulting from the analytical model analysis are then compared to the test data obtained from the full-scale shearwall tests.

1.5 Thesis Organization

Chapter 2 contains a review of the literature, and presents relevant studies regarding four main topics. The topics discussed, in order of presentation, are the behavior of full scale shearwalls sheathed with GWB, shearwall deflection models, joint strength, and finally fastener slip models. For each topic, the extent and limitations of the knowledge and the potential improvements are presented.

Chapter 3 includes the experimental setup information, with material information, explanation of each test setup, and the different test matrices. This information is available for each test performed (joint level test, fastener bending test, embedment strength test and full scale racking test).

Chapter 4 describes the experimental results for all tests performed. This chapter is divided into subsection for each test type. Each subsection includes typical observations, and typical results with associated coefficient of variation.

Chapter 5 provides the discussion portion of the experimental study. Comparisons between each tested group are made and the curve fitting analysis and potential trends observed are discussed. The best model is selected with the help of a decision matrix analysis. The joint level strength is calculated based on component strength and compared to the tested joint strength.

Chapter 6 demonstrates the steps taken to develop a shearwall model based on individual hysteretic joint models using SAPWood. The joint level hysteresis is modeled based on test data and a shearwall model is then completed using the joint level model. The results of the model are compared to full scale tests performed.

Chapter 7 describes the gaps in knowledge that currently exist in the Canadian and US timber design standards and introduces potential provisions that can be used to estimate the stiffness and capacity of GWB shearwalls.

Chapter 8 provides a summary and conclusions obtained from the study.

2. LITERATURE REVIEW

2.1 Experimental Studies on GWB Behaviour in Shearwalls

There have been numerous tests performed on full scale shearwalls sheathed with wood based panels. Relatively fewer tests have been conducted on GWB sheathed shearwalls, but the amount has been substantial enough to provide information on failure modes, ductility and peak strength for different specimen configurations (United States Department of Agriculture (1983), Karacebeyli and Ceccotti (1996), Merrick (1999), Zacher and Gray (1985), Memari and Solnosky (2014), Olivia (1990), Dolan (2003), Sedears et Al. (2008)). The most common test specimen encountered in the literature is 8' x 8' (2440mm x 2440mm) shearwall sheathed with two 4' x 8' (1220mm x 2440mm) vertically placed GWB panel and fastened with GWB nails.

Through review of the literature, common parameter variations in the specimen construction that affect the racking response of the GWB sheathed shearwalls were observed. These variations include fastener type, panel orientation, shearwall length, joint compound type, the effect of including GWB as part of a two sided shearwall with wood based sheathing, and the effect of loading types. The fastener type has shown to have an impact on the peak load of the shearwall, where generally, walls fastened with screws have a higher peak load compared to similar walls fastened with nails (Karacebeyli and Ceccotti, 1996). Full-scale monotonic tests on GWB shearwalls also showed that the panel orientation had an effect on the racking strength of the wall, where walls tested with panels oriented horizontally were more than 40 percent stronger and stiffer than those with panels oriented vertically (United States Department of Agriculture, 1983). The effect of wall length was also examined through monotonic shearwall racking tests and it was concluded that the relationship between the length of wall and racking strength was linearly proportional (United States Department of Agriculture, 1983).

The GWB joint compound type was found to have a significant impact on failure mode, which in turn led to a difference in racking strength and stiffness results. It was determined that compared to the peak shear capacity of the monotonic test on the unfinished specimen, there is a 21% increase in the shear capacity of the non-cement based joint compound walls and 78% increase in shear capacity due to the cement-based joint compound (Memari and Solnosky, 2014).

From the tests performed on the two sided shearwalls (Karacebeyli and Ceccotti (1996), Dolan (2003)), it can be concluded that the GWB does provide additional stiffness and racking strength compared to shearwalls with only a single side of wood based sheathing. More specifically, the study completed by Karacebeyli and Ceccotti (1996), states that the wall strength and stiffness can be assumed to be the sum of

both individual materials (GWB and OSB) up to a drift of 1.3%. Beyond this point, it was found that the addition of GWB to the OSB shearwall contributed to higher peak strength and stiffness but has a lower post-peak ductility. This finding is an essential reason why the current study is important, since the GWB sheathing is expected to have a significant effect on the response of a shearwall and therefore a proper understanding of this response is paramount.

Full-scale racking tests were done on sheathed wood shearwalls for different types of loading protocols with different types of sheathing materials (Olivia (1990), Dolan (2003), Sedears et Al. (2008)). The general conclusion is that effect of different loading protocols on the load-deflections response of wood based sheathing is relatively low. On the other hand, the GWB sheathed shearwalls are affected by the selection of displacement protocol types, since it affects the load-deflection response and the failure modes. Since the cyclic loading protocol is a more realistic scenario when comparing to actual seismic events, it is the more appropriate loading protocol for gypsum wallboard sheathed shearwalls.

Most of the tested GWB wallboard sheathed shearwall have been constructed using ½" (12.7 mm) regular GWB, whereas the CSA-O86 standard requires that only type-X GWB be considered to provide racking strength to shearwalls. This requirement does not imply that regular GWB have no effect on the performance of the shearwalls but it is rather mandated because the manufacturing process of the type-X GWB is more controlled and the performance is therefore expected to be more reliable and repeatable. The present study tested both regular type ½" (12.7 mm) as well as type-X 5/8" (15.9 mm) GWB. A second aspect that is studied is the load-deflection response of GWB sheathed shearwall fastened with GWB screws, which is the most popular fastener used in industry for the construction of GWB sheathed shearwalls.

2.2 Shearwall Deflection Prediction

There are two general models used to predict the deflection of light-frame wood shearwalls. The first, developed by William and McCutcheon (1985), is an energy based method which utilizes the concept that the external energy is the applied force and the internal energy is the energy dissipated by the lumber-to-sheathing connection. The second, which is used by the American (NDS, 2012) and Canadian (CSA-O86, 2010) timber design standards, predicts the deflection by adding the deflection contributions caused by individual components of the shearwall including studs, sheathing, connection and hold-downs.

2.2.1 Energy Model

The energy method was developed to predict the raking response of sheathed wood shear walls (William and McCutcheon, 1985). The concept behind the energy model is the constant equilibrium between the

external and internal energy of the system. In a shearwall system, the external energy is a function of the applied load and is defined as the area under the racking displacement caused by nail distortions versus external racking load curve. The internal energy is the energy absorbed by the nails, which is defined as the sum of the areas under the lateral load-slip curves of the nails.

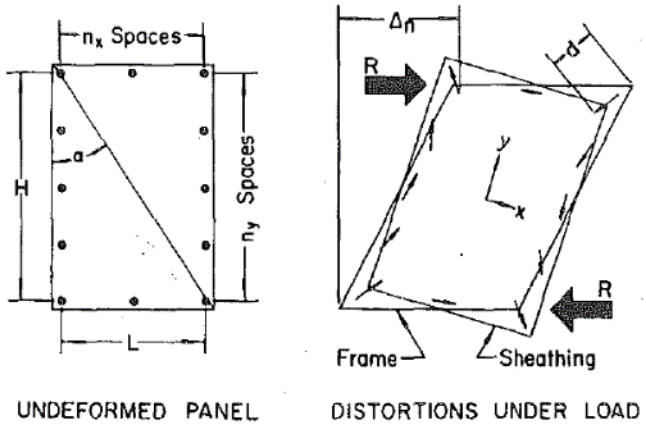

Figure 7: Distortion of Frame and Nails when Panel is subjected to Racking Load (Williams and McCutcheon 1985)

The sheathing to lumber connection is the major factor contributing to the overall response of the shearwall since it is the only source of internal energy for the system. When the power curve is used to define the load-slip behavior at the fastener level, the panel racking is also defined by a power curve. The racking response is:

$$R = \bar{A}\Delta_n^B \tag{2.1}$$

In which, $\bar{A} = A\frac{(\sin\alpha)^{B+1}}{2^B}S$ (2.2)

Where S is the summation of the fastener internal energy and is defined as:

$$S = \sum_{i=1}^{n_x}\left[\sin^2\alpha + \left(2\frac{i}{n_x} - 1\right)^2\cos^2\alpha\right]^{\frac{B+1}{2}} + \sum_{j=1}^{n_y}\left[\left(2\frac{j}{n_y} - 1\right)^2\sin^2\alpha + \cos^2\alpha\right]^{\frac{B+1}{2}} \tag{2.3}$$

R is the external racking load and Δ_n is the horizontal racking displacement due to nail distortions. The parameter α is the angle between the sheathing diagonal and vertical, n_x and n_y are the number of nails in the horizontal and vertical direction, while $i = 0, 1, \ldots, n_x$ and $j = 0, 1, \ldots, n_y$. In addition to the fastener slip, the model includes the shear deformation of the sheathing (second term in equation 2.4). Rearranging the fastener level racking deformation contribution equation, adding the shear deformation contribution and

including the hold-down deflection contribution (for comparison proposes), the total deflection represented in equation 2.4.

$$\Delta_t = \left(\frac{R}{N\bar{A}}\right)^{\frac{1}{B}} + \frac{RH}{NGtL} + \frac{H_s}{L_w}(d_a) \tag{2.4}$$

2.2.2 Four Term Deflection Equation

The Canadian and American timber design standards use the same equation to predict of the shearwall deflection. The equation is a function of four terms: the stud bending, the panel shear, the nail slip and the panel rotation, as shown in Equation 2.5.

$$\Delta_t = \Delta_b + \Delta_v + \Delta_n + \Delta_a \tag{2.5}$$

The shearwall is assumed to be a cantilevered I-beam, where the chords act similar to the flanges of an I-beam (AWC, 2012). Therefore, the bending rigidity of the shearwall is related to the axial rigidity of the chords (*EA*). The equation for the first term is:

$$\Delta_b = \frac{2}{3}\frac{v_s H_s^3}{EAL_W} \tag{2.6}$$

Where v_s is the shear due to specified loads at the top of the wall per unit length, H_s is the height of the shearwall, E is the modulus of Elasticity of the boundary element and A is the cross-sectional area of the boundary member and L_s is the length of the shearwall segment. In the I-beam analogy, the sheathing can be assumed to act as the web; therefore the shear deflection is related to the rigidity of the sheathing.

The equation for the second term is:

$$\Delta_v = \frac{v_s H_s}{B_v} \tag{2.7}$$

Where B_v is the shear-through-rigidity of the sheathing and is obtained from tables found in the Canadian wood design manual (CSA-O86, 2010). There are currently no shear-through-rigidity values for GWB sheathing in the design standards.

The next two parameters are based on experimental tests. The equation for the third term is:

$$\Delta_n = 0.0025 H_s e_n \tag{2.8}$$

Where e_n is the fastener deformations and explained in greater depth in the following section.

The anchorage slip and rotation contribution equation is:

$$\Delta_a = \frac{H_s}{L_W} d_a \tag{2.9}$$

Where d_a is the vertical elongation of the wall anchorage system which is a function of fastener slip, device elongation and anchor or rod elongation at the induced shear load. In the case of shearwalls with no hold-downs the following equation can be used to approximate d_a. Equation 2.10 is found in the Canadian wood design manual and is not present in the American wood design manual.

$$d_a = 2.5 d_f K_m \left[\left(\frac{\left(v H_s - P_{ij} \right) s_n}{L_s} \right) / n_u \right]^{1.7} \tag{2.10}$$

Where d_f is the nail diameter, K_m is the service creep factor, P_{ij} is the uplift restraint force, S_n is the nail spacing around the panel edge and n_u is the lateral nail strength resistance. In summary, the total deflection of a shearwall equation is:

$$\Delta_t = \frac{2}{3} \frac{v_s H_s^3}{E A L_W} + \frac{v_s H_s}{B_v} + 0.0025 H_s e_n + \frac{H_s}{L_W} d_a \tag{2.11}$$

2.3 Joint Strength

The lateral capacity of the joint is a function of the fastener diameter, the fastener yield strength, embedding strength of the main lumber member, the embedding strength of the side plate, the density of the main member and side plate, as well as the thickness of each member (CSA-O86, 2010). There are different models that have been developed to calculate the joint capacity based on different failure modes. These models are developed for joints that have one and two shear planes. The equation and models developed for the dowel type connector failure modes are referred to as the Johansen's yielding equations or European Yield Model (Johansen, 1949).

The expected failure mode for the lumber main member and GWB side plate dowel type single shear connection is Mode III_s. The General Dowel Equations for calculating lateral connection values (American Wood Council, 2014) states that the III_s failure mode is limited by the dowel bearing in the side member

and dowel bending in the main member. Figure 8 is a visual representation of the stresses acting on the connection (Parsons, 2001).

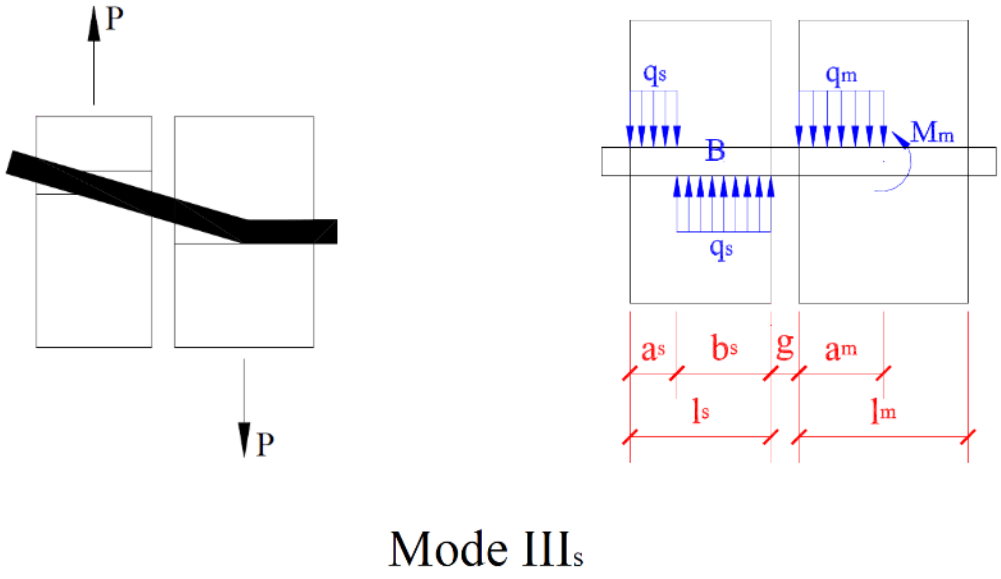

Figure 8: GWB to Lumber Failure Mode (reproduced from Parsons, 2001)

The mathematical derivation of the presented model is completed and described in the study by Parsons (2001). The following equation is obtained for Mode III$_s$ single shear dowel type connection:

$$\left[\frac{1}{4\times q_s}+\frac{1}{(2\times q_m)}\right]P^2+\left(\frac{1}{2}l_s+g\right)P-M_m-\frac{l_s^2\times q_s}{4}=0 \tag{2.12}$$

In which, q_s is the side member dowel bearing resistance, q_m is the main member dowel bearing resistance, l_s is the side member dowel bearing length, g is the gap between members and M_m is the maximum moment developed in the main member. In order to obtain the lateral capacity (P), the quadratic formula is used to obtain the roots which are $+P$ and $-P$ in this case. Therefore the equation used to obtain the maximum lateral capacity is:

$$P=\frac{-B+\sqrt{B^2-4AC}}{2A} \tag{2.13}$$

Where,

$$A = \left[\frac{1}{4 \times q_s} + \frac{1}{(2 \times q_m)}\right] \quad (2.14)$$

$$B = \left(\frac{1}{2} l_s + g\right) \quad (2.15)$$

$$C = -M_m - \frac{l_s^2 \times q_s}{4} \quad (2.16)$$

$$M_m = M_{dm} = \frac{F_b D^3}{6} \quad (2.17)$$

$$q_s = F_{es} D \quad (2.18)$$

$$q_m = F_{em} D \quad (2.19)$$

Where F_b is the dowel bending strength, D is the dowel diameter within the main member, F_{es} is the dowel bearing strength in the side member and F_{em} is the dowel bearing strength in the main member

The embedment strength (bearing strength) is a key parameter in order to obtain the lateral capacity of wood connection. Previous studies have been undertaken to obtain the embedment strength of dowel type connectors in different types of materials that could be used a part of a wood connection. There is extensive data and several studies have been conducted to obtain the embedment strength of dowels in wood. The review by Zhou and Guan (2006) determined the factors affecting embedment strength in wood connections. In this review, the authors state that there are two groups of studies, one in North America by Whale and Smith (1986a,b, 1989) and another in Europe by Ehlbeck and Werner (1992), that are the primary sources of embedment data used in design codes. Zhou and Guan (1992) give a list factors which affect the embedding strength of timber based on the outcomes of historical test results and observations. Beyond dowel diameter, the density (species type) and moisture content are the factors that are most commonly associated with timber embedment strength.

Despite the fact that the wood embedment strength has extensive test data, the same cannot be said for the embedment strength of GWB. As part of the study performed by Smart (2002), the author determined the embedment strength of GWB panels using different manufacturers. The full-hole embedment test, outlined in ASTM D 5764– 97a was used to determine the embedment strength of the GWB panels. The study utilized the actual fastener as the dowel for the embedment tests, where the fasteners were 1-3/8” drywall

nails and 1-1/2" roofing nails. A correlation between the embedment tests and the joint level testing was found, and it was observed that higher embedment strength of GWB with fibers lead to higher joint capacity.

In the current study typical round dowels are used as part of the embedment tests to establish parameter trends. Fasteners used in the joint tests will be used during embedment tests as well in order to use these values in the established yield model to predict joint strength.

2.4 Fastener Slip Models

Wang (2009) provided a detailed literature review for wood based panel sheathing shearwall deflection calculation to determine the contribution of each parameter on the total deflection of the shearwall. It was noted that the most important contributor to the total deflection of the shearwall is the fastener slip term. In addition to contributing to most of the deflection, the fastener slip contribution also provides the non-linearity in the response. It is important to note that the fastener slip contribution varies as a function of the applied load. Caused by the non-linear behavior, the contribution of the fastener slip is greater near peak load while being relatively low at lower loads. Based on this information, it is necessary to develop a fastener level model to obtain a proper full scale deflection model.

The load-deflection response of the laterally loaded nail joints is non-linear and efforts have been made to provide a model capable of describing the response (Foschi (1974, 1977), McLain (1975)), William and McCutcheon (1985), Wang (2009)) and some standards provide equations as well (CSA-O86 (2010), NDS (2012)). All of the presented models predict the response with relatively good accuracy for their intended use. The models are therefore examined to determine potential options for the GWB sheathed joint level deflection model.

The exponential model is developed as part of a study by Foschi (1974) and is further compared to typical connection in a later research study (Foschi 1977). The nail shank was considered as a beam bearing on a non-linear foundation. The nail behaviour is assumed to be elastic up to a yield point. Once the yield point is achieved, crushing of the wood develops under constant or nearly constant load. The load-deflection curve can be expressed as the following exponential equation.

$$y = [p_1 - k_1 x]\left[1 - e^{(-k_0 x/p_1)}\right] \tag{2.20}$$

In equation 2.20, k_0 is the initial stiffness, k_1 is the post-yield stiffness and p_1 is the intercept of the post-yield stiffness slope and the y-axis (load). The variables y and x are the applied load per fastener and the joint level deflection, respectively. The values for the three parameters are obtained by curve fitting to the

test data. The advantage of the model presented in equation 2.20 is that it utilizes material characteristics as equation inputs as opposed to arbitrary curve fitting values. A downside is the relative complexity of the model, since obtaining the displacement with known load values is an iterative process. It is important to note that the equation was developed for joints sheathed with wood based sheathing and connected to lumber using nails.

For the present analysis, both the asymptotic model and the logarithmic model will be considered the same since the terms in the equations can be rearranged to produce both equation types. The models developed by McLain (1975) and Wang (2009) both utilize the asymptotic model (logarithmic model). According to Pellicane et Al. (1991), the logarithmic model is widely used in the United-States to predict the load-slip behavior of laterally loaded nailed joints. Equation 2.21 is the logarithmic model developed in the McLain (1975) study.

$$p = Alog_{10}(1 + Bx) \tag{2.21}$$

Where p is the applied lateral load, A and B are the empirically-derived constants and x is the fastener level displacement. Through testing and data reduction the A parameter can be obtained as a function of the main and side member specific gravity.

The asymptotic model was chosen in the study by Wang (2009) because the shape fits the load-deflection behavior well near the ultimate load. The author placed great importance on this characteristic since the goal was to improve on the existing models, which did not properly predict deflection near ultimate load. The asymptotic model follows the form expressed in Equation 2.22:

$$y = A - BC^x \tag{2.22}$$

Where, A, B and C are curve fitting parameters, x is the fastener deflection and y is the applied lateral load. Using the results from a multitude of tests, the author was able to obtain equations for each of the curve fitting parameters based on sheathing thickness, nail diameter and main member lumber density Wang (2009). It is noteworthy to mention that the models presented in equation 2.21 and 2.22 were developed for joints sheathed with wood based sheathing and connected to lumber using nails.

The power model is a popular model because of its relative simplicity, while still having the benefit of being very accurate at low and moderate load levels. William and McCutcheon (1985) state that this model results in a sufficient description of the slip response because the behaviour of the shearwalls up to design load levels is of primary concern and therefore attempting to predict deflections ultimate strength is less

important. The applicability of the power model is made evident by its implementation in the American and Canadian construction codes. The power curve follows this form:

$$p = Ax^B \tag{2.23}$$

Where p is the applied load, x is the deflection, A is the amplitude and the exponent B is between zero and unity (a value of unity corresponds to a perfectly plastic response). The values for the constants A and B are obtained through experimental lateral joint tests. As part of the William and McCutcheon (1985), joint level load-deflection equations were obtained based on curve fitting of the experimental data.

Gypsum Sheathing: $p = 170x^{0.44}$ (2.24)

Plywood Sheathing: $p = 440x^{0.34}$ (2.25)

These specific equations were not used as part of the previously discussed energy model equation (equation 2.4) but the A and B curve fitting parameters were used to determine the shape of the load-deflection curve of the shearwall in equation 2.1. The equations for GWB and plywood sheathed joints (Equations 2.24 and 2.25) are only applicable for nails. Furthermore, the use of the models are limited to material used in the testing project and could therefore not be generalized.

The Canadian timber design standard (CSA-O86, 2010) and its American counterpart (AWC, 2012) provide an equation to obtain the nail deformation for the purpose of calculating the deflection of shearwalls and diaphragms. Both standards are essentially the same, with some presentation differences. The Canadian timber design standard provides an equation which is a function of the nail diameter, while the American standard has different equations for the different nail diameters. Equation 2.26 is the Canadian version of the nail slip equation and is only valid for wood based sheathing in dry service conditions.

$$e_n = \left(\frac{0.013 v_s}{d_f^2}\right)^2 \tag{2.26}$$

The American standard (AWC, 2012) provides a fastener slip for use in the prediction of full scale shearwall deflection. The equation is a function of the fastener load and there are different equations for the size of nail and the condition of the wood at the time of testing. The first equation is for joints that are fabricated green and tested dry, while the second equation is based on the nail slip equation for dry service conditions.

6d common nail: $e_n = \left(\frac{V_n}{434}\right)^{2.314}$ and $e_n = \left(\frac{V_n}{456}\right)^{3.144}$ (2.27, 2.28)

8d common nail: $e_n = \left(\frac{V_n}{857}\right)^{1.869}$ and $e_n = \left(\frac{V_n}{616}\right)^{3.018}$ (2.29, 2.30)

10d common nail: $e_n = \left(\frac{V_n}{977}\right)^{1.894}$ and $e_n = \left(\frac{V_n}{769}\right)^{3.276}$ (2.31, 2.32)

The values are based on structural panels and lumber with specific gravity of 0.50. The fastener slip is increased by 20% for non-structural grade panels.

For GWB, a nail deformation value of 0.76 mm is assumed for GWB (CSA-O86 (2010), AWC (2012)). The proposed value does not provide an accurate estimate of the fastener deformation since it is not a function of the applied load and does not adequately describe the non-linearity of the fasteners connecting the GWB panel to lumber.

In summary, there are three potential model types that may be used to describe the load-deflection response of a laterally loaded joint: exponential model, asymptotic model and power model. Extensive research exists on models describing the response of joints sheathed with wood-based panels, however, for GWB sheathed joints there is no accurate non-linear load-deflection model that exists. The William and McCutcheon (1985) curve fitted equation (equation 2.24) seems to be the only viable option but it is limited to joints fastened with nails and the materials specific to the testing program. The current study aims to develop an equation that is based on the most appropriate model that will accurately predict the load-deflection response of GWB sheathed joints fastened using both nails and screws. The equation will be developed in such a way that the material characteristics of the joint will be equation inputs.

3. EXPERIMENTAL SETUP

3.1 Materials

Since data for GWB joint tests is very limited in the literature, it is unclear what the effect of the manufacturing process on the performance of the material. It was therefore imperative that data be representative of multiple manufacturers for the different materials. By doing so, the inherent variability that exists due to manufacturing processes is accounted for. This chapter describes all the material involved in the experimental testing program as well as the experimental setup and test procedures.

3.1.1 Gypsum Wallboard (GWB)

Tests involving GWB panels included parameters such as manufacturing, board type, thicknesses and densities. The Gypsum Association ensures that its members produce GWB that meet or exceed the requirements stipulated in the ASTM C1396: Standard Specification for Gypsum Board (ASTM, 2013). There are currently three Canadian gypsum wall board manufacturers that are members of the Gypsum Association: CGC, CertainTeed Gypsum Canada Inc and Georgia-Pacific Gypsum LLC. Products from all three GWB manufacturers were used in the study to ensure an adequate representation of construction in Canada.

Regular and type-X gypsum wall board panels were used in the study. The CSA-O86 states that the gypsum wall board must be type-X gypsum wallboard in order to account for its strength contribution in shear wall design. The type-X gypsum wall board used in the study has a thickness of 5/8" (15.9mm). Regular gypsum wall board panels were also considered to represent "Housing and Small Buildings" (Part 9 of NBCC) since the type-X type panels are not commonly used for this type of application. The regular gypsum wall board used in the study had a thickness of 1/2" (12.7mm). The selection of thickness for each GWB type was based on their commercial material availability.

The gypsum wall board panels were either normal or light-weight panels. The type-X panels used had weights of 9.3 kg/m^2 and 11 kg/m^2, for light-weight and normal weight panels, respectively. The regular type panels had a weight of 6.3-7.0 kg/m^2. Details on the weights measured for GWB panels for the three different manufacturers considered are shown in Table 2.

Table 2: GWB Characteristics

Manufacturer	Type	Thickness	Weight (kg/m^2)
Manufacturer A	Type-X	15.8 mm (5/8")	11.0
	Type-X (Light Weight)	15.8 mm (5/8")	9.3
	Regular	12.7 mm (1/2")	6.34
Manufacturer B	Type-X	15.8 mm (5/8")	11.0
	Regular	12.7 mm (1/2")	6.9
Manufacturer C	Type-X	15.8 mm (5/8")	11.0
	Regular	12.7 mm (1/2")	7.03

3.1.2 Framing Lumber

The most commonly used lumber for construction in eastern Canada is Spruce-Pine-Fir (S-P-F) due to its availability, and was consequently used for this study. A 2x6" (38x140mm) No. 2 grade was chosen for this study to represent typical wall construction. Furthermore, for the joint specimen tests this size allowed for adequate space to drive the fasteners from both sides of the sheathing-wood-sheathing connection without any interference between connectors from opposite directions.

The full size lumber members were first sorted based on their specific gravity in order to obtain high and low density groups. The low density group had an oven dry specific gravity of 0.32-0.35 and the high density group had an oven dry specific gravity of 0.39-0.45. The density test procedure was done according to test method A of ASTM D2395: Standard Test Methods for Specific Gravity of Wood and Wood-Based Materials (ASTM, 2008) and the moisture content was obtained in conformance with ASTM D4442: Standard Test Methods for Direct Moisture Content Measurement of Wood and Wood-Based Materials (ASTM, 2007). The same density test, explained previously, was done on each 8" (203.2 mm) piece after testing to obtain exact density and moisture content at the time of testing for each individual piece. The average moisture content of all tested lumber members is 12.4% (COV: 20.3%).

3.1.3 Fasteners

Nails and screws that are manufactured specifically for application of gypsum wall boards to wood studs were used in this study. The CSA-O86 states that the minimum fastener penetration depth should be 19 mm, which means that a fasteners of 1-5/8" (41.3 mm) and 1-1/2" (38.1 mm) length would be adequate when used together with the 5/8" (15.9 mm) sheathing.

3.1.3.1 GWB Screws

Screws for gypsum wall board applications are deemed adequate to be used to attach GWB panels to wall studs if they are manufactured to the specifications of the ASTM C1002: Standard Specification for Steel Self-Piercing Tapping Screws for the Application of Gypsum Panel Products or Metal Plaster Bases to Wood Studs or Steel Studs (ASTM, 2007). The standard GWB screw was a type W screw with a coarse thread shaft and a pointed end with a number 2 bugle head. Figure 9 shows a typical No.6 GWB screw. The screw manufacturers used for this study are U Can, Gripe Rite, Pro Twist, H.Paulin and Tree Island; all of which follow the ASTM C1002 requirements. In the remainder of the document these manufacturers will be randomly assigned designations as "manufacturer A-E". The purpose of the study is to show trends in the manufacturing process, which can be done without the need to identify the manufacturer. The sizes considered are No.6, No.8 and No.10 screws from different manufacturers, depending on material availability. Table 3 lists all the screws used in this testing program.

Table 3: Screw Characteristics

Manufacturer	Screw Size	Length	Head Diameter	Shaft Diameter	Shaft Diameter with Threads
Manufacturer A	No.6	1-5/8" (41.28 mm)	8.2 mm	2.70 mm	3.80 mm
Manufacturer B	No.6	1-5/8" (41.28 mm)	8.36 mm	2.70 mm	3.80 mm
Manufacturer C	No.6	1-5/8" (41.28 mm)	8.11 mm	2.70 mm	3.80 mm
Manufacturer D	No.6	1-5/8" (41.28 mm)	7.96 mm	2.70 mm	3.80 mm
Manufacturer E	No.6	1-5/8" (41.28 mm)	8.23 mm	2.70 mm	3.80 mm
Manufacturer A	No.8	2-1/2" (63.5 mm)	7.93 mm	3.17 mm	4.31 mm
Manufacturer B	No. 10	1-1/2" (38.1 mm)	8.84 mm	3.82 mm	4.69 mm

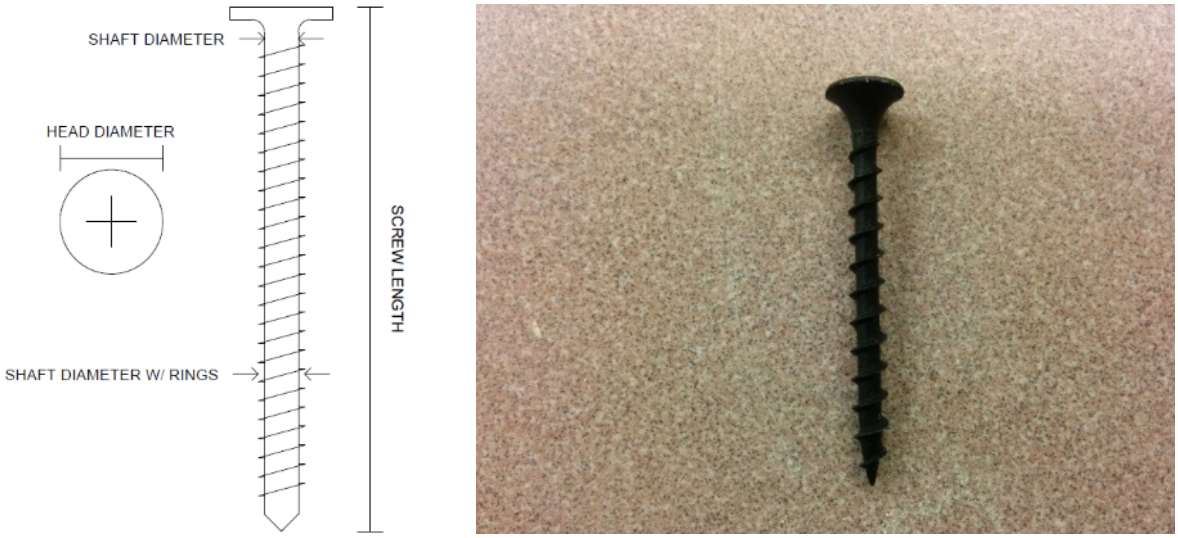

a) GWB Screw Schematic **b) No.6 GWB Screw Picture**

Figure 9: GWB Screw

3.1.3.2 GWB Nails

Using nails as fasteners for gypsum wallboard application is not as common as screws. They are still part of the study since gypsum wallboard nails are still used in practice, manufacturers still produce them and they are the only type of connector referenced in the timber design standard (CSA O86). The nail manufacturers used in this study are Grip Rite, H. Paulin and Tree Island. All three manufacturers follow the ASTM C514: Standard Specifications for Nails for the Application of Gypsum Board (ASTM, 2009), which provides the requirements for the manufacturing of nails for gypsum wall board applications. The standard nail for gypsum wall board application has a large flat head, a ringed shaft and a long diamond point to reduce cracking in the sheathing. Table 4 lists the characteristics for all nails used in the current project and Figure 10 shows a typical 12.5 gauge GWB nail.

Table 4: Nail Characteristics

Manufacturer	Nail Size	Length	Head Diameter	Shaft Diameter	Spike Length
Manufacturer A	12.5 gauge	1-1/2” (38.1 mm)	7.18 mm	2.70 mm	3.93 mm
Manufacturer B	12.5 gauge	1-1/2” (38.1 mm)	7.37 mm	2.70 mm	5.77 mm
Manufacturer D	12.5 gauge	1-1/2” (38.1 mm)	7.81 mm	2.70 mm	6.03 mm

a) GWB Nail Diagram **b) 12.5 Gauge GWB Nail Picture**

Figure 10: Typical GWB Nail

3.1.4 Materials used in Full-Scale Wall Tests

A single manufacturer was represented for each product type used in the construction of the full scale walls. The GWB used is a type-X wall board with a thickness of 5/8" (15.9 mm) and with a weight per surface area of 11.0 kg/m^2. The wallboard panel was fastened with either nails or screws. The screws were No.6 screw with a length of 1-5/8" (41.28 mm), a head diameter of 8.23 mm and a shaft diameter of 3.80 mm (2.70 mm internal diameter). The nail product used was a 12.5 gauge nail with a length of 1-1/2" (38.1 mm), a head diameter of 7.37 mm, a shaft diameter of 2.70 mm and a spike length of 5.77 mm.

The framing lumber selected for the subsystem level test were stud grade S-P-F 2x4" (38x89mm). The grade and species for the full scale tests were consistent with those used in the joint tests. The depth of the stud has no effect on the shear capacity as long as the minimum nail or screw penetration lengths are respected. The average dry relative density and the average moisture content of the lumber within the wall are presented in Table 5. The coefficient of variation for each wall specimen is indicated in brackets next to the average value.

Table 5: Shearwall Lumber Density and Moisture Content

Specimen Number	Average Dry Relative Density	Moisture Content (%)
Wall-3-1	0.42 (9.83%)	17.3 (9.56%)
Wall-3-2	0.42 (6.42%)	17.1 (9.97%)
Wall-4-1	0.42 (8.14%)	17.0 (18.0%)
Wall-4-2	0.42 (8.30%)	16.6 (12.1%)
Wall-5-1	0.42 (9.17%)	15.0 (11.5%)
Wall-6-1	0.41 (5.4%)	16.4 (9.04%)
Wall-7-2	0.42 (10.78%)	17.2 (17.0%)
Wall-8-1	0.42 (9.55 %)	16.5 (17.4%)
Wall-8-2	0.42 (11.3%)	15.5 (14.2%)

3.2 Specimen Fabrication

3.2.1 Joint Level Specimen Fabrication

The test specimens for the joint level tests consisted of two 8 inch long, 2x6" wood pieces with gypsum wall board sheathing fastened with screws or nails on both sides. Figure 11 shows a typical joint level test specimen prior to testing.

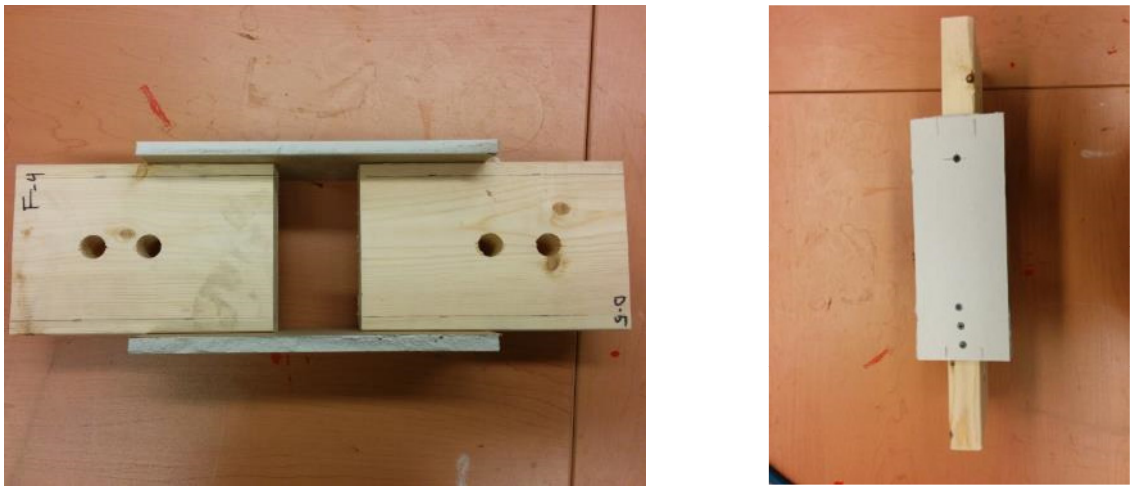

Figure 11: Typical Joint Level Test Specimen

One of the lumber pieces contained the test joint while the other was considered to be the dummy end. As seen in Figure 13, two holes were pre-drilled using a hand-held drill with 3/4" (19.1 mm) drill bit. The fasteners were placed 2" (50.8 mm) from the top of the sheathing, such that no end distance failure occurred. The gypsum wall board sheathing was cut into 4" (101.6 mm) wide and 10.5" (266.7 mm) long sections.

Each specimen had a fastener placed on each side of the stud section at the tested end. The dummy end has three screws placed on each side to minimize the slip of the dummy end during testing. The dummy end screws were examined after each test to ensure the adequacy of this assumption. Figure 12 shows the screws at the dummy end after a test. It should be noted however, that the joint displacement was measured between the GWB panel and the lumber piece at the test end, as shown later in Figure 15. This means that even if slip did take place at the dummy end, it would not affect the result at the tested end.

Figure 12: Straight Dummy End Screws

The tested end nails were driven using a standard hammer and the screws were fastened using a screw driver. Both fastener types were driven in such a way that the head was flush with the sheathing. Figure 13 is a schematic of the joint level test specimen.

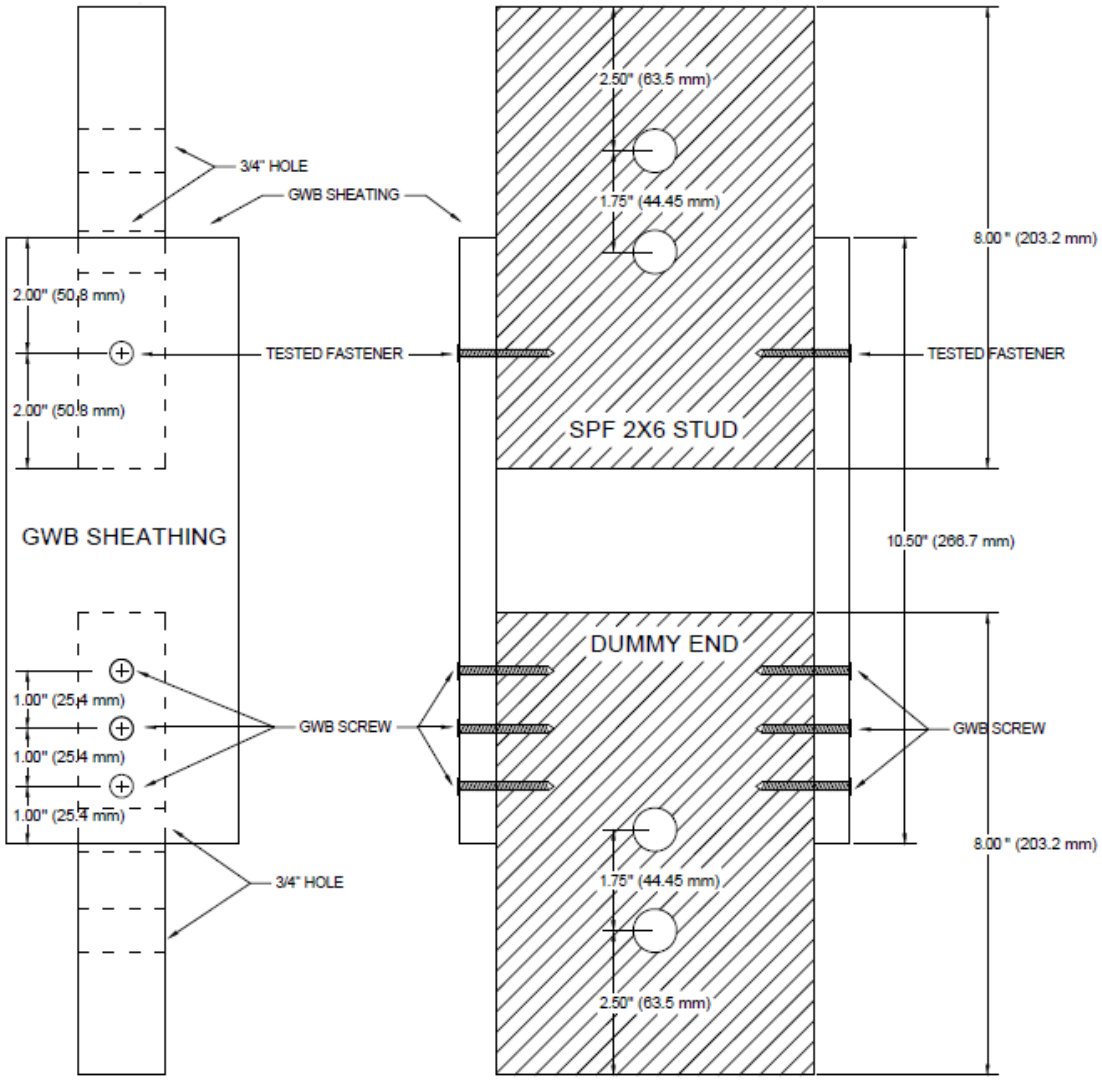

Figure 13: Typical Joint Level Test Specimen Diagram

3.2.2 Fabrication of Full-Scale Wall Specimens

The test specimens for the full-scale wall tests were built to replicate typical shearwall construction details. Twelve 8’ x 8’ (2440x2440 mm) walls were constructed with two top plates, one bottom plate, and two end studs at each end. The studs were spaced 16” (406 mm) apart and were connected to the top and bottom plates using two 3.5” 16d smooth shank common nails. Type-X GWB consisting of 4’x8’ (1220 x 2440 mm) panels with thickness of 5/8” (15.8 mm) were placed on only one side of the wall.

The wall hold-down system used during the full-scale tests was commercially available Simpson Strong-Tie proprietary product (HD3B). Three 5/8" (15.8 mm) bolts were used to connect the end studs to the foundation beam. Figure 14 shows the wall anchorage system used during testing.

a) Front view of Hold-Down **b) Hold-Down placed on wall**

Figure 14: Simpson Strong-Tie HD3B Hold-Down

Tabulated displacement values are provided by the manufacturer literature at strength-level as shown in Table 6. The values include assembly elongation, including fastener slip, hold-down device extension and rotation and anchor bolt elongation. This information will be used later to estimate the overall displacement of the wall assembly.

Table 6: Hold Down Allowable Load and Displacement (Reproduced from Simpson Strong-Tie, 2009)

Model No.	HD3B
Anchor Bolt Diameter	5/8"
Minimum Wood Member Thickness	1-1/2"
Allowable Tensions Load (Strength Level)	2653 lbs (11 801 N)
Displacement	0.207 (5.258 mm)

3.3 Test Set-up and Procedure

3.3.1 Joint Level Test Procedure

The joint specimen tests were performed using a universal testing machine (UTM). The load was measured using a load cell, capable of measuring uni-axial load in tension and compression. The displacement between the GWB sheathing and the lumber stud was measured with two linear variable differential transducers (LVDT) located on each side of the tested end, as shown in Figure 15.

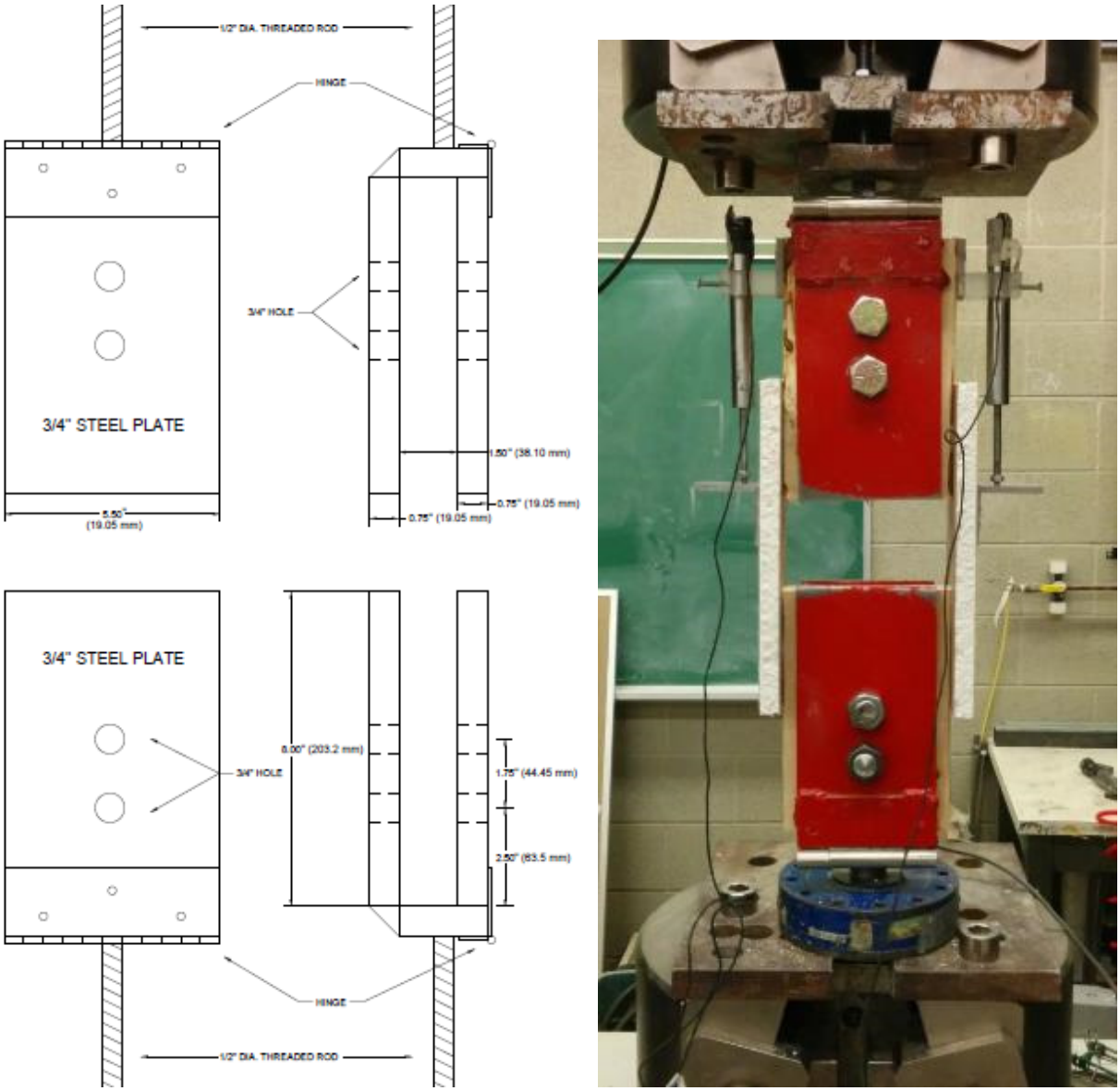

Figure 15: Joint Level Test Setup

The test was first performed using a monotonic displacement protocol to obtain maximum displacement, which formed the basis to develop the reversed cyclic loading protocol. The ASTM E2126: Standard Test Methods for Cyclic (Reversed) Load Test for Shear Resistance of Vertical Elements of the Lateral Force Resisting Systems for Buildings (ASTM, 2011) was used to determine the loading protocol for the joint specimen.

The UTM was pre-programmed with a displacement rate of 2.5mm/minute for monotonic tests. Test method B of the ASTM E2126 uses the ISO 16670 protocol, which involves increasing groups of displacements based on a percentage of the displacement at maximum load obtained from the monotonic tests. The reversed cyclic loading protocol was pre-programmed in the UTM with a displacement rate of 60mm/minute. Figure 16 shows the loading schedule from the ISO 16670 standard which is explained in the ASTM E2126 (ASTM, 2011).

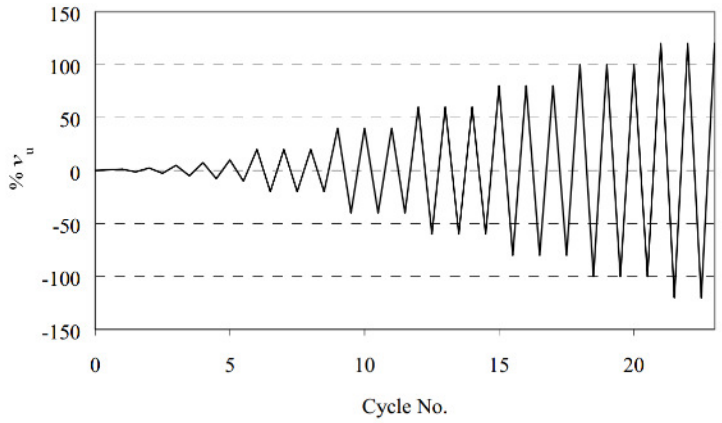

Figure 16: ISO 16670 Loading Protocol (ASTM, 2011)

The joint specimen testing program included three gypsum wallboard manufacturers, two gypsum wallboard types, two gypsum wallboard thicknesses, three nail manufacturers, four screw manufacturers, three screw sizes and two density ranges. Each combination of parameters is shown in Table 7 and is replicated 10 times, which yields a total of 270 tests. It is important to note that, in addition to the tests outlined in the test matrix, monotonic tests were performed for No.8 screw and No.10 screw joint level specimens to obtain the necessary information to complete the reversed cyclic loading protocol.

Table 7: Joint Specimen Test Matrix

JS Group	GWB Manufacturer	GWB Thickness	GWB Type	Fastener Manufacturer	Fastener Type	Fastener Size	Density Range	Loading
JS-1	A	5/8" (15.9mm)	X (L.W)	A	Screw	#6 (3.80mm)	0.39-0.43	Monotonic
JS-2	A	5/8" (15.9mm)	X (L.W)	A	Nail	12.5 gauge	0.39-0.43	Monotonic
JS-3	A	5/8" (15.9mm)	X (L.W)	A	Screw	#6 (3.80mm)	0.39-0.43	Cyclical
JS-4	A	5/8" (15.9mm)	X (L.W)	A	Nail	12.5 gauge	0.39-0.43	Cyclical
JS-5	**A**	5/8" (15.9mm)	X (L.W)	A	Screw	#6 (3.80mm)	0.39-0.43	Cyclical
JS-6	**A**	5/8" (15.9mm)	X (L.W)	B	Screw	#6 (3.80mm)	0.39-0.43	Cyclical
JS-7	**A**	5/8" (15.9mm)	X (L.W)	C	Screw	#6 (3.80mm)	0.39-0.43	Cyclical
JS-8	**A**	5/8" (15.9mm)	X (L.W)	D	Screw	#6 (3.80mm)	0.39-0.43	Cyclical
JS-9	**A**	5/8" (15.9mm)	X (L.W)	B	Nail	12.5 gauge	0.39-0.43	Cyclical
JS-10	**A**	5/8" (15.9mm)	X (L.W)	D	Nail	12.5 gauge	0.39-0.43	Cyclical
JS-11	**A**	5/8" (15.9mm)	X (L.W)	A	Nail	12.5 gauge	0.39-0.43	Cyclical
JS-12	**C**	5/8" (15.9mm)	X	A	Screw	#6 (3.80mm)	0.39-0.43	Cyclical
JS-13	B	5/8" (15.9mm)	X	A	Screw	#6 (3.80mm)	0.39-0.43	Cyclical
JS-30	A	5/8" (15.9mm)	X	B	Screw	#6 (3.80mm)	0.39-0.43	Cyclical
JS-16	**A**	5/8" (15.9mm)	X (L.W)	A	Screw	#8 (4.31 mm)	0.39-0.43	Cyclical
JS-20	**A**	5/8" (15.9mm)	X (L.W)	B	Screw	#10(4.69mm)	0.39-0.43	Cyclical
JS-18	**A**	5/8" (15.9mm)	X (L.W)	D	Screw	#6 (3.80mm)	0.32-0.35	Cyclical
JS-21	**A**	5/8" (15.9mm)	X (L.W)	A	Screw	#6 (3.80mm)	0.32-0.35	Cyclical
JS-22	**A**	5/8" (15.9mm)	X (L.W)	C	Screw	#6 (3.80mm)	0.32-0.35	Cyclical
JS-23	C	5/8" (15.9mm)	X	A	Screw	#6 (3.80mm)	0.32-0.35	Cyclical
JS-17	**A**	5/8" (15.9mm)	X (L.W)	A	Screw	#8 (4.31 mm)	0.32-0.35	Cyclical
JS-19	A	5/8" (15.9mm)	X (L.W)	B	Screw	#10(4.69mm)	0.32-0.35	Cyclical
JS-24	A	5/8" (15.9mm)	X	E	Screw	#6 (3.50mm)	0.39-0.43	Cyclical
JS-25	A	5/8" (15.9mm)	X	B	Nail	12.5 gauge	0.39-0.43	Cyclical
JS-26	**A**	12.7 mm (1/2")	Regular	B	Screw	#6 (3.50mm)	0.39-0.43	Cyclical
JS-27	**C**	12.7 mm (1/2")	Regular	B	Screw	#6 (3.50mm)	0.39-0.43	Cyclical
JS-28	B	12.7 mm (1/2")	Regular	B	Screw	#6 (3.50mm)	0.39-0.43	Cyclical

3.3.2 Center Point Bending Test Procedure

The fastener bending yield strength was obtained through the center point bending test outlined by ASTM F1575: Standard Method for Determining Yield Moment of Nails (ASTM, 2013). Even though the standard is only applicable to nails, since no guidance is give in the literature on how to test yield moment of screws, the ASTM F1575 was adopted to testing the screws as well. The load applicator tip and the supports consisted of rounded edges and had a large enough diameter to ensure distributed stress at the point of load application and supports. The displacement and the load applied were recorded using the instrumentation from the universal testing machine. Figure 17 is a picture taken during a typical center point bending test on a No.6 screw.

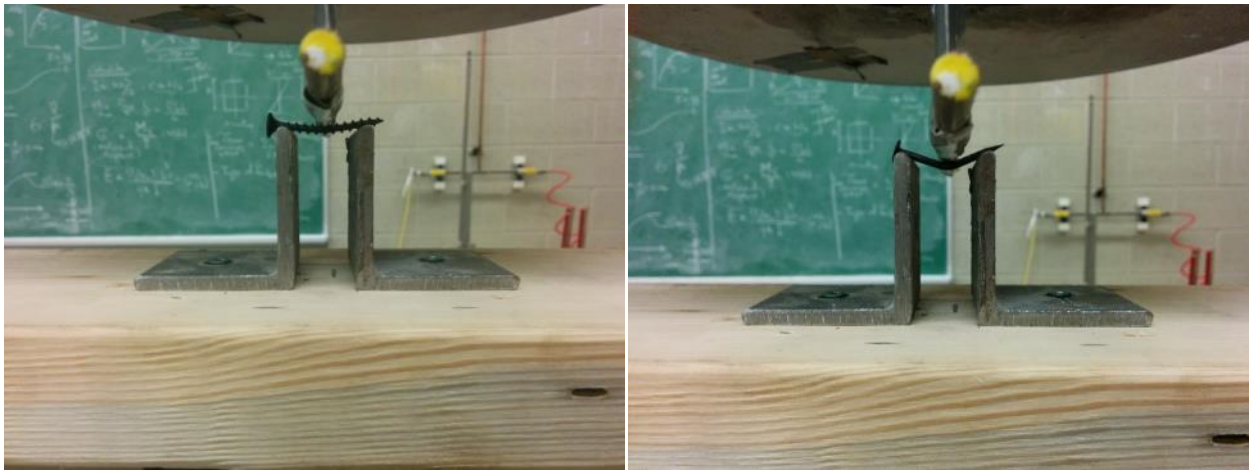

a) No.6 GWB Screw b) 12.5 Gauge GWB Nail

Figure 17: Center Point Bending Test

Each center point bending test was performed on 5 replicates of each screw and nail used in the joint specimen and full scale testing. The load was applied at a rate of 2.5mm/min until failure of the specimen or until the fastener achieved a bending angle of at least 90 degrees. Table 8 presents the center point bending test matrix.

Table 8: Center Point Bending Test Matrix

Fastener Type	Fastener Manufacturer	Diameter Size
Screw	A	No.6
Screw	B	No.6
Screw	C	No.6
Screw	D	No.6
Screw	E	No.6
Screw	D	No.8
Nail	A	12.5 gauge
Nail	B	12.5 gauge
Nail	D	12.5 gauge

3.3.3 Embedment Strength Test Procedure

The full-hole bearing tests were performed in accordance with ASTM D5764: Standard Test Method for Evaluating Dowel-Bearing Strength of Wood and Wood-Based Products (ASTM, 2013). The described method was applied to determine the bearing strength of gypsum wallboard specimens. Two circular dowels with different diameters (6.31 mm and 9.4 mm) were used to determine the effect of the variation in dowel sizes. In addition, No.6, No.8 and No.10 screws were used as dowels to obtain the embedment strength of

the GWB when using screw sizes and shapes used in the study. The nails were not used as part of the study since they would yield during the full hole embedment test and the diameter is too small to use as part of the half hole embedment test. The values used for nails are extrapolated from the trend observed during the testing of the smooth and circular dowels. The tests were performed on each GWB type and manufacturer used in joint level testing.

The tested GWB panel was placed in the top portion of the universal testing machine and held in place by a pneumatic clamp attached to the machine. The steel brackets were placed as close as possible to the GWB panel without actually touching the panels to avoid any friction or interference. The load was applied at a rate of 2.5 mm/minute. Figure 18 shows pictures of the embedment test setup.

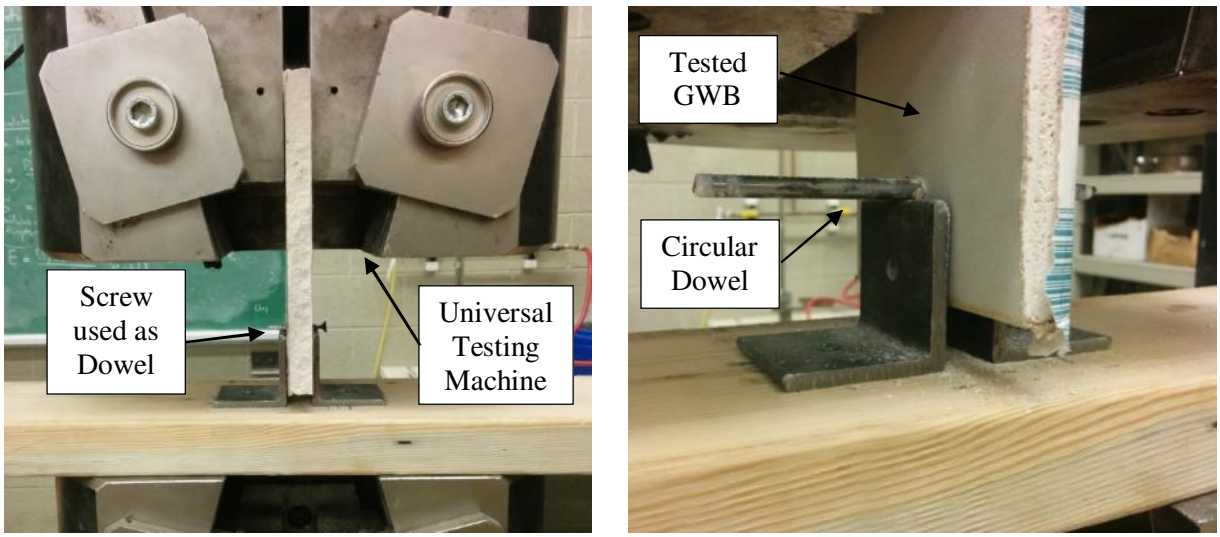

Figure 18: Embedment Strength Test Setup

Embedment tests were completed for each GWB type and manufacturer. In total 100 tests were performed, including five repeats for each configuration. All of the joint level configurations fastened with screws are represented in the embedment tests. Table 9 presents the GWB embedment test matrix.

Table 9: GWB Embedment Test Matrix

GWB Manufacturer	GWB Type	GWB Relative Density	GWB Thickness (mm)	Dowel Type	Dowel Diameter
A	Type-X	0.69	15.8	Dowel 1	6.31 mm
				Dowel 2	9.4 mm
				Screw	No. 6
B	Type-X	0.69	15.8	Dowel 1	6.31 mm
				Dowel 2	9.4 mm
				Screw	No. 6
C	Type-X	0.69	15.8	Dowel 1	6.31 mm
				Dowel 2	9.4 mm
				Screw	No. 6
A	Type-X (L.W)	0.59	15.8	Dowel 1	6.31 mm
				Dowel 2	9.4 mm
				Screw	No. 6
				Screw	No. 8
				Screw	No. 10
A	Regular	0.5	12.7	Dowel 1	6.31 mm
				Dowel 2	9.4 mm
				Screw	No. 6
B	Regular	0.54	12.7	Dowel 1	6.31 mm
				Dowel 2	9.4 mm
				Screw	No. 6
C	Regular	0.55	12.7	Dowel 1	6.31 mm
				Dowel 2	9.4 mm
				Screw	No. 6

3.3.4 Full-scale wall Test Procedure

The top plates of the shearwall specimen were attached to a load transfer HSS beam using four 19 mm bolts. The load transfer beam was displaced at a pre-programmed rate, using an actuator with an attached load cell to measure the applied force. The bottom of the specimen was placed on a wood plate (38x89 mm) and attached to a steel beam using four 19 mm anchor bolts and two additional bolts for the hold-down. The bottom wood plate was used to ensure that the sheathing panel has sufficient room to rotate. In total, seven LVDTs were used to measure the wall displacements. LVDT 1 and 2 measured the slip of the bottom plate of the specimen on each side, LVDT 3 and 4 measures the uplift at the base on each side, LVDT 5 and 6 measure displacements at the top of the wall on each side and LVDT 7 measure the separation between the two GWB panels. A schematic of the test setup is shown in Figure 19 and a picture of the setup is shown in Figure 20.

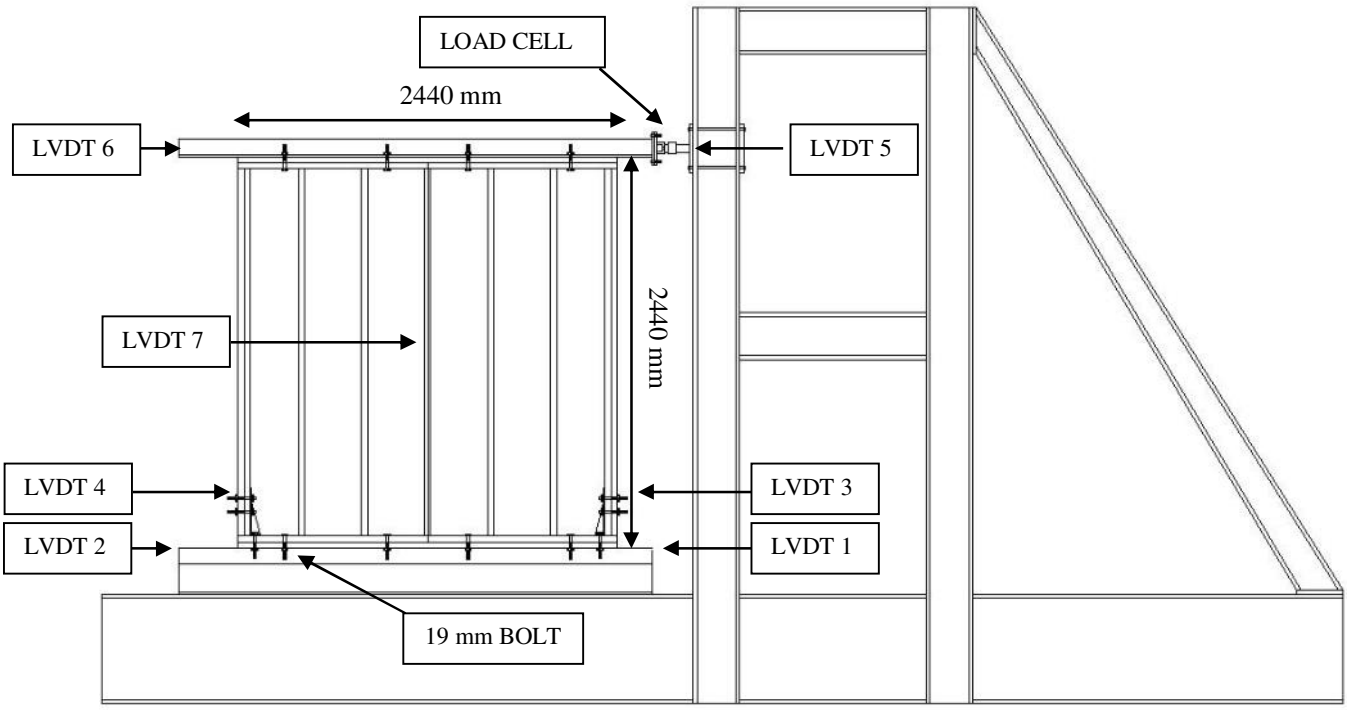

Figure 19: Full Scale Test Setup Schematic

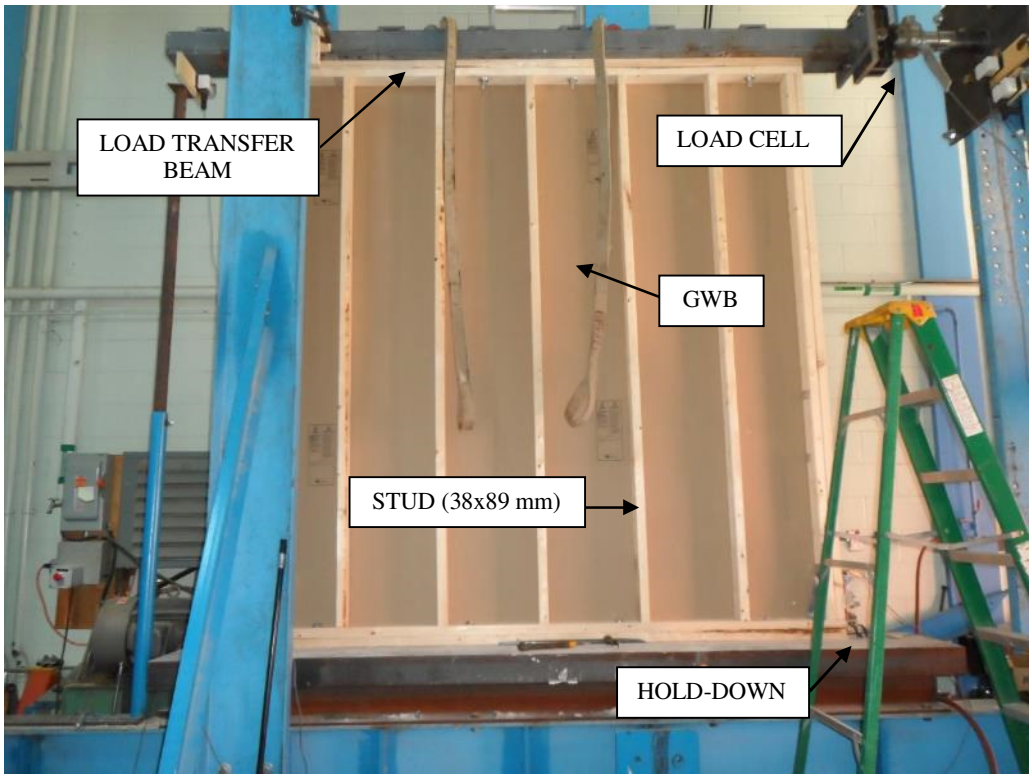

Figure 20: Full Scale Test Setup

The same two displacement protocols, used at the joint level, were used for the wall tests. One wall fastened with nails and another fastened with screws were subjected to monotonic to obtain the maximum displacement. The maximum displacement is then used as part of the ISO 16670 protocol reversed cyclic displacement protocol, shown in Figure 16. The displacement rates are similar to the ones used in the joint level and are applied at the top of the wall through the load transfer device.

The parameters studied during the shearwalls testing were fastener type, fastener spacing at panel edges and panel end/edge distance. The field screw spacing of 300 mm remained constant. Table 10 lists the wall test matrix.

Table 10: Shearwall Test Matrix

	Sheathing Thickness (GWB)	**Fastener Type**	**Fastener Size**	**Panel End/Edge Distance***	**Fastener Spacing at Panel Edges**	**Loading**
Wall – 1	5/8" (15.9mm)	Screw	No.6	Setup 1	150 mm	**Monotonic**
Wall – 2	5/8" (15.9mm)	Nail	12.5 gauge	Setup 1	150 mm	**Monotonic**
Wall – 3	5/8" (15.9mm)	**Screw**	No.6	Setup 1	150 mm	Cyclical
Wall – 4	5/8" (15.9mm)	**Nail**	12.5 gauge	Setup 1	150 mm	Cyclical
Wall – 5	5/8" (15.9mm)	Screw	No.6	**Setup 2**	150 mm	Cyclical
Wall – 6	5/8" (15.9mm)	Screw	No.6	**Setup 3**	150 mm	Cyclical
Wall – 7	5/8" (15.9mm)	Screw	No.6	**Setup 4**	150 mm	Cyclical
Wall – 8	5/8" (15.9mm)	Screw	No.6	Setup 1	**50 mm**	Cyclical

*See Table 11 for "Setup" definition

The fasteners' end and edge distance were varied between 19 mm and 9 mm. The minimum spacing requirement (9 mm) was selected based on the 2009 CSA O86 Standard provisions. The selection of 19 mm for edge spacing was chosen based on it being an upper boundary since this is exactly half of the 38 mm width of the stud used.

Table 11: Panel End/Edge Distance Definition

	Intermediate Stud	**End Studs**	**Top and Bottom**
Setup 1	9 mm	19 mm	19 mm
Setup 2	9 mm	9 mm	9 mm
Setup 3	9 mm	9 mm	19 mm
Setup 4	9 mm	19 mm	9 mm

4. EXPERIMENTAL TEST RESULTS

4.1 Joint Level

4.1.1 Observations

For all test configurations and parameters studied, the joint level tests showed consistent failure modes, where factors contributing to the fastener slip consisted of crushing in the wood member, crushing in the GWB panel and yielding of the steel connector.

The crushing of the wood member was caused by the bending of the fastener, embedded in the member. Wood crushing is a ductile failure, although it cannot provide consistent ductility in reversed cyclic response since a gap is formed during crushing, as seen in Figure 21.

Figure 21: Wood Crushing

The crushing of the GWB panel exhibited similar characteristics as that observed in wood. The GWB crushing creates a void in the panel which eliminates any resistance during a reversed cyclic event once the load is reversed, unless higher displacement occurs. Figure 22 shows a typical GWB crushing failure.

Figure 22: Gypsum Wallboard crushing

Another element contributing to the deflection of the joint is the bending of the fastener. Steel is known for maintaining the ability to dissipate energy during cyclic loading. Since sufficient end distance in both the lumber and GWB was provided during these tests, the ultimate failure always occurred in the steel connector. Figure 23 illustrates the fastener behaviour. The bent screws shown in the picture are taken from the monotonic loading.

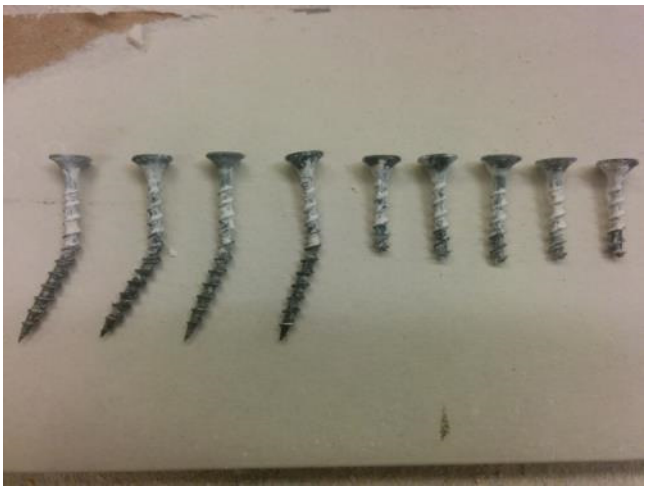

Figure 23: Bent and Ruptured Screws

4.1.2 Joint Level Load-Deflection Response

The joint level test specimens consisted of panels placed on both sides of the lumber piece and the sheathing to lumber deflection was measured on both sides. The average displacement was then obtained, which yielded the load-deflection response per fastener. The load-deflection behaviour of all tested joints was consistent and involved the characteristic pinching behavior, strength and stiffness degradation, as shown in Figure 24. The joint level hysteresis shown in Figure 24 is the seventh repetition of the JS-5 group.

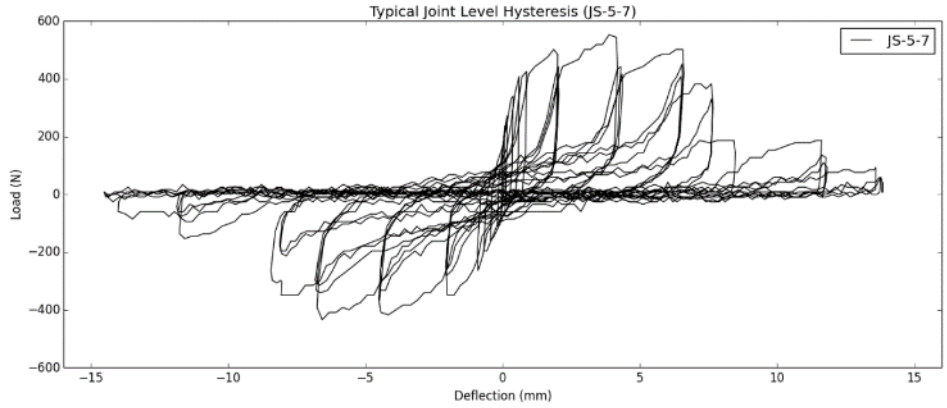

Figure 24: Typical Joint Level Hysteresis

The pinching behavior in the hysteresis is caused by the gap that is created by the crushing of the GWB and wood members. The average of the positive and negative envelope curve of the joint level hysteresis was obtained for each test. The average backbone curves for the JS-5 group represents a typical result and is shown in Figure 25.

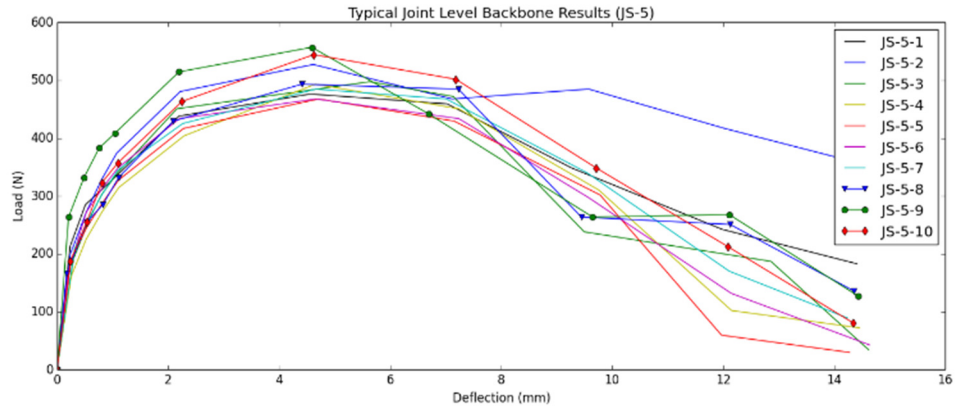

Figure 25: Typical Joint Level Average Envelope

4.1.3 EEEP Analysis Results

ASTM E2126 (ASTM, 2011) describes the EEEP model as an idealized elastic-plastic curve circumscribing an area equal to the area enclosed by the envelop curve between the origin, the ultimate displacement and the displacement axis. The initial stiffness is based on the slope of the line connecting (0,0) and the point on the load-deflection response corresponding to 40% of the peak load. The initial portion of the bi-linear curve follows this slope until an intersection is made with a horizontal line connecting the yield load and the point of 80% of Peak load, past the peak point of the response. The yield load is obtained by requiring the same amount of are under the curve for both curves. The EEEP curve is used as a tool to compare the effect of the different parameters of the joint specimen as well the response at full scale. The parameters examined using this method are the elastic initial stiffness (k_e), yield load (P_y) and the ductility ratio ($\Delta u/\Delta_{yield}$). Figure 26 shows an example of the EEEP model compared to the average envelope curve.

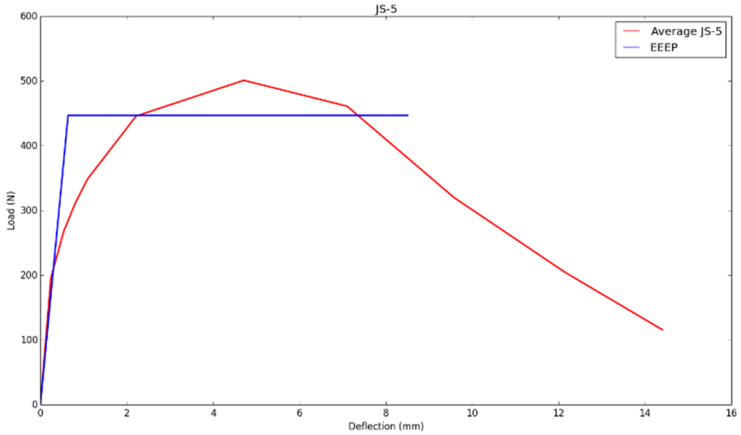

Figure 26: Typical EEEP Model

The EEEP results for all analyzed tests are tabulated in Table 12. The analysis was performed on each test group and the average is given with the coefficient of variation in brackets. The joint specimen groups start at JS-5 since JS-1 to JS-4 groups were used to determine the effect of loading types (cyclical and monotonic)

Table 12: Characteristics of Fastener Joint Specimens for Different Screw Manufacturers

JS Group	Peak Load (N)	Deflection at Peak Load (mm)	Average Lumber Relative Density	Initial Stiffness (N/mm)	Yield Load (N)	Ductility Ratio ($\Delta u/\Delta_{yield}$)
JS-5	500.85 (6.28%)	4.71 (7.07%)	0.40 (3.40%)	738.22 (29.5%)	446.82 (5.74%)	13.86 (24.6%)

JS-6	539.49 (4.32%)	4.41 (3.76%)	0.38 (2.91%)	1280.7 (24.3%)	489.68 (5.07%)	25.64 (27.5%)
JS-7	500.00 (6.20%)	4.51 (3.32%)	0.43 (3.89%)	836.70 (30.2%)	436.7 (6.82%)	14.66 (26.1%)
JS-8	516.51 (8.73%)	4.44 (2.60%)	0.41 (5.07%)	868.22 (48.0%)	455.86 (6.15%)	14.57 (37.2%)
JS-9	409.01 (7.75%)	4.86 (14.96%)	0.41 (2.56%)	262.79 (27.2%)	364.15 (6.32%)	6.97 (20.9%)
JS-10	449.4 (8.30%)	4.56 (4.34%)	0.43 (4.55%)	437.3 (38.5%)	398.02 (7.3%)	8.96 (39.3%)
JS-11	494.05 (5.16%)	4.42 (6.44%)	0.40 (2.00%)	819.73 (62.8%)	437.15 (6.58%)	17.74 (70.3%)
JS-12	592.26 (6.22%)	4.37 (5.62%)	0.39 (3.29%)	1496.96 (25.2%)	532.77 (5.62%)	23.4 (25.0%)
JS-13	621.6 (7.47%)	4.53 (2.79%)	0.37 (6.87%)	1569.82 (26.5%)	561.29 (7.65%)	26.87 (25.9%)
JS-30	755.53 (3.85%)	4.26 (9.88%)	0.41 (1.82%)	2129.35 (38.3%)	678.23 (4.43%)	23.95 (33.8%)
JS-16	576.11 (6.35%)	4.2 (13.4%)	0.43 (3.59%)	953.71 (31.82%)	530.26 (5.65%)	15.62 (34.7%)
JS-17	539.12 (4.83%)	4.72 (13.5%)	0.35 (1.49%)	1042.88 (39.28%)	492.95 (4.69%)	21.18 (36.9%)
JS-18	504.68 (4.09%)	4.39 (10.8%)	0.36 (10.89%)	1247.28 (43.04%)	461.58 (4.56%)	22.42 (38.8%)
JS-19	663.74 (5.33%)	16.32 (31.0%)	0.32 (9.53%)	2009.3 (52.0%)	663.74 (5.33%)	125.74 (53.9%)
JS-20	797.11 (2.54%)	14.15 (3.85%)	0.43 (3.59%)	2983.75 (55.2%)	754.41 (6.97%)	84.01 (62.9%)
JS-21	537.13 (9.14%)	4.50 (6.80%)	0.33 (2.96%)	1273.04 (33.4%)	482.76 (9.58%)	24.44 (29.4%)
JS-22	490.22 (4.91%)	4.44 (4.12%)	0.33 (2.20%)	967.16 (39.3%)	442.88 (5.37%)	21.73 (40.3%)
JS-23	644.56 (7.87%)	4.29 (8.00%)	0.34 (2.58%)	1536.07 (29.8%)	575.81 (6.44%)	24.87 (34.4%)
JS-24	661.56 (5.39%)	4.18 (7.69%)	0.41 (6.54%)	1458.24 (32.5%)	591.69 (5.98%)	24.92 (28.0%)
JS-25	501.28 (6.29%)	4.62 (2.39%)	0.41 (6.54%)	367.17 (42.1%)	446.19 (4.90%)	7.84 (37.6%)
JS-26	472.79 (6.24%)	4.40 (3.94%)	0.43 (3.13%)	1045.08 (25.4%)	434.18 (6.36%)	19.79 (33.3%)
JS-27	523.81 (5.58%)	4.25 (4.47%)	0.41 (7.26%)	1772.41 (30.2%)	472.15 (5.28%)	27.76 (31.7%)
JS-28	538.37 (6.15%)	4.48 (7.9%)	0.44 (5.94%)	1804.07 (17.1%)	485.83 (6.32%)	30.46 (26.9%)

4.2 Center Point Bending Test

The results of the center point bending tests provided estimates of the yield capacity of the fastener. The ASTM F1575 standard (ASTM, 2013) describes the method of obtaining the bending yield strength of the

fasteners by plotting the initial elastic stiffness at an offset of 5% of the fastener diameter, as seen in Figure 29. The intersection of this line with the load deflection curve, obtained from the experimental tests, defines the yield load of the fastener for a particular case. The bending yield strength is obtained by calculating the moment and dividing it by the section modulus of the fastener. The results for all fastener types, manufacturers, and diameter sizes tested are shown in Table 13.

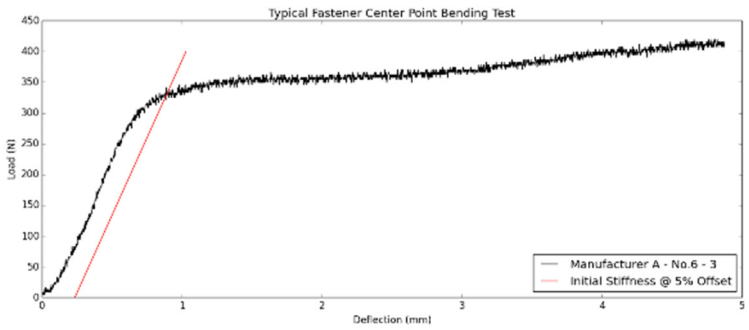

Figure 27: Typical Fastener Center Point Bending Test (Manufacturer A - No.6)

The screw diameter used for the analysis is the effective diameter, which is equal to the average of the diameter with and without the screw threads. The average bending strength of the No.6 and No. 8 GWB screws and the 12.5 gauge GWB nails was found to be 646.9 MPa (COV: 8.90%), 749.4 MPa (COV: 2.98%) and 585.7 MPa (COV: 4.66%), respectively.

Table 13: Fastener Center Point Bending Results

Fastener Type	Fastener Manufacturer	Diameter Size	Yield Moment Capacity (Nmm)	Bending Yield Strength (MPa)
Screw	B	No.6	3958.3	660.8 (8.42%)
Screw	D	No.6	3801.5	634.7 (7.50%)
Screw	E	No.6	3807.4	635.7 (8.86%)
Screw	A	No.6	4122.7	688.3(9.19%)
Screw	C	No.6	3684.5	615.2 (10.7%)
Screw	A	No.8	6326.0	749.4 (2.98%)
Nail	B	12.5 gauge	2079.3	633.8 (3.11%)
Nail	D	12.5 gauge	1858.1	566.6 (2.53%)
Nail	A	12.5 gauge	1826.5	556.8 (8.33%)

The tested nail specimens all reached a deflection angle of 90 degrees prior to failure. The screw specimens all failed prior to attaining the deflection angle of 90 degrees. Figure 28 shows typical screws and nails

after testing. The screws shown in Figure 28 are considered broken since a crack was formed and the capacity of the fastener was null.

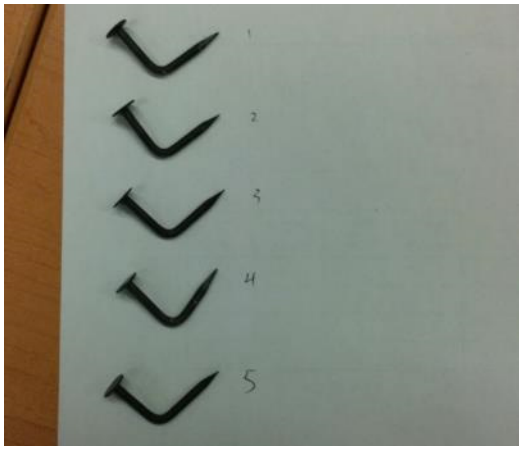

a) **Typical Bending Nail Failure**

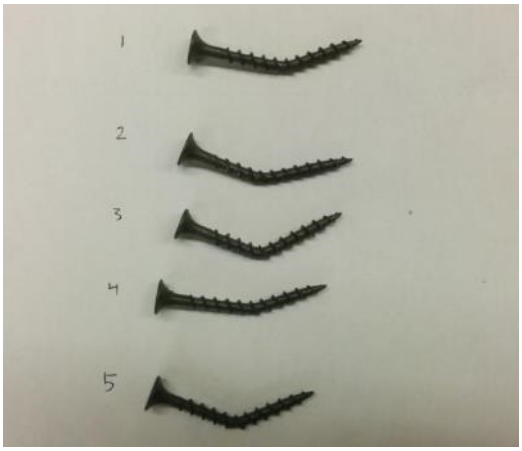

b) **Typical Bending Screw Failure**

Figure 28: Post-Test Fasteners

4.3 Embedment Test Results

The embedment tests were performed according to the ASTM D5764 standard (ASTM, 2013), and they were used to obtain the yield strength of the gypsum wallboard.

The yield strength of the specimen was obtained by plotting the initial elastic stiffness at an offset of 5% of the fastener diameter. The intersection point is considered the yield load. Figure 29 illustrates a typical result of the embedment test for GWB with the associated initial stiffness line plotted to determine the yield strength.

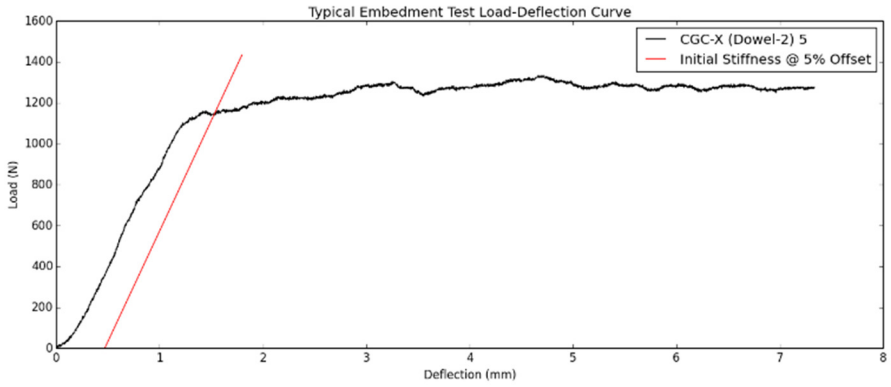

Figure 29: Typical Embedment Test (CGC-X (Dowel-2) 5)

The tests were performed using two different sizes of smooth dowels as well as GWB screws. The dowel diameters were 6.31 mm and 9.4 mm, while the screws used were No.6, No.8 and No.10 screws.

The embedment strengths for different types of gypsum wallboard are presented in Table 14. The coefficient of variation for each set of test is indicated in brackets next to the embedment strength values.

Table 14: Embedment Strength of GWB

GWB Manufacturer	GWB Relative Density	GWB Thickness (mm)	Dowel Type	Dowel Diameter	Load (N) (COV)	Embedment Strength (MPa)
A – Type-X	0.69	15.8	Dowel 1	6.31 mm	791.1 (6.4%)	7.90
			Dowel 2	9.4 mm	1063.3 (9.5%)	7.13
			Screw	No. 6	422.7 (5.0%)	8.07
B– Type-X	0.69	15.8	Dowel 1	6.31 mm	782.9 (6.8%)	7.82
			Dowel 2	9.4 mm	1162.9 (5.3%)	7.79
			Screw	No. 6	450.5 (12.5%)	8.60
C– Type-X	0.69	15.8	Dowel 1	6.31 mm	656.2 (4.2%)	6.55
			Dowel 2	9.4 mm	865.1 (10.5%)	5.80
			Screw	No. 6	382.2 (3.4%)	7.30
A– Type-X (L.W)	0.59	15.8	Dowel 1	6.31 mm	605.7 (11.2%)	6.05
			Dowel 2	9.4 mm	887.6 (4.4%)	5.95
			Screw	No. 6	370.0 (14.0%)	7.06
			Screw	No. 8	379.2 (5.3%)	6.4
			Screw	No. 10	392.9 (6.9%)	5.78
A-Regular	0.5	12.7	Dowel 1	6.31 mm	456.2 (7.1%)	6.69
			Dowel 2	9.4 mm	604.9 (12.6%)	5.07
			Screw	No. 6	233.9 (9.4%)	5.58
B-Regular	0.54	12.7	Dowel 1	6.31 mm	415.6 (11.3%)	5.19
			Dowel 2	9.4 mm	574.6 (6.8%)	4.81
			Screw	No. 6	283.1 (14.9%)	6.75
C-Regular	0.55	12.7	Dowel 1	6.31 mm	409.6 (11.3%)	5.11
			Dowel 2	9.4 mm	525.7 (13.2%)	4.40
			Screw	No. 6	230.0 (12.7%)	5.49

Consistent failure mode was observed for all GWB types, with the dowel crushing the GWB panel as shown in Figure 30 a) and b).

a) Dowel: No.6 GWB Screw b) Dowel: 9.4 mm diameter dowel

Figure 30: GWB Embedment Test Failure Modes

4.4 Full Scale Shearwall Experimental Test Results

4.4.1 General Observations

The typical failure modes observed during the joint level testing were also observed during full scale tests. For example, it was confirmed in the full scale tests that the wood crushing was a relatively minor contributor to the fastener slip. Figure 31 illustrates a typical wood crushing observed after testing at the top plate of the shearwall.

a) Context View b) Close-up View

Figure 31: Full Scale Wood Crushing

The crushing of the gypsum wallboard contributed more significantly to fastener slip in full scale shear walls. The gypsum wall board crushing caused by the fastener is shown in Figure 32. It can be seen that the GWB crushing occurred at an angle, which was a function of the location of the fastener in the panel and the panel aspect ratio. Due to the homogeneity of the material, it could be assumed that the joint level tests are still representative of the failure at full scale. In addition to the GWB crushing, the ultimate failure was a function of the end distance, as illustrated in Figure 32. This issue will be addressed later in this section as well as in the Discussion Chapter.

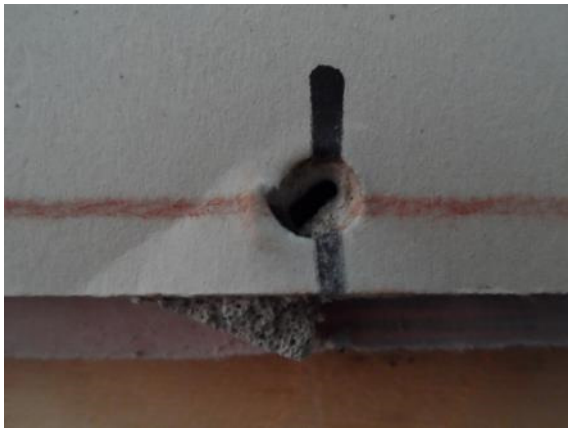

Figure 32: Full Scale Gypsum Wallboard Crushing

The magnitude of fastener deflection was dependent on its location on the panel edge. Figure 33 illustrates the different amount of bending observed in each fastener from the same shearwall and indicates the location on the shearwall from which they were taken.

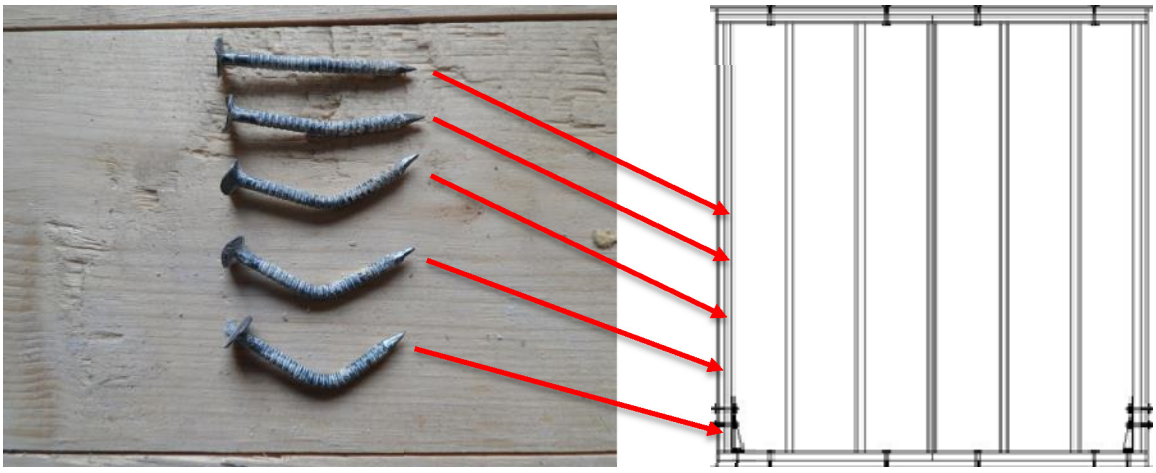

Figure 33: Full Scale Fastener Bending

4.4.2 Shearwall Load-Deflection Response

The average of the measured displacement at the top left and top right of the wall was obtained and plotted against the load measure by the load cell. A typical example of the results obtained from the full scale shearwall reversed cyclic racking tests can be seen in Figure 34. The shearwall hysteresis shown is the first repetition of the Wall-3 setup.

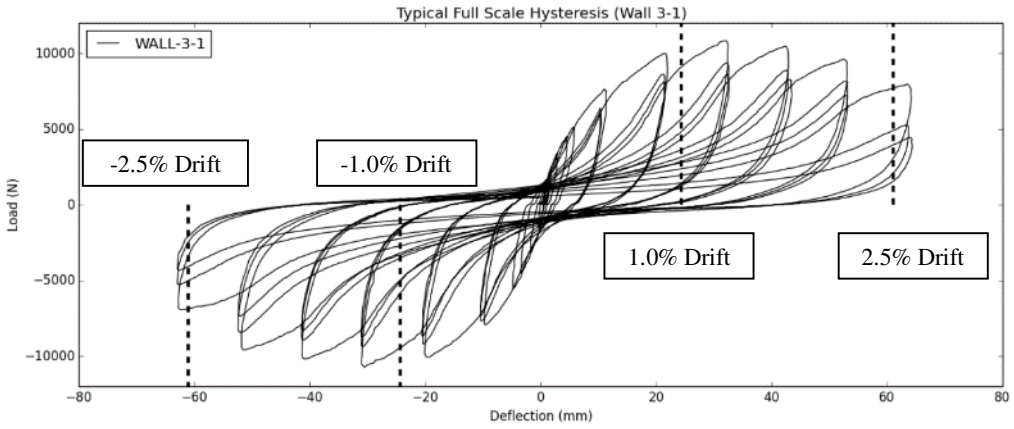

Figure 34: Typical GWB Sheathed Shearwall Hysteresis

Similar characteristics as those found during the joint tests, such as pinching behavior, strength and the stiffness degradation, were also observed in the full scale tests. The same approach used in the joint specimen tests to obtain the average backbone curve was also used for the full scale shearwall analysis. The average of the positive and negative sides of each test was used in the comparison between the various wall configurations. The average backbone curves for all walls are shown in Figure 35.

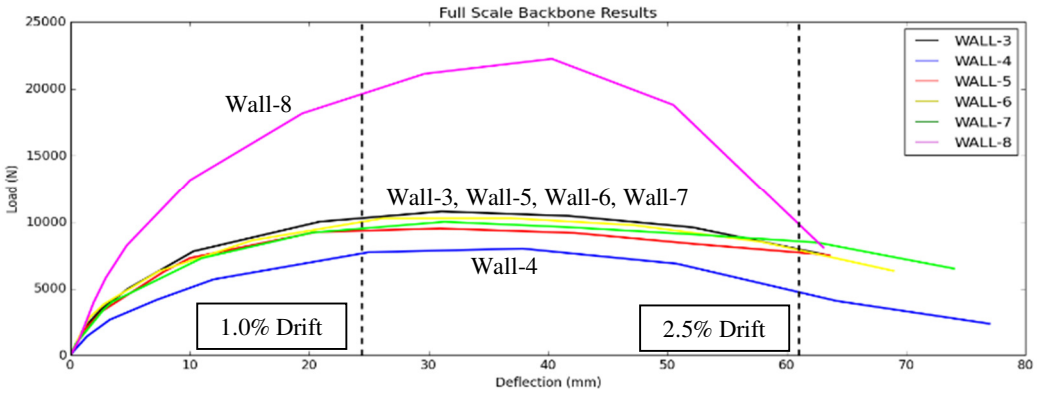

Figure 35: Full Scale Load-Deflection

Drift limits at 1 and 2.5% are also indicated in Figure 35 because these are important design requirements. The behaviour of the various walls with respect to this limit will be further discussed in the following chapter.

4.4.3 EEEP Analysis Results

The geometry at the full scale shearwalls tests causes additional failure modes when compared to those observed at the fastener level. The following sections present the data obtained from the EEEP analysis, failure modes and the unique characteristics observed at each test group. A complete summary of each tested wall can be seen in Appendix 1. The EEEP analysis results summary for each wall is shown in Table 15.

4.4.3.1 Wall-3 and Wall-4

The Wall-3 specimen construction consisted of type-X GWB fastened to studs with an average relative density of 0.42 using No.6 GWB screws spaced at 150 mm and with an end/edge distance of 19 mm. Wall-4 was constructed similarly to Wall-3 but with 12.5 gauge GWB nails.

Wall-3 and Wall-4 specimens failed in a combination of fastener rupture and GWB crushing leading to fastener pulling through the edges of the panel, as shown in Figure 36 and Figure 37. In Wall-3 specimens, slightly more than half of the screws ruptured compared to 10% pulling through the edge, while the rest of screws are bent but remained unbroken. More than half the nails in the Wall-4 specimens are ruptured compared to 20% of the nails pulling through the edge and the remaining nails are bent but unbroken. In both the Wall-3 and Wall-4 specimens, the fasteners that pulled through the edge of the GWB panel were located at the corners of the panel

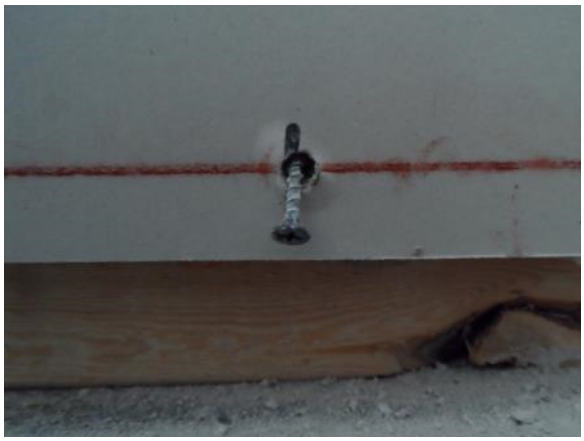

a) **Ruptured Screw at Bottom Edge (Wall-3-1)**

b) **Edge Pull-Through at Bottom Edge (Wall-3-1)**

Figure 36: Wall-3 Failure Modes

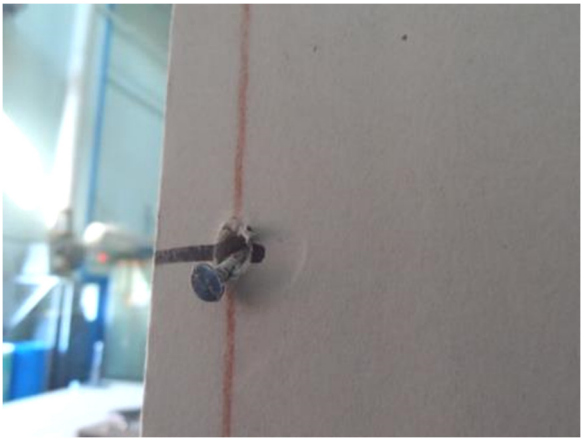

a) **Ruptured Nail at Bottom Edge (Wall-4-1)**

b) **Edge Pull-Through at Bottom Edge (Wall-4-1)**

Figure 37: Wall-4 Failure Modes

4.4.3.2 Wall-5, Wall-6, Wall-7

Wall-5, Wall-6 and Wall-7 specimens all had different variation of panel end/edge distance. Wall-5 had end/edge distance at all panel edges of 9 mm, Wall-6 had end/edge distance of 19 mm at the top and bottom of the panel and 9 mm at both vertical sides of the wall, and finally Wall-7 had end/edge distance of 9 mm at the top and bottom of the panel and 19 mm at both vertical sides of the wall. All of the walls were constructed using No.6 GWB screws spaced at 150 mm, which were used to attach type-X GWB to the lumber frame.

The reduced fastener end/edge distance in Wall-5 resulted in a slight variation in the failure modes. The predominant failure mode for this wall configuration was GWB crushing with the fasteners pulling through the edge of the panel. Most of the screws at the bottom and top of the wall pulled through the edge of the panel prior to the screws rupturing. The screws located at the vertical outer edge studs were a mixture of pull through failure, ruptured screws and bent screws.

In the case of Wall-6, the screws on the vertical outer edge studs pulled through prior to the ones located at the bottom and top of the panels, while the opposite occurred for the Wall-7 specimen. For Wall-6 specimens, approximately half of the screws located at the top and bottom failed in panel edge pull through and a quarter of the screws ruptured, leaving the rest slightly bent. For the screws located at the vertical outer wall edges, a quarter of the screws pulled through the edge, more than half are ruptured and the remaining were slightly bent. In the Wall-7 specimen, most of the screws located at the top and bottom of the wall pulled through the panel edge and none of the screws were ruptured. Most of the screws located at the vertical outer panel edges were ruptured and no screws have pulled through. Figure 38, Figure 39 and Figure 40 show the failure modes for Wall-5, Wall-6 and Wall-7, respectively.

a) Top and Edge Pull-Through (Wall-5-1)

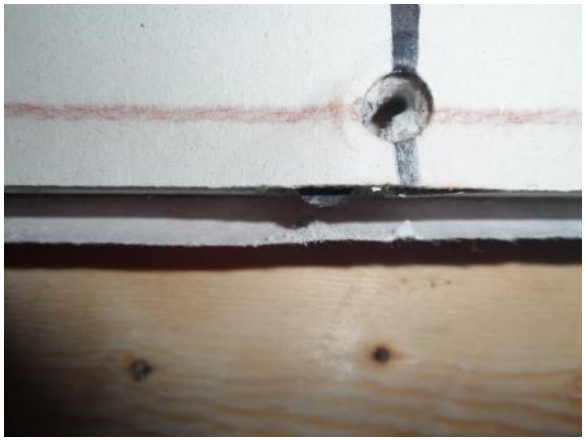

b) Bottom Edge Pull-Through (Wall-5-1)

Figure 38: Wall-5 Failure Modes

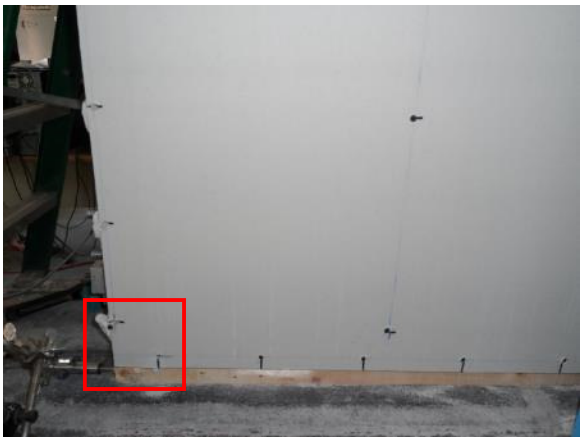

a) Side Edge Pull-Through Prior to Bottom Edge (Wall-6-1)

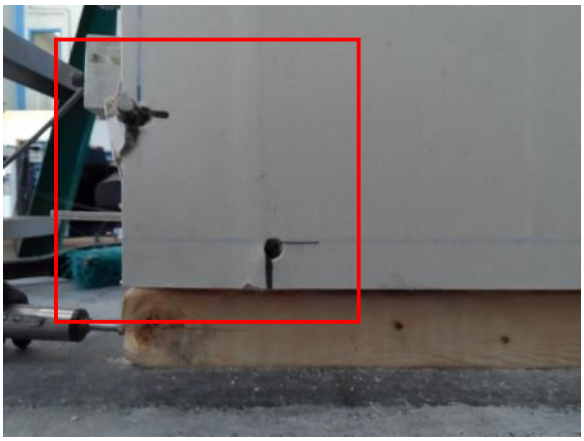

b) Close-up View of (a)

Figure 39: Wall-6 Failure Modes

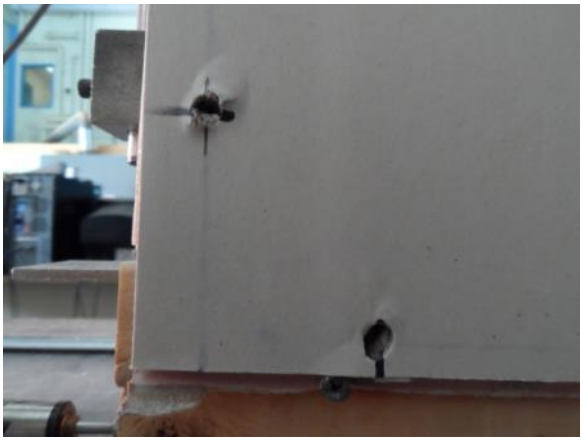

a) Bottom Edge Pull-Through Prior to Side Edge (Wall-7-1)

b) Edge Pull-Through at Bottom Edge (Wall-7-1)

Figure 40: Wall-7 Failure Modes

4.4.3.3 Wall -8

Wall-8 construction included screw spacing of 50 mm at the panel edges. The decreased spacing between the fasteners led to a crack of the GWB forming along the edges of the panel which causes a sudden loss of capacity. The failure mode observed was also reproduced in the test replicate for this particular wall setup. Due to the increase in load obtained in this wall configuration, several other modes of failure were observed. These include: yielding and withdrawal of the end nailing of studs, and increased hold-down deflection due

to crushing of the wood caused by the anchor bolts. Figure 41 shows the different failure modes observed for the Wall-8 specimens.

a) Wall 8-2 GWB Fissure Failure Mode

b) Wall 8-2 End Nails Yielding and Withdrawal

c) Wall 8-1 Hold-Down Deflection

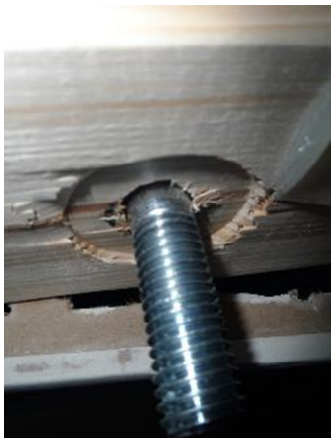

d) Wall 8-1 Wood Crushed by Anchor Bolt

Figure 41: Wall-8 Failure Modes

4.4.3.4 Shearwall Specimen Results Summary

The EEEP method of analysis is explained in the joint specimen section. Table 15 lists the results of this analysis for the full scale tests.

Table 15: Full Scale Shearwalls EEEP Analysis Results

Wall No.	Peak Load (N)	Deflection at Peak Load (mm)	Initial Stiffness (N/mm)	Yield Load (N)	Ductility Ratio ($\Delta u/\Delta_{yield}$)
Wall – 3-1	10780	31.34	1134.7	9620.5	6.69
Wall – 3-2	10785	30.86	1136.5	9768.6	6.74
Wall – 4-1	7760.0	38.10	771.33	6916.0	5.90
Wall – 4-2	8235.0	37.70	627.05	7340.4	4.54
Wall – 5-1	9505.0	30.97	1081.3	8613.9	7.83
Wall – 6-1	10025	31.26	1273.2	8882.3	8.62
Wall – 6-2	10915	31.76	1270.4	9830.3	7.26
Wall – 7-1	10005	31.33	1140.2	8887.1	8.37
Wall – 8-1	19375	41.13	1728.2	16972	4.80
Wall – 8-2	25145	39.54	1834.2	21911	4.52

5.0 DISCUSSION

5.1 Selection of Test Protocol

As mentioned in the literature review, several studies had found that the test protocol had insignificant effect on the behavior of nail or screw joints in light frame wood shearwalls where the sheathing consisted of OSB or plywood panels (Olivia (1990), Dolan (2003), Sedears et Al. (2008)). However, it is not widely known whether the test protocol has any effect on the joint behavior when GWB panel is used. In the current study, the monotonic protocol tests were used to determine the ultimate deflection of the specimens, which in turn was used to develop the reversed cyclic loading protocol. Having both curves (monotonic and the backbone from the cyclic loading) allowed for the comparison of the behavior at both the joint as well as the full scale levels. Figure 42 presents the comparison between two groups with identical construction details and with the testing protocol being the only variable, at both the joint level and the full scale level.

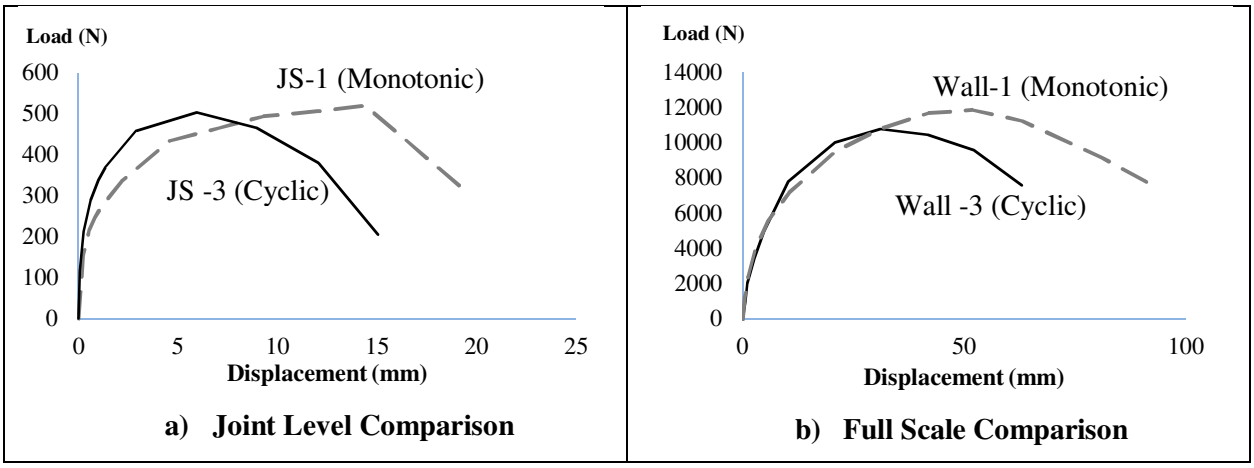

Figure 42: Displacement Protocol Type Comparison

For both the joint level and the full scale tests it can be observed that the displacement protocol has a significant effect on the load-displacement response of the specimen. The initial responses are relatively similar but once peak load is approached, the two responses behave differently. It is obvious from Figure 42 that using the cyclic protocol for both joint as well as full scale tests is more appropriate than using the monotonic test protocol.

5.2 Joint Level

The results from the EEEP analysis were evaluated and possible trends identified. This section describes the factors that affect the load-deflection response at the joint level, in order to develop an appropriate fastener slip model for GWB used in light frame wood construction.

5.2.1 Material Variability Comparison

Since data for connections including GWB was found to be very limited in the literature, it was decided to investigate the effect of the manufacturing process on the performance of the material. By investigating material from different manufacturers, the inherent variability that exists due to manufacturing processes is accounted for. Three GWB manufacturers, four GWB screws manufacturers and three GWB nail manufacturers were included in this study as part of the joint level tests.

In order to examine the screw manufacturers' variability, a total of 40 joint level tests were performed using light-weight type-X GWB and fastened with No.6 GWB screws, where only the screw manufacturer differs for each set of tests (JS-5, JS-6, JS-7 and JS-8). The average values and coefficient of variation for all forty tests combined were 514.2 N (COV: 6.38%) for capacity, 931.0 N/mm (COV: 33.0%) for initial stiffness and 17.18 (COV: 28.9%) for ductility ratio. Figure 43 compares the results obtained for the peak load (a), initial stiffness (b) and ductility ratio (c) for each GWB screw manufacturer.

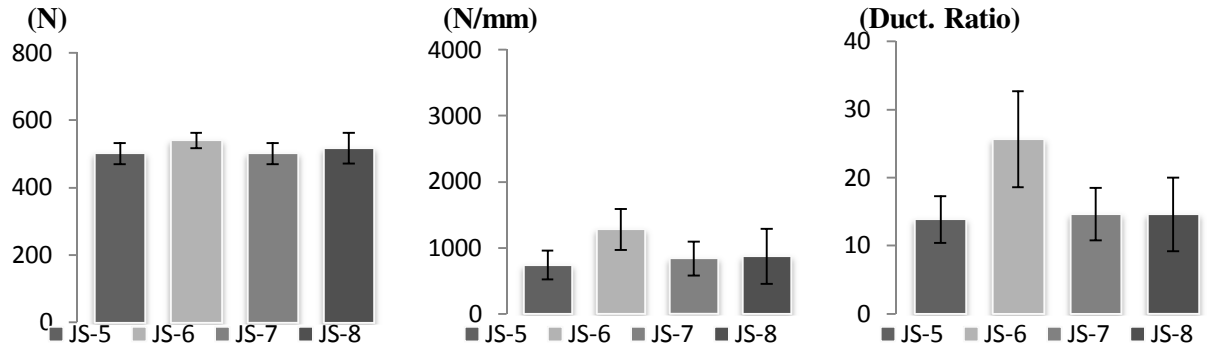

a) Peak Load b) **Initial Stiffness** **c) Ductility Ratio**

Figure 43: Parameter Comparisons of No.6 Screws with Different Manufacturers

Figure 43 shows that the results obtained for peak load are fairly consistent for each tested manufacturer when accounting for the variability within each group. In other words, it can be assumed that regardless of which type of available screw is used in construction, estimate of the capacity would be obtained with reasonable precision. With the exception of joint JS-6, which uses Manufacturer B, the results for stiffness

and ductility also seemed to be relatively similar between different manufacturers. The tests based on screws from manufacturer B showed a significantly stiffer behaviour and higher ductility ratios relative to other manufacturers. The timber design standard (CSA O86) does not stipulate any design requirements on the stiffness and ductility of connections; however, such parameters are extremely important when stiffness, deflection and ductility of shearwalls are to be assessed. Stiffness and ductility is notoriously more difficult to estimate than peak load. Stiffness is highly influenced by the specimen construction, initial friction, etc. and the determination of ductility is complicated by the definition of the yield point. Every effort has been made to construct the test specimens in a similar manner, and the yield point was determined using the same procedure (EEEP curve). It can therefore be assumed that what is presented in Figure 43 is a reasonable depiction of the true variability that may be found in the joints of similar detailing but using different manufacturers.

Variability due to different nail manufacturer was also investigated by testing joints constructed with same size nails produced by three different manufacturers. Each joint was repeated 10 times to account for the variability of constructing the same joint. All other parameters remained constant. 12.5 gauge GWB nails were used together with lumber of similar density range and using light weight type-X GWB panels (JS-9, JS-10 and JS-11). The average values and coefficient of variation for all joints was found to be 450.8 N (COV: 7.07 %) for capacity, 506.6 N/mm (COV: 76.1%) for initial stiffness and 9.95 (COV: 52.9%) for ductility ratio. Figure 44 compares the results obtained for the peak load (a), initial stiffness (b) and ductility ratio (c) for each GWB nail manufacturer.

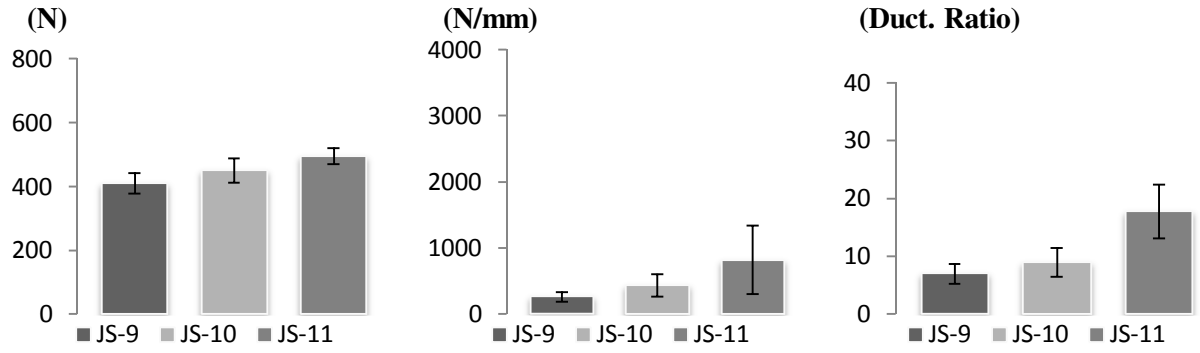

a) Peak Load **b) Initial Stiffness** **c) Ductility Ratio**

Figure 44: EEEP Parameter Comparisons of 12.5 gauge Nails with Different Manufacturers

Similar to the case with GWB screws, the capacity of the joints was found to be similar for all tested GWB

nail manufacturers. Significant differences were found between manufacturers when considering initial stiffness and ductility ratios. Differences could be attributed, as mentioned earlier, to the stiffness being influenced by the construction details and the ductility being dependent on the yield point.

Finally, the variability in GWB panel manufacturer was examined and a total of 30 joint level tests were performed using regular-weight type-X GWB and fastened with No.6 GWB screws and using lumber in the same density range (JS-12, JS-13 and JS-30). The only varying construction parameter was the GWB manufacturer. The average values and coefficient of variation for the joints, without considering the change in manufacturer is 656.5 N (COV: 19%) for the capacity, 1732.1 N/mm (COV: 35.9%) for the initial stiffness and 24.74 (COV: 27.9%) for the ductility ratio. Figure 45 compares the results obtained for the peak load (a), initial stiffness (b) and ductility ratio (c) for each GWB manufacturer.

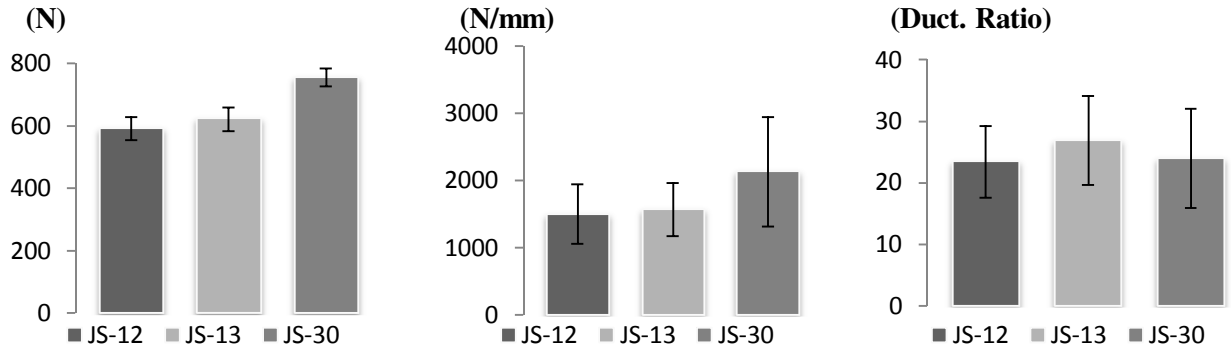

a) Peak Load **b) Initial Stiffness** **c) Ductility Ratio**

Figure 45: Parameter Comparisons of Type-X GWB with Different Manufacturers

Test joints using manufacturer A (JS-30) exhibited slightly higher peak load than the other two manufacturers. However, variability within manufacturers seems to be relatively low for peak load. Some differences can be found between manufacturers with regard to initial stiffness and ductility ratios; however the difference seems to fall in the variability range found within each manufacturer.

Based on the results, it can be concluded that the variability found between manufacturers is relatively low when considering the peak load. As expected, the variability within as well as between manufactures was found to be more pronounced when it comes to stiffness and ductility. The variability in results is taken into consideration but ultimately the components with the same characteristics, even with different manufacturers, are considered as a single group to account for this effect during the development of a joint level fastener slip model.

5.2.2 Lumber Density Comparison

As mentioned in the Experimental Result section, the observed failure in the joint level tests was dominated by lumber crushing, GWB crushing and fastener bending. The density and embedment strength of lumber was found to be significantly higher than GWB. This was corroborated by embedment strength tests (presented in Chapter 4) as well as observed sizes of gaps in the material after the test. Figure 46 compares the peak load for joint level tests where on lumber densities is varied. The figure defines two groups for the lumber density. The "high" and "low" density values refer to ranges of relative density values between 0.39-0.45 and 0.32-0.35, respectively.

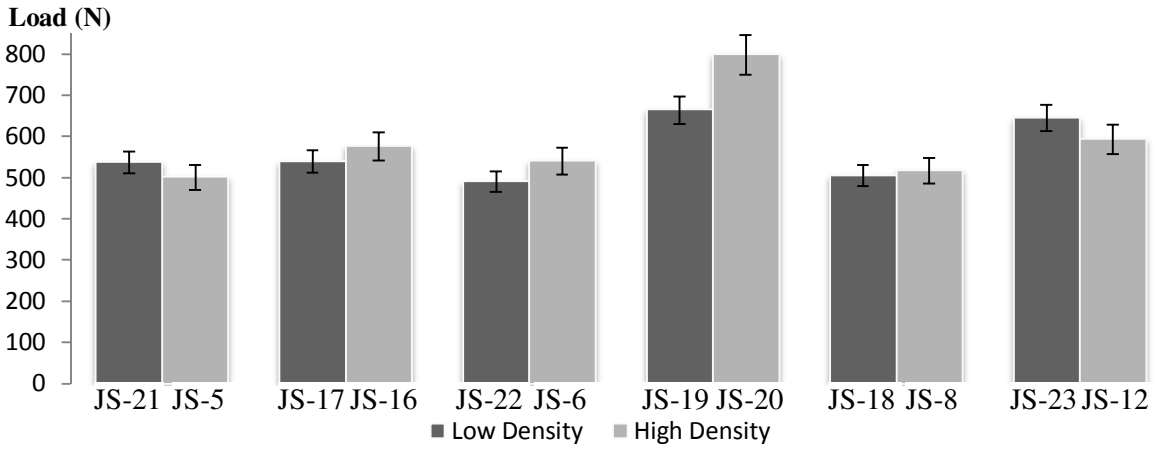

Figure 46: Peak Load Comparison with Different Lumber Densities

Two out of the six comparisons cases appears to have a lower peak load when using higher lumber density. Most of the differences in values can be attributed variability observed in the materials used, and hence no conclusion can be drawn on whether denser wood yields higher joint peak load. The only groups that show a significant increase in joint capacity as function of higher density is the JS-19 to JS-20 comparison, in which No.10 GWB screws are used. This result was expected because the No.10 screw has larger diameter than the other screws used and would therefore not bend as easily. This would cause more pronounced lumber crushing, thereby emphasizing the effect of lumber density. The fact that no conclusive statement could be made about the effect of density does not mean that density does not play an important role, it simply implies that the lumber density was not engaged in these tests primarily due to the use of GWB where the majority of the deformation took place. It can therefore be suggested that within the parameters and ranges used in this study, the effect of lumber density can be ignored when considering peak load.

Figure 47 compares the initial stiffness of tests completed on specimens with different lumber densities.

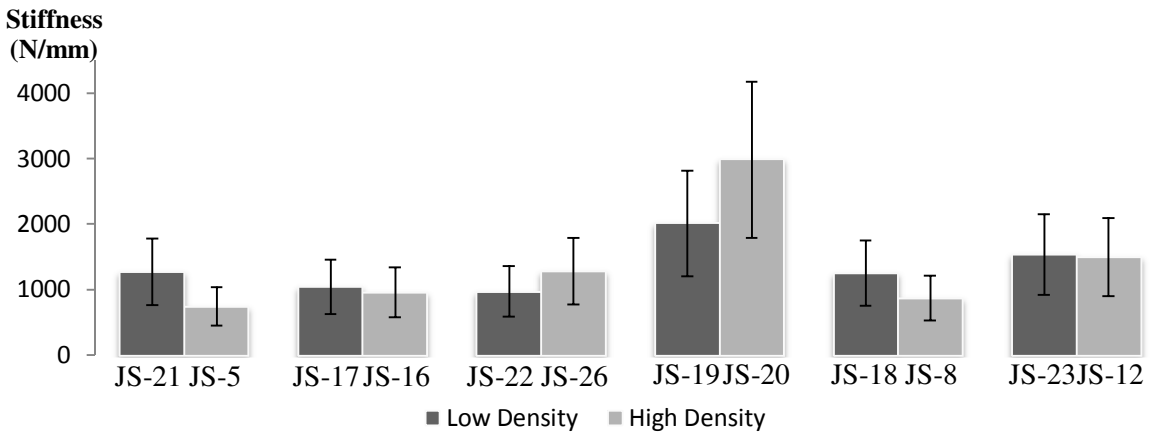

Figure 47: Initial Stiffness Comparison with Different Lumber Densities

Again here, no clear trend can be observed, and the values, when including the variability within each group, seem relatively close for the two densities considered. Half of the comparison groups have a larger initial stiffness for low density lumber, while the opposite is true for the other half. It can be noted that the coefficient of variation is large within each group which makes it impossible to separate many of the comparison groups.

Table 16 compares the ductility ratio for joint tests with different lumber densities, while all other parameters remained constant. The values presented in Table 16 represent the ratio of the ductility obtained from the test group with the high lumber density relative to those obtained from test group with the low density. A value greater than 1.0 would therefore indicate that the higher lumber density test group has a greater ductility ratio.

Table 16: Ductility Ratio Comparison with Different Lumber Densities

JS-21 vs JS-5	JS-17 vs JS-16	JS-22 vs JS-26	JS-19 vs JS-20	JS-18 vs JS-8	JS-23 vs JS-12
0.57	0.74	1.18	0.67	0.65	0.94

The majority of the test results (5 out of 6) show higher ductility ratio for tests completed with low density lumber. One possible explanation could be that low density allows for more displacement and crushing in the lumber. However, again here, there does not seem to be any conclusive tendency on the effect of density on the ductility of the joint.

The above analysis shows that lumber density does not have an impact on the joint level response and therefore density will not be considered as a parameter in the fastener slip model described later in this chapter.

5.2.3 GWB Type Comparison

The gypsum wallboard crushing contributed significantly to the overall deflection of the joint level. Variation in GWB panel weight and type was therefore investigated. Joint configurations JS-6, JS-30 and JS-26 have consistent parameters except for their GWB densities, where the JS-6 group consisted of light-weight type-X GWB, the JS-30 group had regular-weight type-X GWB and the JS-26 group was constructed using regular GWB. It is important to note that the regular GWB has a ½" (12.7 mm) thickness, while both type-X GWB have 5/8" (15.9 mm) thickness. The reason for not testing 5/8" regular GWB was that this thickness was not available in the market. Similarly, ½" type-X GWB was also not found. This obviously puts limitations on what can be concluded in this comparison. For the purpose of this evaluation, the slight difference in panel thickness (3.2 mm) was ignored. The thickness of the panel is, of course, taken into account when the design of such a joint is performed. The results obtained for the peak load (a), initial stiffness (b) and ductility ratio (c) for each GWB type, using manufacturer A are shown in Figure 48 .

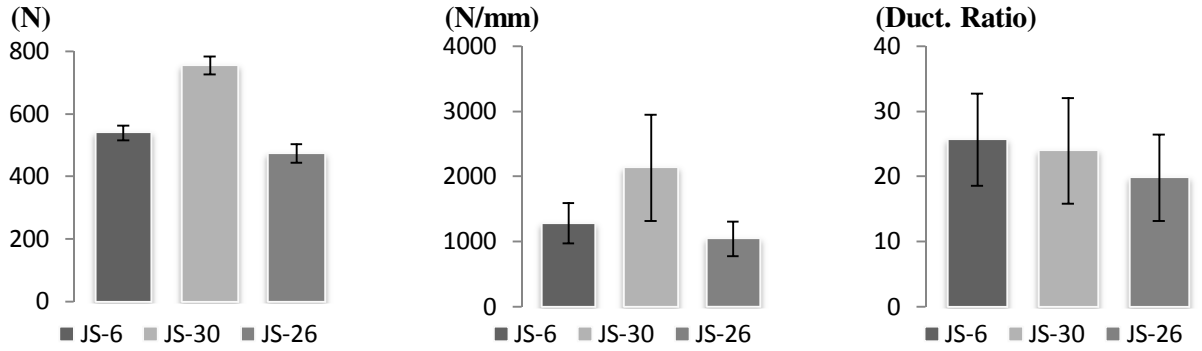

a) Peak Load **b) Initial Stiffness** **c) Ductility Ratio**

Figure 48: Parameter Comparisons of Different GWB Types

Figure 48 clearly shows that joints using lightweight panel (JS-6) have reduced peak load and initial stiffness when compared with regular-weight type-X GWB (JS-30). The ductility is observed to be similar for both joint combinations, with a slight tendency to achieve higher ductility when using the lighter weight GWB material. The reduced capacity of the joint can be attributed to the lower embedment strength of the GWB panel with light weight and lower density. This observation was corroborated by the embedment strength tests as described in Chapter 4.

Comparing the results of the light-weight GWB and the regular GWB of similar density, it can be seen that despite the slight difference in panel thickness, the capacity, initial stiffness and ductility (to a slightly lesser degree) are within the same range, especially when considering the variability within each material.

5.2.4 Fastener Type Comparison

The fasteners used during this study are GWB nail and screws. The diameter of the 12.5 gauge nail and the No.6 screw are similar; but since they are not exactly the same, the comparisons made must be done while keeping this statement in mind. The root diameter of the No.6 GWB screw is 2.7 mm and the diameter with the threads are 3.8 mm, while the diameter of the GWB nail is 2.7 mm. Figure 49 compares the peak load obtained for the joints fastened with screws and the joints fastened with nails. The average peak load values obtained for the screw and nail joints are 514.2 N and 450.8 N, respectively.

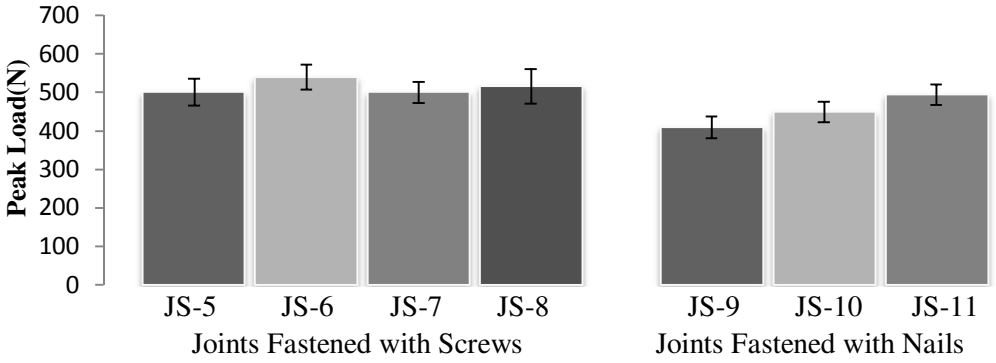

Figure 49: Peak Load Comparison for Screws and Nails

Figure 49 shows that screws exhibited a slightly higher joint capacity compared to the nails, which can be attributed to the slight difference in fastener diameter and possibly the type of metal composition of which they consist.

Figure 50 compares the initial stiffness obtained for the joints fastened with screws and the joints fastened with nails.

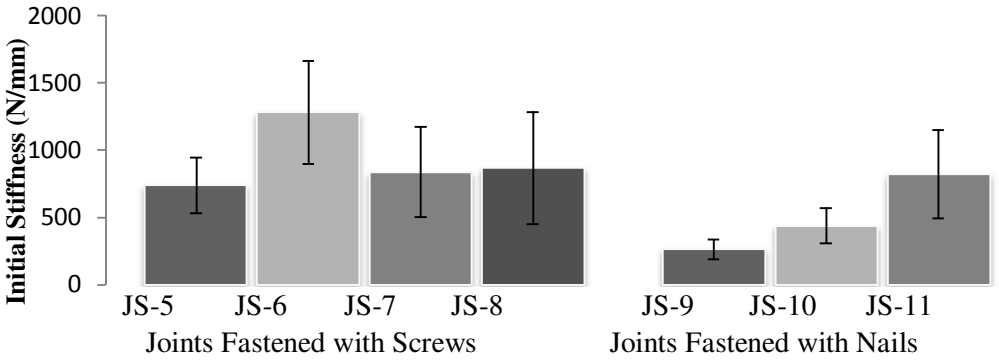

Figure 50: Initial Stiffness Comparison for Screws and Nails

The joint level initial stiffness for all tested screws was higher than those obtained from nails. Some of the increase in stiffness stems from the slight increase in diameter but also comes from the manufacturer type. The threads of the screws increase the withdrawal resistance of the fastener, which in turn would increase the initial stiffness.

Figure 51 compares the ductility obtained for the joints fastened with screws and the joints fastened with nails.

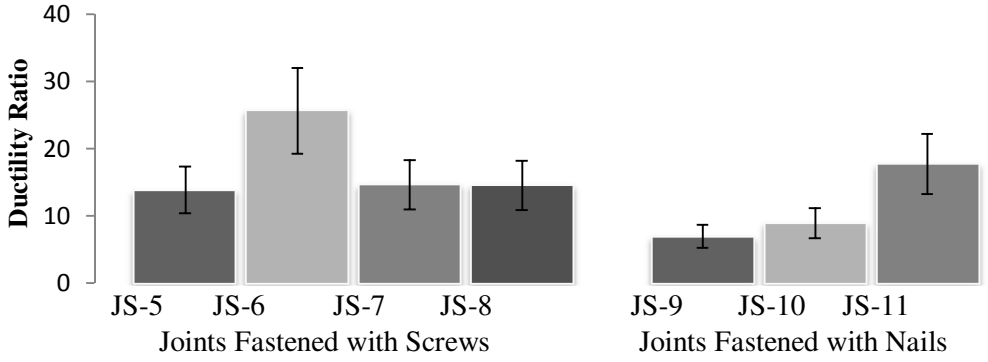

Figure 51: Ductility Comparison for Screws and Nails

The average ductility ratio of joints fastened with typical screws available in light frame wood construction seems higher than those obtained from joints fastened with nails. This result was not expected since nails are typically considered to be more ductile compared to the brittle behavior of a typical screw. This was also corroborated by the results obtained from the nail and screw bending tests. It is important to note that the comparison is made using the ductility ratio, which is defined as the ultimate displacement divided by the yield displacement. The ductility ratio is a dimensionless ratio that is suitable for comparing two

products with same or similar characteristics (initial stiffness, yield point, ultimate capacity etc.), and it may therefore be misleading to draw general conclusions regarding the behavior of two systems (screw vs. nail joints) due to the significant difference in behavior observed between the two joints. The brittle behavior of the screws was clearly shown when component testing was performed to obtain the yield moment of the fasteners. None of the joint tests observed fastener bending near 90 degrees, and due to the additional stiffness and early onset of yield in the fastener as well as the GWB crushing observed, more ductility was found for the screw connectors. Similar joints used in a shearwall are expected to have even less slip than those tested in the joint level tests in this study. Therefore, within the slip range observed and expected, the screws' ductility seems to be consistent and slightly higher than those found in nails. The difference in the behaviour of GWB nails and screws was significant enough and meant that these connectors could not be treated together for the purpose of development of the slip models.

5.2.5 Fastener Size Comparison

The fastener size was varied only for the GWB screws since they are the most available GWB fastener type and the most commonly used during construction. The most common screw size is the No.6 screw, which is available with every manufacturer used during this study. The No.8 and No.10 screws are not common and therefore are only tested for a single manufacturer. For the purpose of this study, the comparison is made between No.6 and No.8 screws obtained from manufacturer A, as well as No.6 and No.10 screws obtained from manufacturer B. Figure 52 compares the results obtained for the peak load (a), initial stiffness (b) and ductility ratio (c) for different fastener diameter sizes.

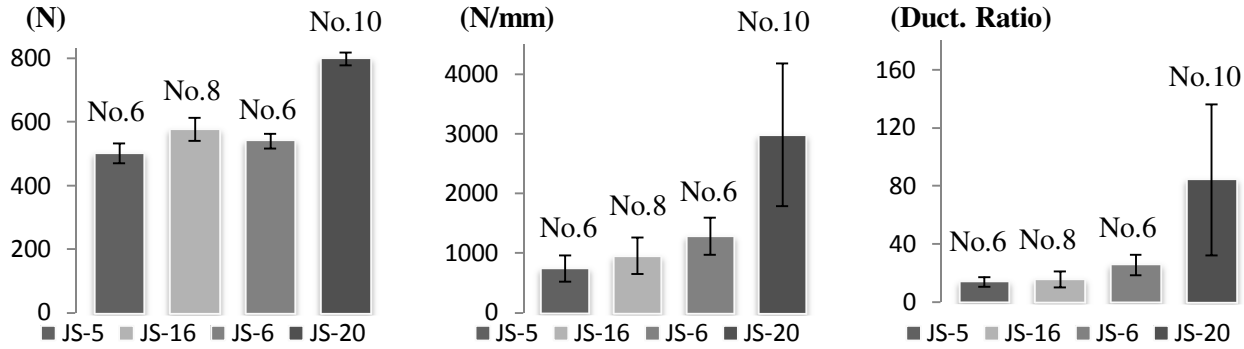

a) **Peak Load** b) **Initial Stiffness** c) **Ductility Ratio**

Figure 52: Parameter Comparison for Different Screw Sizes

The results show that the peak load, initial stiffness and ductility ratios are increased with increase in screw diameter. The increase in capacity and initial stiffness is expected due to the larger screw diameter,

however, the increase in ductility for the larger diameter screw of the No.10 screw is substantial. This could possibly be explained, as mentioned earlier, by the engagement of more wood crushing. Whether this observation can be extended to full scale shearwalls with GWB needs more investigation due to the end/edge distance limitation in the full scale tests relative to the joint level tests. This will be discussed later in this Chapter when the full scale results are examined. Quantifiable trends relating to screw diameter will be determined at the load-deflection model development stage, in order to use the fastener diameter as an input parameter.

5.2.6 Statistical Analysis

The EEEP analysis parameters are obtained and evaluated for each set of tests in the previous section. Some conclusions were drawn to determine which construction characteristics will affect the load-deflection response sufficiently enough to consider them as same or different groups. The lumber density variation was not found to be significant enough since the analysis determined that it does not affect the joint level load-deflection response. The fastener type, diameter and GWB type will be used during the curve fitting analysis to determine trends which will be then used as part of the fastener slip equations. Table 17 presents the groups used in the curve fitting analysis. The first column of the table is the group number which will be used as a reference throughout the section. The following two columns list the construction characteristics and the final column lists the joint level test groups that will be considered as a single group.

Table 17: Parameter Influence Groups

Group	GWB Type	Fastener Diameter	JS Group
1	Lower Density – X (5/8")	No. 6	JS-5, JS-6, JS-7, JS-8, JS-18, JS-21, JS-22
2	Higher Density- X (5/8")	No. 6	JS-12, JS-13 JS-23, JS-24, JS-30
3	Lower Density – X (5/8")	No. 8	JS-16, JS-17
4	Lower Density – X (5/8")	No. 10	JS-19, JS-20
5	Regular GWB (1/2")	No. 6	JS-26, JS-27, JS-28
6	Lower Density – X (5/8")	Nails – 12.5 gauge	JS-9, JS-10, JS-11

The groups chosen were subjected to a t-Test analysis. The test was done to determine if there is sufficient difference between two data sets in order to consider them as part of same or two separate groups. This test is based on the mean value and variance of the two data sets. The confidence level for this analysis is 95%,

$$if \quad -t_{crit} \leq t_{stat} \leq t_{crit} \quad the\ null\ hypothesis\ is\ rejected$$

The data that is formatted in bold in Table 18, indicates the groups that are similar enough to consider as a single group for a given parameter. The groups referred to in the first column are defined in Table 17.

Table 18: T-Test Analysis Results

Group Comparison	Initial Stiffness		Ductility		Peak Load	
	tStat	tCritical	tStat	tCritical	tStat	tCritical
1-vs-2	6.66	1.66	3.66	1.66	14.6	1.66
1-vs-3	**0.28**	**1.66**	**0.61**	**1.66**	4.96	1.66
1-vs-4	7.40	1.66	10.68	1.66	18.2	1.66
1-vs-5	4.84	1.66	3.29	1.66	**0.24**	**1.66**
2-vs-5	**0.89**	**1.66**	**0.48**	**1.66**	10.3	1.66
1-vs-6	5.79	1.66	4.67	1.66	6.96	1.66

The t-test analysis further supports the conclusions made earlier in this section based on the observations of the EEEP analysis. The comparison of Group 1 to Group 2 examines the effect of GWB density and the t-test shows that there is a statistical difference between the two groups when considering the initial stiffness, ductility and peak load. The comparison of Group 1 to Group 3 and Group 1 to Group 4 examines the effect of fastener diameter where the only parameter with a clear difference is the peak load. The GWB types are compared in the Group 1 to Group 5 and the Group 2 to Group 5. Both Group 1 and Group 2 are compared to Group 5 since the regular GWB does not have the same density ranges as the type-X GWB; therefore a comparison to both groups is required. From the analysis, it is seen that the regular GWB has a similar peak load to the lightweight type-X GWB, while sharing a similar initial stiffness and ductility with the normal weight type-X GWB. By evaluating Group 1 to Group 6, the fastener types are compared, and the results clearly show that the differences in initial stiffness, ductility and peak load are substantial enough to consider them as different groups.

The established groups all have at least one EEEP parameters which is statistically different enough to be considered as a separate group. When establishing trends during the development of the fastener slip equation, the trends will be based on parameters which are determined to be statistically different.

5.2.7 Curve Fitting Analysis

The curve fitting analysis is completed for each set of joint tests. The developed models predict values up to maximum load; therefore will not address the prediction of the ductility of the joint. The least squared method was used to approximate the load-slip behavior of the fastener joints. The least squared method reduces the error of the approximate curve by reducing the sum of the difference of the squared approximation and the data points. There are three empirical model types that are examined as a potential

fastener slip model of the GWB sheathed joint. All three models are viable options and have been proven to be effective for predicting the load-deflection response of a laterally loaded lumber joint. These models are the power model (CSA O86, 2010; APA, 2005; William and McCutcheon, 1985), the exponential model (Foschi, 1974) and the asymptotic model (McLain, 1975; Wang, 2009).

The equations are presented below:

Power Model: $x = A\left(\frac{y}{1000}\right)^{B}$ (5.1)

Exponential Model: $y = [p_1 - k_1 x]\left[1 - e^{(-k_0 x/p_1)}\right]$ (5.2)

Asymptotic Model: $y = C - DE^{x}\ or\ x = (\log\left(\frac{C-y}{D}\right))/\log(E)$ (5.3)

Where:

x is the fastener slip (mm)

y is the applied load on an individual fastener (N)

A and B are constants used for power model curve fitting

C, D and E are constants used for asymptotic model curve fitting

k_0 is the initial tangent stiffness

k_1 is the final tangent stiffness

p_1 is the intercept of k_1 on the load axis

Figure 53 illustrates the parameters used for the exponential model.

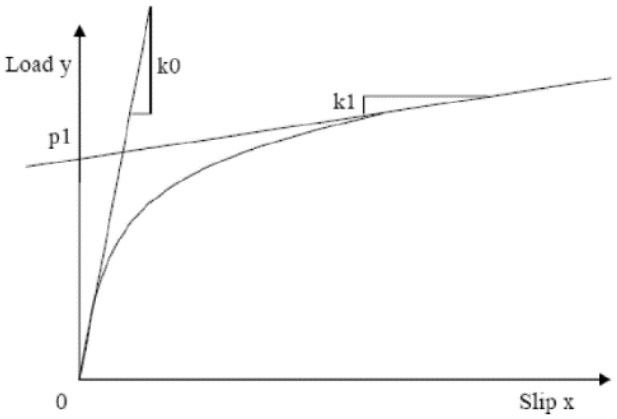

Figure 53: Exponential Model (Foschi 1974)

In the following section the parameters are obtained for each set of test configuration. Table 19 to Table 24 present the curve fitting parameter results for each set of joint level tests. The results are separated by the groups that were defined during the t-test analysis, which are presented in Table 17.

Table 19: Group 1 Curve Fitting Parameters

JS	Power Model			Exponential Model				Asymptotic Model			
Group	**A**	**B**	**R^2**	**K0 (N/mm)**	**K1(N/mm)**	**P1(N)**	**R^2**	**C**	**D**	**E**	**R^2**
JS-5	81.53	4.2	0.97	941.48	-36.78	335.99	0.99	483.13	454.77	0.28	0.97
JS-6	132.27	5.4	0.98	1932.30	-39.41	361.18	0.99	493.78	458.55	0.12	0.94
JS-7	65.24	3.9	0.99	1159.00	-46.45	301.48	0.99	477.24	441.97	0.27	0.96
JS-8	56.30	3.9	0.99	1177.29	-48.12	314.28	0.99	494.34	458.31	0.27	0.97
JS-18	217.24	5.8	0.96	2748.07	-68.40	480.99	0.98	479.02	445.52	0.15	0.97
JS-21	92.06	4.9	0.99	1547.65	-37.07	354.20	0.99	501.17	460.09	0.17	0.95
JS-22	97.44	4.3	0.99	1478.57	-45.00	296.30	0.99	457.53	418.06	0.22	0.96

Table 20: Group 2 Curve Fitting Parameters

JS	Power Model			Exponential Model				Asymptotic Model			
Group	**A**	**B**	**R^2**	**K0 (N/mm)**	**K1(N/mm)**	**P1(N)**	**R^2**	**C**	**D**	**E**	**R^2**
JS-12	90.79	5.9	0.96	1771.33	-42.39	419.46	0.99	561.03	525.33	0.14	0.97
JS-13	58.54	5.4	0.99	2552.26	-48.01	415.85	0.99	562.77	526.87	0.09	0.94
JS-23	31.24	4.6	0.99	3767.65	-16.87	604.20	0.97	606.73	550.37	0.19	0.95
JS-24	22.21	4.0	0.99	2056.06	-66.75	389.58	0.99	613.21	562.05	0.19	0.95
JS-30	17.45	5.1	0.98	2748.07	-68.40	480.99	0.98	707.43	645.30	0.14	0.96

Table 21: Group 3 Curve Fitting Parameters

JS	Power Model			Exponential Model				Asymptotic Model			
Group	A	B	R^2	K0 (N/mm)	K1(N/mm)	P1(N)	R^2	C	D	E	R^2
JS-16	67.50	5.1	0.96	1771.33	-42.39	419.46	0.99	555.00	532.89	0.20	0.99
JS-17	128.74	5.4	0.96	2552.26	-48.01	415.85	0.99	513.04	481.87	0.20	0.97

Table 22: Group 4 Curve Fitting Parameters

JS	Power Model			Exponential Model				Asymptotic Model			
Group	A	B	R^2	K0 (N/mm)	K1(N/mm)	P1(N)	R^2	C	D	E	R^2
JS-19	4846.3	15	0.95	1732.86	-20.69	534.06	0.98	622.16	598.48	0.06	0.98
JS-20	1063.6	17	0.90	1242.26	-34.45	382.93	0.99	700.71	645.62	0.04	0.95

Table 23: Group 5 Curve Fitting Parameters

JS	Power Model			Exponential Model				Asymptotic Model			
Group	A	B	R^2	K0 (N/mm)	K1(N/mm)	P1(N)	R^2	C	D	E	R^2
JS-26	231.68	5.5	0.91	2202.18	-40.89	357.80	0.98	460.94	427.18	0.17	0.97
JS-27	247.75	6.5	0.94	1256.11	-31.49	347.25	0.97	504.01	457.37	0.12	0.95
JS-28	803.78	8.1	0.90	2196.05	-41.32	366.78	0.97	499.31	451.30	0.12	0.95

Table 24: Group 6 Curve Fitting Parameters

JS	Power Model			Exponential Model				Asymptotic Model			
Group	A	B	R^2	K0 (N/mm)	K1(N/mm)	P1(N)	R^2	C	D	E	R^2
JS-9	53.59	2.7	0.98	352.96	-22.58	297.41	0.99	412.58	400.61	0.48	0.99
JS-10	44.67	2.9	0.98	550.24	-40.55	269.45	0.99	451.74	425.11	0.44	0.98
JS-11	58.52	3.6	0.98	1035.96	-50.11	273.53	0.98	470.18	431.59	0.32	0.96

The experimental data is compared to the empirical models and the R^2 values are obtained. From the values indicated in the tables, it is very clear that all three curve fitting options are suitable to represent the load-deflection data of the joint specimens sheathed with gypsum wallboard. Figure 54 compare the different empirical model to typical test data.

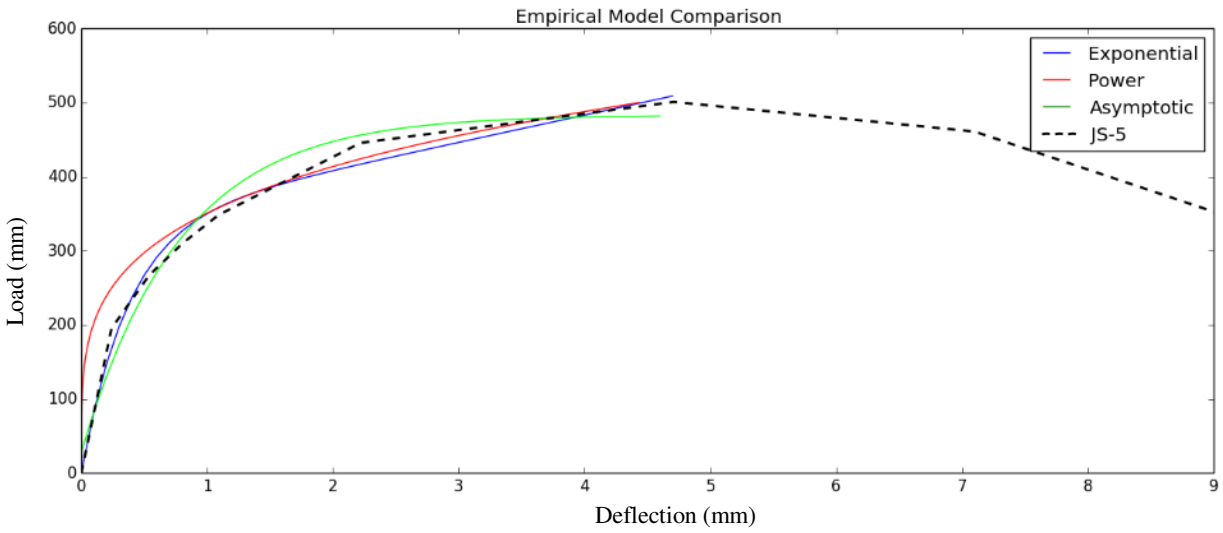

Figure 54: Empirical Model Comparison

The figure illustrates the potential applicability of all three model types to be used as fastener slip models for GWB sheathed joints. It can be seen that the initial stiffness of the load-deflection curve is overestimated by the power model, but is accurate past the 0.8 mm mark. The other two models are accurate throughout. It is important to note the scale of the graph, since a small difference in this case does not greatly affect the response. This is made evident by the accuracy of all three models, displayed in this section.

5.2.8 Development of Fastener Slip Equations

The following section quantifies the trends by plotting the construction characteristic inputs against the values obtained for the model parameters during the curve fitting analysis to develop a model to predict the load-deflection response of the fastener joint. It is noteworthy to reiterate that the construction characteristics that cause variations in the load-deflection response were the fastener diameter, the gypsum wallboard density and the fastener type. The equations developed are limited to the material characteristics tested.

The variables used in the models are explained below:

e_n: Fastener Deformation (mm)

γ_{GWB}: Type-X Gypsum wallboard weight per area (kg/m^2)

d_s: Diameter of screw (mm)

v_f: Load per fastener (N)

5.2.8.1 Power Model Equation

The power model equation (5.1) has two model parameter constants. The parameter "A" constant modifies the amplitude of the curve while the parameter "B" constant, which is the exponent, modifies the shape of the curve. It was determined that the shape of the curve remains constant for all GWB sheathed joints fastened with screws and differs only for those fastened with nails. A single value is chosen to be used as the "B" parameter for all joints fastened with screws and a second is chosen for the joints fastened with nails. The method used to choose the optimal parameter B was to separate the tests into the previously defined groups, shown in Table 17, and determine the average summation of error obtained from the least squared error by optimizing for the parameter A. The average error was then obtained for each group parameter "B" and was varied until a minimum error was found. The value of parameter "B" was found to be 5.5 for screws and 3.0 for nails. Parameter "A" is the only one the will be affected by the construction characteristic inputs. The trends are plotted and presented in Appendix B.

The screw diameter and GWB density quantified trends are obtained from these figures and are presented as the following equations. Equations 5.4, 5.5 and 5.6 express Parameter "A" as a function of screw diameter, GWB density for joints fastened with screws, and GWB density for joints fastened with nails, respectively.

$$Parameter\ A = (845.85 - 171.71 d_s\ ) \tag{5.4}$$

$$Parameter\ A = (868.73 - 73.44 \gamma_{GWB}) \tag{5.5}$$

$$Parameter\ A_{NAILS} = (145.28 - 19.86 \gamma_{GWB}) \tag{5.6}$$

The power empirical model equations for joints fastened with screws and nails are developed using the established trends and are presented below.

Screw Joints:

$$e_n = (4.92 - 0.42\gamma_{GWB})(4.926 - d_s)\left(0.00255 v_f\right)^{5.5} \tag{5.7}$$

Nail Joints:

$$e_n = (2.64 - 0.18\gamma_{GWB})\left(0.00374 v_f\right)^{3} \tag{5.8}$$

5.2.8.2 Exponential Model Equation

The exponential model has three varying parameters, for which the trends are presented in Appendix B. The screw diameter and GWB density quantified trends are obtained from these figures and are presented as the following equations. Equations 5.9 and 5.10 represent parameter "k0" and "k1", respectively, as function of GWB density for joints fastened with screws. Equation 5.11 expresses Parameter "P1" as function of screw diameter. Equation 5.12 and 5.13 express Parameter "P1" as a function of GWB density for joints fastened with screws and nails, respectively.

$$k_0 = 580.06\gamma_{GWB} - 3798.3 \tag{5.9}$$

$$k_1 = 49.55 - 9.77\gamma_{GWB} \tag{5.10}$$

$$P_1 = 218.75d_s - 499.03 \tag{5.11}$$

$$P_1 = 51.8\gamma_{GWB} - 144.82 \tag{5.12}$$

$$P_{1NAILS} = 42.66\gamma_{GWB} - 111.61 \tag{5.13}$$

The exponential empirical model equations for joints fastened with screws and nails are presented below.

$$v_f = [p_1 - k_1 e_n]\left[1 - e^{(-k_0 e_n / p_1)}\right] \tag{5.14}$$

Where,

$$k_0 = 580.06\gamma_{GWB} - 3798.3\ (Screw\ Joints) \tag{5.15}$$

$$k_1 = 49.55 - 9.77\gamma_{GWB}\ (Screw\ Joints) \tag{5.16}$$

$$P_1 = (0.154\gamma_{GWB} - 0.43)(218.75d_s - 499.03)\ (Screw\ Joints) \tag{5.17}$$

$$k_0 = 810.87\ (Nail\ Joints) \tag{5.18}$$

$$k_1 = -36.70\ (Nail\ Joints) \tag{5.19}$$

$$P_1 = (42.66\gamma_{GWB} - 111.61)\ (Nail\ Joints) \tag{5.20}$$

5.2.8.3 Asymptotic Model Equation

The asymptotic model has three varying parameters, for which the trends are obtained and presented in Appendix B. The screw diameter and GWB density quantified trends are obtained from these figures and

are presented as the following equations. Equation 5.21 and 5.22 express parameter "C" as function of screw diameter and GWB density for joints fastened with screws, respectively. Equation 5.23 is the parameter "D" vs the screw diameter, equation 5.24 is the Parameter "D" vs the GWB density for joints fastened with screws, equation 5.25 is the Parameter "C" vs the GWB density for joints fastened with nails and equation 5.26 is the Parameter "D" vs the GWB density for joints fastened with nails.

$$C = 183.98d_s - 218.85 \tag{5.21}$$

$$C = 76.72\gamma_{GWB} - 228.68 \tag{5.22}$$

$$D = 181.78d_s - 242.37 \tag{5.23}$$

$$D = 67.26\gamma_{GWB} - 172.83 \tag{5.24}$$

$$C_{NAILS} = 37.21\gamma_{GWB} + 105.89 \tag{5.25}$$

$$D_{NAILS} = 42.94\gamma_{GWB} + 27.12 \tag{5.26}$$

The asymptotic empirical model equations for joints fastened with screws and nails are presented below.

$$e_n = (\log\left(\frac{C - y}{D}\right))/\log(E) \tag{5.27}$$

Where,

$$C = (0.158\gamma_{GWB} - 0.468)(183.98d_s - 218.85)\ (Screw\ Joints) \tag{5.28}$$

$$D = (0.149\gamma_{GWB} - 0.382)(181.78d_s - 242.37)\ (Screw\ Joints) \tag{5.29}$$

$$E = 0.20\ \ (No.6\ Screws), \mathrm{E} = 0.20\ (\mathrm{No.8\ Screws}), \mathrm{E} = 0.05\ (\mathrm{No.10\ Screws}) \tag{5.30}$$

$$C = (37.21\gamma_{GWB} + 105.89)\ (Nail\ Joints) \tag{5.31}$$

$$D = (42.94\gamma_{GWB} + 27.12)\ (Nail\ Joints) \tag{5.32}$$

$$E = 0.41\ (Nail\ Joints) \tag{5.33}$$

5.2.8.4 Model Accuracy Comparison

The joint level displacement for each of the tested joint configurations is evaluated using the previously defined equations. The predicted deflection data is compared to the test data for each joint level group and

is presented in Figure 55, Figure 56 and Figure 57 for the power, exponential and asymptotic models, respectively. The diagonal line represents the perfect prediction line.

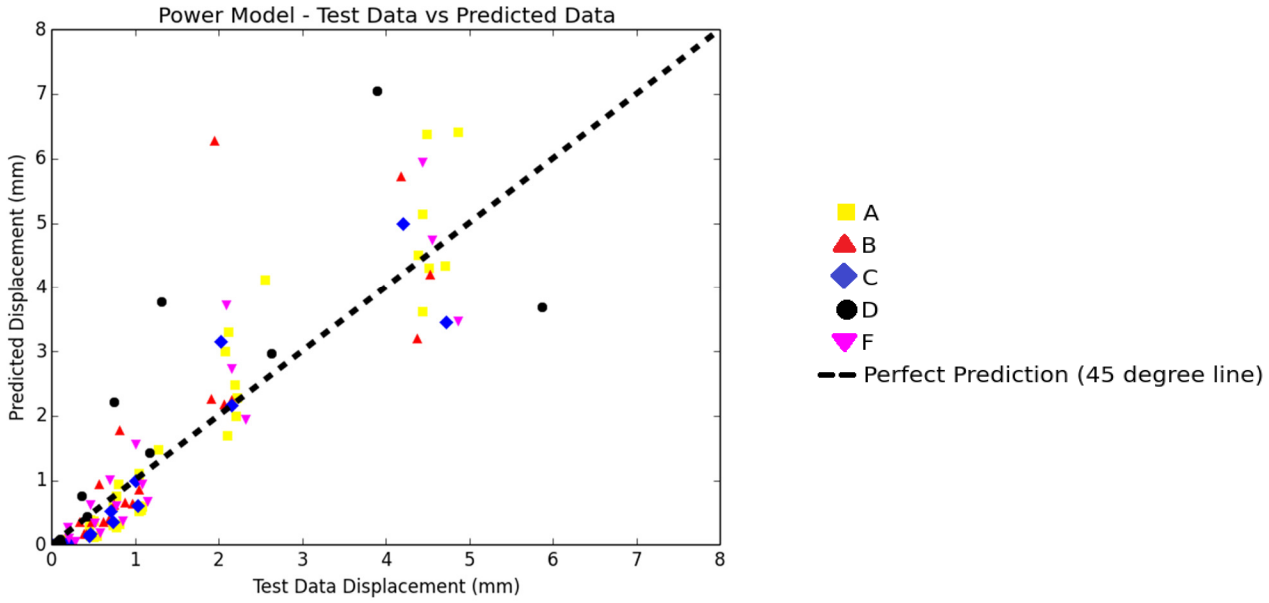

Figure 55: Power Model - Test Data vs Predicted Data

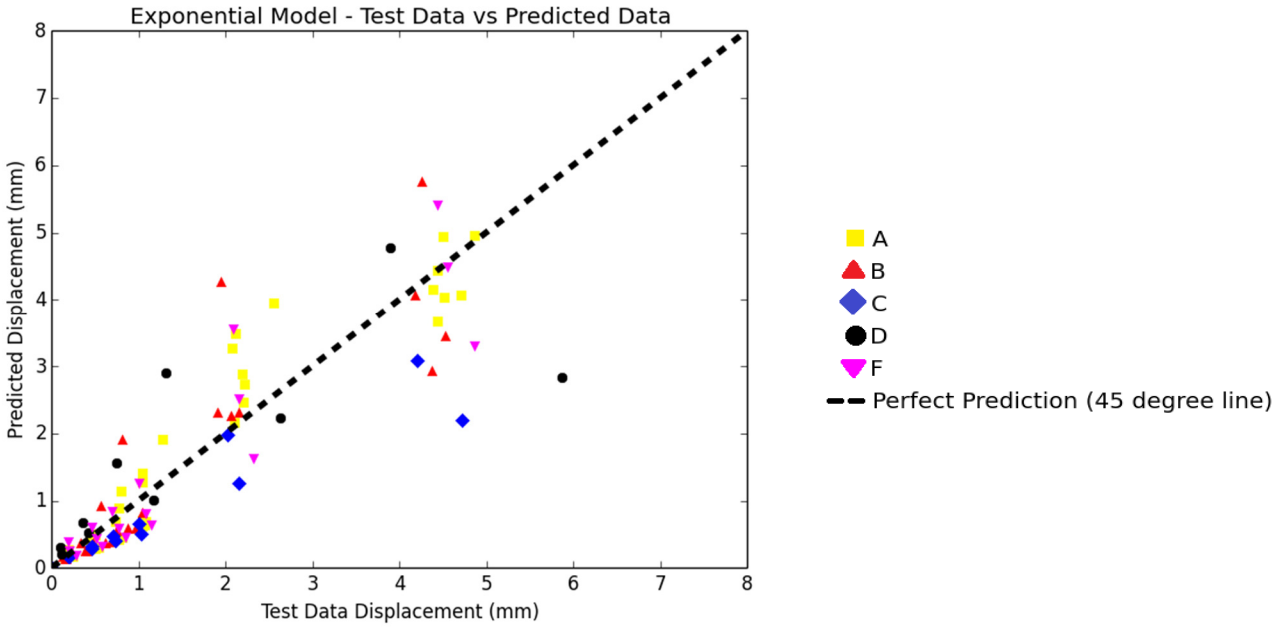

Figure 56: Exponential Model - Test Data vs Predicted Data

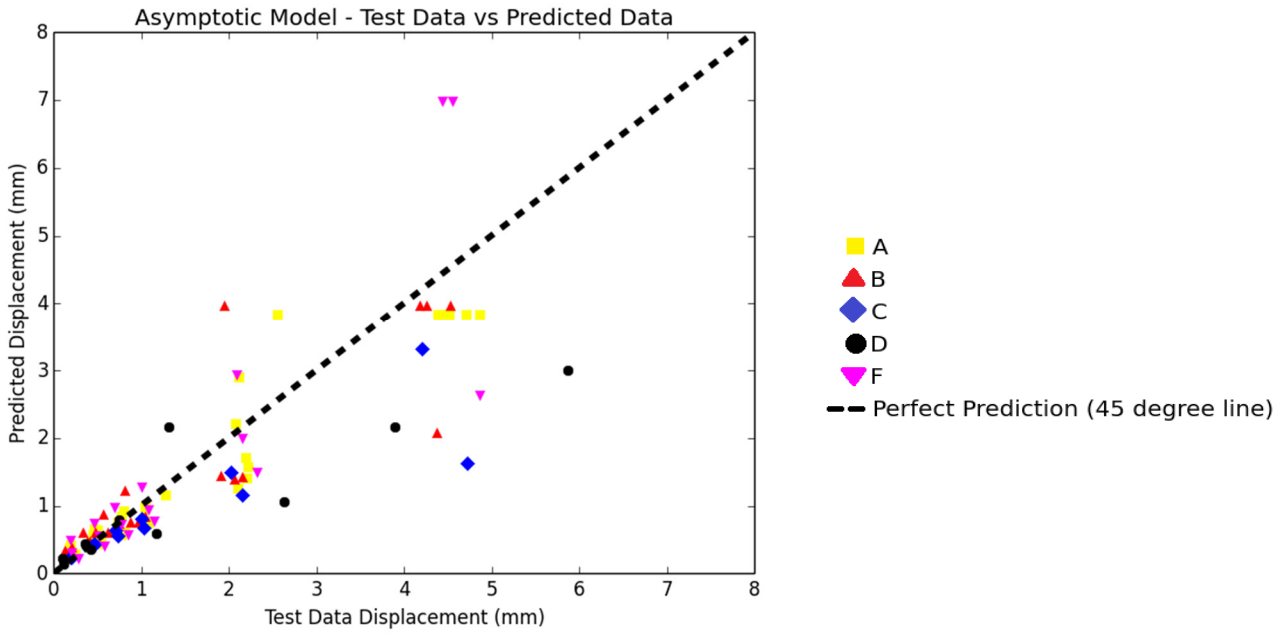

Figure 57: Asymptotic Model - Test Data vs Predicted Data

The results evaluated visually and by means of the R^2 values show that all three models have reasonable ability to predict the test results. As expected, the models are more accurate at low load levels, while the prediction is not as accurate near peak load levels. However, this may be acceptable from a design point of view since the model is mainly required to estimate low and moderate load levels. The models will be used to predict quantities such as initial stiffness (probably up to 50% of design capacity) or displacement (up to full design capacity). It can be argued however that design capacity in timber constitute roughly 50% of ultimate capacity, which means that any data point beyond the 50% mark (3 mm displacement) in Figure 55 to Figure 57 have no practical use in design.

The results from the exponential model (Figure 56) indicate that this model had the best R^2 value of 0.82 compared to the power model ($R^2 = 0.75$) and the asymptotic model ($R^2 = 0.77$).

A concern with the asymptotic model is that the model under-predicts the displacements near the peak values. Although the prediction at higher load levels is not as important compared to lower loads, the fact that the model under-predicts the displacement could have significant implications on estimating important parameters such as drift and period. This behaviour can be attributed to the nature of the logarithmic function, and its sensitivity to small changes near the peak of the function.

5.3 GWB Embedment Strength

The embedment strength (in MPa) of GWB decreased with the increase of dowel diameter. This result is consistent with that observed for embedment strength expressions found in the CSA-O86 for lumber members and lumber side plates. An expression can be developed for the embedment strength based on the material density and the diameter of the dowel, following the same format as those found in the timber design standard (CSA-O86). The format used for the embedment equation is shown in the following equation.

$$f = C_1 G\left(1 - C_2 d_f\right) \tag{5.30}$$

Where, f is the embedding strength, C_1 and C_2 are constants based on the type of material, G is the mean relative density of the material and d_f is the fastener diameter. The constants were determined by completing the least squared method to reduce the difference between the predicted values and tested values. The values found after the analysis are 12 and 0.02 for C_1 and C_2, respectively. The embedment equation for GWB, as function of its density and the fastener diameter used, can therefore be expressed as:

$$f = 12G\left(1 - 0.02 d_f\right) \tag{5.31}$$

The following table compares the predicted and tested embedment strength values and lists the percentage difference between the two.

Table 25: GWB Tested and Predicted Embedment Strength Comparison

Manufacturer	Dowel	G	d_f (mm)	$f_{predicted}$ (MPa)	f_{tested} (MPa)	Difference (%)
A – Type-X	Dowel 1	0.69	6.31	7.24	7.90	-9.2
	Dowel 2	0.69	9.40	6.72	7.13	-6.0
A – Type-X	Dowel 1	0.59	6.31	6.19	6.05	2.3
(L.W)	Dowel 2	0.59	9.40	5.75	5.95	-3.5
C – Type-X	Dowel 1	0.69	6.31	7.24	6.55	9.5
	Dowel 2	0.69	9.40	6.72	5.80	13.8
B – Type-X	Dowel 1	0.69	6.31	7.24	7.82	-8.0
	Dowel 2	0.69	9.40	6.72	7.79	-15.9
A - Regular	Dowel 1	0.5	6.31	5.66	5.19	8.4
	Dowel 2	0.5	9.40	5.26	4.81	8.5
B - Regular	Dowel 1	0.54	6.31	5.77	5.11	11.4
	Dowel 2	0.54	9.40	5.36	4.40	17.8
C - Regular	Dowel 1	0.55	6.31	5.24	5.69	-8.6
	Dowel 2	0.55	9.40	4.87	5.07	-4.0

One average the error difference is approximately 9% with a maximum error found to be 17.8%. The differences from the tested values to the predicted values arise from the aforementioned manufacturer variability. Essentially the developed equation takes into account all manufacturers; therefore manufacturers with embedment values that do not coincide with the average will be relatively different from the predicted value. However, as mentioned earlier, the presented data is consistent with manufacturing processes available in the market across the country, and as such the presented error in predicting the embedment strength is realistic.

The embedment strength will be used to estimate the joint capacity using established mechanics models in the following section.

5.4 Joint Level Yield Strength Prediction

This section describes the method used to obtain the joint level yield strength of the tested specimens based on material component testing. The yield strength is used for comparison since this value is well defined in the component testing ASTM standards (ASTM, 2013). The failure mode observed during testing of the joint specimens is Mode III and is described in the Literature Review chapter. This failure mode is limited by the dowel bearing in the side member and dowel bending in the main member. The value of P, in the equation derived in Parsons (2001), represents the lateral capacity of the joint.

The required information to determine the yield strength of the joint specimen are: side member dowel bearing resistance (q_s), main member dowel bearing resistance (q_m), side member dowel bearing length (l_s), dowel bending strength and diameter. The values for GWB embedment strength and the values for the bending strength of the fasteners are obtained through component testing, while the wood main member bearing strength was obtained from a concurrent study on S-P-F lumber according to ASTM D5764 (ASTM, 2013) (Plesnik, 2014). The relevant results are summarized in Table 26.

Table 26: SPF Lumber Embedment Strength (Reproduced from Plesnik, 2014)

Dowel Diameter (mm)	Lumber Embedment Strength (MPa)
2.87	45.95
3.33	44.71
3.76	53.25
4.11	49.24

The GWB embedment strength is taken directly from the embedment tests performed using the screws as dowels since it is difficult to determine an effective diameter for the screw, therefore the test results will give an exact value without the need of determining an effective diameter. It is important that the value used is representative since the embedding strength of the GWB has a very significant impact on the lateral capacity of the joint. The side member dowel bearing resistance (q_s), main member dowel bearing resistance (q_m), side member dowel bearing length (l_s), dowel bending strength and diameter of each joint specimen group are found in Appendix D. Figure 58 presents the comparison between the test lateral yield capacities and the calculated capacity based on the yielding failure mode observed for each joint level test group. The darker bars represent the predicted values using the yield equations.

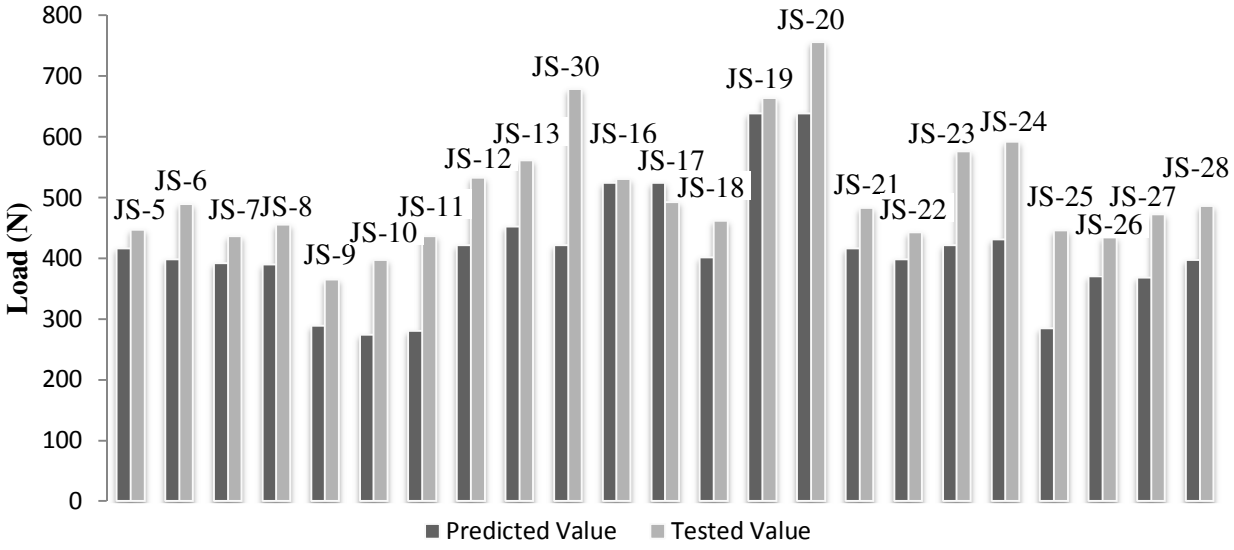

Figure 58: Lateral Yield Strength Prediction Accuracy Comparison

On average the error difference is approximately 24.7% with a maximum error found to be 60.6%. The main reason for the relatively large differences comes from the value selected for the yield load for the joint level tests. The yield load is a value that is often difficult to quantify when dealing with a laterally loaded wood joint because of the non-linearity exhibited in the load-deflection responses. On the other hand, the components of the joint (lumber embedment, fastener bending, and GWB embedment) all offer relatively bi-linear load-deflection responses which facilitates the method of obtaining a yield load. The nailed joints, which have a more pronounced non-linearity compared to the joints fastened with screws are consistently under-predicted (JS-9, JS-10, JS-11, JS-25) which would make the yield load of the joint more difficult to quantify accurately.

The differences could also potentially stem from the fact that the failure mode is idealized, whereas the actual failure could be a slightly modified version of the idealized failure or a combination of other failure

modes. Taking this into account, the results from the predicted value compared to the tested value are quite reasonable.

5.5 Full-Scale Shearwall Analysis

The EEEP analysis was performed on all tested walls and the results were presented in Section 4. As part of the analysis the ductility ratio, the initial stiffness and the peak load are obtained and used for the comparison of the tested shearwall specimens.

5.5.1 Effect of Fastener End/Edge Distance

The effect of varying the panel end/edge distance is compared by analyzing the results from Wall-3, Wall-5, Wall-6 and Wall-7. The walls were all constructed using the same GWB, lumber density and No.6 GWB screws. Wall-3 specimens have a panel end/edge distance of 19 mm, while the other three walls have a variation of reduced panel end/edge distance compared to Wall-3. The detailed characteristics of the end/edge distance used for each wall is described in Chapter 3. Figure 59 compares the results obtained for the peak load (a), initial stiffness (b) and ductility ratio (c) for Wall-3, Wall-5, Wall-6 and Wall-7.

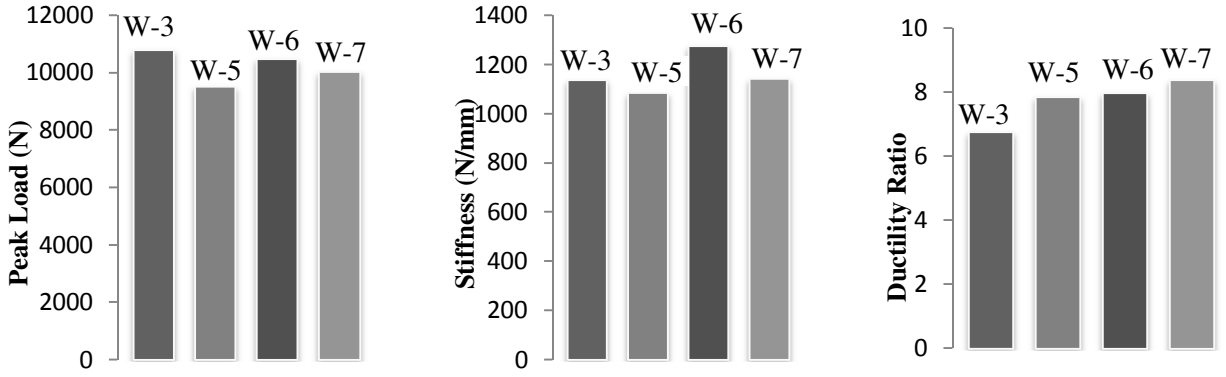

a) Peak Load **b) Initial Stiffness** **c) Ductility Ratio**

Figure 59: Parameter Comparisons for Panel End/Edge Distance Variation

As can be seen from Figure 59, the results for the panel end/edge distance variation shearwall specimens are very similar, which leads to the conclusion that the effect is minimal. There are still a few conclusions that can be drawn from these results. As expected, the results from the full scale shearwall testing showed that the wall with the largest end and edge distances (Wall-3) also had the highest peak load compared to those with reduced end and edge distances whether on the vertical or horizontal panel edges. The failure mechanism of the walls with reduced end/edge distance (compared to Wall-3) was characterized more by fasteners pulling through the edges of the GWB panel. An example of a wall failure that ultimately resulted

in pull through the end/edge of the panel can be seen in Figure 60. The fastener pull-through failure was dependent on the location of the fastener. As Figure 60 illustrates, the first three fasteners (starting from the left) pulled through the end of the panel while the other two are still providing some resistance.

Figure 60: Wall 5-2 End Distance Failure

Table 27 shows the calculated ratio of the peak load and ductility ratio of the walls with lower end/edge distance (Wall-5, Wall-6 and Wall-7) compared to Wall-3.

Table 27: End/Edge Distance Comparison Ratio

Wall No.	Peak Load	Ductility Ratio
Wall – 5	0.88	1.17
Wall – 6	0.97	1.18
Wall – 7	0.93	1.25

Since the values in the second column are smaller than 1.0, it can be seen that while the capacity slightly reduced in the three walls with shorter end/edge distance, the ductility of the wall is still maintained. The relatively similar values for peak load and ductility ratio for Wall-3, Wall-5, Wall-6 and Wall-7 leads to the conclusion that there is little to no effect to the response of the shearwall when the panel edge/end distance are varied from 19 to 9 mm. Even with the biggest difference between ductility ratios when comparing Wall-3 to Wall-7, the responses are very similar.

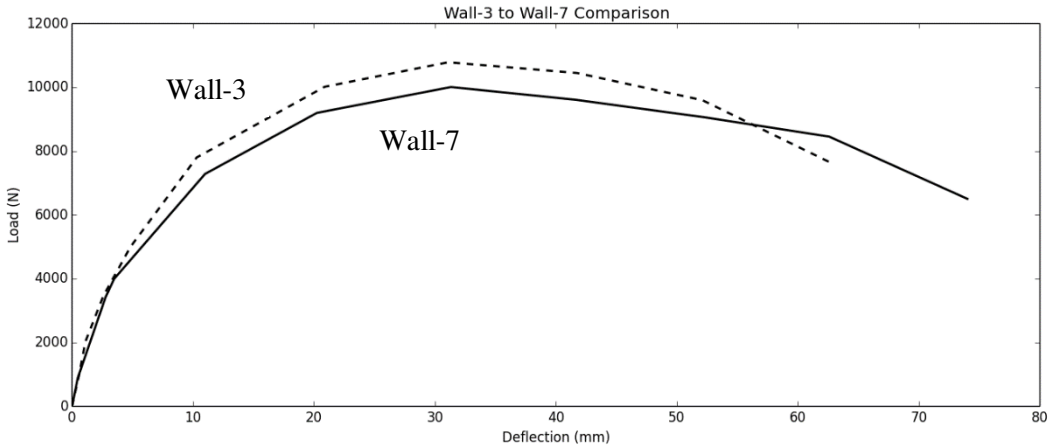

Figure 61: Wall-3 to Wall-7 Comparison

From Figure 61, it can be seen that despite a 25% increase in the ductility ratio for Wall-7 compare to Wall-3, the responses are very similar. The increase in ductility ratio stems from the way it is calculated. The ductility ratio is calculated by obtaining a ratio between the yield displacement and the displacement at 80% of peak load (past the point of peak load). Hence, the increase for Wall-7 is obtained because it reaches a lower peak load and maintains the same load for longer, compared to Wall-3. In summary, the end/edge distance variation (19 mm – 9mm) has no impact on the load-deflection response of GWB sheathed shearwalls.

5.5.2 Effect of Fastener Type

The fastener type variation was tested at the joint level. It was found that the type of fastener had a significant impact on the load-deflection response. The joints fastened with screws had higher peak load, higher initial stiffness and higher ductility compared to the joints fastened with nails. Wall-3 and Wall-4 had the same construction parameters expect the fasteners used to connect the sheathing panel to the lumber. Wall-3 used No.6 GWB screws, which had a root diameter of 2.7 mm and a threaded diameter of 3.8 mm, and the Wall-4 specimens used 12.5 gauge GWB nails, which had a diameter of 2.7 mm. Figure 62 compares the results obtained for the peak load (a), initial stiffness (b) and ductility ratio (c) for the average values of Wall-3 and Wall-4.

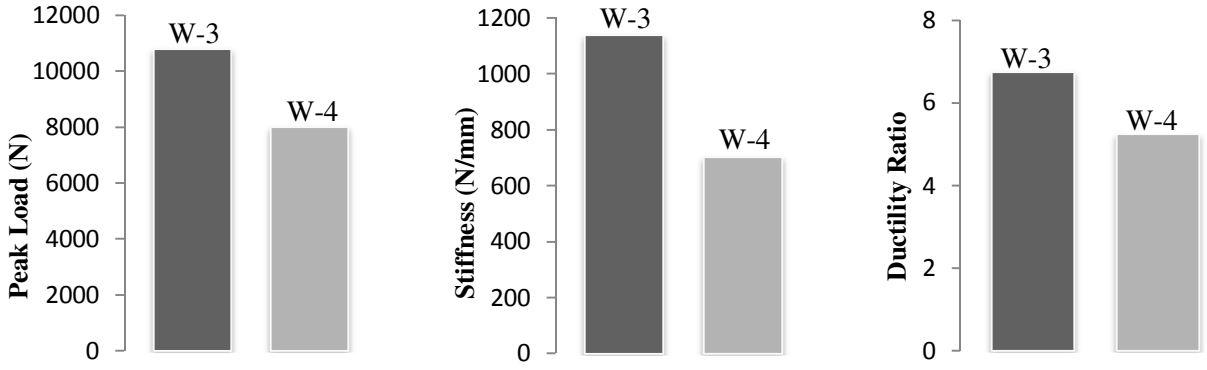

a) Peak Load **b) Initial Stiffness** **c) Ductility Ratio**

Figure 62: Parameter Comparisons for Fastener Type Variation

A similar result to the joint level tests is obtained for the full scale shearwall tests, where the walls fastened with screws exhibit greater strength, a higher initial stiffness and an increased ductility ratio, compared to the walls fastened with nails. This can be partly explained by the increased withdrawal resistance of the screws caused by the threads. A major result that is reproduced at the shearwall level is the increased ductility ratio for shearwalls fastened with screws compared to those fastened with nails. The average ductility ratios of the wall fastened with screws (Wall-3) and nails (Wall-4) are 6.72 and 5.22, respectively. During testing it was observed that the walls fastened with screws had an increase in deflection caused by the bending of the studs, while the walls fastened with nails did not reach a load that was sufficient to achieve this effect.

5.5.3 Effect of Fastener Spacing at Panel Edge

Wall-3 and Wall-8 specimens were both constructed using the same parameters, with the one exception being the fastener spacing. Wall-3 had No.6 GWB screws spaced at 150 mm, while Wall-8 specimens used the same fasteners but spaced at 50 mm. Figure 63 compares the results obtained for the peak load (a), initial stiffness (b) and ductility ratio (c) for the average values of Wall-3 and Wall-8.

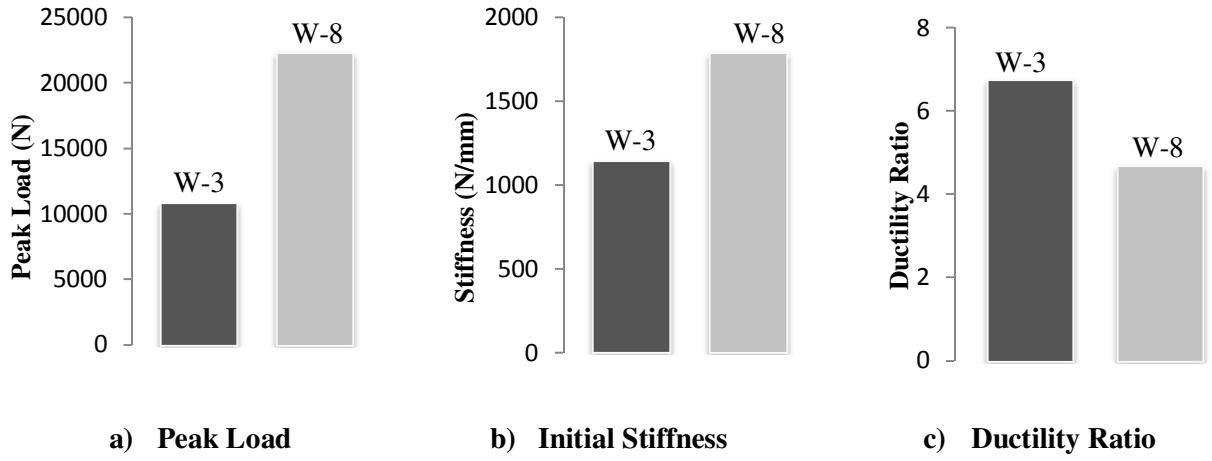

a) Peak Load **b) Initial Stiffness** **c) Ductility Ratio**

Figure 63: Parameter Comparisons for Fastener Spacing Variation

By decreasing the fastener spacing, the amount of fasteners used increases. Wall-8 with 50 mm fastener spacing had a peak load of 22,260.0 N compared to Wall-3 which had a peak load of 10,782.5 N. The increased number of fasteners present in Wall-8 (3 times the number of screws) led to a peak load that is 2.1 times larger. Usually an increase in the number of fasteners is directly proportional to the increase in capacity. This requires however that the failure mode is consistent. The decrease in fastener spacing caused a shift in the failure mode has and a more brittle failure was obtained. The ductility ratio was 6.72 and 4.66 for Wall-3 and Wall-8, respectively. The decreased spacing between the fasteners led to a sudden crack of the GWB along the edges of the panel which causes a sudden loss of capacity. The failure mode observed was also reproduced in both test replicates. It is worth mentioning that the timber design standard (CSA O86) does not supply strength values for shearwalls with 50 mm fastener spacing, therefore it is inferred that this particular wall setup is not acceptable according to the standard.

5.5.4 Shearwall Deflection Prediction Using Developed Fastener Slip Models

The response of the shearwall tests is used to validate the accuracy of the fastener slip models. Joint level tests were performed with the same materials and specifications as the full scale shear wall specimens. These specifications included the type and manufacturer of fastener, the thickness and manufacturer of gypsum wall board as well as the stud type and density. Equation (5.32), from the CSA-O86, is used to obtain the static deflection at the top of the shearwall segment with wood-based panels used as sheathing. The fastener slip equation derived from the joint specimen tests for gypsum wall board is used to replace the e_n value in the four term deflection equation. The goal is to investigate whether including the slip model developed in this study into the four-term deflection equation could yield reasonable results in predicting the wall deflection.

$$\Delta s = \frac{2v_s H_s^3}{3EAL_w} + \frac{v_s H_s}{B_v} + 0.0025 H_s e_n + \frac{H_s}{L_w}\Delta_a \quad (5.32)$$

The four terms of equation 5.32 are explained in detail in literature review section (Section 2) and the variable definitions are explained in the following.

v_s = Applied shear force at the top of the wall per unit length (N/mm)

H_s = Height of the shearwall (mm)

B_v = Shear-through-thickness rigidity of sheathing (N/mm). B_v is obtained from tests following the ASTM D2719, where the modulus of rigidity (G) is obtained. The product of the modulus of rigidity and the thickness of the sheathing is the B_v value.

E = Modulus of elasticity of end studs (MPa)

A = Cross-sectional area of end studs (mm^2)

L_w = Length of shearwall (mm)

Δ_a = Total vertical elongation of the wall anchorage system (mm)

e_n = fastener slip (mm). e_n is obtained using the curve fitting equations developed for the tests performed on the full scale replicate joint specimens

The values used in the prediction, are the values obtained from the curve fitting of the joint level test data, using the same construction characteristics as the tested shearwall. The parameters for each model type are presented in Table 28.

Table 28: Curve Fitting Parameters for Fastener Joint Specimens (Full Scale Replicates)

JS	Power Model		Exponential Model			Asymptotic Model		
Group	A	B	K0 (N/mm)	K1(N/mm)	P1(N)	C	D	E
JS-24	22.21	4.0	2056.06	-66.75	389.58	613.21	562.05	0.19
JS-25	27.13	2.6	460.11	-36.84	332.79	509.57	495.12	0.48

All of the tested walls are used as part of this analysis. Walls Wall-3, Wall-5, Wall-6 and Wall-7 are placed in the same figure since they all have the same input parameters for the CSA-O86 equation. Wall-4 uses a different type of fastener therefore the fastener slip model parameters are different. Finally Wall-8 uses the same fastener slip model as Wall-3, Wall-5, Wall-6 and Wall-7 but has lower fastener spacing, which is

why it is treated separately. The following table lists the CSA-O86 deflection equation inputs based on the wall characteristics.

Table 29: Shearwall Characteristics

	Wall-3, 5, 6, 7	Wall-4	Wall-8
Height of Shearwall (H_s)	2440 mm	2440 mm	2440 mm
Shear-through-thickness rigidity (B_v)	8958 N/mm	8958 N/mm	8958 N/mm
Modulus of Elasticity (E)	9000 MPa	9000 MPa	9000 MPa
Cross-Sectional Area (A)	3382 mm^2	3382 mm^2	3382 mm^2
Length of Shearwall (L_w)	2440 mm	2440 mm	2440 mm
Elongation of Anchorage (Δa)	$0.445x10^{-3}$ mm/N	$0.445x10^{-3}$ mm/N	$0.445x10^{-3}$ mm/N
Fastener Spacing	150 mm	150 mm	50 mm
Fastener Type	Screws	Nails	Screws

The following equations are used as input for the fastener slip. Equations 5.34, 5.35 and 5.36 are the power, exponential and asymptotic model and are used for Wall-3, Wall-5, Wall-6, Wall-7 and Wall-8. Equations 5.37, 5.38 and 5.39 are the power, exponential and asymptotic model used for Wall-4.

$$e_n = 22.21\left(v_f\right)^{4.0} \tag{5.34}$$

$$v_f = [389.58 + 66.75e_n]\left[1 - e^{(-2056.06e_n/389.58)}\right] \tag{5.35}$$

$$e_n = (\log\left(\frac{613.21 - v_f}{562.05}\right))/\log(0.19) \tag{5.36}$$

$$e_n = 27.13(y)^{2.6} \tag{5.37}$$

$$v_f = [332.79 + 36.84e_n]\left[1 - e^{(-460.1e_n/332.79)}\right] \tag{5.38}$$

$$e_n = (\log\left(\frac{509.57 - v_f}{495.12}\right))/\log(0.48) \tag{5.39}$$

The developed models are valid only up to peak load; therefore the peak load of the shearwalls is based on the maximum load per fastener obtained from the joint level tests. Figure 64 to Figure 72 present the three models compared to the three different types of shearwall configuration.

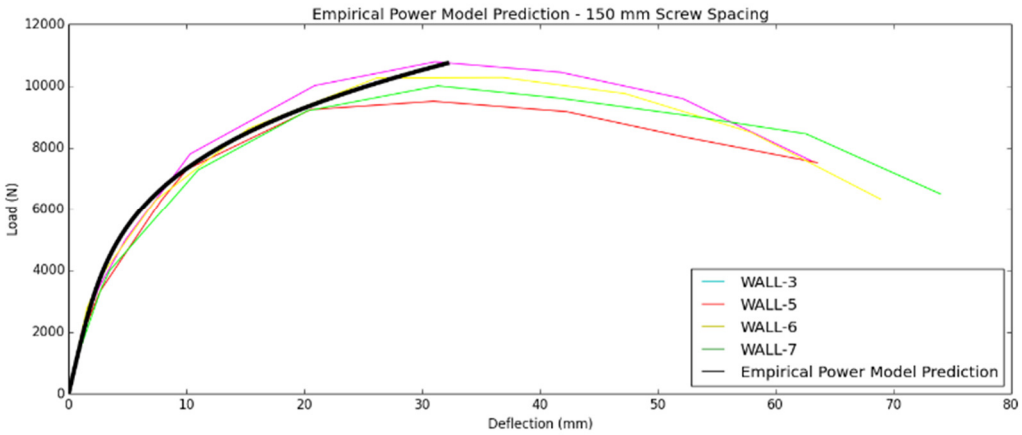

Figure 64: Power Model Prediction - 150 mm Screw Spacing

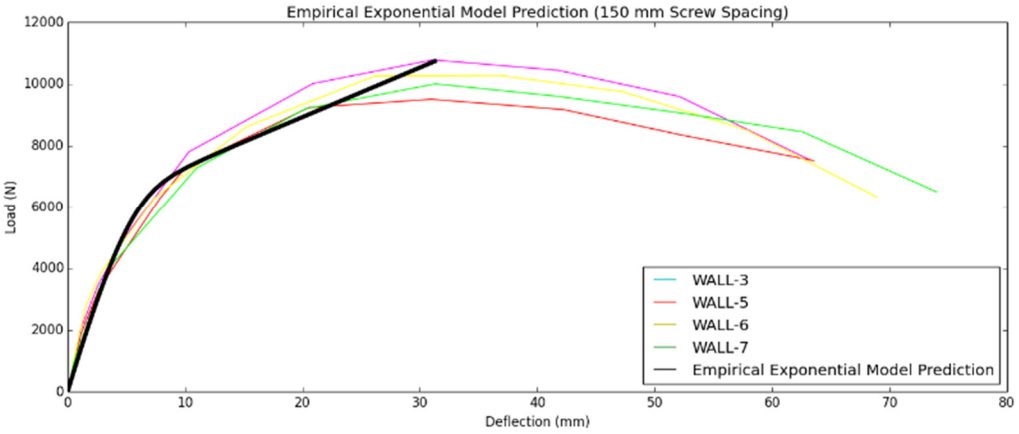

Figure 65: Exponential Model Prediction - 150 mm Screw Spacing

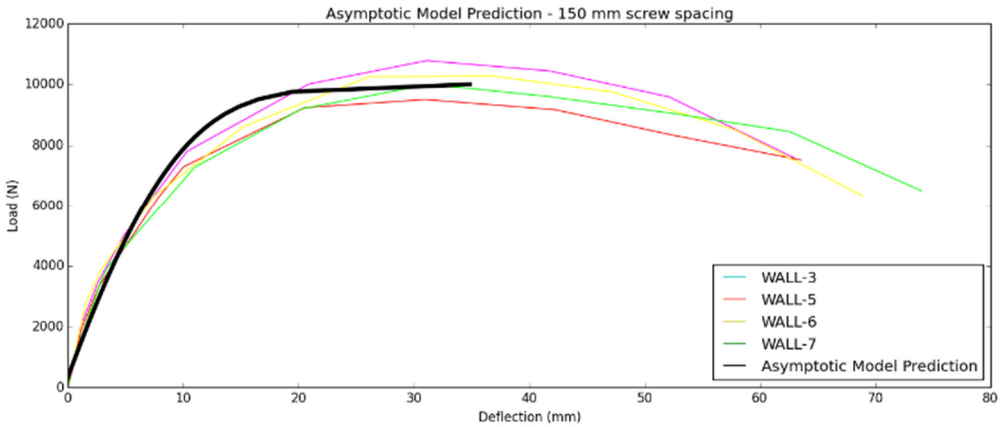

Figure 66: Asymptotic Model Prediction - 150 mm Screw Spacing

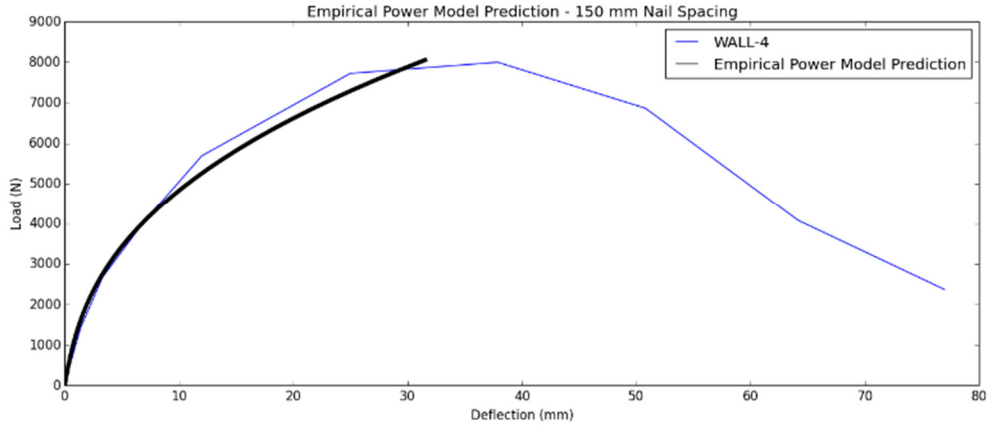

Figure 67: Power Model Prediction - 150 mm Nail Spacing

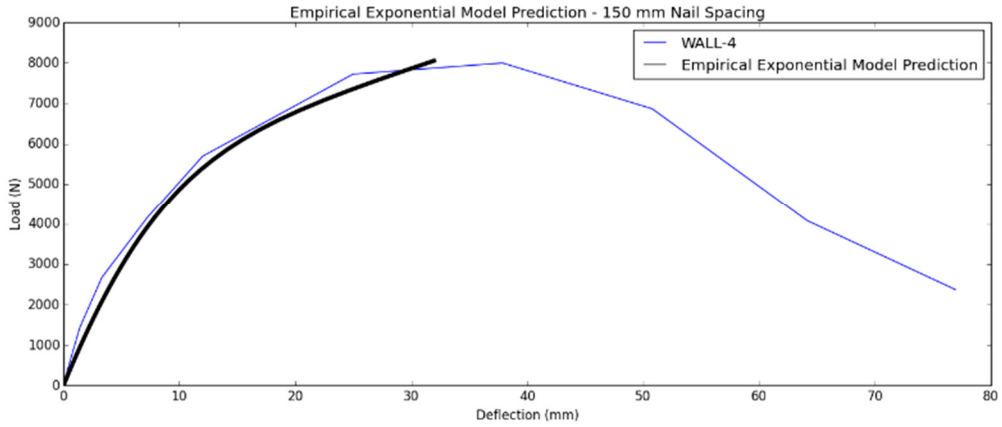

Figure 68: Exponential Model Prediction - 150 mm Nail Spacing

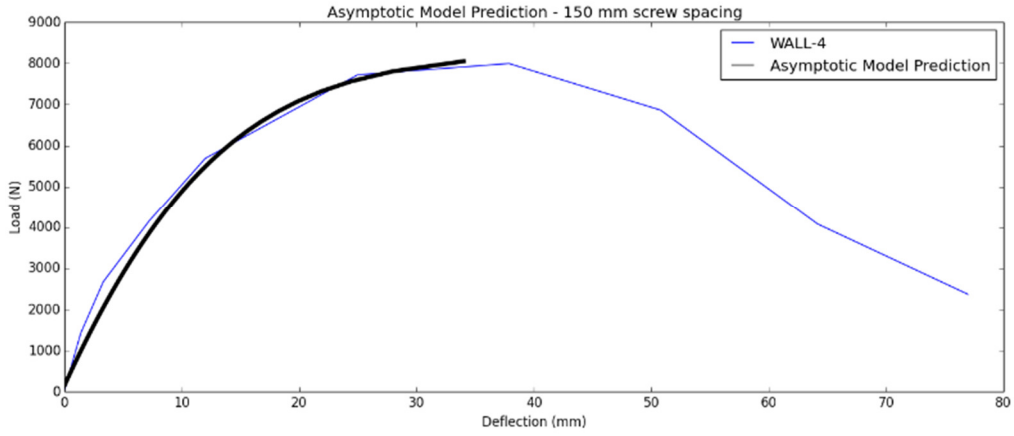

Figure 69: Asymptotic Model Prediction - 150 mm Nail Spacing

All three predictive models seem to be able to replicate the wall behaviour with reasonable accuracy. The power model seems to have a similar response to the test data up to peak load compared to the other two models.

The Figure 67, Figure 68 and Figure 69 present the prediction of the load deflection response of the shearwall fastened with nails, using the different model types. The bilinear behavior that was observed for the specimens fastened with screws is not as noticeable for the walls fastened with nails, which occur at lower load compared to the walls fastened with screws. The asymptotic and exponential model types were selected for this study based on the recommendations of previous studies (Foschi, 1974; McLain, 1975; Wang, 2009). The previous studies that were used for this purpose mainly focus on joints fastened with nails, it is therefore expected that these two model types are more suitable for shearwalls fastened with GWB nails. There is little to no observable difference in the predicted responses for each of the different models and they also have a very accurate load-deflection response compared to the average test data of the Wall-4 specimens.

It was observed in the previous section that the failure mode for the Wall-8 specimen configuration is different compared to the other tested walls. The reduced fastener spacing caused a premature failure at the wall edge. The failure mode developed at the full scale level was obviously not observed during the joint level tests, and is therefore also not reflective in the slip model developed. Although the model is not accurate at high load levels, the initial portions of all three model predictions follow the load-deflection response. The power model accurately describes the response up to 5.4 mm (41% of tested specimen peak load), the exponential model accurately describes the response up to 6.7 mm (45% of tested specimen peak load) and the asymptotic model is accurate up to 8.3 mm (53% of tested specimen peak load).

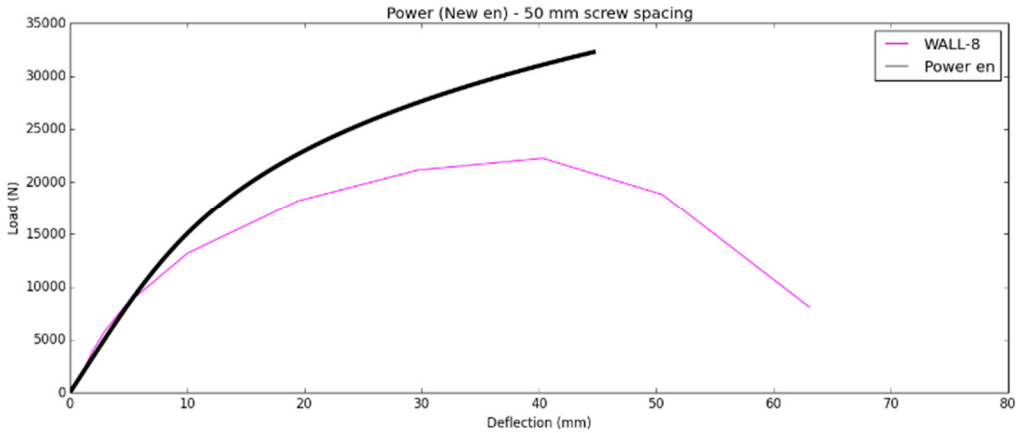

Figure 70: Power Model Prediction - 50 mm Screw Spacing

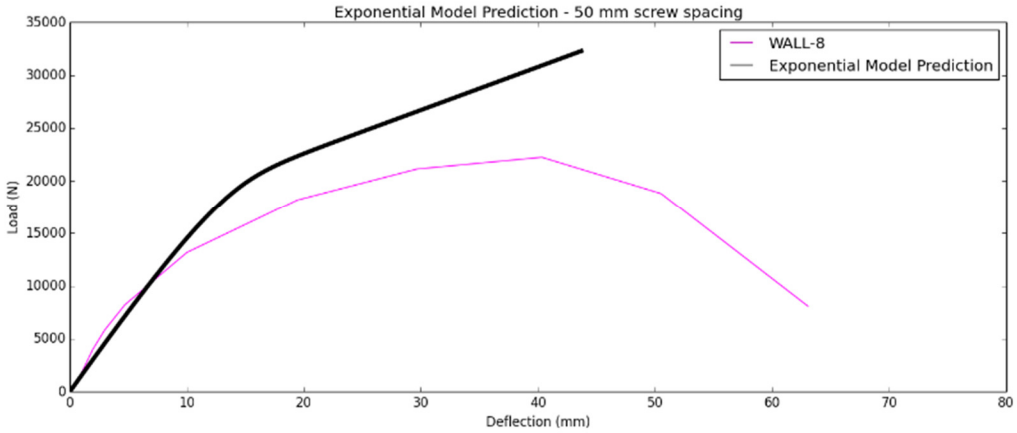

Figure 71: Exponential Model Prediction - 50 mm Screw Spacing

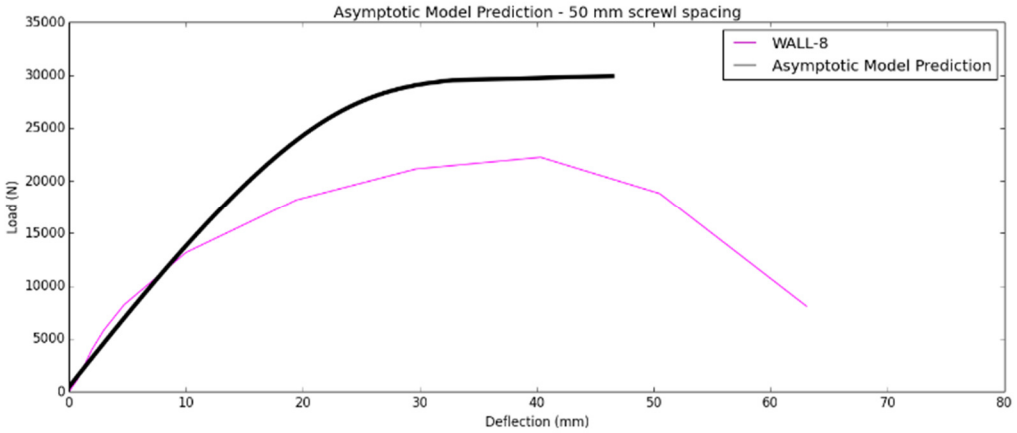

Figure 72: Asymptotic Model Prediction - 50 mm Screw Spacing

The following tables present the average tested and predicted initial stiffness, the displacement at peak load, the peak load and the displacement at 40% of peak load. The difference in percentage is also presented in order to compare the effectiveness of each model to predict the tested values. The predicted initial stiffness (K_P) and tested initial stiffness (K_T) are obtained based on the method from the EEEP analysis, where the initial stiffness is the slope from (0,0) to the 40% of peak load and the associated displacement point from the load-deflection graph. The differences will be used to select the best model, as part of the decision matrix analysis.

Table 30: Test values versus predicted values - Power Model

	Initial Stiffness (kN/mm)			Peak Load (kN)			Displacement at Peak (mm)			Displacement at 40% Peak (mm)		
	K_T	K_P	D (%)	P_T	P_P	D (%)	D_T	D_P	D (%)	D_{T40}	D_{P40}	D (%)
Wall-3	1.1	1.7	-50.8	10.7	10.8	0.2	31.1	34.0	-9.3	3.80	2.50	34.2
Wall-4	0.7	1.7	-143.9	8.0	8.2	-1.9	37.9	32.2	15.0	4.64	1.89	59.3
Wall-5	1.1	1.7	-58.4	9.5	10.8	-13.2	31.0	34.0	-9.7	3.52	2.50	29.0
Wall-6	1.3	1.7	-34.7	10.5	10.8	-2.8	37.9	34.0	10.3	3.29	2.50	24.0
Wall-7	1.1	1.7	-50.2	10.0	10.8	-7.5	31.3	34.0	-8.6	3.51	2.50	28.8
Wall-8	1.8	1.7	3.9	22.3	32.3	-45.0	40.3	44.7	-10.9	4.98	4.53	9.0

Table 31: Test values versus predicted values - Exponential Model

	Initial Stiffness (kN/mm)			Peak Load (kN)			Displacement at Peak (mm)			Displacement at 40% Peak (mm)		
	K_T	K_P	D (%)	P_T	P_P	D (%)	D_T	D_P	D (%)	D_{T40}	D_{P40}	D (%)
Wall-3	1.1	1.7	-50.8	10.7	10.8	0.2	31.1	32.2	-3.5	3.80	2.51	33.9
Wall-4	0.7	1.7	-143.9	8.0	8.2	-1.9	37.9	32.8	13.4	4.64	1.88	59.5
Wall-5	1.1	1.7	-58.4	9.5	10.8	-13.2	31.0	31.0	-0.1	3.52	2.51	28.7
Wall-6	1.3	1.7	-34.7	10.5	10.8	-2.8	37.9	31.0	18.2	3.29	2.51	23.7
Wall-7	1.1	1.7	-50.2	10.0	10.8	-7.5	31.3	31.0	1.1	3.51	2.51	28.5
Wall-8	1.8	1.7	3.9	22.3	32.3	-45.0	40.3	43.7	-8.3	4.98	4.53	9.0

Table 32: Test values versus predicted values - Asymptotic Model

	Initial Stiffness (kN/mm)			Peak Load (kN)			Displacement at Peak (mm)			Displacement at 40% Peak (mm)		
	K_T	K_P	D (%)	P_T	P_P	D (%)	D_T	D_P	D (%)	D_{T40}	D_{P40}	D (%)
Wall-3	1.1	1.8	-61.7	10.7	10.0	7.2	31.1	34.8	-11.9	3.80	2.18	42.6
Wall-4	0.7	1.6	-130.4	8.0	8.2	-1.9	37.9	38.5	-1.6	4.64	2.00	56.9
Wall-5	1.1	1.8	-69.8	9.5	10.0	-5.2	31.0	34.8	-12.4	3.52	2.18	38.1
Wall-6	1.3	1.8	-44.3	10.5	10.0	4.5	37.9	34.8	8.1	3.29	2.18	33.7
Wall-7	1.1	1.8	-61.0	10.0	10.0	0.0	31.3	34.8	-11.1	3.51	2.18	37.9
Wall-8	1.8	1.6	11.7	22.3	30.0	-34.4	40.3	46.5	-15.3	4.98	3.45	30.7

5.6 Fastener Slip Model Selection – Decision Matrix Analysis

Seven criteria were used to determine the effectiveness of the developed fastener slip models to predict the load-deflection response of the tested shearwall specimens. These are: simplicity of the equations, response shape, displacement at 40% of peak load, initial stiffness, peak load and the associated deflection, and the R^2 value obtained from the joint level analysis. Each criterion is assigned a certain weight based on its importance to the model selection. The criterion importance is discussed and the weights are tabulated in the following table.

The simplicity of the equation is an advantage for a design situation. In the current study, the simplest model is the power model since it only has one varying parameter compared to three parameters for the other two models. The exponential model is deemed the most complex model of the three since it becomes an iterative process to obtain the deflection with a given load.

It is important to have a similar response shape to the test data since this ensures the accuracy of the stiffness throughout the load-deflection response. The power model exhibits the most similar shape to the test data since it has a constant curve up to maximum. The exponential and asymptotic model shapes have an almost bilinear shape which affects the predicted post-yield stiffness. The asymptotic model is deemed the worst in this regard since the function predicts a stiffness approaching zero near peak load.

An important emphasis is placed on the ability for a model to predict the displacement at low to moderate loads since it coincides with design level loading and displacement. The displacement at 40% of peak load is used for comparison since it coincides with the value used in the EEEP analysis to obtain the initial stiffness.

The initial stiffness is, as mentioned earlier, very important for the estimation of parameters such as period of buildings. It was previously determined that the initial stiffness had a very large coefficient of variance within the joint level groups. All three models overestimate the initial stiffness with similar percentage of error.

The peak load and the deflection at peak load are given the same importance. A lower emphasis is placed on these criteria, compared to the lower load deflection, since a slip model is not usually used to predict the ultimate response. The accuracy of the models is determined by examining the percentage difference between the tested and predicted data.

The R^2 value is given some consideration but an emphasis is not placed on this criterion since it is very similar for all three models. The values used for this criterion stem from the analysis performed at the joint level.

Table 33 presents the weights associated to each criterion that will be used as part of the decision matrix analysis. It is recognized that this analysis is subjective, and that a different conclusion could be achieved if the values assigned were different. However, the attempt here is to use a rational method that can combine more than one criterion that may have different impact or weight into deciding which model is most suitable to use.

Table 33 Decision Matrix Criteria Weights

Criterion	Weight (%)
Simplicity of the function	15
Response Shape	25
Deflection at 40% Peak Load	25
Deflection at Peak Load	10
Initial Stiffness	10
Peak Load	10
R^2	5

A scale from 0 (worst) to 10 (best) was used to rate each criterion. Where possible, the percentage of difference was used as a basis to obtain the performance rating. Quantifying parameters such as "simplicity" is of course difficult and subjective.

Table 34: Decision Matrix Ranking Scale

Performance Level	Percentage Difference	Value
Useless	100%	0
Inadequate	90%	1
Very Poor	80%	2
Poor	70%	3
Tolerable	60%	4
Adequate	50%	5
Satisfactory	40%	6
Good	30%	7
Very Good	20%	8
Excellent	10%	9
Perfect	0%	10

The following table presents the criteria and the associated score to each model.

Table 35: Model Features and Scores

	Power Model	Exponential Model	Asymptotic Model
Simplicity of the function (15%)	1 parameter	3 parameters Iterative process to obtain displacement	3 parameters
Score	9	5	7
Response Shape (25%)	Constant curve function	Bilinear function with transition	Bilinear function with transition Slope is zero at peak loads
Score	8	7	6
Deflection at 40% Peak Load (25%)	Average Difference to Test Value: 30.7%	Average Difference to Test Value: 30.6%	Average Difference to Test Value: 40.0%
Score	7	7	6
Deflection at Peak Load (10%)	Overestimates peak load deflection Average Difference to Test Value: 10.6%	 Average Difference to Test Value: 7.4%	Underestimates peak load deflection Average Difference to Test Value: 10%
Score	9	9	9
Initial Stiffness (10%)	Average Difference to Test Value: 56.9%	Average Difference to Test Value: 56.9%	Average Difference to Test Value: 63%
Score	4	4	4
Peak Load (10%)	Average Difference to Test Value: 11.7%	Average Difference to Test Value: 11.7%	Average Difference to Test Value: 8.9%
Score	9	9	9
R^2 (5%)	$R^2 = 0.75$	$R^2 = 0.82$	$R^2 = 0.77$
Score	7	8	8

Table 36 shows the matrix evaluating which model is the most suitable to predict the load-deflection response of the tested shearwalls. A ratio of each score of each model is obtained for each criterion in order for the analysis to be consistent. The average score ratio is obtained for each model type and criterion and presented as the value C in Table 36. The weights given in Table 33 are used as a factor to multiply the C values obtained for each model and for each criterion. Finally the summary value presented in Table 36 is the sum of each $W*P_i$ value, with the largest value belonging to the best selection.

Table 36: Decision Matrix – Fastener Model Selection

	Weight (W)		Power Model	Exponential Model	Asymptotic Model
Simplicity of the function	0.15	C1	0.43	0.24	0.33
		W*C1	0.06	0.06	0.05
Response Shape	0.25	C2	0.38	0.33	0.29
		W*C2	0.10	0.08	0.07
Deflection at 40% Peak Load	0.25	C3	0.35	0.35	0.30
		W*C3	0.09	0.09	0.08
Deflection at Peak Load	0.10	C4	0.33	0.33	0.33
		W*C4	0.03	0.03	0.03
Initial Stiffness	0.10	C5	0.33	0.33	0.33
		W*C5	0.03	0.03	0.03
Peak Load	0.10	C6	0.33	0.33	0.33
		W*C6	0.03	0.03	0.03
R^2	0.05	C7	0.30	0.35	0.35
		W*C7	0.02	0.02	0.02
Summary			**36.04%**	**31.9%**	**30.98%**

According to the decision matrix analysis the best fastener slip model is the power model. This is also corroborated by ad-hoc observation made on the simplicity of the model and its ability to fit the response shape accurately. A strong emphasis was placed on the simplicity of the model type since one of the goals of the study is to provide a model for design situations. As it is clearly indicated from this result, the difference between the three models is small, and any of the models can essentially be used to predict the shear wall behaviour with reasonable accuracy.

6. ANALYTICAL PREDICTIONS AND DISCUSSION

Analysis program (SAPWood) was used to model the joint level hysteresis as a hysteretic spring with 10 model fitting parameters (Pei and Van de Lindt, 2010). The developed joint level hysteretic model was then used to represent the fasteners connecting the sheathing panels to the lumber framing in the construction of the full-scale shearwall model. The shearwall model was subjected to reversed cyclic loading and the resulting hysteresis was compared with the results obtained from the full scale shearwall tests. There are three shearwall models developed using two different joint level hysteretic models. Wall-3 and Wall-8 specimens were modeled using a screw model and Wall-4 specimen was modeled using a nail model. The wall specimen configurations are explained in Chapter 3. The main goal of this section is validate the joint level results and to establish whether a linkage can be made between the performance of the joints and the overall behaviour of the wall.

6.1 Introduction to the SAPWood program

The SAPWood analysis program is developed based on the Seismic Analysis of Woodframe Structures (SAWS) and the Computer Program for the Cyclic Analysis of Shearwalls (CASHEW) (Pei and Van de Lindt, 2010). SAPWood enables the user to model and analyze light-frame wood shearwalls with nonlinear connectors using the NP-Model Builder tool. The NP-Model Builder consists of the following components: panels, studs and connectors (sheathing-to-lumber, lumber-to-lumber and hold-downs). Any model developed using this tool has 3 degrees-of-freedom on every component and the components will undergo rigid body displacement with the restraint of the fasteners connecting them together. The full-scale model is independent of the sheathing type or the lumber density since these characteristics are taken into account in the development of the joint level hysteresis.

6.2 Joint Level Hysteresis Model

Several researchers have investigated the behaviour of light frame wood shearwalls by developing sophisticated finite element models, which model the connection based on its individual components (Foschi 1974, 2000; Chui et al. 1998). The connection models were comprised of individual modeled elements for the sheathing, the fastener and the main lumber member. These models were reasonably accurate and versatile but became computationally demanding when dealing with a shearwall, which is comprised of multiple connections. The simple alternative is to develop a hysteretic load-deflection model capable of reproducing the hysteretic behavior of the joint as a whole, without modeling each component of the joint. Folz and Filliatrault (2001) discuss the developed model in which the sheathing to lumber connection is modeled and the shearwall is subjected to a quasi-static displacement protocol. The study also

compares the analytical results to full scale tested shearwalls. The CASHEW program was used in the study and it was shown to accurately predict the load-displacement response and energy dissipation of wood shearwalls. The present study utilizes the calibrating procedure developed by Folz and Filliatrault (2001) as part of the SAPWood program, which calibrates a single degree-of-freedom system to predict the nonlinear dynamic response of shearwalls under reversed cyclic loading.

The developed hysteretic model is presented in Figure 73. The model path is based on a set of rules, which are governed by ten parameters. The parameters are identified and briefly explained in Figure 73.

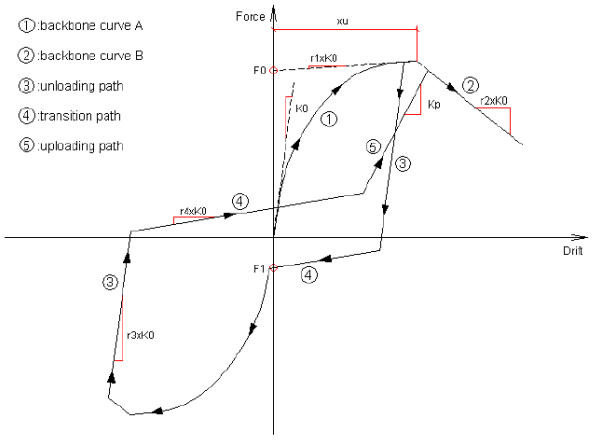

K0: Initial Stiffness
F0: The Resistance Force Parameter of the Backbone
F1: Pinching Residual Resistance Force
R1: The stiffness ratio parameter of the backbone
R2: The ratio of the degrading backbone stiffness to K0
R3: The ratio of the unloading path stiffness to K0
R4: The ratio of the pinching load path stiffness to K0
Xu: The drift corresponding to the maximum restoring force of the backbone curve
Alpha: Stiffness degradation parameter (≈ 0.5-0.9)
Beta: Strength degradation parameter (≈ 1.01-1.5)

Figure 73: Loading Path and Parameters of CASHEW Model (Reproduced from Pei and W. van de Lindt, 2010)

The loading path is separated into five different sections, which are indicated on Figure 73. The first section is the initial portion of the backbone curve and is a combination of the initial stiffness (K0), the post yield stiffness (R1xK0) and a nonlinear transition between the two. The first section ends at a drift associated with the maximum force exhibited by the connection (X_u). The second portion is governed by the degrading backbone stiffness and follows the post-peak backbone curve. The third portion consists of a linear unloading path and is governed by the unloading stiffness (R3xK0). The fourth portion is the transition phase, which takes into account the pinching behavior of the response and is governed by the pinching load path stiffness (R4xK0). Finally the fifth loading path portion, the reloading phase, which is linear and has the same slope as the initial stiffness. The stiffness and strength degradation are taken into account by introducing the Alpha and Beta parameters. The Alpha and Beta parameters reduce the inputted initial stiffness and strength parameters after every cycle.

6.3 Shearwall Model

The light-frame wood shearwall model consisted of four basic components: the wood framing, sheathing, anchorage hold-down system and the lumber to sheathing connection. All of the components are taken into account in the "NP Model" section of the SAPWood program.

6.3.1 Wood Framing and Sheathing

The wood framing and sheathing components each have three degrees of freedom. The components undergo rigid body deformation and therefore no stud bending is incorporated into the model. The lumber and sheathing are restrained by the fasteners that are connecting them together.

6.3.2 Lumber-to-Sheathing Connection

The hysteresis manual fitting tool is used to obtain the model parameters required to accurately describe the joint level hysteresis test data. A representative joint level hysteresis is uploaded to the program and an automatic first iteration of the model fit is completed by the program. The previously described model parameters are obtained based on the EEEP analysis results and the other parameters (alpha and beta) are varied until the model fits the test data. A joint level test result which was representative of the group average was chosen to obtain the "alpha" and "beta" parameters. Table 37 presents the parameter values used to model the screw and nail joint hysteresis.

Table 37: Fastener Hysteresis Model Parameters

Fastener	K0 (N/m)	F0 (N)	F1 (N)	R1	R2	R3	R4	Xu (m)	Alpha	Beta
Screws	1.46×10^6	584.1	0.0001	0.0128	-0.0322	10	0.0001	0.00418	0.5	1.1
Nails	3.67×10^5	422.7	0.0001	0.0461	-0.0752	10	0.0001	0.00462	0.5	1.1

The joint level hysteresis models are compared to test data in Figure 74 and Figure 75 for joints fastened with screws and nails, respectively.

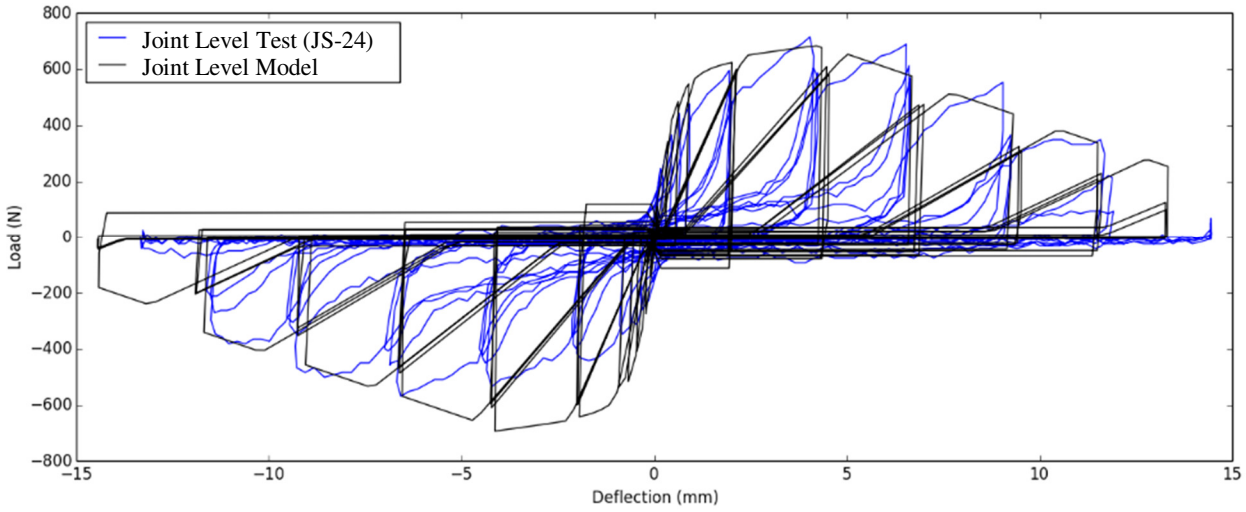

Figure 74: Screw Joint Level Hysteresis Model Comparison

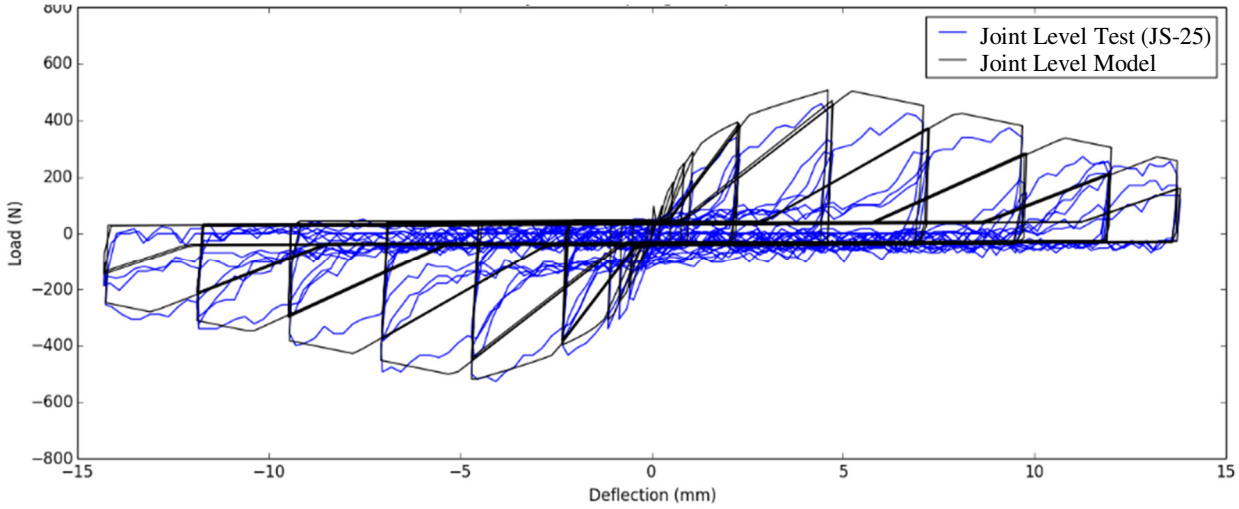

Figure 75: Nail Joint Level Hysteresis Model Comparison

The modeled wall specimen is subjected to the same quasi-static reversed cyclic load protocol which was used during the full scale shearwall tests. The load is applied at the top of the wall by selecting the DoF (Degree of Freedom) as 1X, which corresponds to the top horizontal plate and the in-plane direction of the shearwall. A sub-step of 20 is selected for the analysis since this is the value that was selected during the joint level hysteresis manual fitting and provided the most accurate fit.

6.4 Results

Figure 76 presents a typical hysteresis obtained from subjecting the shearwall model to the displacement protocol. The shearwall model presented has the same configuration as Wall-3.

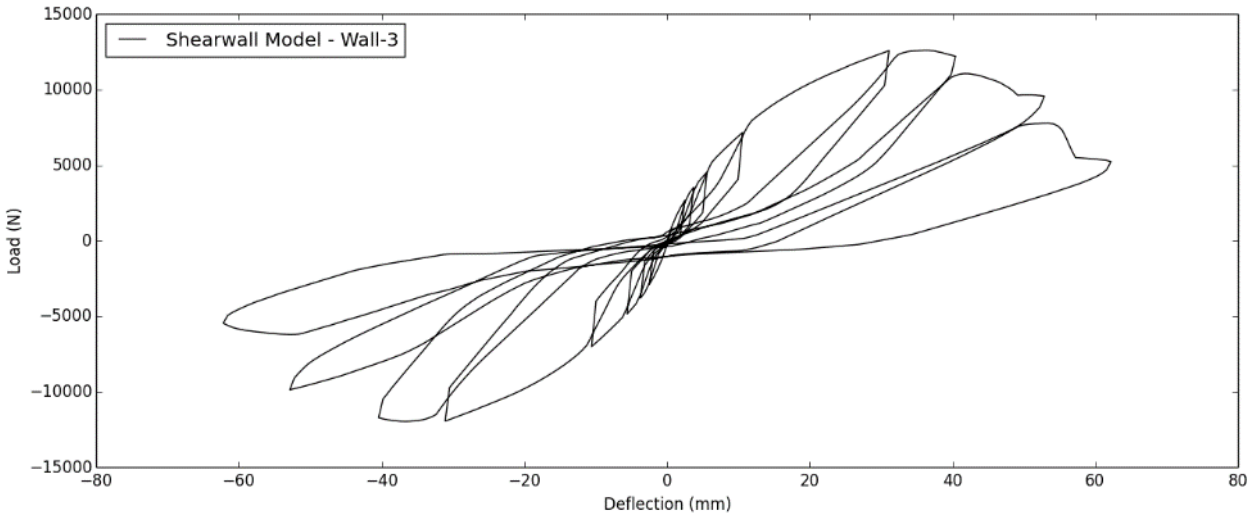

Figure 76: Typical Shearwall Model Hysteresis

The average of the positive and negative sides of each test was obtained and compared with the model data for the various wall configurations. Figure 77 presents the average envelope of the hysteresis for each model in addition to the associated tested specimen hysteresis average envelope.

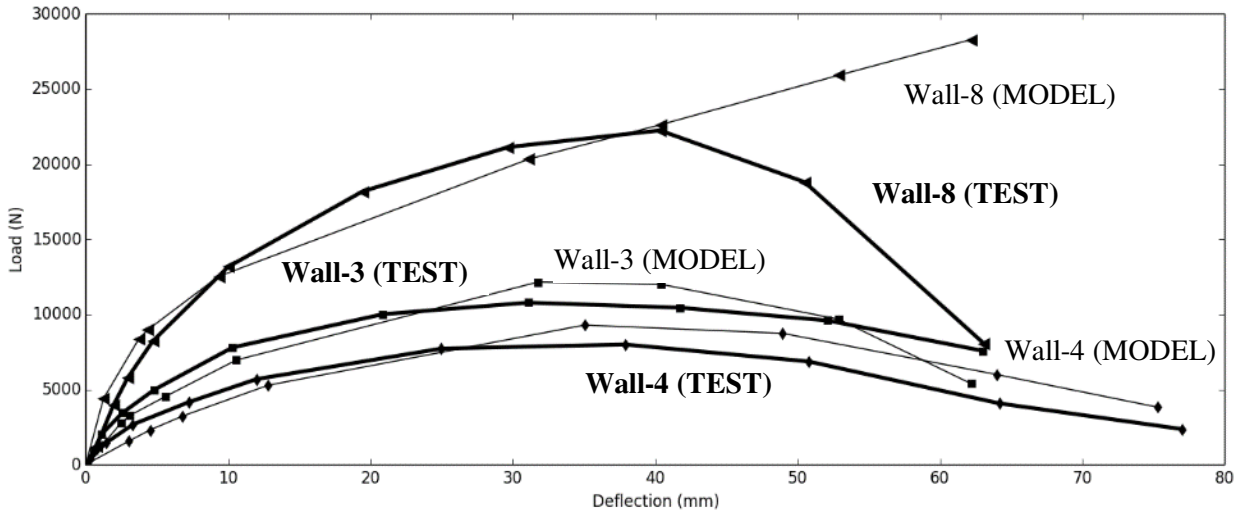

Figure 77: Model and Test Average Envelope Comparison

The results show reasonable fit between the model prediction and those obtained from the shearwall tests. Wall-3 and Wall-4 models seem to accurately predict the behaviour throughout the response range, while the accuracy of predicting the behaviour of Wall-8 is limited up to peak load. The model obviously lacks the ability at this rather extreme case of tight nail/screw spacing to predict the brittle failure mode.

Table 38 presents the results of the EEEP analysis performed on the average backbone curves of the models' hysteresis.

Table 38: Shearwall Models EEEP Analysis Results

MODEL Wall No.	Peak Load (N)	Deflection at Peak Load (mm)	Initial Stiffness (N/mm)	Yield Load (N)	Ductility Ratio ($\Delta u/\Delta_{yield}$)
Wall – 3	12154	31.78	957.59	10218.5	4.93
Wall – 4	9290.1	35.04	505.60	7922.2	3.58
Wall – 8	N/A	N/A	2031.8	N/A	N/A

6.5 Model Discussion

Table 39 presents a comparison, by means of ratios, between the EEEP analysis values obtained for the model and the shearwall tests.

Table 39: Ratios of Values Obtained from the Model to Tested Values

Wall No.	Peak Load	Deflection at Peak Load	Initial Stiffness	Yield Load	Ductility Ratio
Wall – 3-1	1.13	1.01	0.84	1.06	0.74
Wall – 3-2	1.13	1.03	0.84	1.05	0.73
Wall – 4-1	1.20	0.92	0.66	1.15	0.61
Wall – 4-2	1.13	0.93	0.81	1.08	0.79
Wall – 8-1	N/A	N/A	1.18	N/A	N/A
Wall – 8-2	N/A	N/A	1.11	N/A	N/A

As seen in Table 39, the model slightly over-estimates the capacity of the shearwall. The model's prediction of the deflection obtained at the peak load is very close to that obtained from the experimental testing. The predicted initial stiffness is lower than the tested value for Wall-3 and Wall-4 specimens because the actual stiffness will typically be affected by construction details and initial conditions including friction. The ductility ratio was under predicted by the model for Wall-3 and Wall-4 specimens.

Examples showing the comparison between the hysteresis obtained during testing and those obtained from the model for Wall-3 and Wall-4 can be seen in Figure 78 and Figure 79 respectively.

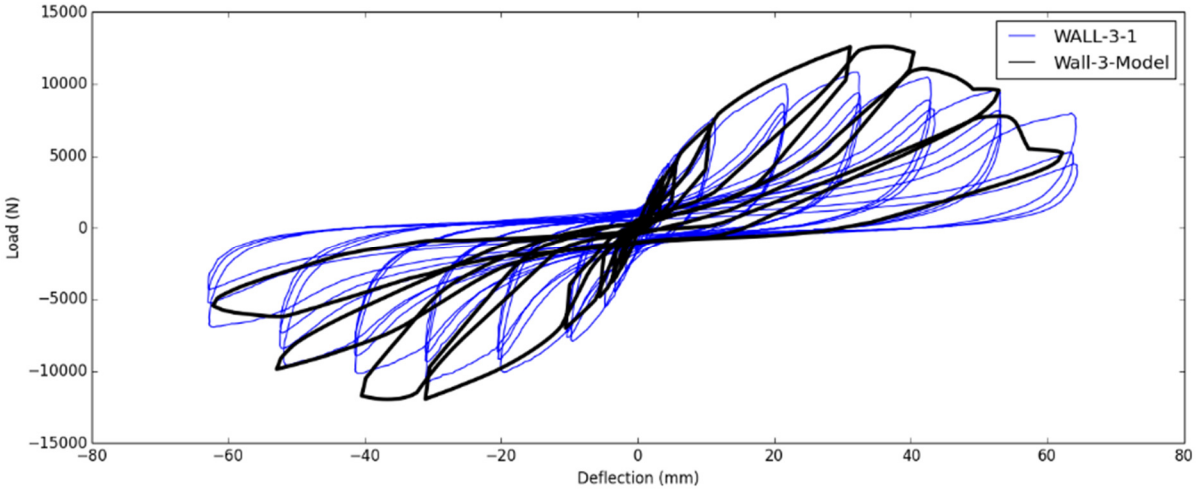

Figure 78: Wall-3 Model and Test Hysteresis Comparison

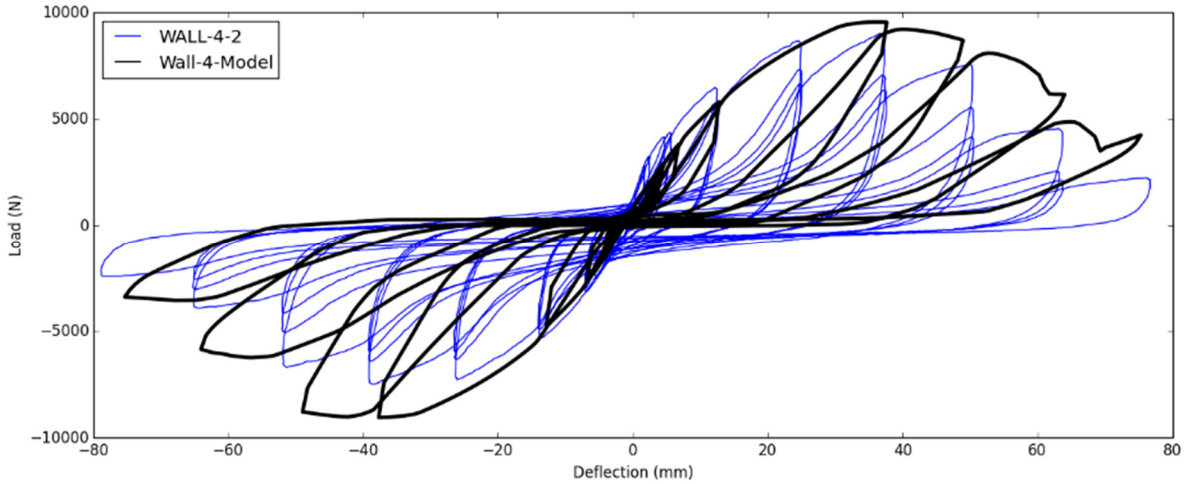

Figure 79: Wall-4 Model and Test Hysteresis Comparison

As seen in Figure 78 and Figure 79, the model is capable of predicting the shearwall behaviour with a reasonable level of accuracy, with the model having a slight tendency to over-estimate the peak capacity. This could be attributed to the fastener's pull-through failure mode, which was observed during shearwall racking testing, and is not represented in the model.

Figure 80 shows the comparison between Wall-8 and the model prediction. There are clearly observable differences between the two behaviours. The reason for the difference is that the model is not able to capture the brittle failure mode observed in the full scale test. Caution should therefore be used when interpreting model results for atypical connectors and for fastener spacing where no experimental data exist.

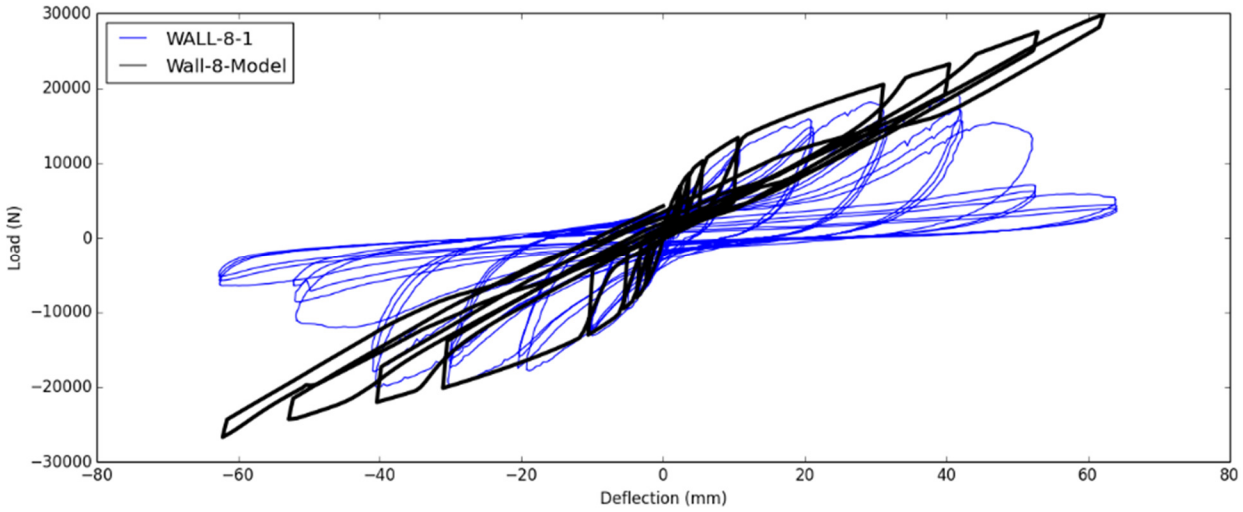

Figure 80: Wall-8 Model and Test Hysteresis Comparison

The results presented here show that it is feasible to predict the overall wall behaviour simply based on joint tests, as long as the failure mode observed in the full scale tests are consistent with failure in the joints only. If the failure mode changes to a more brittle failure mode, relying on joint level behaviour to predict the overall wall behaviour becomes no longer valid.

7.0 CODE CONSIDERATIONS

This chapter attempts to fill the voids currently existing in the Canadian and US timber design standards by introducing a slip model for GWB connected to wood frames walls with nails or screws based on the experimental work in the current study. The chapter also provides arguments that support the ability to predict full scale shearwall strength based on knowledge about joint strength when predictable and consistent failure modes are expected at the shearwall level.

7.1 Existing Code Provisions

7.1.1 Existing Fastener Slip Equations

The Canadian timber design standard (CSA-O86, 2014) currently contains provisions to estimate the deformation for nail fasteners connecting wood-based sheathing panels to stud members, as presented in Equation 7.1.

$$e_n = \left(\frac{0.013 v_s}{d_f^2}\right)^2 \tag{7.1}$$

Where e_n is the joint deflection (mm), v_s is the load per fastener and d_f is the fastener diameter (mm).

The 2014 edition of the design standard (CSA, 2014) was the first edition to introduce provisions related to slip of nail fasteners when GWB panels are used. The standard stipulates that the joint deformation can be taken as 0.76 mm. This provision is consistent with what had been used in the US (NDS, 2012) however it has obvious limitations, as the value of the displacement is constant and independent of the joint configuration and the load level.

The value of 0.76 mm displacement provided by the CSA-O86 was compared to test data obtained from the experimental study in the current project, and it was concluded that although the constant value itself was crude in estimating the displacement, it seemed to align well with the yield point of the joint, as obtained by the EEEP analysis. The tested data that was similar to the proposed value was the joint tests with a No.6 screw.

Replacing the constant value of 0.76 mm with a straight line connecting the origin with the yield point provides a fairly reasonable depiction of the slip behaviour up to that point. This approximation requires of course that one knows where the intersecting point is, and as such a load limit needs to be defined as well.

Figure 81 presents the average backbone load-deflection response of the JS-5 tests (No.6 screw) compared to the linear equation using 0.76 mm as the yield deflection.

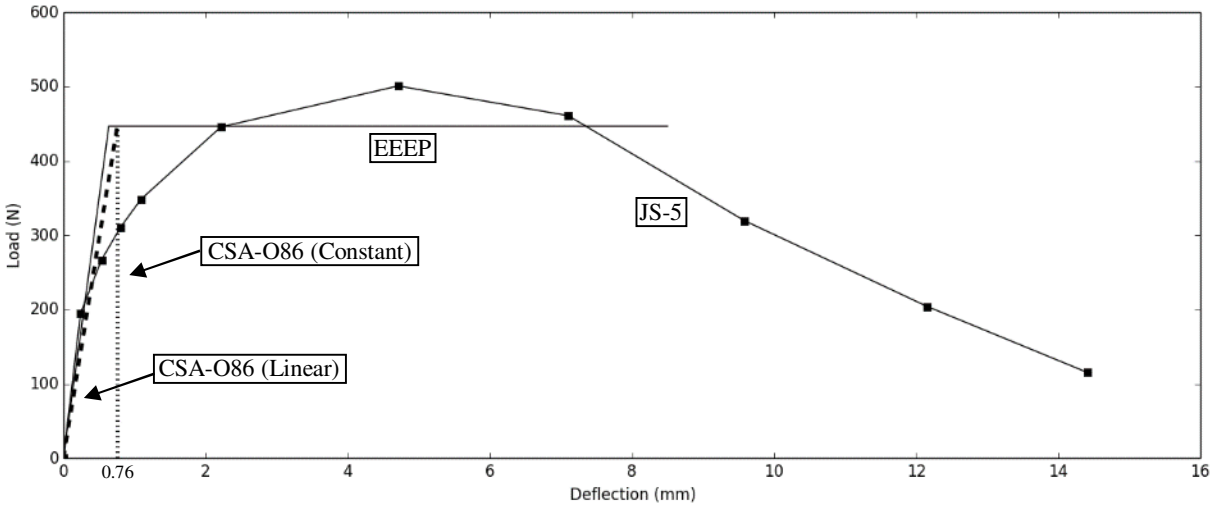

Figure 81: Fastener Slip Prediction Using Current CSA-O86 Standard

Figure 81 provides evidence that the linear equation shown as the dashed line could be a suitable option for GWB joints using the same characteristics as joint test JS-5. The yield point does not stay similar for all test groups, which necessitates a more general and comprehensive equation with joint characteristics as input (GWB density, fastener type and fastener diameter). It is also necessary to improve to accuracy of the fastener slip equation past the yield points, which the newly proposed equation does.

7.1.2 Existing GWB Shearwall Capacity Provisions

The current Canadian timber design standard (CSA-O86, 2014) introduced a new method to determine the shear strength of shearwalls sheathed with wood based panels (OSB and plywood). The method relies of the capacity of the sheathing to framing joints and includes a check to ensure that sheathing panel buckling does not occur. The standard provides strength values for GWB shearwalls based on full scale testing. The Canadian Wood Council Commentary (WDM, 2010) states that the allowable shear force, presented in the tables, are approximately equal to the average ultimate load carrying capacity of tested shearwalls divided by a safety factor of 3. The specified shear strength for GWB shearwalls with 200 mm fastener spacing at panel edges is given directly based on tested capacity, while the capacity values for GWB shearwalls with fastener spacing of 150 mm and 100 mm at panel edges are increased by 25% and 50%, respectively. This method limits the configurations that can potentially be used in design to those tested experimentally. The

proposed model allows for design of GWB shearwalls in a similar fashion to those of wood based panels by comparing and linking the joint level capacity to that of the wall full scale capacity.

7.2 Proposed Changes

7.2.1 Proposed Fastener Slip Equation

The power law model was deemed the best option for a design situation because of its accuracy and simplicity relative to the two other examined model types (exponential and asymptotic). The developed fastener slip equation has a different fixed exponent constant for joints fastened with nails and screws; therefore there are two distinct equations, one for each case. The screw joint equation is developed for type-X 5/8" GWB (9.3 kg/m^2 ≤ γ_{GWB} ≤ 11.0 kg/m^2) fastened with No.6 (d_s = 3.80 mm), No.8 (d_s = 4.31 mm) or No.10 (d_s = 4.69 mm) GWB screws.

The joint slip, e_n, may be calculated using equation 7.2a or 7.2b and equation 7.3, for GWB joints using screws and nails, respectively.

Screw Joints:

$$e_n = (4.92 - 0.42\gamma_{GWB})(4.926 - d_s)\left(0.0026v_f\right)^{5.5} \tag{7.2a}$$

The same equation can be slightly altered to follow the CSA-O86 format.

$$e_n = (4.92 - 0.42\gamma_{GWB})\left(\frac{0.016v_f}{d_s^{1.33}}\right)^{5.5} \tag{7.2b}$$

The nail joint equation is developed for type-X 5/8" GWB (9.3 kg/m^2 ≤ γ_{GWB} ≤ 11.0 kg/m^2) fastened with 12.5 gauge nails.

Nail Joints:

$$e_n = (2.64 - 0.18\gamma_{GWB})\left(0.0037v_f\right)^{3.0} \tag{7.3}$$

In which,

e_n: Fastener Deformation (mm)

γ_{GWB}: Type-X Gypsum wallboard weight per area (kg/m^2)

d_s: Diameter of screw – including threads (mm)

v_f: Load per fastener (N)

7.2.2 Proposed GWB Shearwall Capacity Provision

It is proposed that the factored shear resistance for a shearwall segment with GWB sheathing panels be taken as the smaller resistance governed by the sheathing-to-framing connection (a), or sheathing panel buckling (b). The sheathing-to-framing connection resistance equation will include factors to adjust strength for fastener spacing, and account for blocking and hold-down. The specified strength of the shearwall for part (a) is proposed to be based on the lateral strength resistance of the sheathing-to-framing connection along the panel edges, per fastener. This value will be calculated based on the European Yield Model equations with the lumber as the main member and the GWB as the side member. It was shown in the Discussion Chapter (Chapter 5) that using the capacity of the individual components of the connection (fastener bending moment capacity, GWB embedment strength and lumber embedment strength) as part of the Johansen Yielding Equation; it was possible to calculate the capacity of the joint with relatively good accuracy.

In Chapter 5 the embedment equation for GWB was developed, as function of its density and the fastener diameter used, and can therefore be expressed as:

$$f = 12G\left(1 - 0.02d_f\right) \tag{7.5}$$

It is important to note that the values obtained using equation 7.5 are yield strength values which have not been modified for design level. In addition, more tests are required to ensure the accuracy of the developed equation because of the relatively high variability within and between each manufacturer.

7.3 Proposed Changes Comparison to Existing Code

7.3.1 Fastener Slip Equations Comparison

In the Discussion section (Chapter 5), the deflection of the full-scale shearwall was calculated using the CSA-O86 shearwall deflection equation with the aid of the developed fastener slip models. The fastener slip models used in the Chapter 5 comparisons are based on curve fitting of joint level tests with the same construction characteristics and manufacturers as the full scale shearwall tests. The following comparisons are made using the same shearwall deflection equation proposed by the CSA-O86 but utilizing equations 7.2 and 7.3, which both take into account the material variability inherent to the different manufacturers. Wall-3, Wall-5, Wall-6 and Wall-7 specimens utilize the No.6 GWB screw as a fastener and the Wall-4 specimen uses the 12.5 gauge GWB nail. All shearwalls are constructed with type-X GWB, with a weight

per area of 11 kg/m^2. Figure 82 and Figure 83 present the load-deflection prediction compared to test data for shearwalls fastened with screws and nails, respectively.

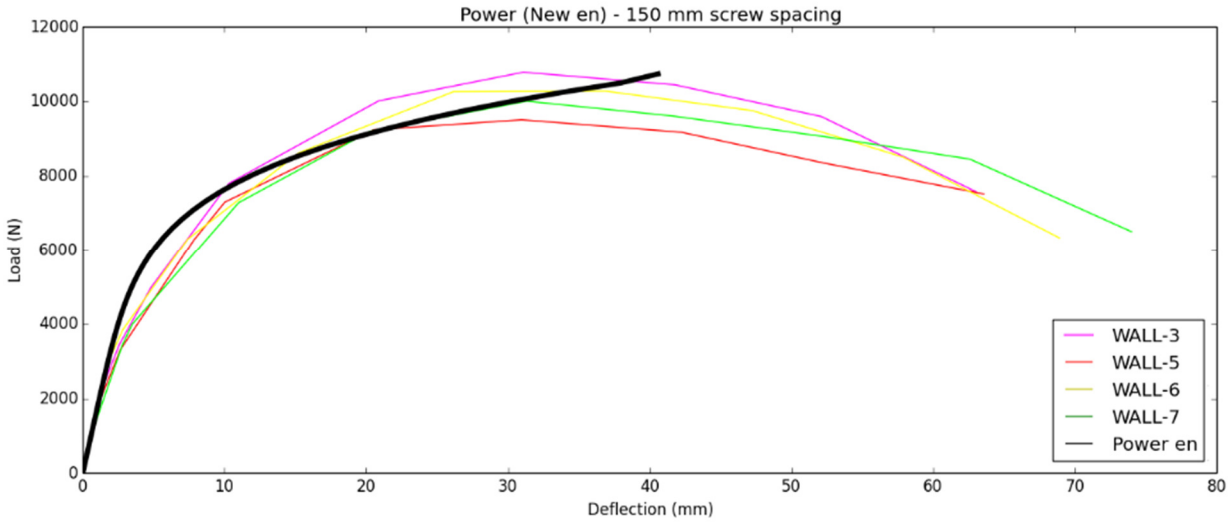

Figure 82: Power Model Fastener Equation - 150 mm Screw Spacing

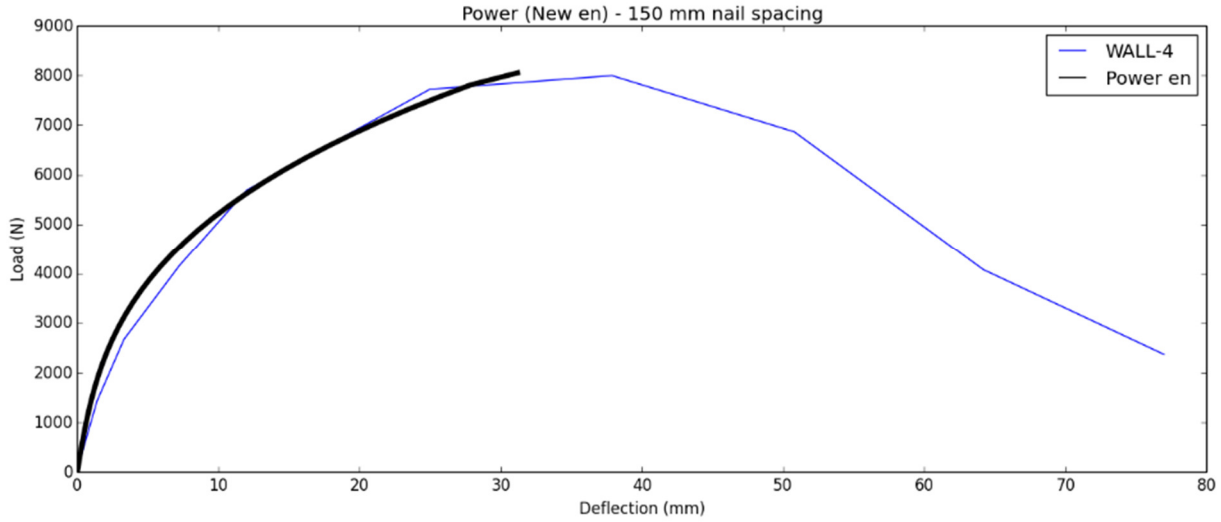

Figure 83: Power Model Fastener Equation - 150 mm Nail Spacing

It is evident from Figure 82 and Figure 83 that the proposed fastener slip equation significantly improves the prediction of the joint slip compared to existing provisions. A non-linear model is essential to capturing the entirety of the response in order to provide an accurate estimation of the deflection and stiffness.

7.3.2 GWB Shearwall Capacity Comparison

In order to demonstrate the applicability of using the joint level capacity to describe the capacity of the full scale shearwall, the tested peak load of the shearwall was compared to the peak load obtained from the joint level capacity The JS-24 tests have the same construction characteristics as the Wall-3, Wall-5, Wall-6, Wall-7 and Wall-8 shearwalls and JS-25 tests have the construction characteristics as the Wall-4 shearwalls. The values presented in Table 40 are the values obtained from the full scale tests and those obtained from the joint level capacity multiplied by the number of fasteners at the edge of the shearwall. Table 40 shows the comparisons in terms of percentage difference.

Table 40: Joint Level to Shearwall Peak Load Comparison

Wall No.	Peak Load (N)	Peak Load based on Joint Tests (N)*	% Difference
Wall – 3-1	10780	10761	0.17 %
Wall – 3-2	10785	10761	0.22 %
Wall – 4-1	7760.0	8154	5.08 %
Wall – 4-2	8235.0	8154	0.98 %
Wall – 5-1	9505.0	10761	13.22 %
Wall – 6-1	10025	10761	7.35 %
Wall – 6-2	10915	10761	1.41 %
Wall – 7-1	10005	10761	7.56 %
Wall – 8-1	19375	32284	66.63 %
Wall – 8-2	25145	32284	28.39 %

$*P = Joint\ Capacity(Length\ of\ wall/fastener\ spacing)$

The percentage difference, presented in column 4 of Table 40, is the difference between the tested peak load of the shearwall and the calculated peak load based on the joint level capacity. This comparison results in a relatively good fit between the two values but some obvious limitations exist. For Wall-3, Wall-4, Wall-5, Wall-6 and Wall-7 configurations, the difference for the compared values are low. Excluding the Wall-8 configuration, the average error is 4.50% with a maximum error of 13.2%. The Wall-8 configuration, which has a fastener spacing of 50 mm at the panel edges and had a brittle failure mode, a very large difference between the two compared values exists. It will be important to limit the fastener spacing or to take the reduced capacity into account if such an approach is implemented in the design standard.

8.0 SUMMARY AND CONCLUSIONS

8.1 Summary

As part of this study, 270 GWB sheathed joints were subjected to reversed cyclic loading with variations including GWB type, GWB thickness, fastener type, fastener size and manufacturer variations for all materials. Curve fitting analysis and comparisons were completed from the resulting load-deflection responses. In turn, the curve fitting analysis aided in the development of fastener slip equations for GWB sheathed joints fastened with either GWB nails or GWB screws.

Component testing was performed on the GWB and the fasteners. The embedding strength of the different GWB types and manufacturers were obtained through testing and a GWB embedment strength equation was developed. The bending yield capacity of the fasteners were obtained through center point bending tests. The component test results were used as part of established yield models to calculate the joint capacity and compared to the tested joint capacity.

A total of 12 full-scale GWB sheathed shearwalls were tested and subjected to the same reversed cyclic loading as the joint level tests. The parameters studied during the shearwalls testing were fastener type, fastener spacing at panel edges and panel end/edge distance. The load-deflection responses were compared to determine the effect of the parameters and the responses were compared to calculated deflection based on the CSA-O86 four term deflection equation with the newly developed fastener slip equations.

8.2 Conclusions

The conclusions from this study are as follows:

1) For both the joint level and the full scale tests it was observed that the displacement protocol has a significant effect on the load-displacement response of the specimen and that a cyclic loading protocol is more appropriate when investigating the behaviour of shearwalls with GWB panels.
2) The construction parameters which affect the load-deflection response of GWB sheathed joints were identified as GWB type, GWB density, fastener size, and fastener type.
3) The power model was found to be the most suitable to describe the fastener slip behaviour. A strong emphasis was placed on the simplicity of the model for the purpose of design. It was shown, however, that all considered models could be used to predict the shear wall behaviour with reasonable accuracy.

4) It was found that the joint level capacity could be calculated using the component capacities in the European Yield Model. It was also found that the shearwall capacity could be predicted by considering the joint level capacity while accounting for the number of joints at a panel edge.
5) The construction parameters which affect the load-deflection response of GWB sheathed shearwalls were found to be: fastener type and fastener spacing at panel edge. The shearwalls with fastener spacing of 50 mm at the panel edge led to brittle failure mode compared to a spacing of 150 mm and did not reach the calculated peak capacity. The fastener panel edge/end distance did not have an impact on the response of the shearwall, when varying the distance between 9 mm and 19 mm.
6) The GWB sheathed shearwall deflection could be calculated using the CSA-O86 four term deflection equation when the proposed fastener slip equation is incorporated into the deflection equation. The proposed equation represents a significant improvement to the existing CSA-O86 recommendation.
7) A GWB shearwall analytical model, using the joint level hysteresis and shearwall geometry as input, was used to validate full-scale GWB hysteresis results. A limitation to the model was identified for walls with fastener spacing that falls outside the code provisions.

9.0 REFERENCES

American Forest & Paper Association, Inc., 2005. "National Design Specifications (NDS) for Wood Construction with Commentary and Supplement: Design Values for Wood Construction 2005 Edition.

ASTM. 2005. Standard Specification for Driven Fasteners: Nails, Spikes and Staples. ASTM F1667-05, American Society for Testing and Materials. West Conshohocken, PA, US.

ASTM. 2007. Standard Test Methods for Specific Gravity of Wood and Wood-Based Materials. ASTM D2395-07a, American Society for Testing and Materials. West Conshohocken, PA, US.

ASTM. 2007. Standard Test Methods for Direct Moisture Content Measurement of Wood and Wood-Based Materials. ASTM D4442-07, American Society for Testing and Materials. West Conshohocken, PA, US.

ASTM. 2009. Standard Specification for Nails for the Application of Gypsum Board. ASTM C514-04, American Society for Testing and Materials. West Conshohocken, PA, US.

ASTM. 2011. Standard Test Methods for Cyclic (Reversed) Load Test for Shear Resistance of Vertical Elements of the Lateral Force Resisting Systems for Buildings. ASTM E2126-11, American Society for Testing and Materials. West Conshohocken, PA, US.

ASTM. 2012. Standard Test Methods for Mechanical Fasteners in Wood. ASTM D1761-12, American Society for Testing and Materials. West Conshohocken, PA, US.

ASTM. 2012. Standard Test Methods for Physical Testing of Gypsum Panel Products. ASTM C473-12, American Society for Testing and Materials. West Conshohocken, PA, US.

ASTM. 2012. Standard Practice for Static Load Test for Shear Resistance of Framed Walls for Buildings. ASTM E564-06, American Society for Testing and Materials. West Conshohocken, PA, US.

ASTM. 2013. Standard Specification for Steel Self-Piercing Tapping Screws for the Application of Gypsum Panel Products or Metal Plaster Bases to Wood Studs or Steel Studs. ASTM C1002-07, American Society for Testing and Materials. West Conshohocken, PA, US.

ASTM. 2013. Standard Specification for Gypsum Board. ASTM C1396/C1396M-13, American Society for Testing and Materials. West Conshohocken, PA, US.

ASTM. 2013. Standard Specification for Steel Self-Piercing Tapping Screws for the Application of Gypsum Panel Products or Metal Plaster Bases to Wood Studs or Steel Studs. ASTM C1002-07, American Society for Testing and Materials. West Conshohocken, PA, US.

ASTM. 2013. Standard Practice for Force Verification of Testing Machines. ASTM E4-13, American Society for Testing and Materials. West Conshohocken, PA, US.

ASTM. 2013. Standard Test Methods for Determining Bending Yield Moment of Nails. ASTM F1575-03, American Society for Testing and Materials. West Conshohocken, PA, US.

ASTM. 2013. Standard Test Method for Evaluating Dowel-Bearing Strength of Wood and Wood-Based Products. ASTM D5764, American Society for Testing and Materials. West Conshohocken, PA, US.

CWC. 2005. Wood Design Manual. Canadian Wood Council. Ottawa, ON.

Dolan, D. J., and Madsen, B., 1992. "Monotonic and Cyclic Nail Connection Tests," *Canadian Journal of Civil Engineering,* vol. 19, no. 3, pp. 97-104.

Dolan, D. J., and Madsen, B., 1992. "Monotonic and Cyclic Tests of Timber Shear Walls," *Canadian Journal of Civil Engineering,* vol. 19, no. 3, pp. 415-422.

Falk, R. H., and Itani, R. Y, 1987. "Monotonic and Cyclic Tests of Timber Shear Walls," *Journal of Structural Engineering,* vol. 113, no. 6, pp. 1357-1370.

Folz, B., and Filiatrault, A., 2001. "Cyclic Analysis of Wood Shear Walls," *Journal of Structural Engineering,* vol. 127, pp. 433-441.

Foschi, R. O., 1974. “Load-Slip Characteristics of Nailed Joints,” *Journal of Wood Science,* vol. 7, No. 1, pp. 69-76.

Foschi, R. O., and Bonac, T., 1977. “Load-Slip Characteristics for Connections with Common Nails,” *Journal of Wood Science,* vol. 9, No. 3, pp. 118-123.

Goodall, S. and Gupta, R., 2011. ”Improving the Performance of Gypsum Wallboard in Wood Frame Shear Walls.” J. Perform. Constr. Facil., 25(4), 287–298.

Gupta, A. K., and Kuo, G. P., 1984. “Behavior of Wood-Framed Shear Walls,” *Journal of Structural Engineering,* vol. 111, no. 8, pp. 1722-1733.

Gypsum Association, 2015. “What is Gypsum?” www.gypsum.org/about/gypsum-101/what-is-gypsum.

Gypsum Association, 2015. “What is Gypsum Board?” www.gypsum.org/about/gypsum-101/gypsum-board.

Gypsum Association, 2015. “Making Gypsum Board” www.gypsum.org/about/gypsum-101/making-gypsum-board.

Hunt, R. D., and Bryant, A. H., 1990. “Laterally Loaded Nail Joints in Wood,” *Journal of Structural Engineering,* vol. 116, no. 1, pp. 111-124.

Johansen, K. W., 1949. “Theory of Timber Connections,” IABSE Publications. Copenhagen, Denmark.

Karacabeyli, E. and Ceccotti, A., 1996. “Test results on the lateral resistance of nailed shear walls.” *Proceedings,* International Wood Engineering Conference, Baton Rouge, LO.

McCutcheon, B., 1985. “Racking Deformations in Wood Shear Walls,” *Journal of Structural Engineering,* vol. 111, no. 2, pp. 257-269.

McMullin, K. M., and Merrick, D., 2001. “Seismic Performance of Gypsum Walls – Experimental Test Program,” *San Jose State University*, San Jose, CA.

Memari, A. M., and Solnosky, R. L., 2014. "In-Plane Shear Performance of Wood-Framed Drywall Sheathing Wall Systems under Cyclic Racking Loading," *Open Journal of Civil Engineering,* vol. 4, pp. 54-70.

Oliva, Michael G., 1990. "Racking Behavior of Wood-Framed Gypsum Panels under Dynamic Load," Report No. UCB/EERC-85/06, Earthquake Engineering Research Center, University of California, Berkeley.

Parsons, W. R., 2001. "Energy-Based Modelling of Dowel-Type Connections in Wood-Plastic Composite Hollow Sections," M.Sc. Thesis, Washington State University, Pullman, WA, US.

Pelicane, P. J., Stone, J. L., and Vanderbilt, M. D., 1991. "Generalized Model for Lateral Load Slip of Nailed Joints," *Journal of Materials in Civil Engineering,* vol. 3, No.1, pp. 60-77.

Plesnik, T., 2014. "Effect of an Intermediate Material Layer on the Lateral Load-Slip Characteristics of Nailed Joints," M.App.Sc. Thesis, Carleton University, Ottawa, ON, Canada.

Sà Ribeiro, R. A., and Pellicane, P. J., 1992. "Modeling Load-Slip Behavior of Nailed Joints," *Journal of Structural Engineering,* vol. 4, no. 4, pp. 385-398.

Seaders, P., Gupta, R., and Miller, T. H., 2009. "Monotonic and Cyclic Load Testing of Partially and Fully Anchored Wood-Frame Shear Walls," *Wood and Fiber Science,* vol. 41, No.2, pp. 146-156.

Shenton III, H. W., Dinehart, D. W., and Eliott, T. E., 1998. "Stiffness and Energy Degradation of Wood Frame Shear Walls," *Canadian Journal of Civil Engineering,* vol. 25, pp. 412-423.

Smart, J. V., 2002. "Capacity Resistance and Performance of Single-Shear Bolted and Nailed Connections: An Experimental Investigation," M.Sc. Thesis, Virginia Polytechnic Institute, Blacksburg, VA, US.

Toothman, A. J., 2003. "Monotonic and Cyclic Performance of Light-Frame Shear Walls with Various Sheathing Materials," M.Sc. Thesis, Virginia Polytechnic Institute, Blacksburg, VA, US.

White, M. W., and Dolan, J. D., 1995. "Nonlinear Shear-Wall Analysis," *Journal of Structural Engineering,* vol. 121, pp. 1629-1635.

Wolf, R. W., 1984. "Contribution of Gypsum Wallboard to Racking Resistance of Light-Frame Walls," United States Department of Agriculture. Madison, Wis, US.

Zacker, Edwin G. and Gray, Ralph Gareth, 1985. “Dynamic Tests of Wood Framed Shear Walls.” *Proceedings,* Structural Engineers Association of California Annual Convention. San Diego, CA.

Zhou, T., and Guan, Z., 2006. “Review of Existing and Newly Developed Approaches to Obtain Timber Embedding Strength,” *Prog. Struct. Engng Mater.,* vol. 8, pp. 49-67.

10.0 APPENDIX

10.1 Appendix A: Summary of Results for Full Scale Shearwall Specimens

Specimen Number	Wall-3-1	**EEEP Results**	
Sheathing Thickness (GWB)	5/8" (15.9mm)	**Peak Load (N)**	10780
Fastener Type	Screw	**Displacement at peak (mm)**	31.335
Fastener Size	No.6	**Initial Stiffness (N/mm)**	1134.72
Panel End/Edge Distance	Setup 1	**Yield Load (N)**	9620.5
Fastener Spacing at Panel Edges	150 mm	**Ductility Ratio ($\Delta u/\Delta_{yield}$)**	6.69
Loading Type	Cyclical		
Top and Bottom Plates Relative Density	Plate 1	0.46	Average: 0.42
	Plate 2	0.37	COV (%): 9.83
	Plate 3	0.35	
Vertical Stud Relative Density	Stud 1	0.41	
	Stud 2	0.38	
	Stud 3	0.46	
	Stud 4	0.46	
	Stud 5	0.43	
	Stud 6	0.44	
	Stud 7	0.46	
	Stud 8	0.41	
	Stud 9	0.37	

Hysteresis

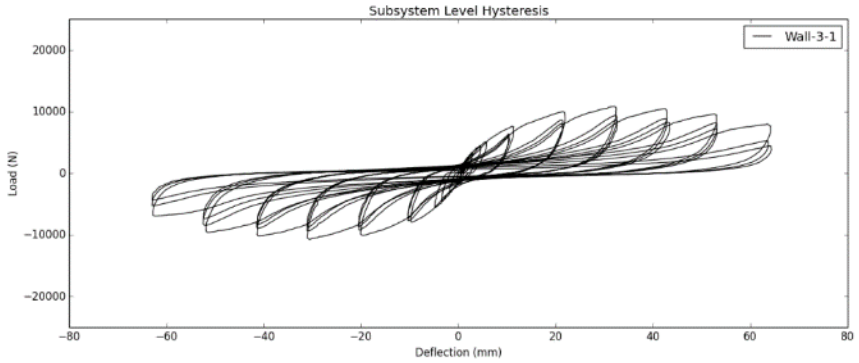

Specimen Number	Wall-3-2	**EEEP Results**	
Sheathing Thickness (GWB)	5/8" (15.9mm)	**Peak Load (N)**	10785
Fastener Type	Screw	**Displacement at peak (mm)**	30.86
Fastener Size	No.6	**Initial Stiffness (N/mm)**	1136.46
Panel End/Edge Distance	Setup 1	**Yield Load (N)**	9768.61
Fastener Spacing at Panel Edges	150 mm	**Ductility Ratio ($\Delta u/\Delta_{yield}$)**	6.74
Loading Type	Cyclical		
Top and Bottom Plates Relative Density	Plate 1	0.44	Average: 0.42
	Plate 2	0.42	COV (%): 6.92
	Plate 3	0.39	
Vertical Stud Relative Density	Stud 1	0.45	
	Stud 2	0.44	
	Stud 3	0.45	
	Stud 4	0.37	
	Stud 5	0.45	
	Stud 6	0.40	
	Stud 7	0.43	
	Stud 8	0.44	
	Stud 9	0.38	

Hysteresis

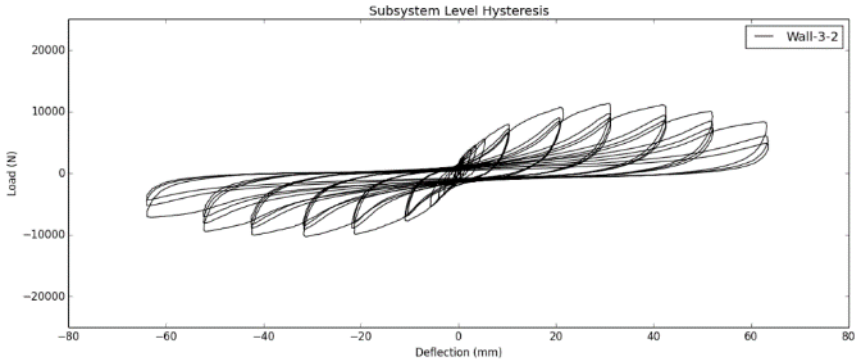

Specimen Number	Wall-4-1	**EEEP Results**	
Sheathing Thickness (GWB)	5/8" (15.9mm)	**Peak Load (N)**	7760
Fastener Type	Nail	**Displacement at peak (mm)**	38.03
Fastener Size	12.5 gauge	**Initial Stiffness (N/mm)**	771.33
Panel End/Edge Distance	Setup 1	**Yield Load (N)**	6916.00
Fastener Spacing at Panel Edges	150 mm	**Ductility Ratio ($\Delta u/\Delta_{yield}$)**	5.90
Loading Type	Cyclical		
Top and Bottom Plates Relative Density	Plate 1	0.42	Average: 0.42
	Plate 2	0.39	COV (%): 8.14
	Plate 3	0.51	
Vertical Stud Relative Density	Stud 1	0.41	
	Stud 2	0.43	
	Stud 3	0.40	
	Stud 4	0.41	
	Stud 5	0.41	
	Stud 6	0.43	
	Stud 7	0.40	
	Stud 8	0.40	
	Stud 9	0.47	

Hysteresis

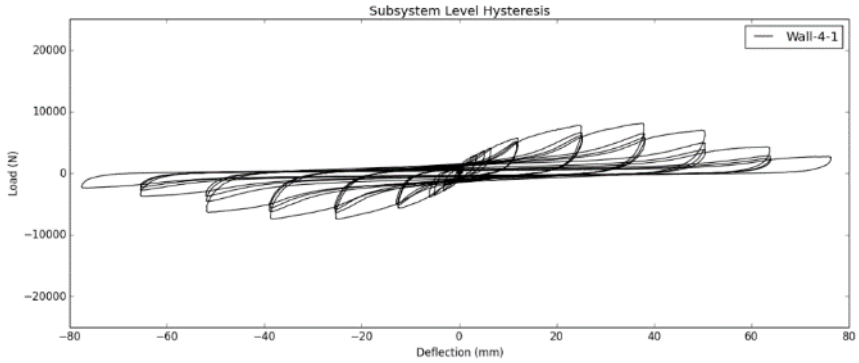

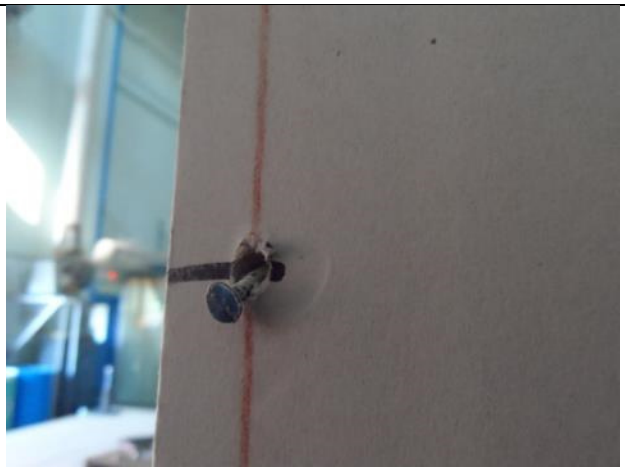

Specimen Number	Wall-4-2	**EEEP Results**	
Sheathing Thickness (GWB)	5/8" (15.9mm)	**Peak Load (N)**	8235.0
Fastener Type	Nail	**Displacement at peak (mm)**	37.73
Fastener Size	12.5 gauge	**Initial Stiffness (N/mm)**	627.05
Panel End/Edge Distance	Setup 1	**Yield Load (N)**	7340.4
Fastener Spacing at Panel Edges	150 mm	**Ductility Ratio ($\Delta u/\Delta_{yield}$)**	4.54
Loading Type	Cyclical		
Top and Bottom Plates Relative Density	Plate 1	0.39	Average: 0.42
	Plate 2	0.44	COV (%): 8.30
	Plate 3	0.40	
Vertical Stud Relative Density	Stud 1	0.38	
	Stud 2	0.39	
	Stud 3	0.39	
	Stud 4	0.38	
	Stud 5	0.39	
	Stud 6	0.45	
	Stud 7	0.46	
	Stud 8	0.46	
	Stud 9	0.46	

Hysteresis

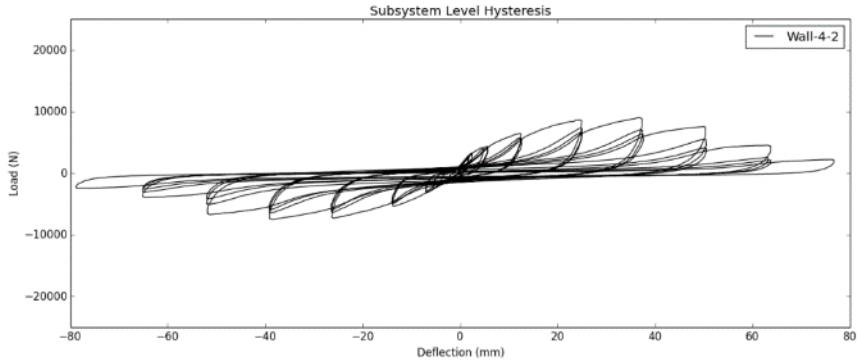

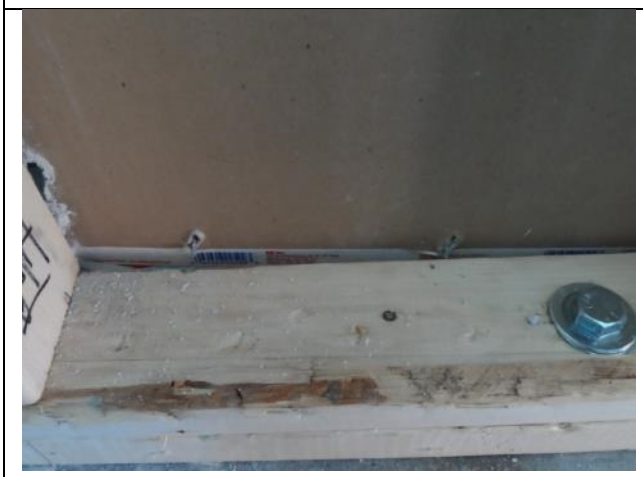

Specimen Number	Wall-5-1	**EEEP Results**	
Sheathing Thickness (GWB)	5/8" (15.9mm)	**Peak Load (N)**	9505.0
Fastener Type	Screw	**Displacement at peak (mm)**	30.97
Fastener Size	No.6	**Initial Stiffness (N/mm)**	1081.34
Panel End/Edge Distance	Setup 1	**Yield Load (N)**	8613.89
Fastener Spacing at Panel Edges	150 mm	**Ductility Ratio ($\Delta u/\Delta_{yield}$)**	7.83
Loading Type	Cyclical		
Top and Bottom Plates Relative Density	Plate 1	0.37	Average: 0.42
	Plate 2	0.39	COV (%): 9.17
	Plate 3	0.46	
Vertical Stud Relative Density	Stud 1	0.39	
	Stud 2	0.46	
	Stud 3	0.46	
	Stud 4	0.39	
	Stud 5	0.38	
	Stud 6	0.44	
	Stud 7	0.37	
	Stud 8	0.43	
	Stud 9	0.46	

Hysteresis

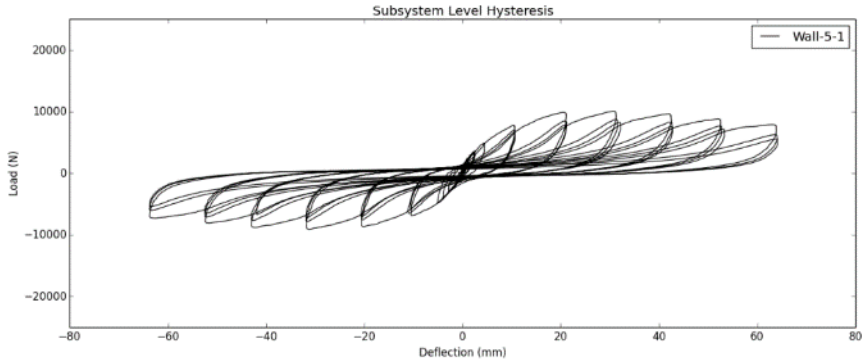

Specimen Number	Wall-6-1	**EEEP Results**	
Sheathing Thickness (GWB)	5/8” (15.9mm)	**Peak Load (N)**	10025
Fastener Type	Screw	**Displacement at peak (mm)**	31.26
Fastener Size	No.6	**Initial Stiffness (N/mm)**	1273.23
Panel End/Edge Distance	Setup 3	**Yield Load (N)**	8882.30
Fastener Spacing at Panel Edges	150 mm	**Ductility Ratio ($\Delta u/\Delta_{yield}$)**	8.62
Loading Type	Cyclical		
Top and Bottom Plates Relative Density	Plate 1	0.42	Average: 0.41
	Plate 2	0.39	COV (%): 5.40
	Plate 3	0.41	
Vertical Stud Relative Density	Stud 1	0.40	
	Stud 2	0.40	
	Stud 3	0.43	
	Stud 4	0.40	
	Stud 5	0.39	
	Stud 6	0.41	
	Stud 7	0.47	
	Stud 8	0.42	
	Stud 9	0.43	

Hysteresis

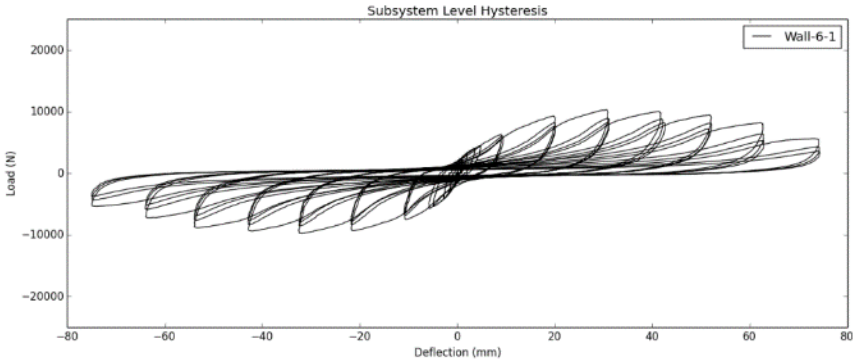

Specimen Number	Wall-6-2	**EEEP Results**	
Sheathing Thickness (GWB)	5/8" (15.9mm)	**Peak Load (N)**	10915
Fastener Type	Screw	**Displacement at peak (mm)**	31.76
Fastener Size	No.6	**Initial Stiffness (N/mm)**	1270.43
Panel End/Edge Distance	Setup 3	**Yield Load (N)**	9830.28
Fastener Spacing at Panel Edges	150 mm	**Ductility Ratio ($\Delta u/\Delta_{yield}$)**	7.26
Loading Type	Cyclical		
Top and Bottom Plates Relative Density	Plate 1	0.37	Average: 0.42
	Plate 2	0.45	COV (%): 8.88
	Plate 3	0.40	
Vertical Stud Relative Density	Stud 1	0.48	
	Stud 2	0.44	
	Stud 3	0.39	
	Stud 4	0.38	
	Stud 5	0.40	
	Stud 6	0.40	
	Stud 7	0.38	
	Stud 8	0.45	
	Stud 9	0.46	

Hysteresis

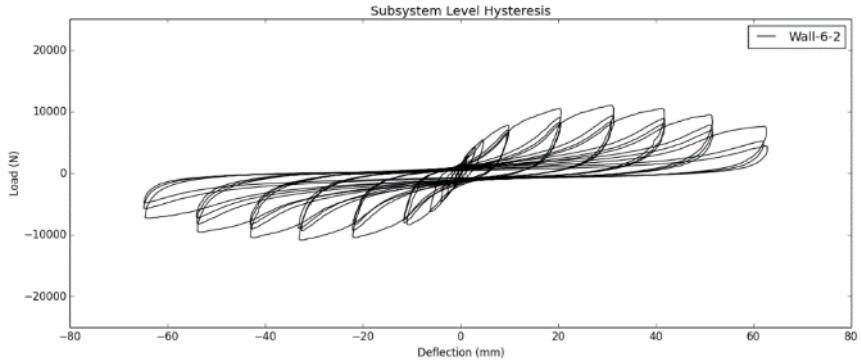

Specimen Number	Wall-7-1	**EEEP Results**	
Sheathing Thickness (GWB)	5/8" (15.9mm)	**Peak Load (N)**	10005
Fastener Type	Screw	**Displacement at peak (mm)**	31.3
Fastener Size	No.6	**Initial Stiffness (N/mm)**	1140.2
Panel End/Edge Distance	Setup 4	**Yield Load (N)**	8887.1
Fastener Spacing at Panel Edges	150 mm	**Ductility Ratio ($\Delta u/\Delta_{yield}$)**	8.37
Loading Type	Cyclical		
Top and Bottom Plates Relative Density	Plate 1	0.45	Average: 0.42
	Plate 2	0.39	COV (%): 7.68
	Plate 3	0.35	
Vertical Stud Relative Density	Stud 1	0.43	
	Stud 2	0.43	
	Stud 3	0.43	
	Stud 4	0.47	
	Stud 5	0.41	
	Stud 6	0.44	
	Stud 7	0.39	
	Stud 8	0.41	
	Stud 9	0.40	

Hysteresis

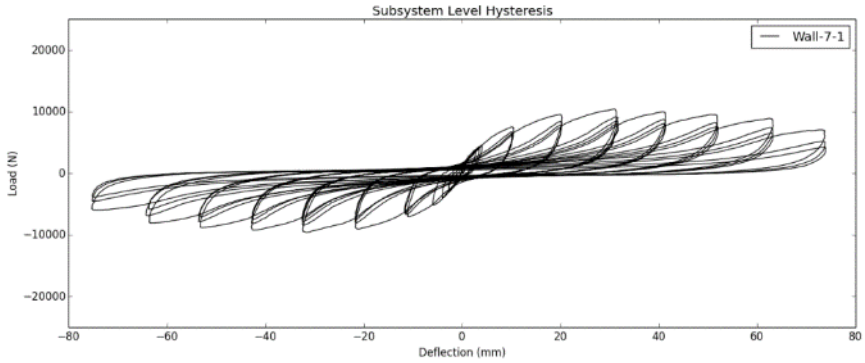

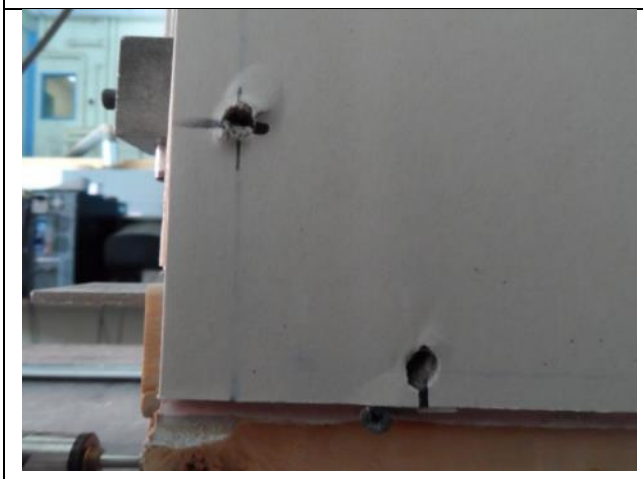

Specimen Number	Wall-8-1	**EEEP Results**	
Sheathing Thickness (GWB)	5/8" (15.9mm)	**Peak Load (N)**	19375
Fastener Type	Screw	**Displacement at peak (mm)**	41.13
Fastener Size	No.6	**Initial Stiffness (N/mm)**	1728.2
Panel End/Edge Distance	Setup 1	**Yield Load (N)**	16971.59
Fastener Spacing at Panel Edges	50 mm	**Ductility Ratio ($\Delta u/\Delta_{yield}$)**	4.80
Loading Type	Cyclical		
Top and Bottom Plates Relative Density	Plate 1	0.49	Average: 0.42
	Plate 2	0.35	COV (%): 9.55
	Plate 3	0.38	
Vertical Stud Relative Density	Stud 1	0.46	
	Stud 2	0.47	
	Stud 3	0.40	
	Stud 4	0.44	
	Stud 5	0.42	
	Stud 6	0.40	
	Stud 7	0.40	
	Stud 8	0.41	
	Stud 9	0.40	

Hysteresis

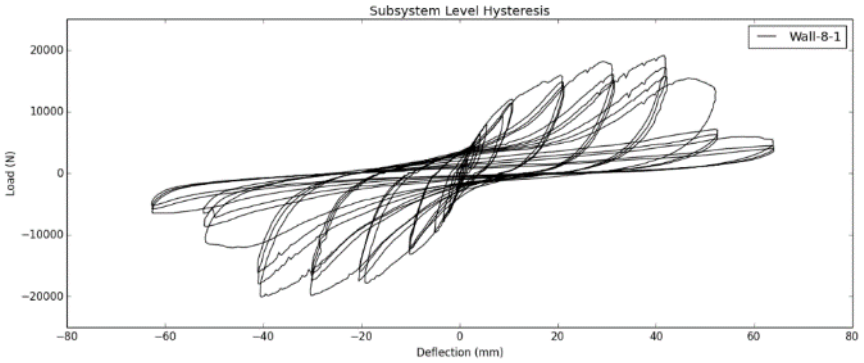

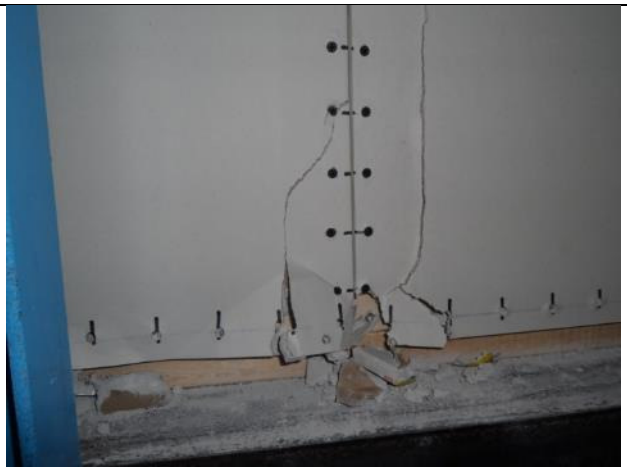

Specimen Number	Wall-8-2	**EEEP Results**	
Sheathing Thickness (GWB)	5/8" (15.9mm)	**Peak Load (N)**	25145.0
Fastener Type	Screw	**Displacement at peak (mm)**	39.54
Fastener Size	No.6	**Initial Stiffness (N/mm)**	1834.2
Panel End/Edge Distance	Setup 1	**Yield Load (N)**	21910.76
Fastener Spacing at Panel Edges	50 mm	**Ductility Ratio ($\Delta u/\Delta_{yield}$)**	4.52
Loading Type	Cyclical		
Top and Bottom Plates Relative Density	Plate 1	0.37	Average: 0.42
	Plate 2	0.39	COV (%): 11.30
	Plate 3	0.49	
Vertical Stud Relative Density	Stud 1	0.46	
	Stud 2	0.45	
	Stud 3	0.45	
	Stud 4	0.38	
	Stud 5	0.35	
	Stud 6	0.46	
	Stud 7	0.46	
	Stud 8	0.38	
	Stud 9	0.38	

Hysteresis

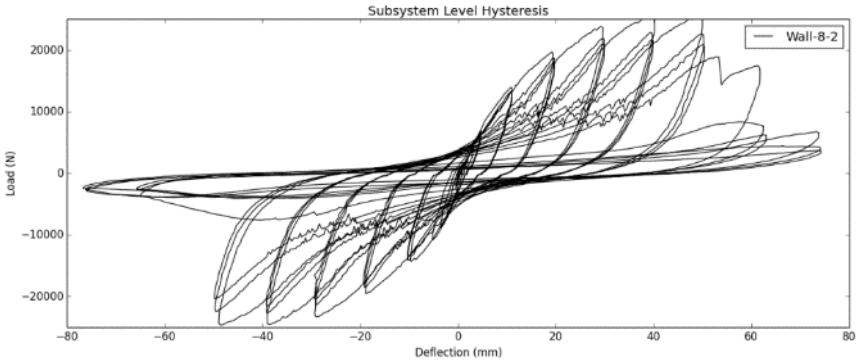

10.2 Appendix B: Paraneter Trends used to develop fastener slip models

Parameter A Trend

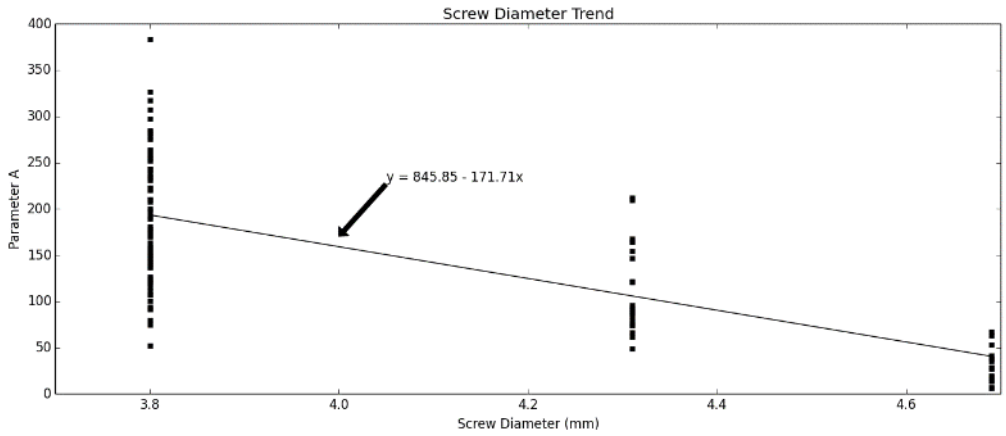

Figure 84: Screw Diameter Trend – Parameter A

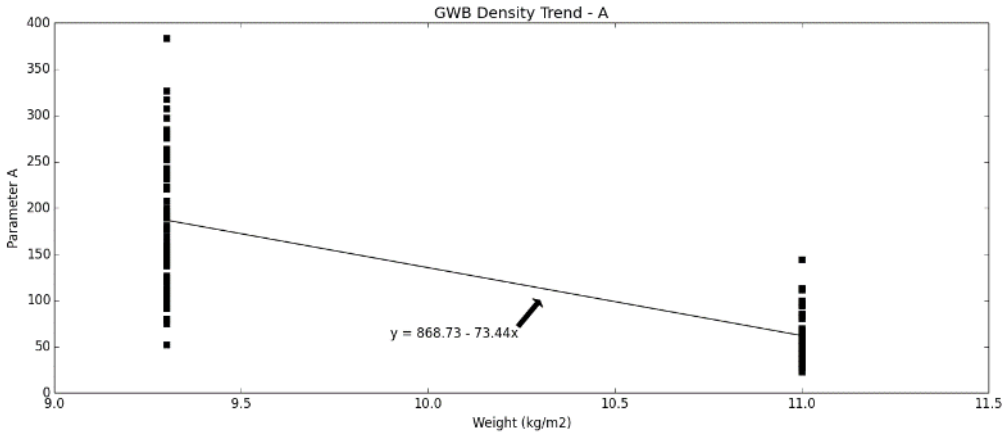

Figure 85: GWB Density Trend - Parameter A

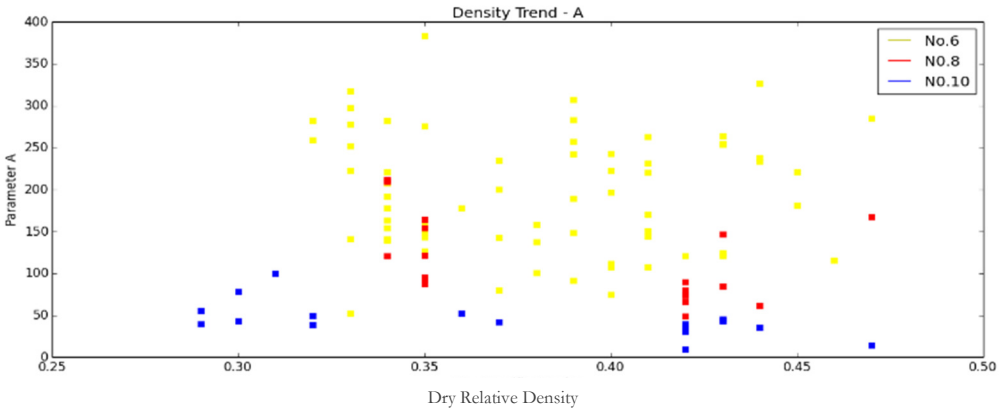

Figure 86: Lumber Density Trend - Parameter A

Parameter K0 Trend

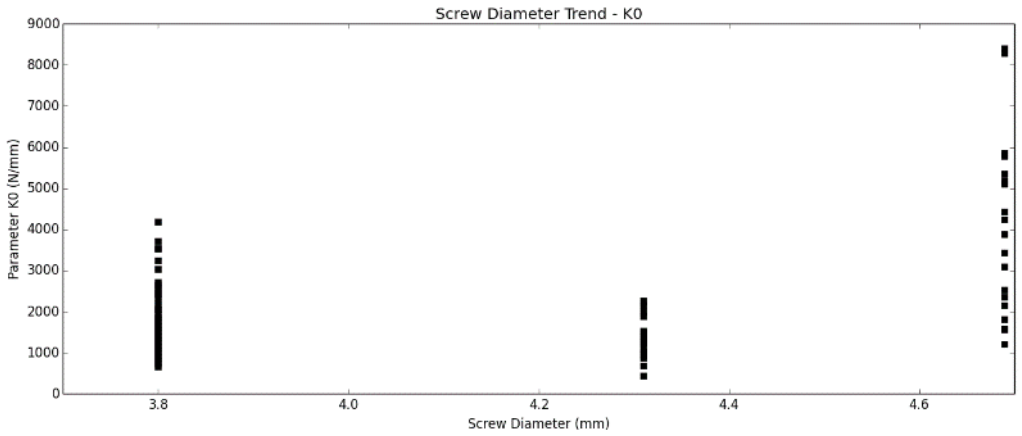

Figure 87: Screw Diameter Trend - K0

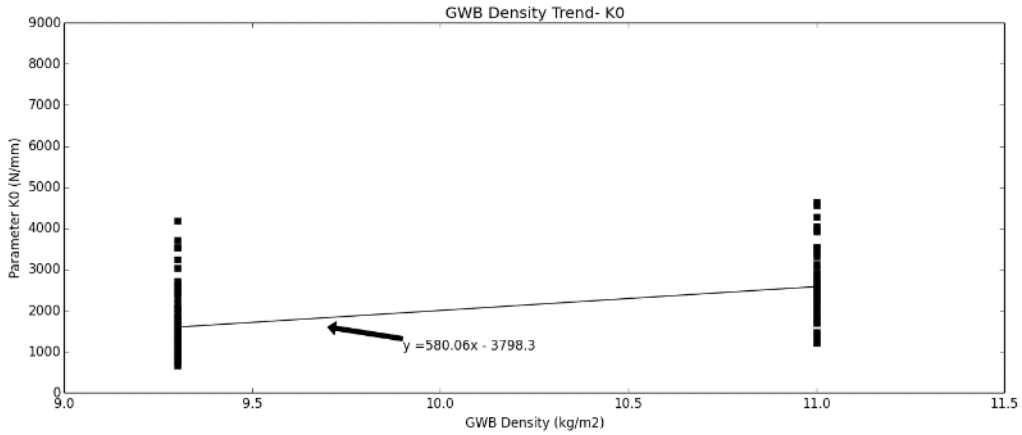

Figure 88: GWB Density Trend - K0

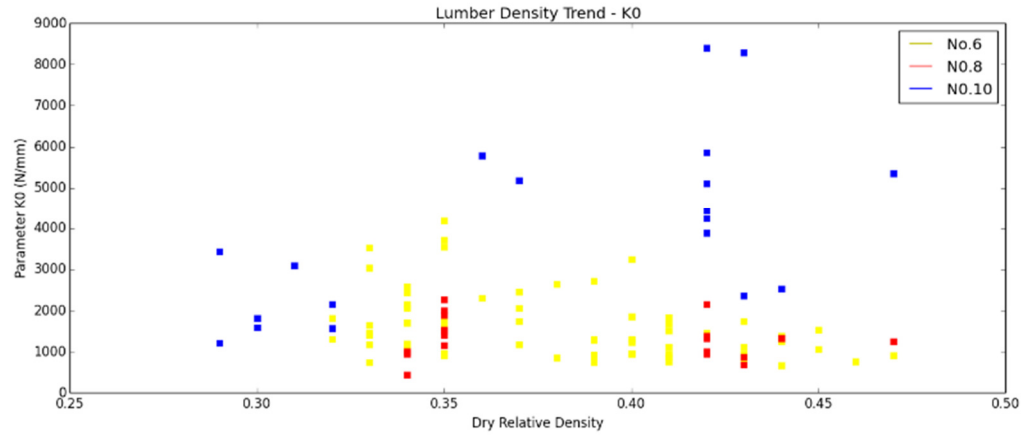

Figure 89: Lumber Density Trend - K0

Parameter K1 Trend

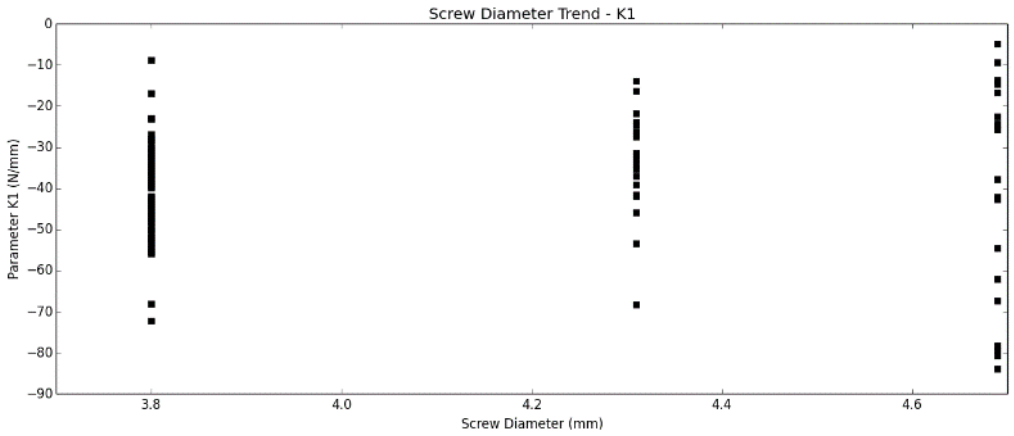

Figure 90: Screw Diameter Trend - K1

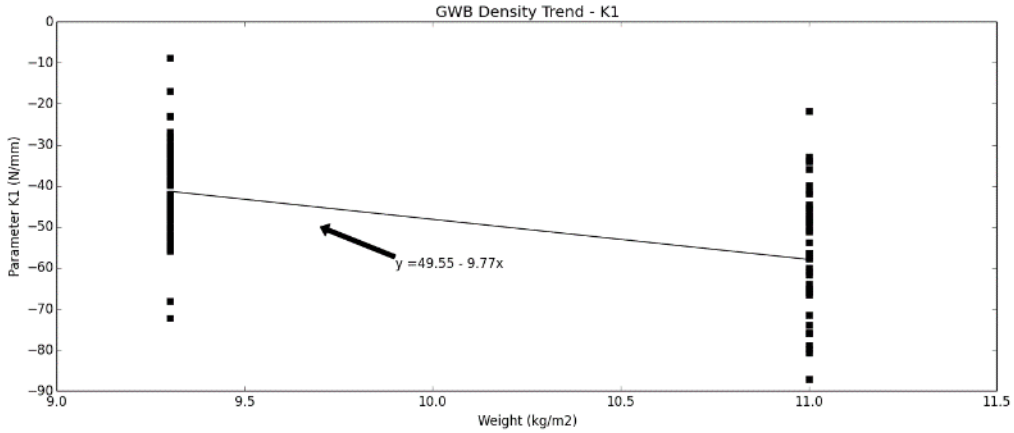

Figure 91: GWB Density Trend - K1

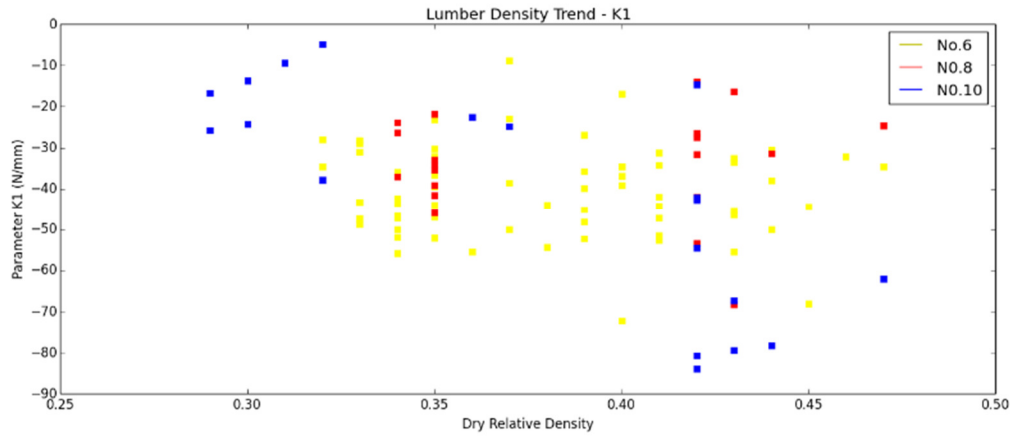

Figure 92: Lumber Density Trend - K1

Parameter P1 Trend

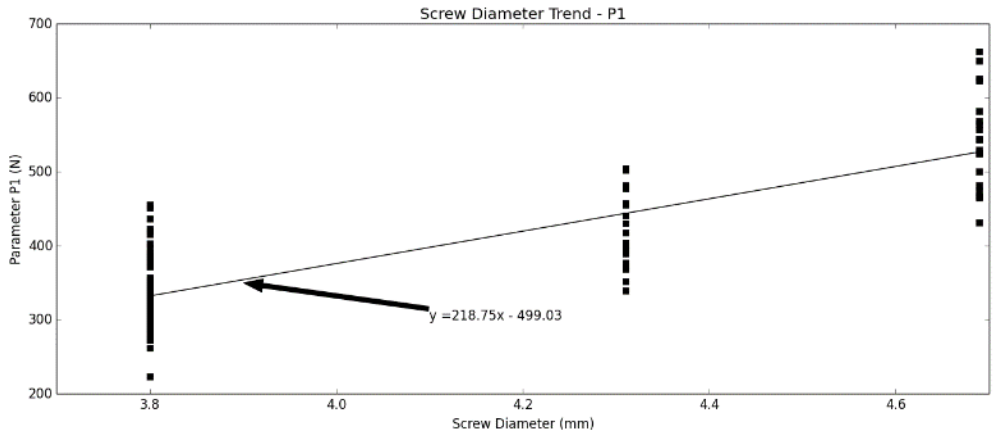

Figure 93: Screw Diameter Trend - P1

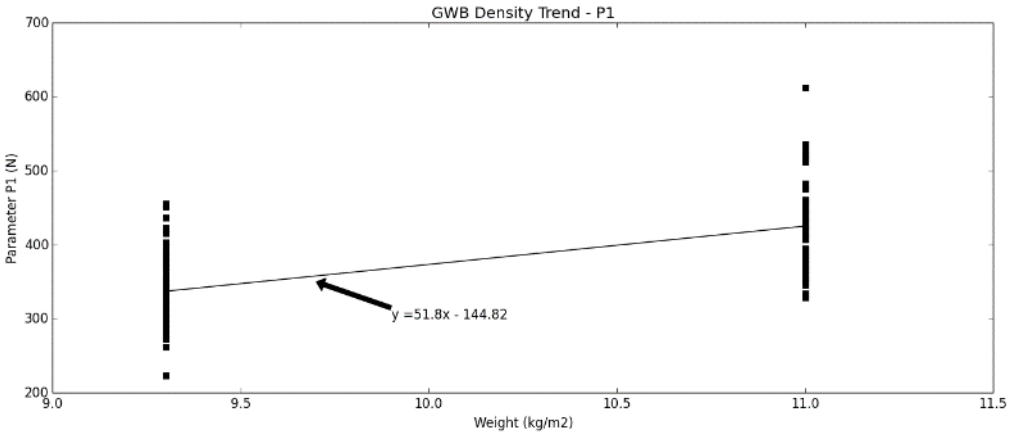

Figure 94: GWB Density Trend - P1

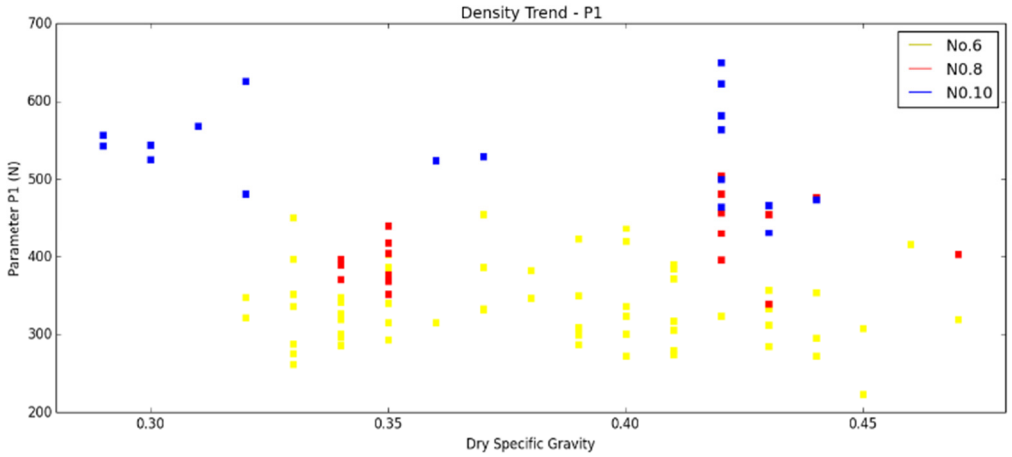

Figure 95: Lumber Density Trend - P1

Parameter C Trend

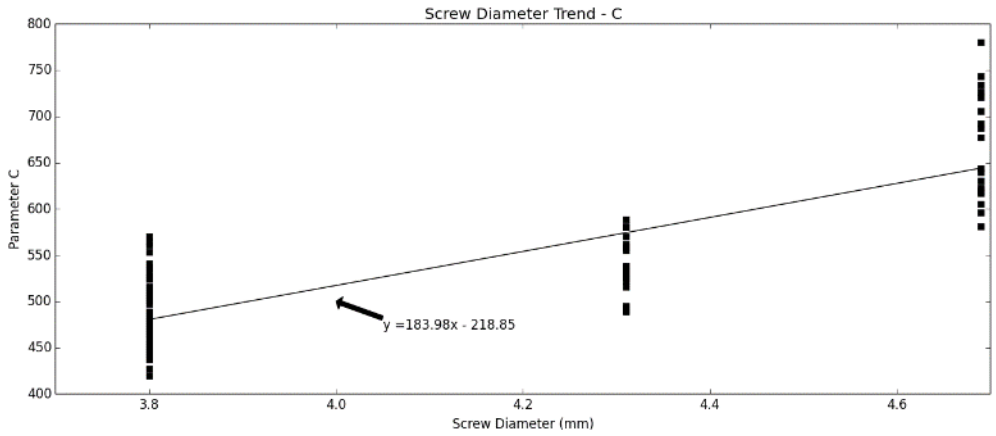

Figure 96: Screw Diameter Trend - C

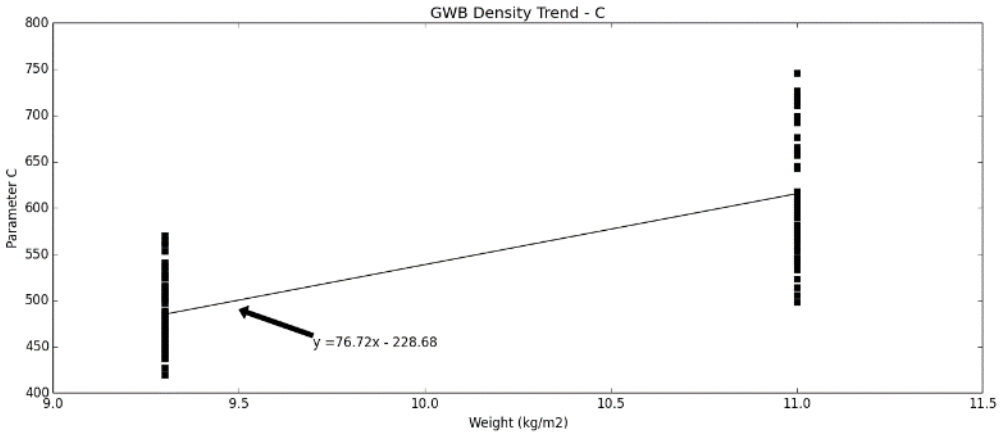

Figure 97: GWB Density Trend - C

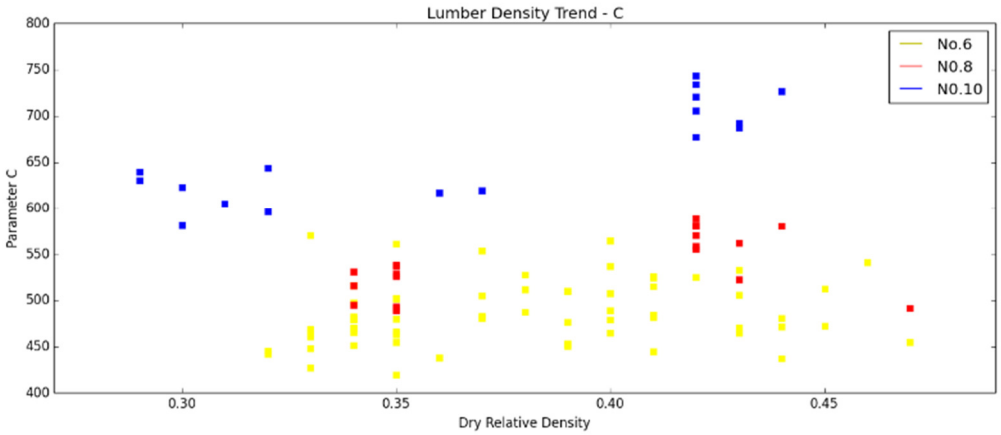

Figure 98: Lumber Density Trend - C

Parameter D Trend

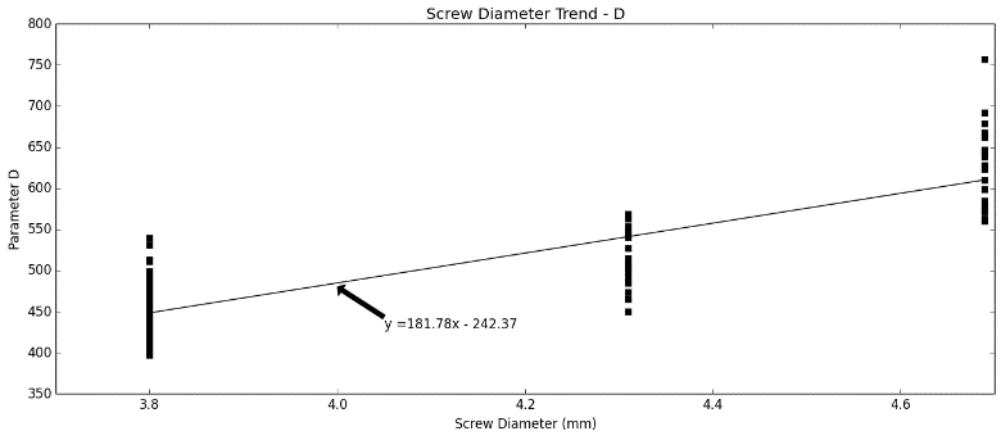

Figure 99: Screw Diameter Trend – D

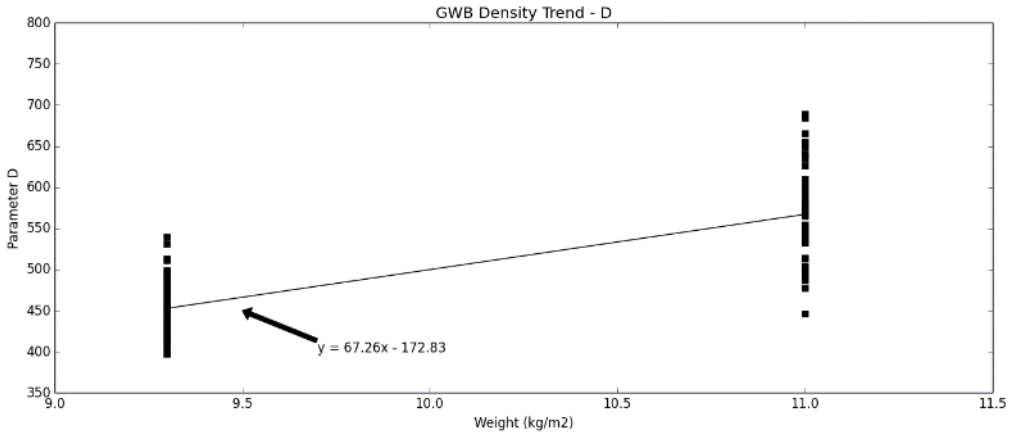

Figure 100: GWB Density Trend – D

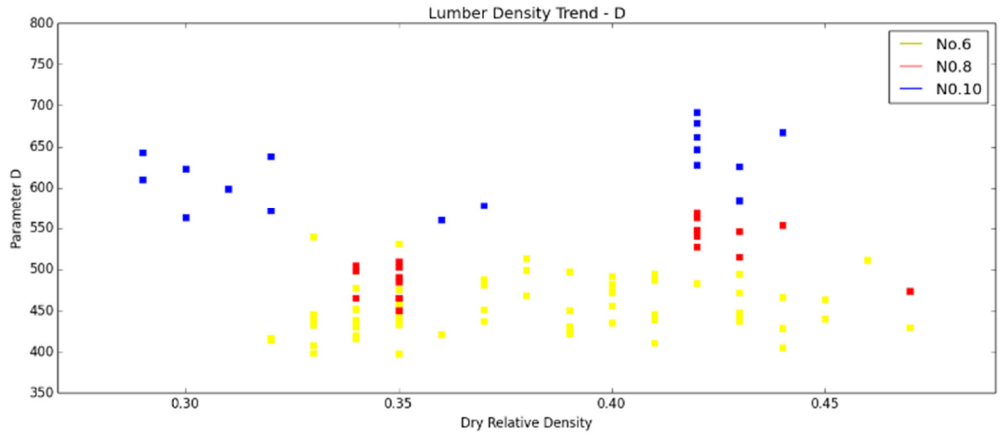

Figure 101: Lumber Density Trend - D

Parameter E Trend

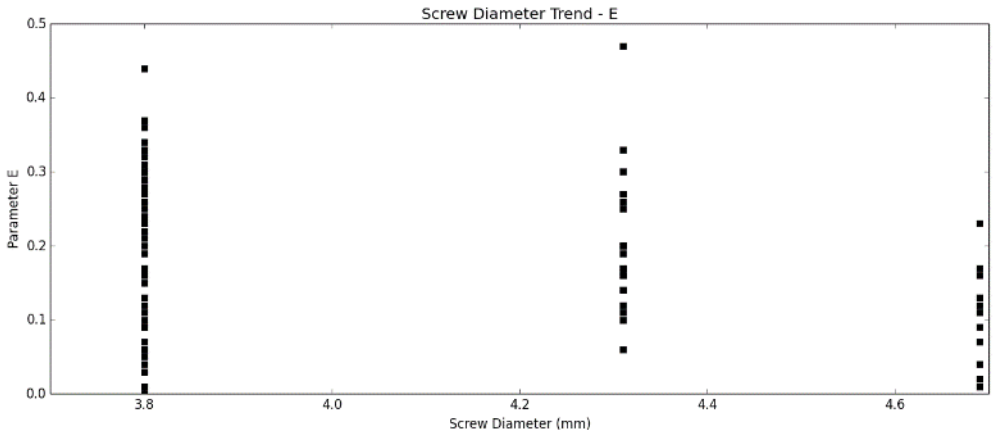

Figure 102: Screw Diameter Trend - E

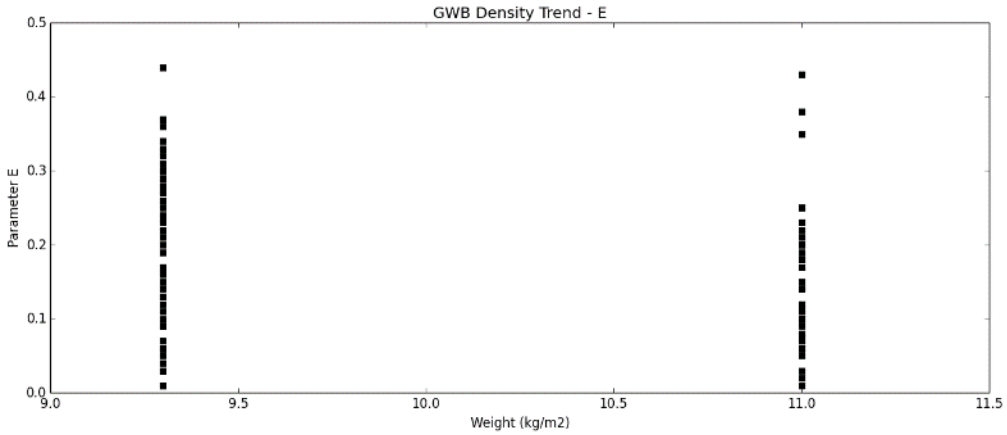

Figure 103: GWB Density Trend - E

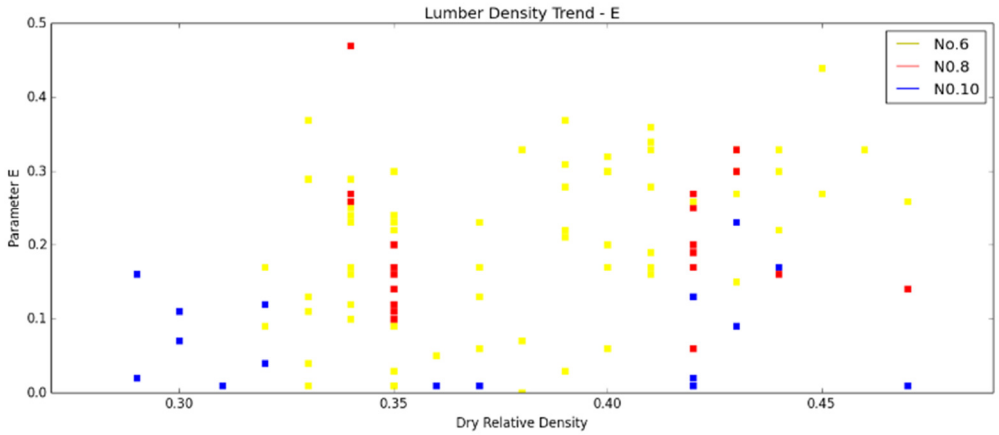

Figure 104: Lumber Density Trend – E

GWB Density Trends using nails as fasteners

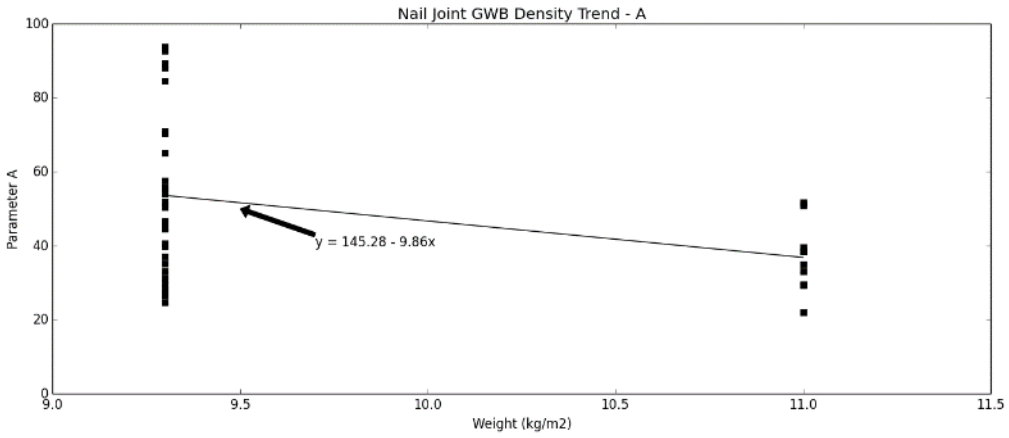

Figure 105: Nail Joint GWB Density Trend – A

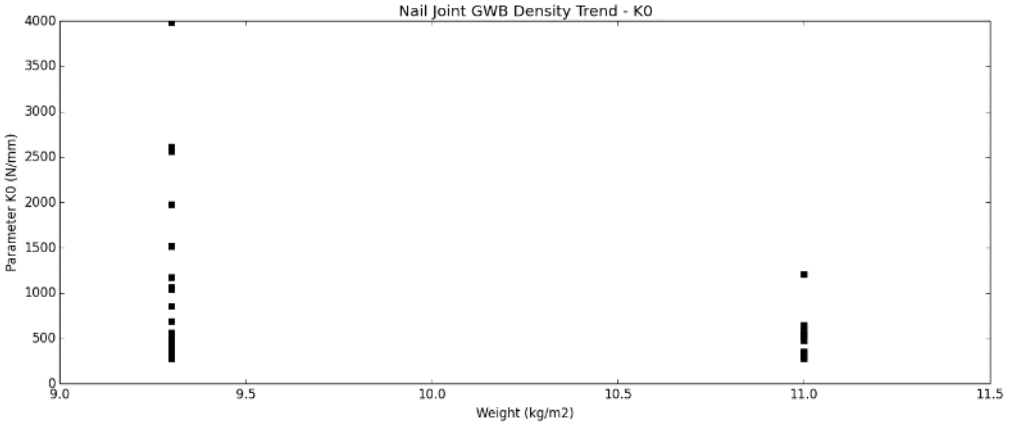

Figure 106: Nail Joint Density GWB Trend - K0

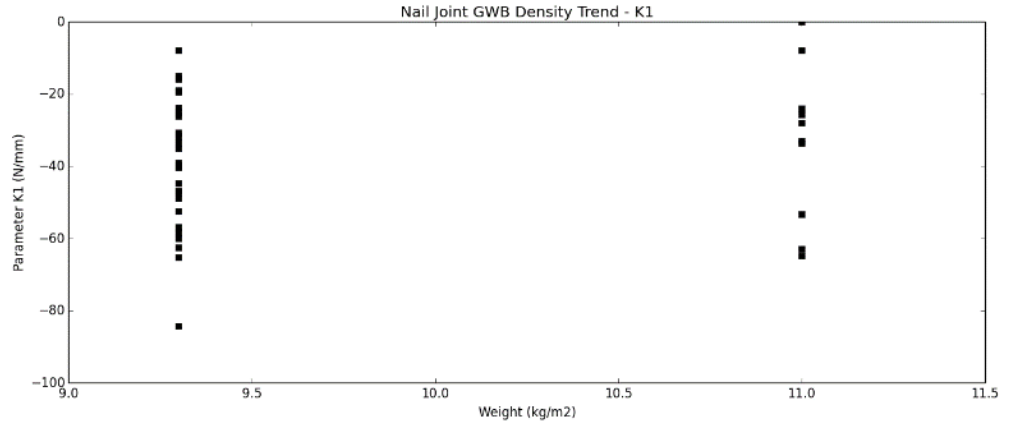

Figure 107: Nail Joint GWB Density Trend - K1

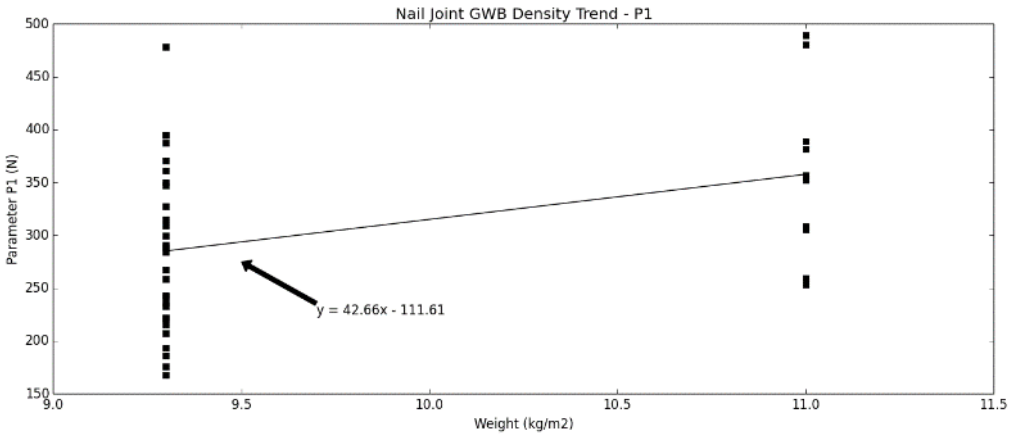

Figure 108 : Nail Joint GWB Density Trend - P1

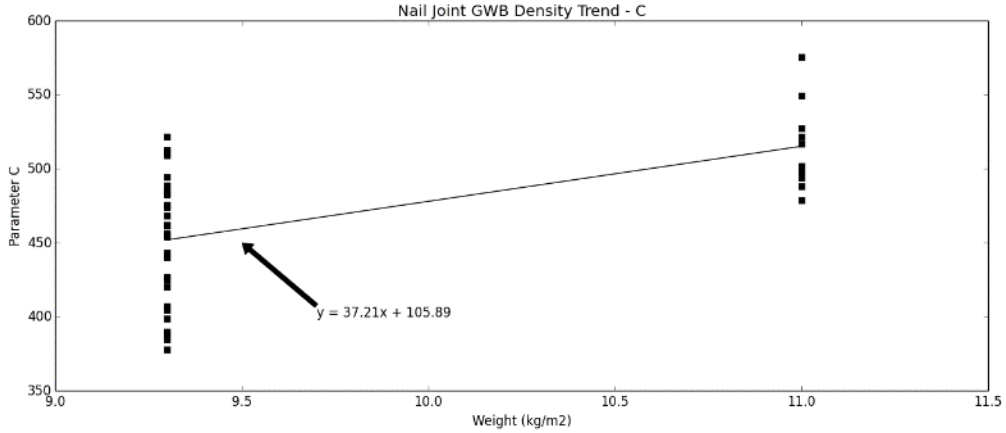

Figure 109: Nail Joint GWB Density Trend - C

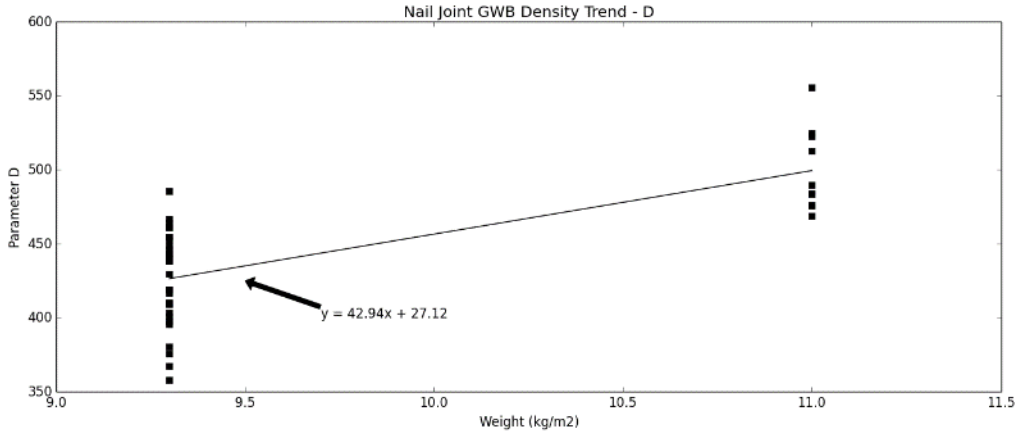

Figure 110: Nail Joint GWB Density Trend - D

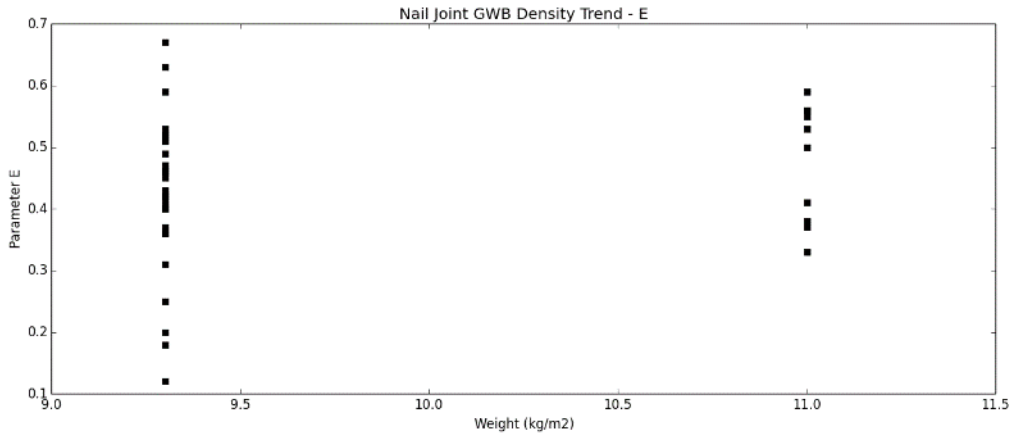

Figure 111: Nail Joint GWB Density Trend – E

10.3 Appendix C: Parameters Used in Joint Level Strength Prediction

JS	JS-5	JS-6	JS-7	JS-8	JS-9	JS-10	JS-11	JS-12	JS-13	JS-30	JS-16	JS-17	JS-18	JS-19	JS-20	JS-21
GWB Relative Density	0.59	0.59	0.59	0.59	0.59	0.59	0.59	0.69	0.69	0.69	0.59	0.59	0.59	0.59	0.59	0.59
Side member Bearing (N/mm)	23.3	23.3	23.3	21.7	21.7	21.7	23.3	24.1	28.3	26.6	23.9	23.9	23.3	24.7	24.7	23.3
Length of penetration in side member (mm)	15.9	15.9	15.9	15.9	15.9	15.9	15.9	15.9	15.9	15.9	15.9	15.9	15.9	15.9	15.9	15.9
Bending Strength of Fastener (MPa)	692.7	637.3	618.9	648.5	636.0	564.9	549.2	692.7	692.7	637.3	705.1	705.1	648.5	637.3	637.3	692.7
Wood Relative Density	0.4	0.4	0.4	0.4	0.4	0.4	0.4	0.4	0.4	0.4	0.43	0.35	0.36	0.32	0.43	0.33
Main Member Bearing (N/mm)	191.2	191.2	191.2	191.2	191.2	191.2	191.2	191.2	191.2	191.2	223.7	223.7	191.2	251.4	251.4	191.2
Predicted Lateral Yield Capacity of Joint (N)	416.3	398.6	392.7	390.3	287.7	273.0	280.1	422.2	452.3	422.2	524.3	524.3	402.2	638.2	638.2	416.3
Tested Avergae Lateral Yield Capacity of Joint (N)	446.8	489.7	436.7	455.9	364.2	398.0	437.2	532.8	561.3	678.2	530.6	493	461.6	663.7	754.5	482.8
Predicted vs Tested Difference	-7.3	-22.8	-11.2	-16.8	-26.6	-45.8	-56.1	-26.2	-24.1	-60.6	-1.2	6.0	-14.8	-4.0	-18.2	-16.0

JS	JS-22	JS-23	JS-24	JS-25	JS-26	JS-27	JS-28
GWB Relative Density	0.59	0.69	0.69	0.69	0.5	0.55	0.54
Side member Bearing (N/mm)	23.3	24.1	26.6	21.2	18.4	18.1	22.3
Length of penetration in side member (mm)	15.9	15.9	15.9	15.9	12.7	12.7	12.7
Bending Strength of Fastener (MPa)	637.3	692.7	665.6	636	637.3	637.3	637.3
Wood Relative Density	0.33	0.34	0.41	0.41	0.43	0.41	0.44
Main Member Bearing (N/mm)	191.2	191.2	191.2	191.2	191.2	191.2	191.2
Predicted Lateral Yield Capacity of Joint (N)	398.6	422.2	431.5	284.4	369.5	367.2	397.9
Tested Avergae Lateral Yield Capacity of Joint (N)	442.9	575.8	591.7	446.2	434.2	472.2	485.8
Predicted vs Tested Difference	-11.1	-36.4	-37.1	-56.9	-17.5	-28.6	-22.1

10.4 Appendix D: Joint Level Test Results

JS-#	Density (SG)	Moisture Content (%)
JS-5-1	0.39	12.00
JS-5-2	0.41	12.12
JS-5-3	0.40	13.01
JS-5-4	0.39	12.62
JS-5-5	0.39	12.00
JS-5-6	0.39	12.87
JS-5-7	0.43	14.63
JS-5-8	0.41	12.96
JS-5-9	0.41	13.08
JS-5-10	0.38	12.87

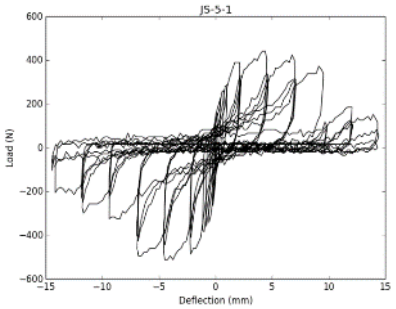

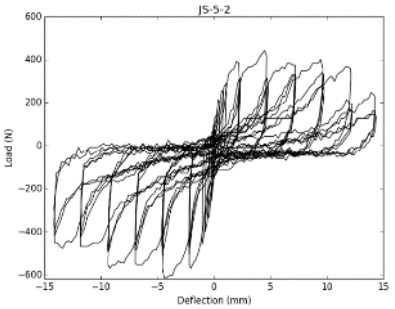

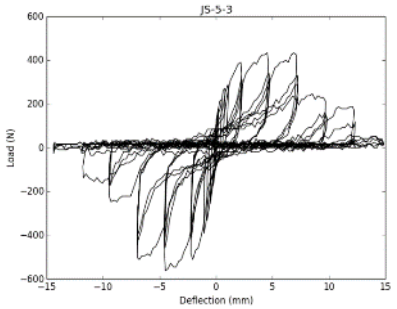

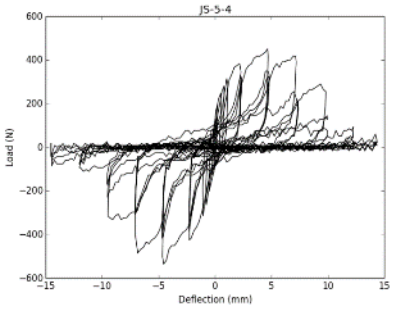

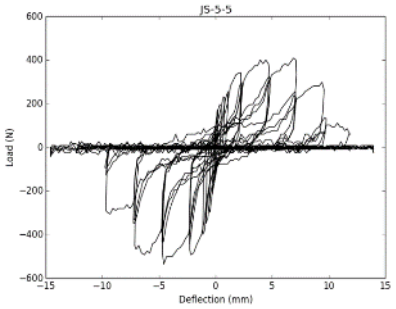

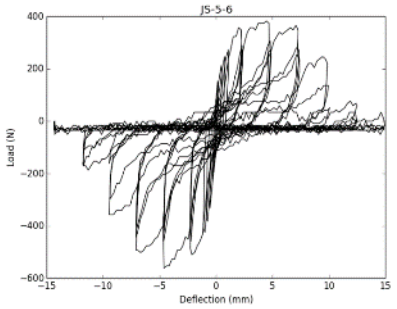

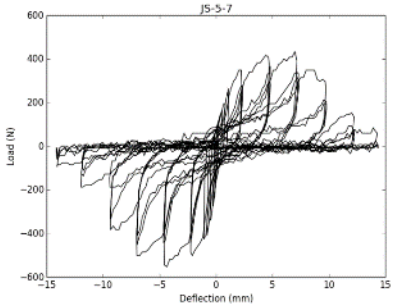

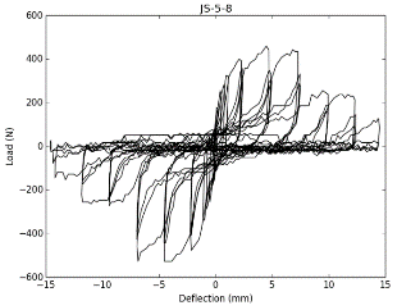

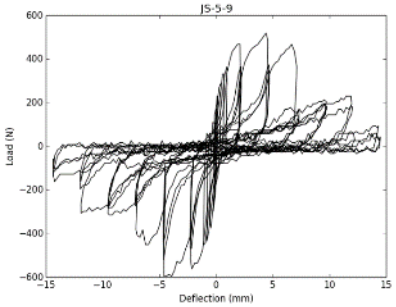

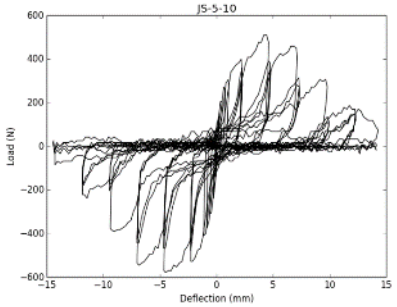

JS-#	Density (SG)	Moisture Content (%)
JS-6-1	0.38	12.00
JS-6-2	0.39	13.21
JS-6-3	0.40	11.82
JS-6-4	0.38	12.00
JS-6-5	0.37	12.37
JS-6-6	0.37	12.63
JS-6-7	0.37	13.13
JS-6-8	0.40	12.96
JS-6-9	0.39	11.32
JS-6-10	0.39	12.24

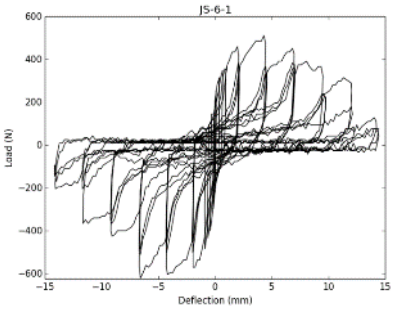

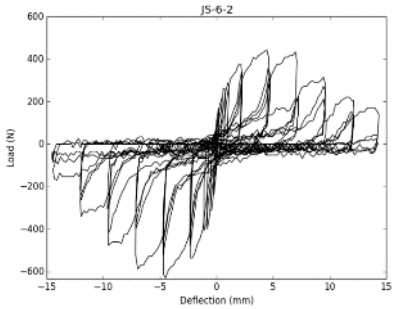

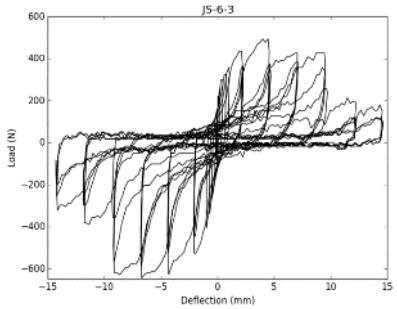

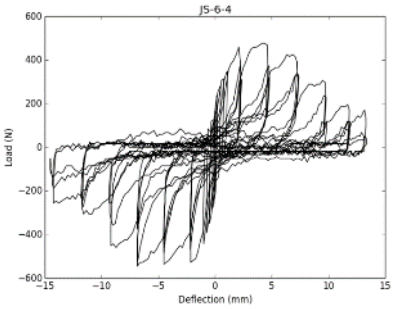

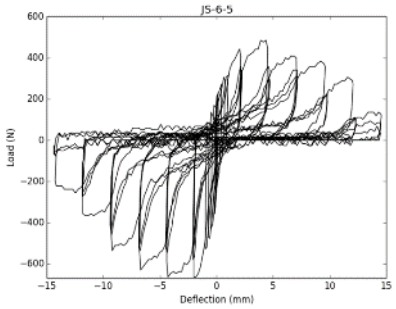

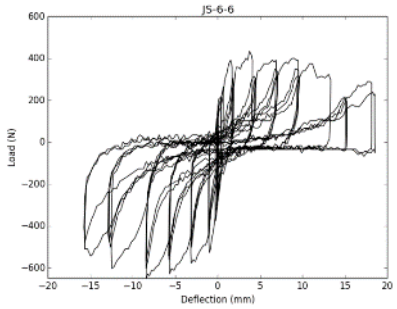

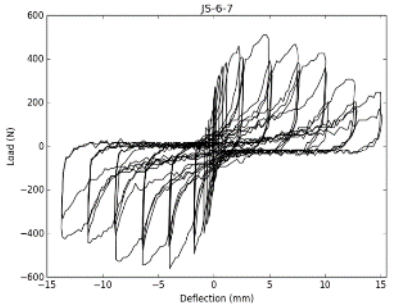

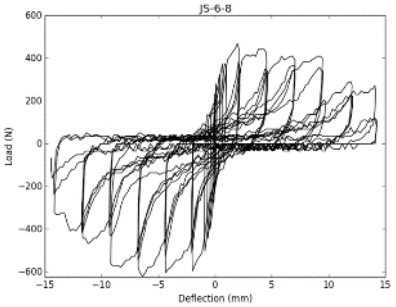

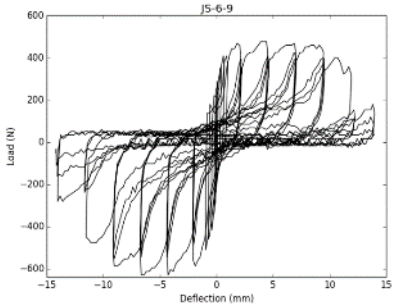

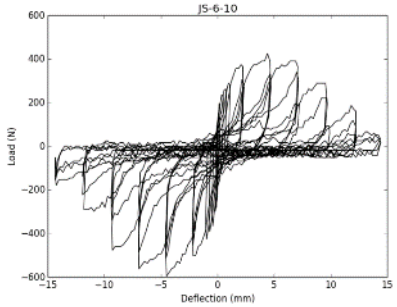

JS-#	Density (SG)	Moisture Content (%)
JS-7-1	0.40	11.76
JS-7-2	0.45	12.39
JS-7-3	0.44	12.73
JS-7-4	0.44	12.84
JS-7-5	0.43	11.93
JS-7-6	0.43	12.04
JS-7-7	0.45	12.50
JS-7-8	0.43	11.93
JS-7-9	0.44	11.82
JS-7-10	0.41	11.43

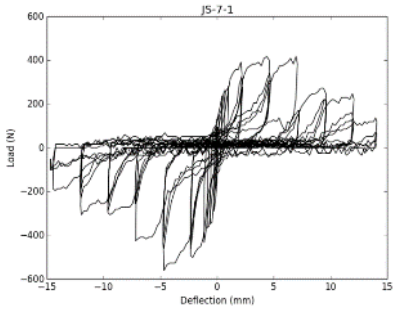

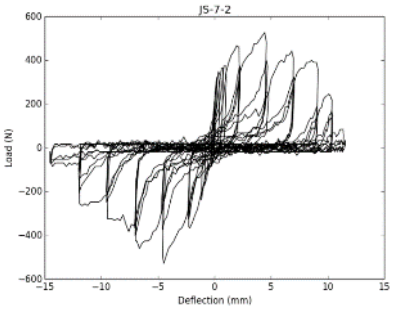

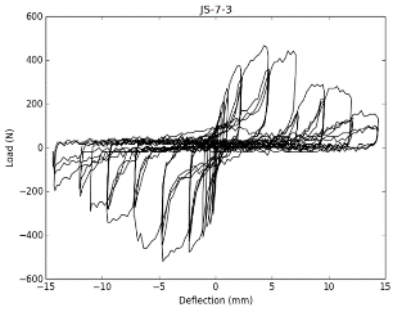

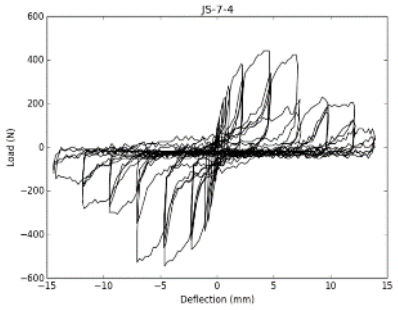

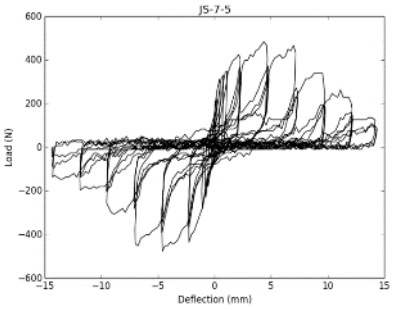

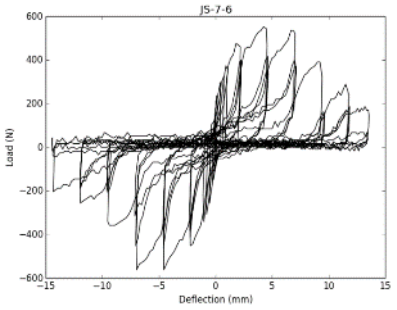

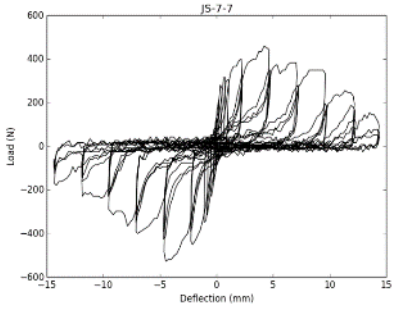

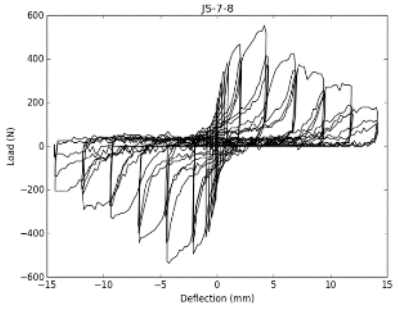

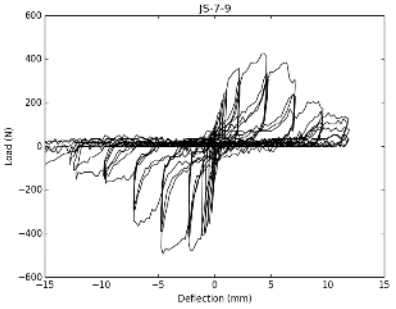

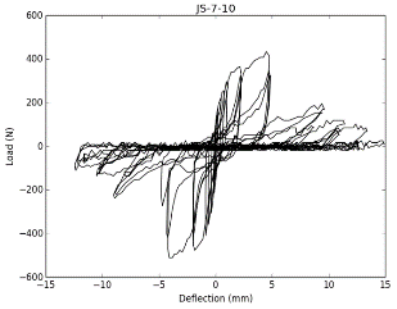

JS-#	Density (SG)	Moisture Content (%)
JS-8-1	0.40	12.00
JS-8-2	0.40	12.12
JS-8-3	0.47	13.01
JS-8-4	0.41	12.62
JS-8-5	0.41	12.87
JS-8-6	0.43	12.50
JS-8-7	0.40	12.37
JS-8-8	0.41	13.13
JS-8-9	0.42	13.16
JS-8-10	0.41	12.75

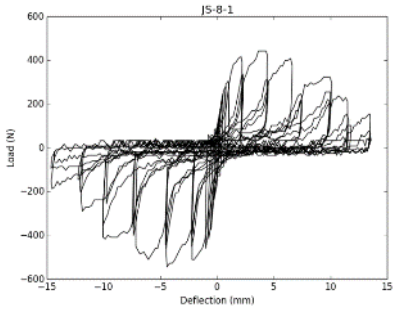

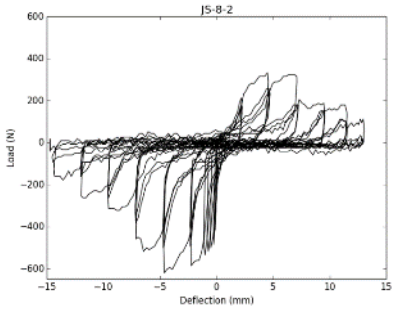

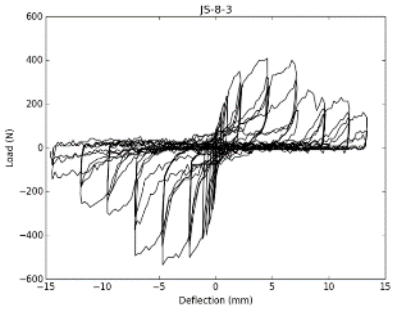

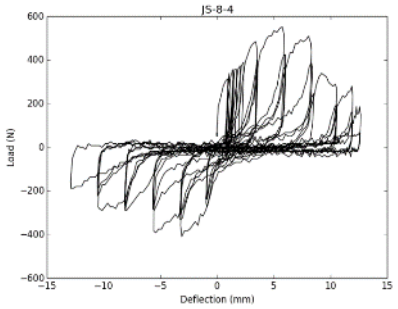

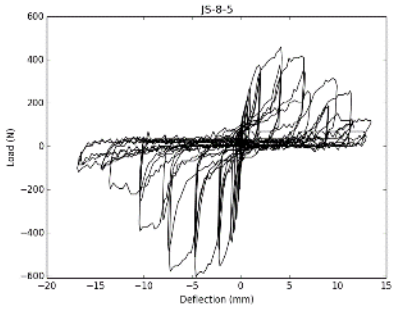

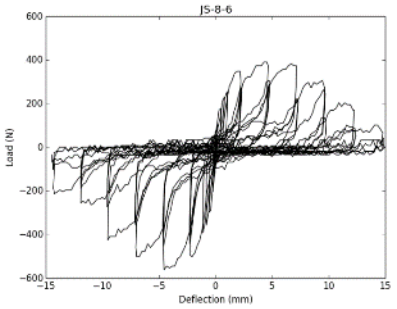

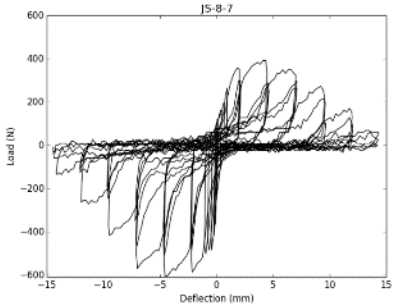

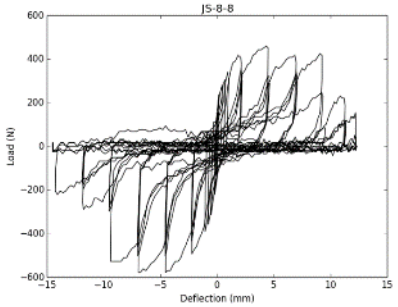

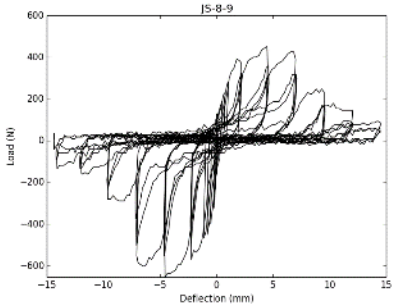

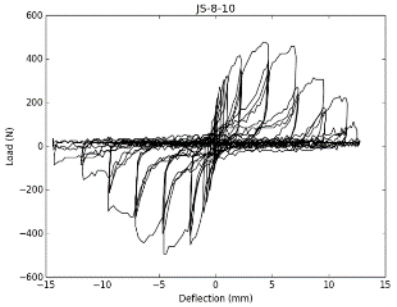

JS-#	Density (SG)	Moisture Content (%)
JS-9-1	0.40	13.00
JS-9-2	0.43	12.50
JS-9-3	0.40	12.87
JS-9-4	0.40	13.59
JS-9-5	0.41	13.08
JS-9-6	0.40	12.87
JS-9-7	0.42	14.63
JS-9-8	0.41	12.96
JS-9-9	0.40	13.08
JS-9-10	0.41	12.87

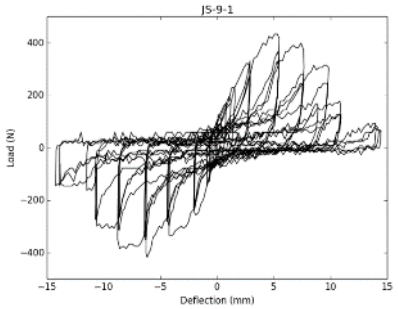

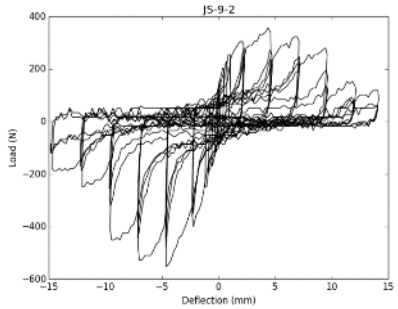

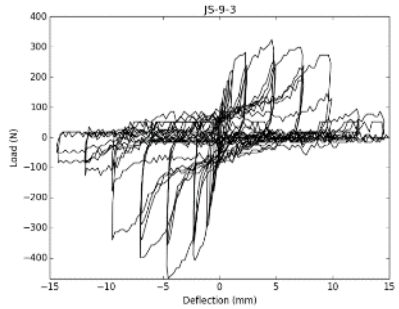

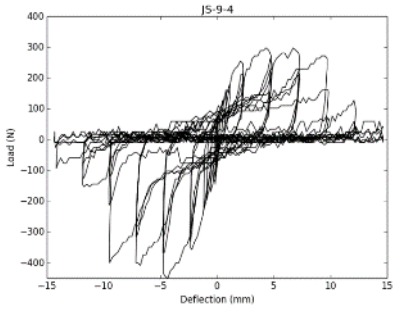

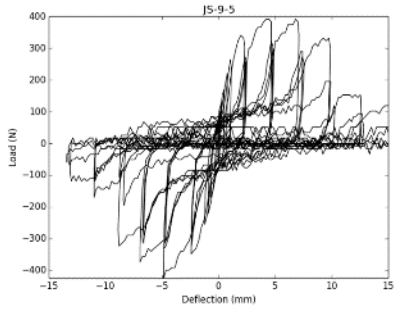

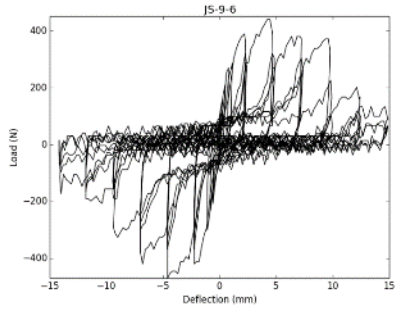

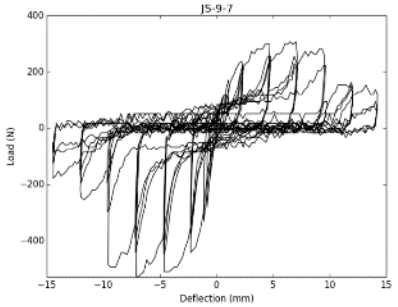

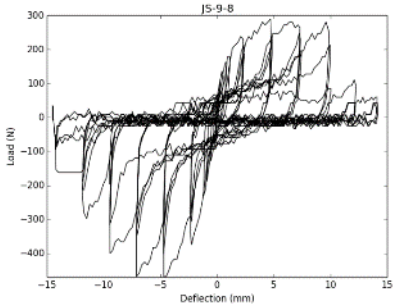

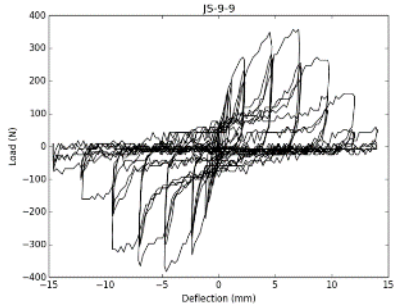

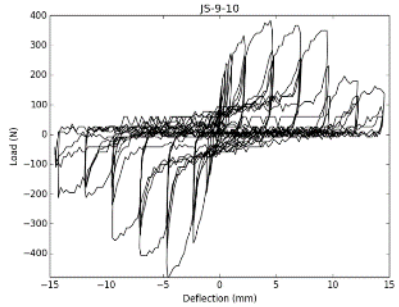

JS-#	Density (SG)	Moisture Content (%)
JS-10-1	0.41	24.75
JS-10-2	0.46	13.22
JS-10-3	0.45	11.97
JS-10-4	0.45	13.33
JS-10-5	0.43	18.02
JS-10-6	0.41	12.84
JS-10-7	0.41	13.89
JS-10-8	0.42	13.16
JS-10-9	0.43	13.51
JS-10-10	0.43	12.28

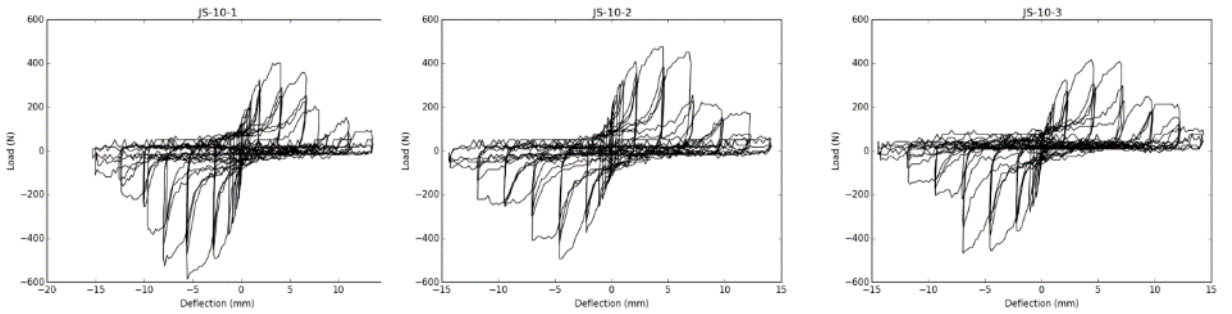

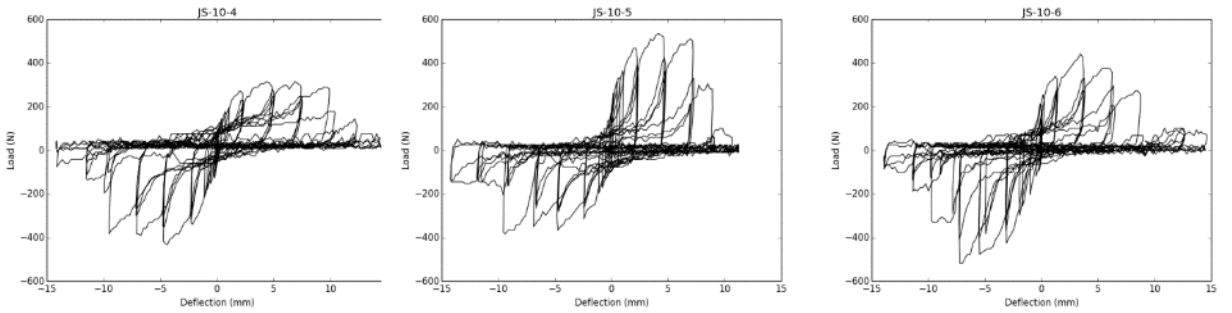

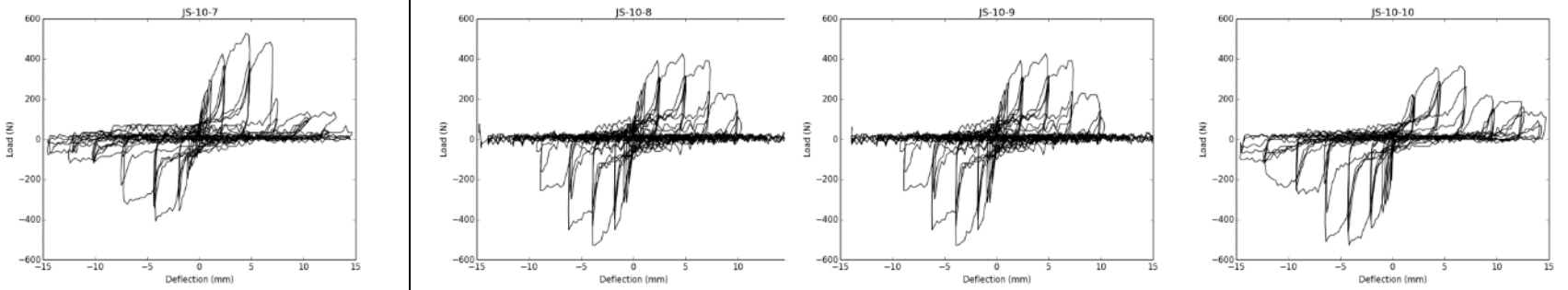

JS-#	Density (SG)	Moisture Content (%)			
JS-11-1	0.41	11.50	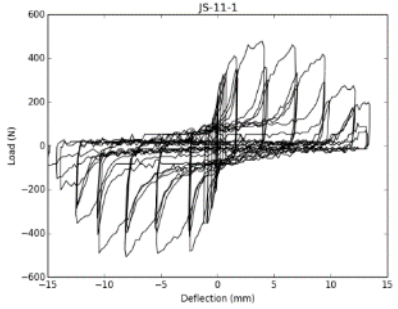	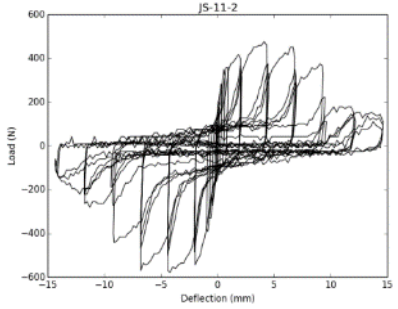	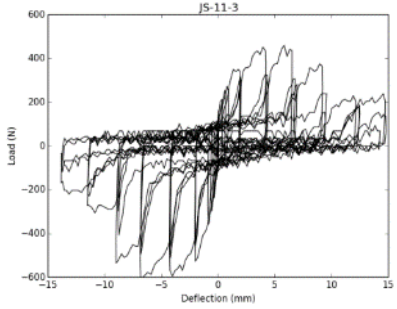
JS-11-2	0.40	11.54			
JS-11-3	0.39	12.75			
JS-11-4	0.40	11.65			
JS-11-5	0.40	10.91			
JS-11-6	0.42	11.40	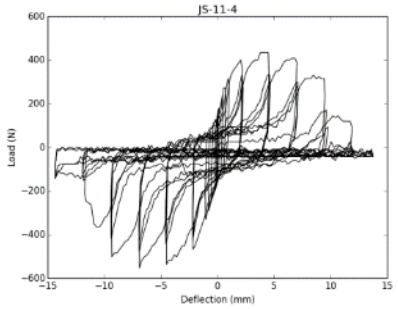	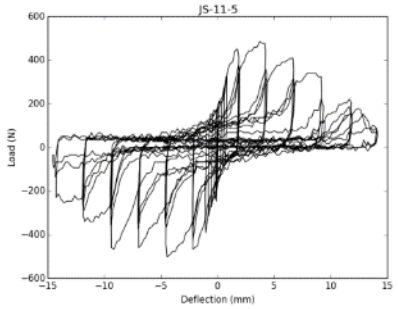	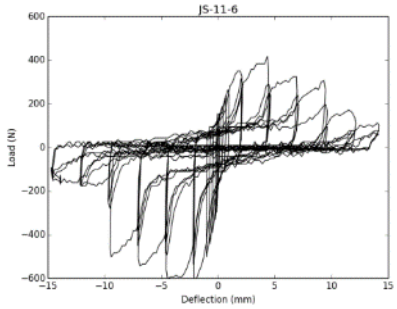
JS-11-7	0.40	11.61			
JS-11-8	0.40	11.32			
JS-11-9	0.40	4.42			
JS-11-10	0.39	11.32			
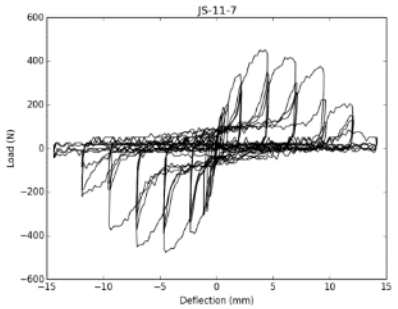			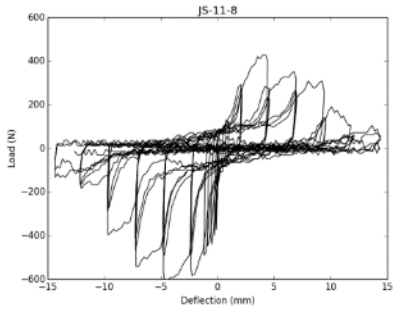	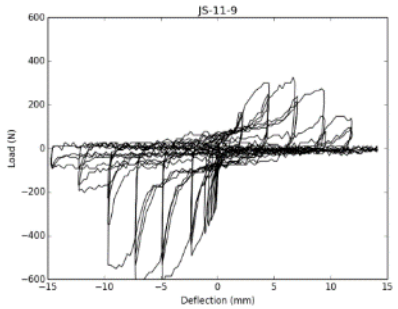	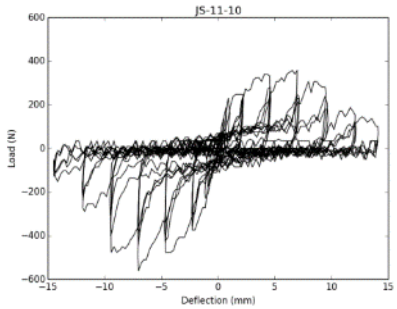

JS-#	Density (SG)	Moisture Content (%)			
JS-12-1	0.38	13.00	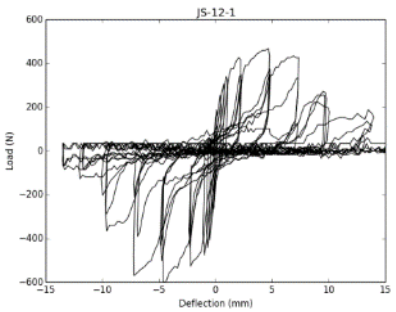	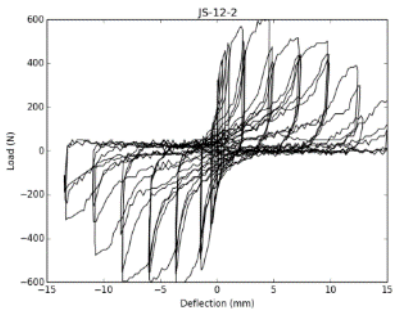	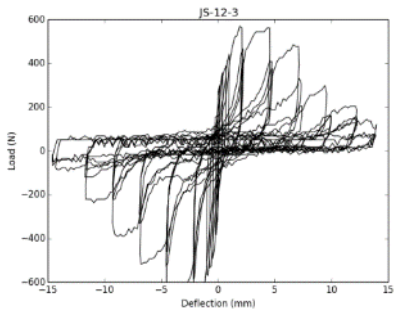
JS-12-2	0.41	12.84			
JS-12-3	0.39	12.12			
JS-12-4	0.39	13.86			
JS-12-5	0.38	13.46			
JS-12-6	0.40	12.50	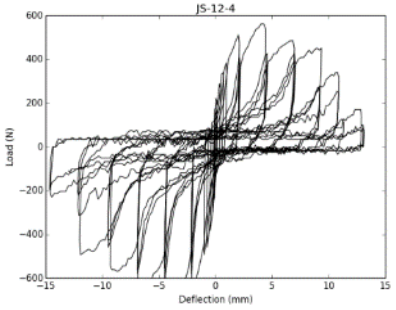	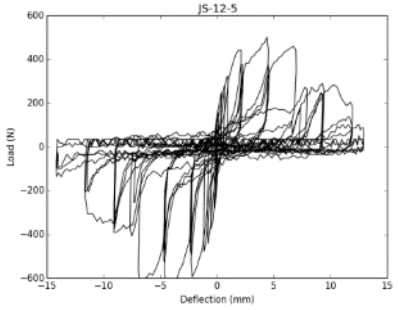	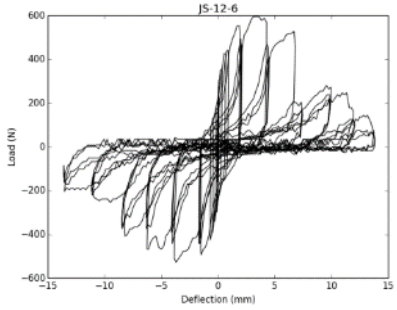
JS-12-7	0.42	13.64			
JS-12-8	0.39	13.00			
JS-12-9	0.38	10.89			
JS-12-10	0.38	13.13			
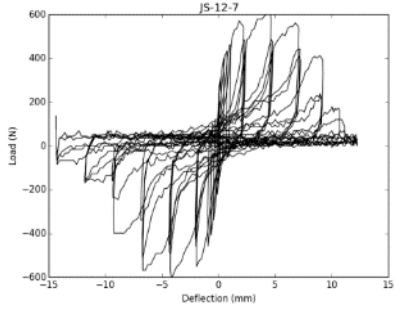	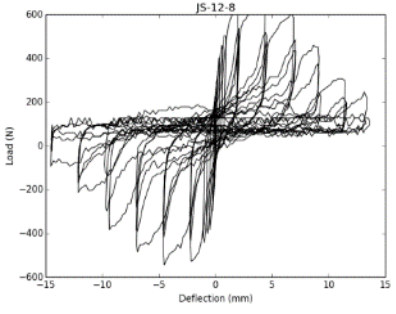	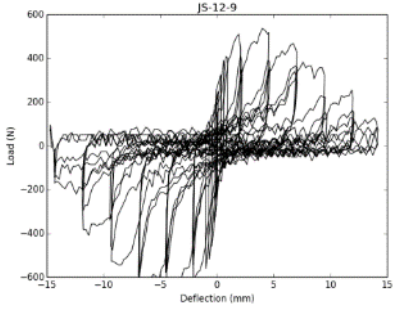	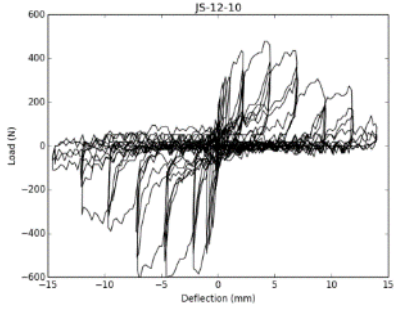		

JS-#	Density (SG)	Moisture Content (%)			
JS-13-1	0.38	11.22	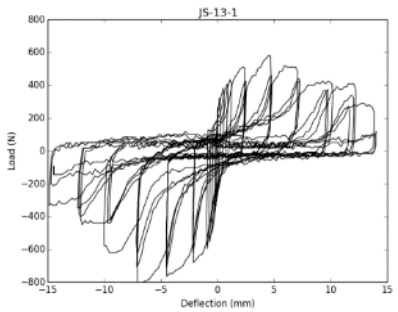	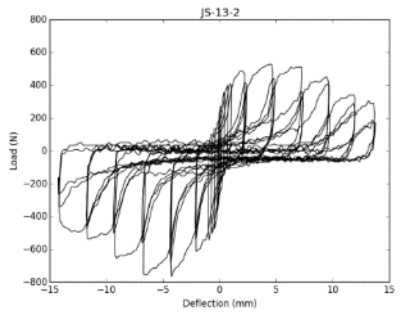	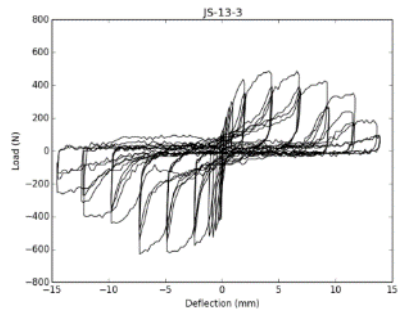
JS-13-2	0.39	12.24			
JS-13-3	0.40	8.82			
JS-13-4	0.38	14.04			
JS-13-5	0.36	13.04			
JS-13-6	0.37	11.96	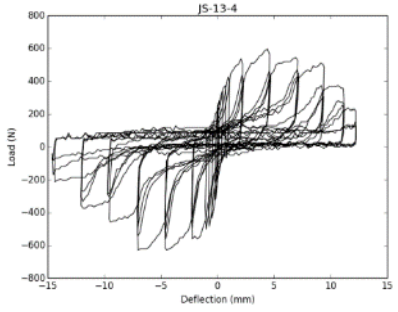	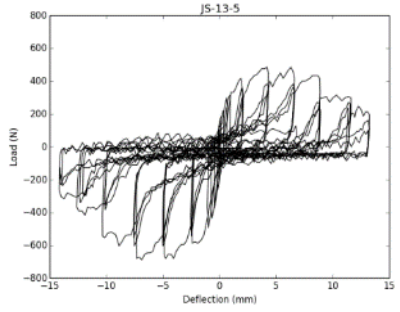	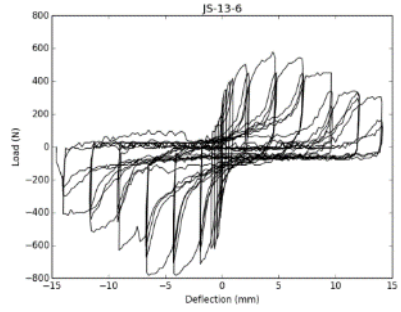
JS-13-7	0.35	11.96			
JS-13-8	0.37	4.35			
JS-13-9	0.32	9.53			
JS-13-10	0.41	7.48			
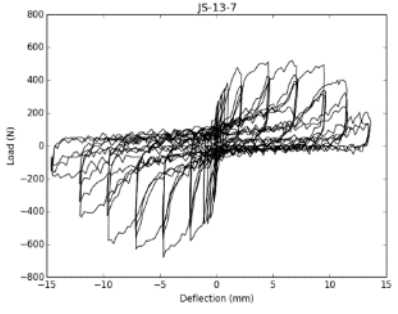	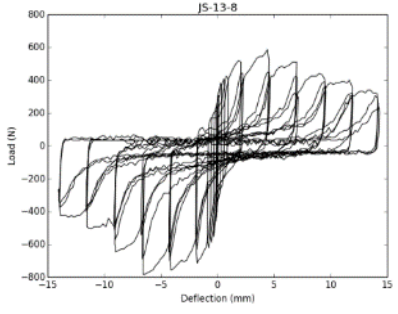	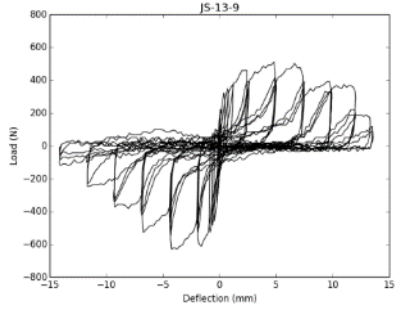	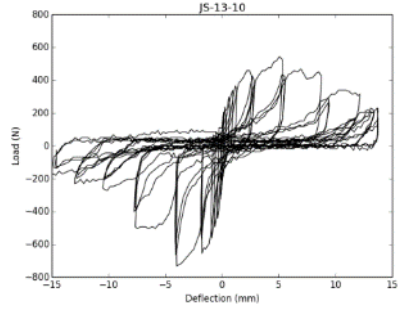		

JS-#	Density (SG)	Moisture Content (%)			
JS-16-1	0.42	12.15	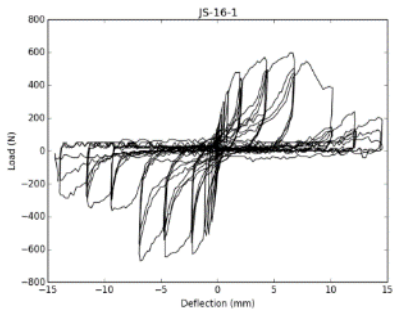	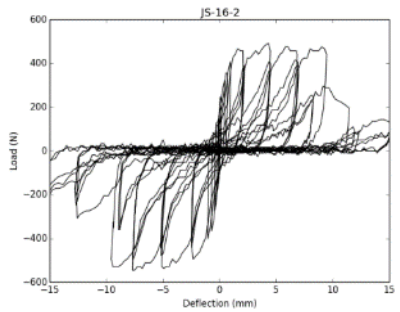	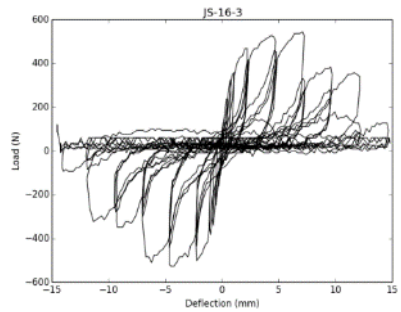
JS-16-2	0.47	14.04			
JS-16-3	0.43	12.15			
JS-16-4	0.42	12.08			
JS-16-5	0.44	12.28			
JS-16-6	0.42	13.21	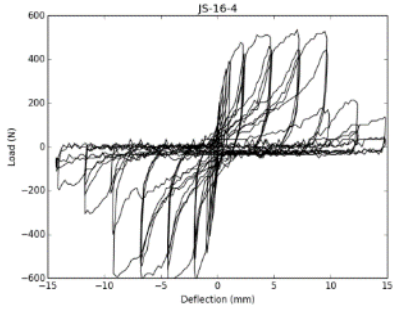	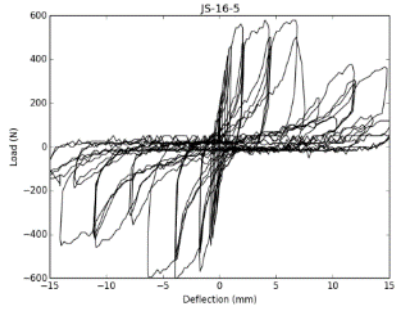	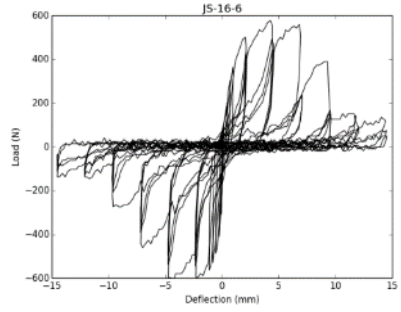
JS-16-7	0.43	12.39			
JS-16-8	0.42	11.93			
JS-16-9	0.42	13.33			
JS-16-10	0.42	13.04			
			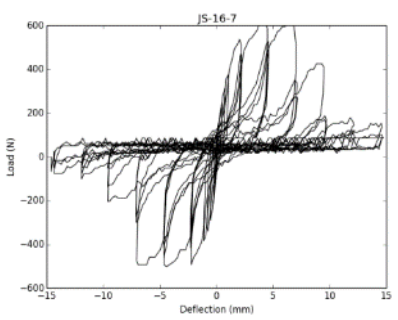	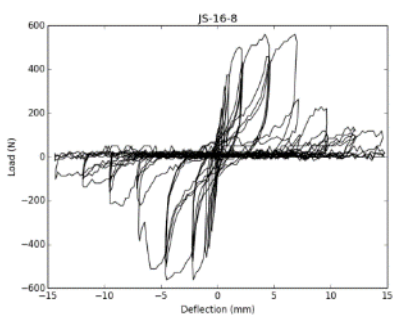	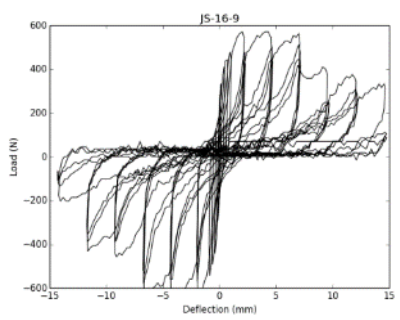	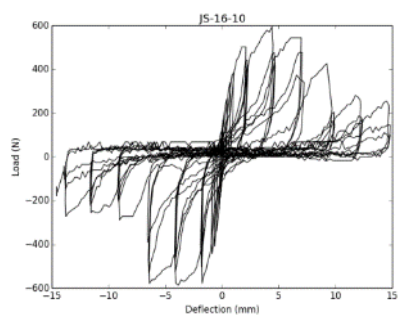

JS-#	Density (SG)	Moisture Content (%)			
JS-17-1	0.34	11.96	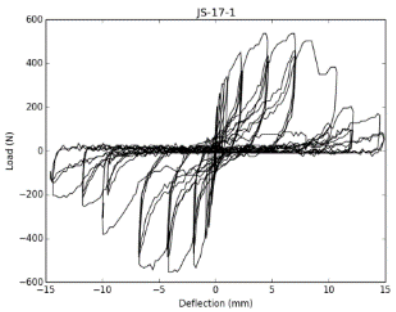	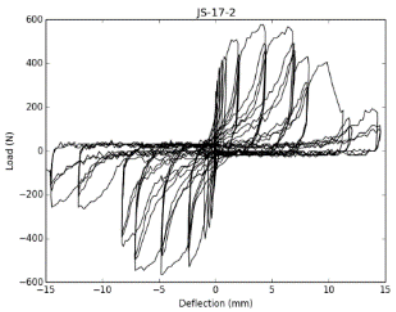	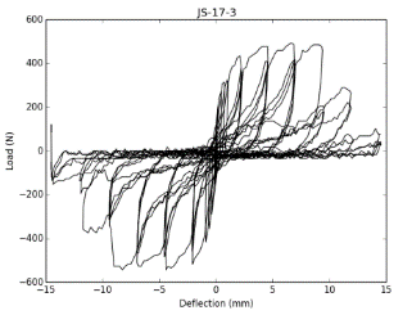
JS-17-2	0.35	11.96			
JS-17-3	0.35	11.96			
JS-17-4	0.35	11.83			
JS-17-5	0.35	11.83			
JS-17-6	0.35	10.64	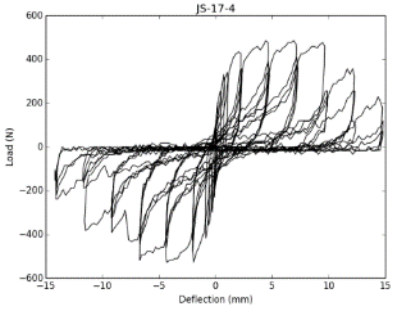	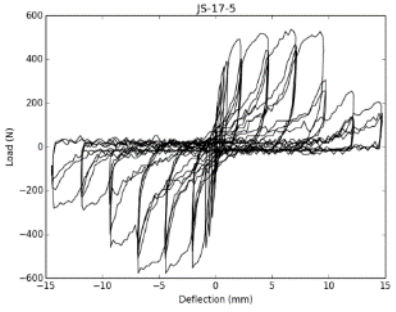	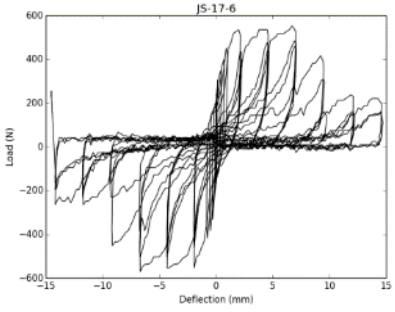
JS-17-7	0.34	11.24			
JS-17-8	0.35	11.70			
JS-17-9	0.35	11.83			
JS-17-10	0.34	11.83			
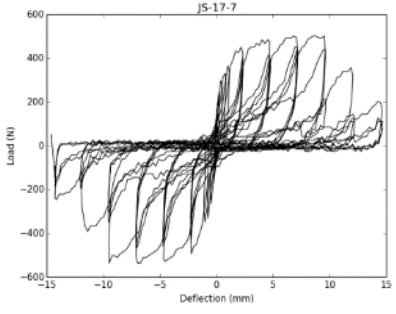			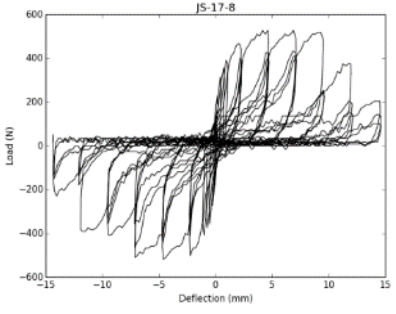	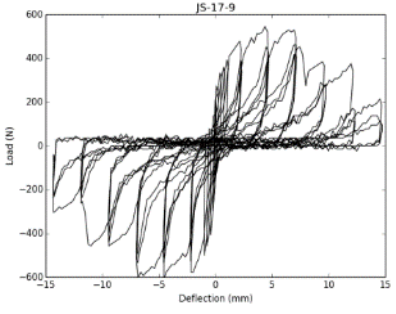	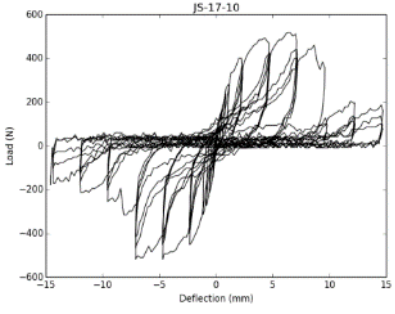

JS-#	Density (SG)	Moisture Content (%)			
JS-18-1	0.33	10.99	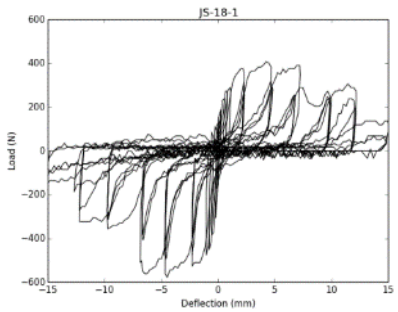	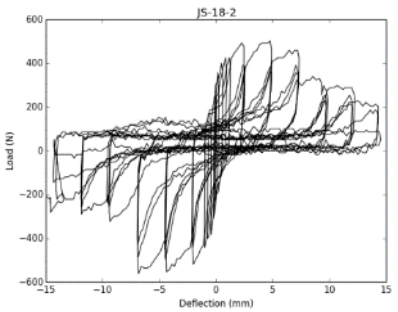	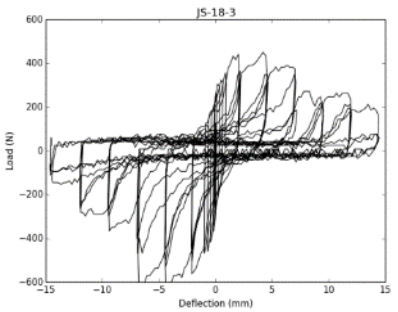
JS-18-2	0.33	12.36			
JS-18-3	0.35	11.46			
JS-18-4	0.37	12.12			
JS-18-5	0.34	13.04			
JS-18-6	0.35	11.34	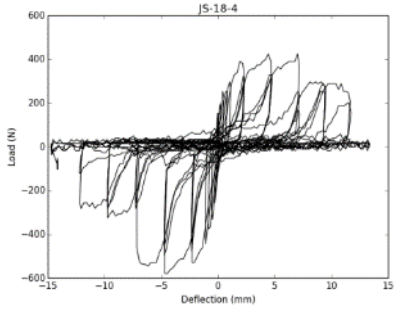	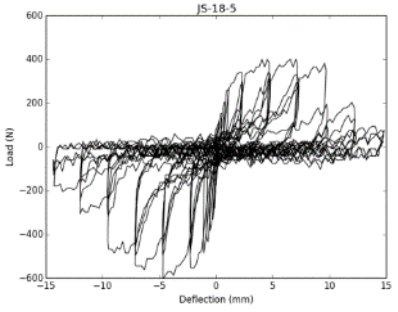	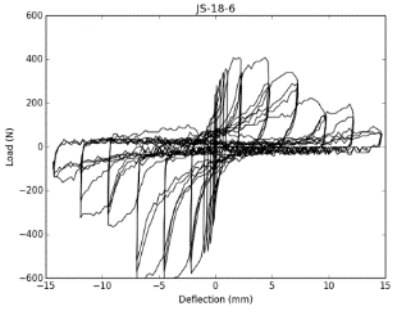
JS-18-7	0.46	11.63			
JS-18-8	0.35	12.24			
JS-18-9	0.36	11.76			
JS-18-10	0.35	12.37			
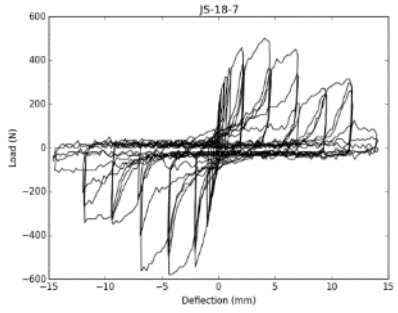	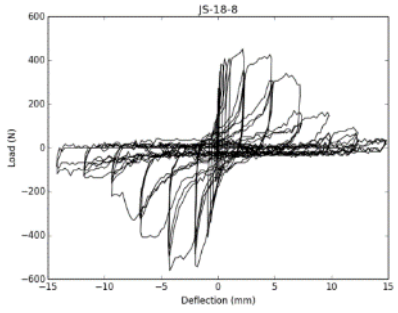	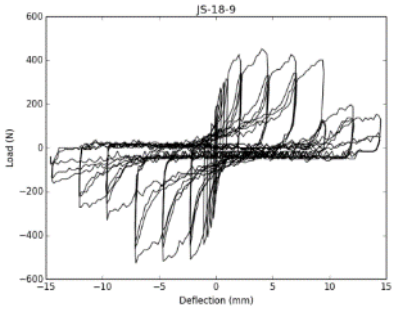	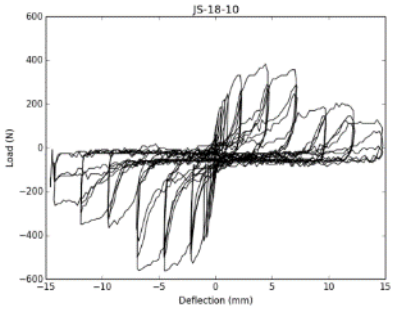	

JS-#	Density (SG)	Moisture Content (%)			
JS-19-1	0.30	12.50	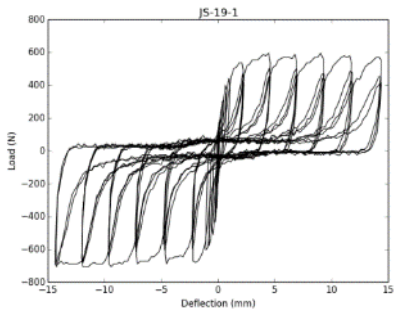	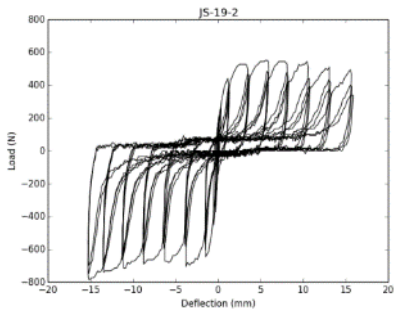	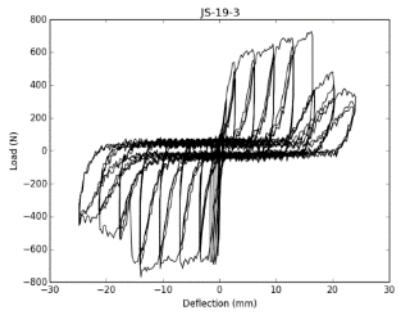
JS-19-2	0.32	12.94			
JS-19-3	0.37	12.62			
JS-19-4	0.31	13.10			
JS-19-5	0.29	12.99			
JS-19-6	0.29	14.10	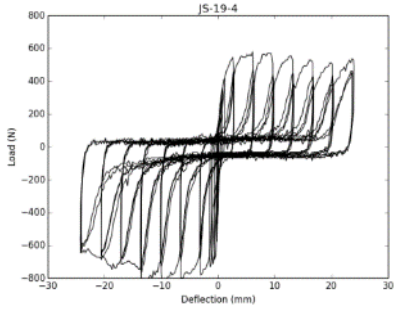	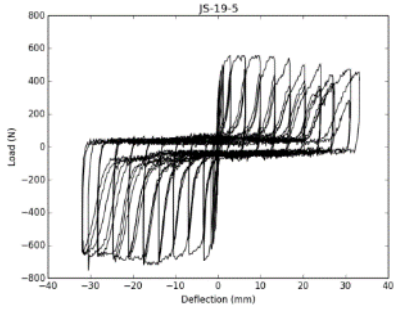	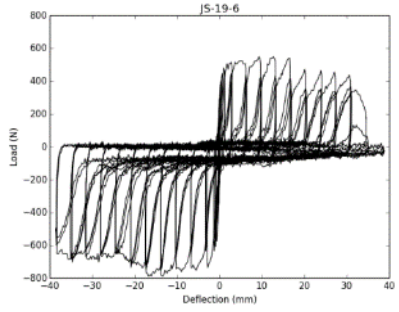
JS-19-7	0.31	11.76			
JS-19-8	0.36	12.63			
JS-19-9	0.30	12.50			
JS-19-10	0.37	12.62			
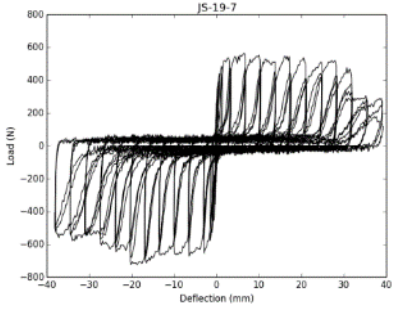	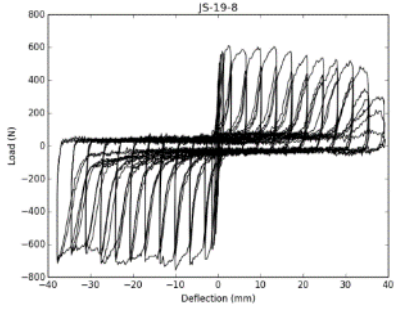	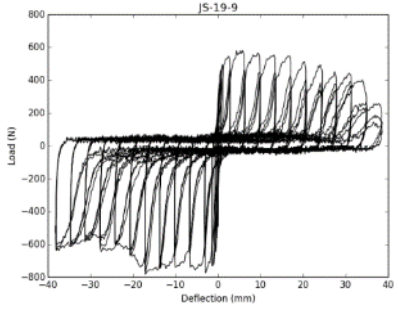			

JS-#	Density (SG)	Moisture Content (%)			
JS-20-1	0.42	12.15	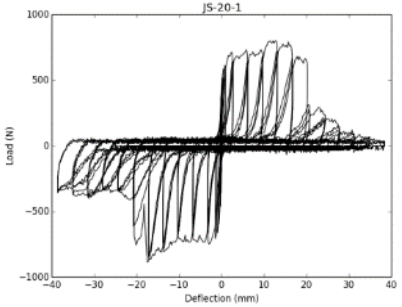	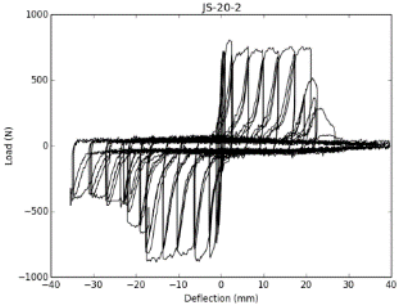	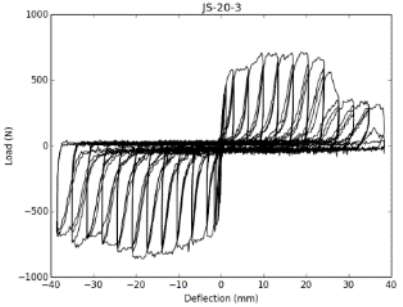
JS-20-2	0.47	14.04			
JS-20-3	0.43	12.15			
JS-20-4	0.42	12.08			
JS-20-5	0.44	12.28			
JS-20-6	0.42	13.21	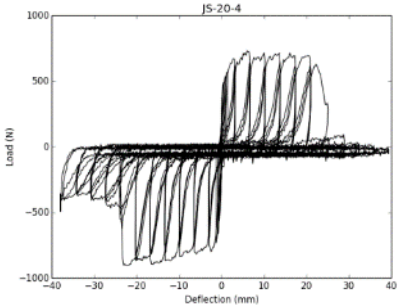	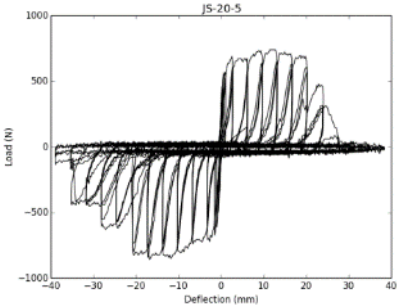	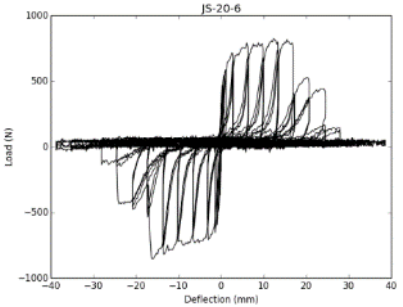
JS-20-7	0.43	12.39			
JS-20-8	0.42	11.93			
JS-20-9	0.42	13.33			
JS-20-10	0.42	13.04			
			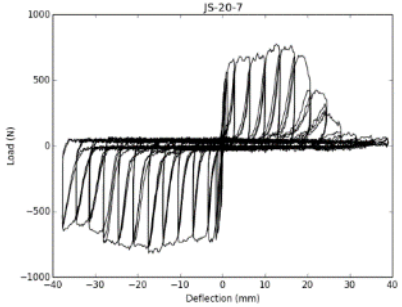	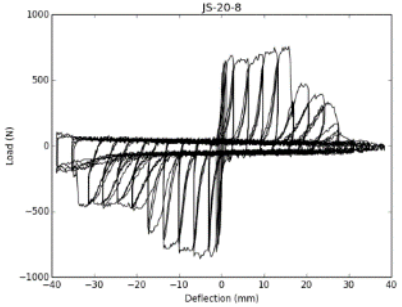	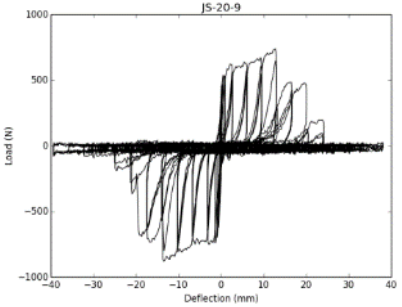	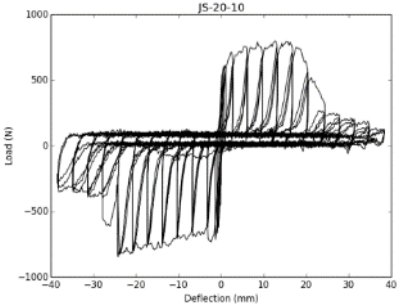

JS-#	Density (SG)	Moisture Content (%)			
JS-21-1	0.32	12.64	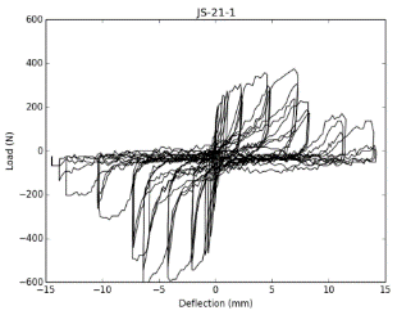	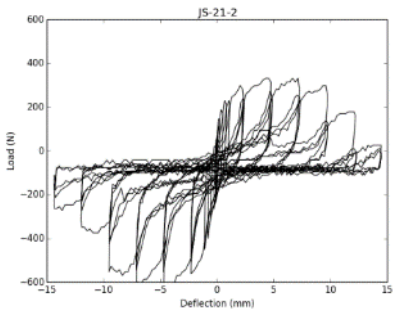	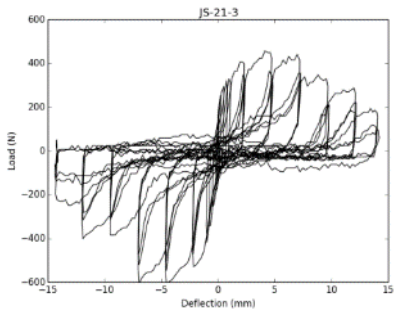
JS-21-2	0.33	11.24			
JS-21-3	0.33	12.36			
JS-21-4	0.32	11.90			
JS-21-5	0.34	12.50			
JS-21-6	0.34	12.63	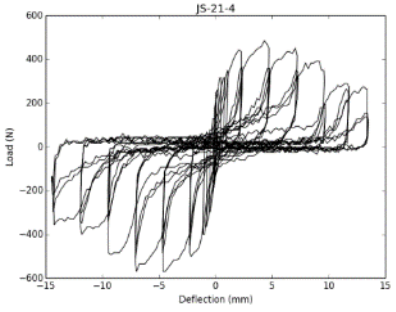	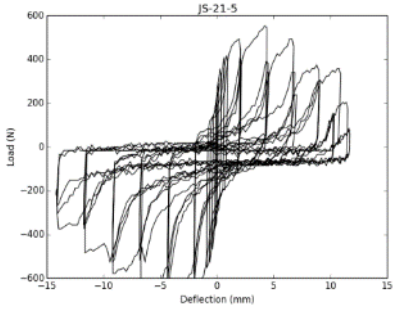	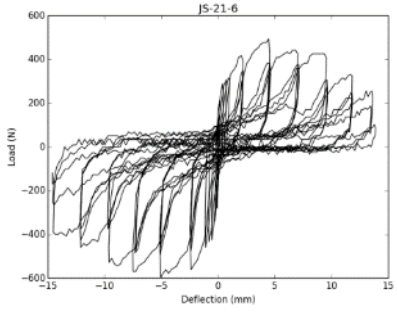
JS-21-7	0.35	12.24			
JS-21-8	0.33	12.22			
JS-21-9	0.34	11.96			
JS-21-10	0.34	12.09			
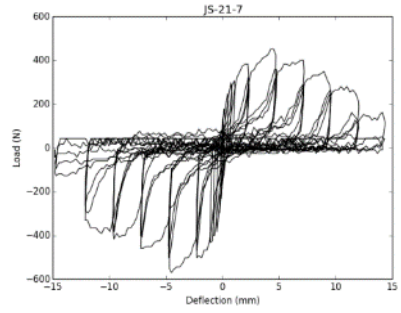	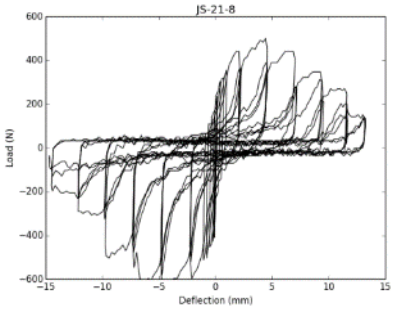	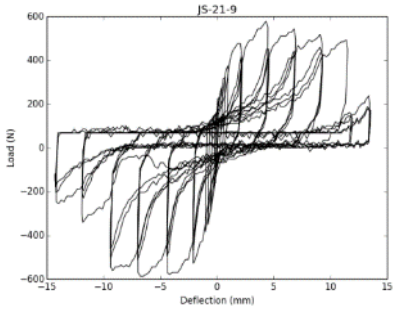			

JS-#	Density (SG)	Moisture Content (%)			
JS-22-1	0.33	11.36	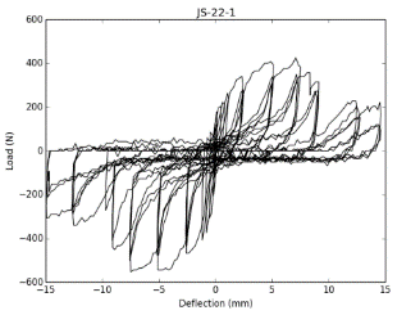	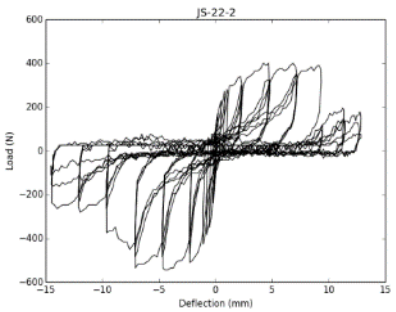	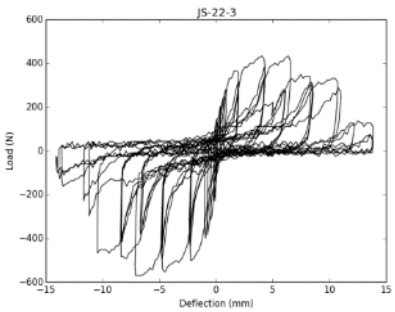
JS-22-2	0.32	12.64			
JS-22-3	0.34	12.22			
JS-22-4	0.35	11.11			
JS-22-5	0.34	12.50			
JS-22-6	0.33	12.64	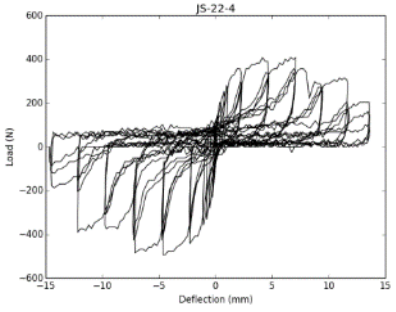	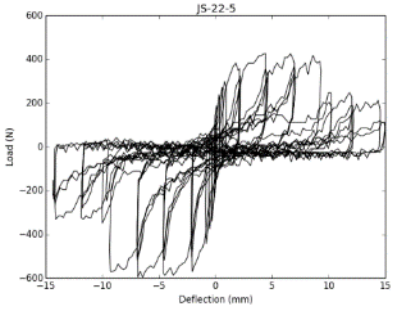	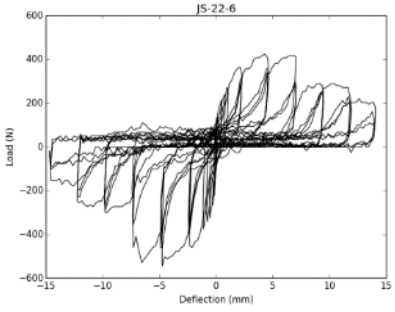
JS-22-7	0.34	13.04			
JS-22-8	0.33	12.79			
JS-22-9	0.34	13.79			
JS-22-10	0.33	12.64			
			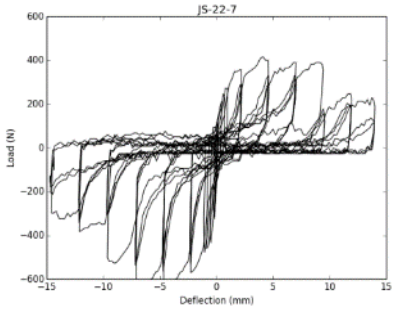	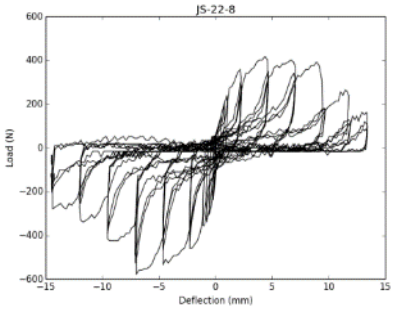	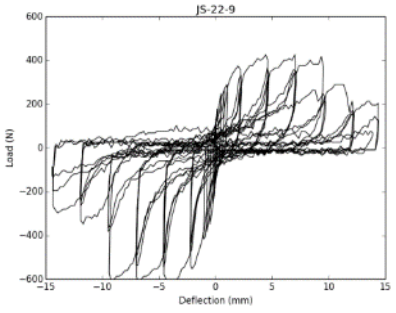	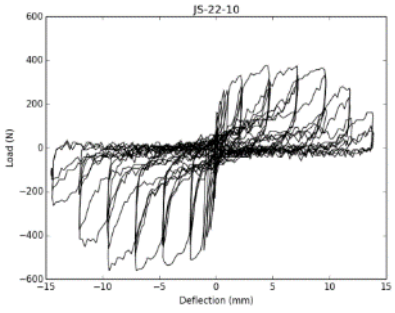

JS-#	Density (SG)	Moisture Content (%)			
JS-23-1	0.35	11.70	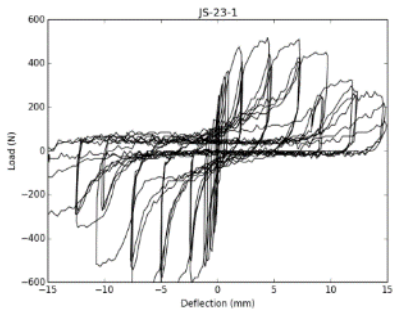	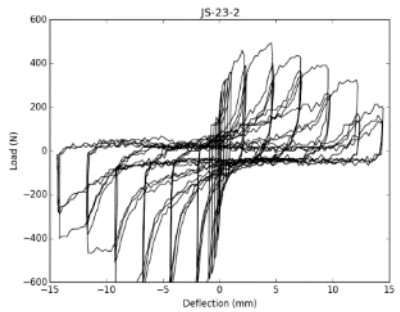	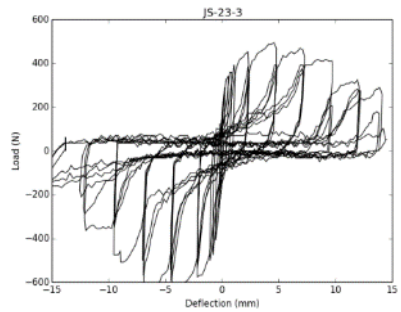
JS-23-2	0.34	12.09			
JS-23-3	0.35	12.24			
JS-23-4	0.34	12.36			
JS-23-5	0.33	12.50			
JS-23-6	0.33	11.11	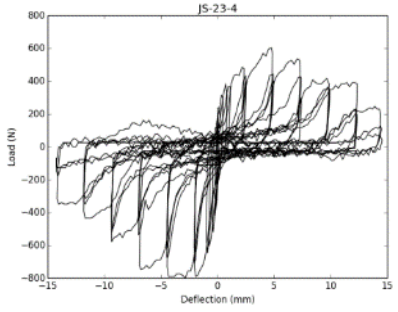	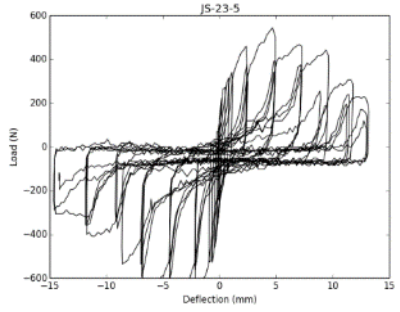	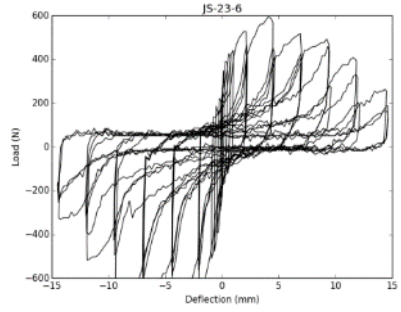
JS-22-7	0.35	11.58			
JS-23-8	0.33	23.26			
JS-23-9	0.34	11.11			
JS-23-10	0.33	12.09			
			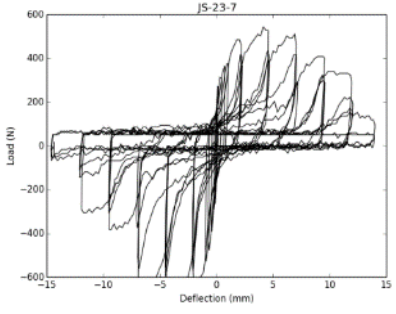	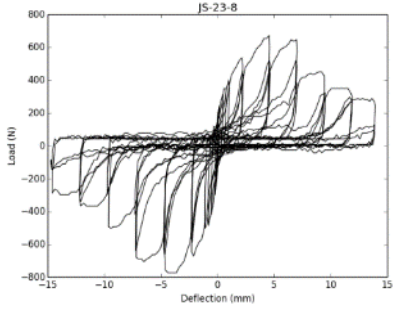	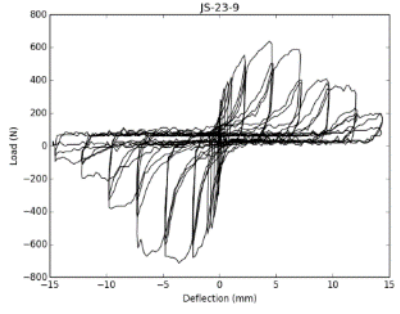	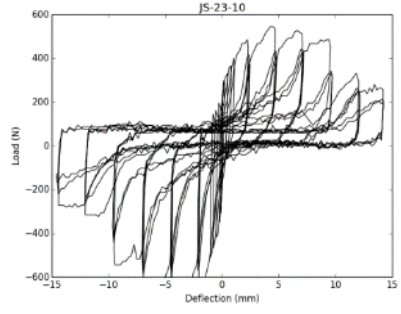

JS-#	Density (SG)	Moisture Content (%)			
JS-24-1	0.41	11.54	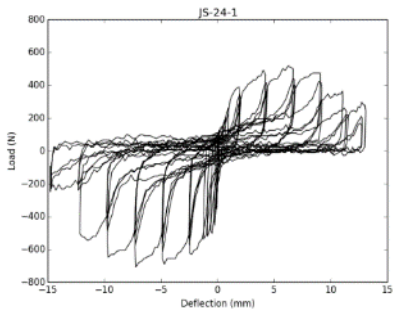	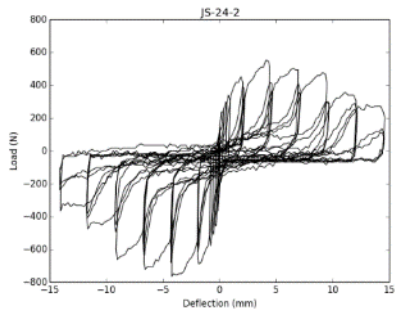	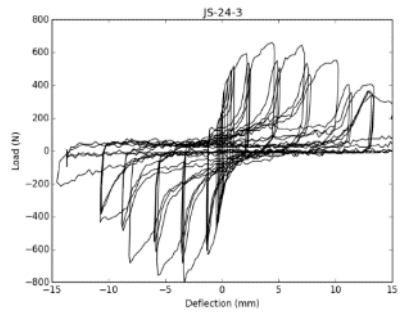
JS-24-2	0.40	11.11			
JS-24-3	0.43	10.81			
JS-24-4	0.39	11.22			
JS-24-5	0.41	10.89			
JS-24-6	0.40	11.22	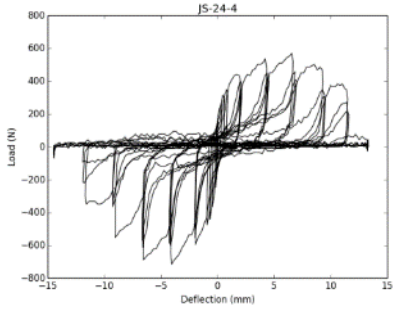	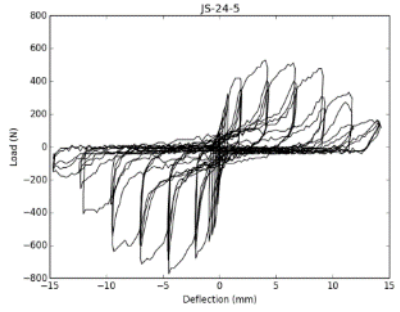	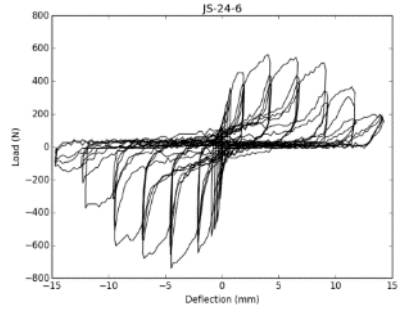
JS-24-7	0.39	11.22			
JS-24-8	0.48	11.02			
JS-24-9	0.42	11.43			
JS-24-10	0.40	10.89			
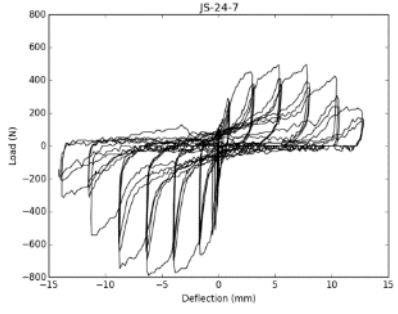			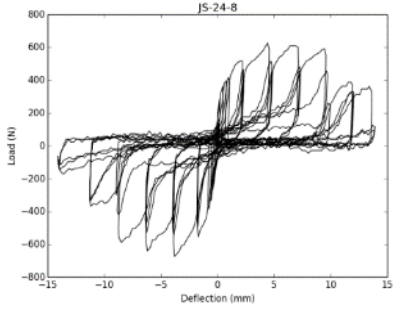	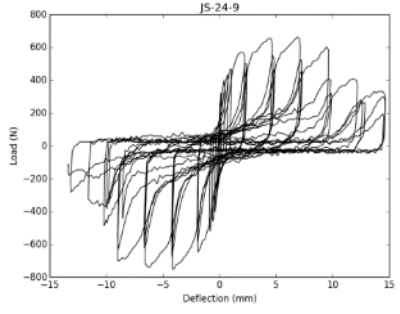	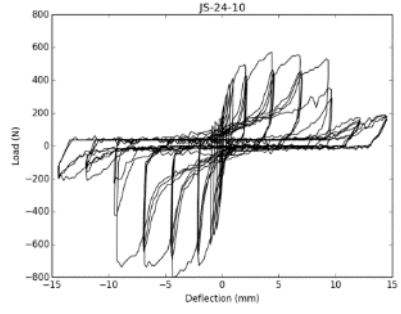

JS-#	Density (SG)	Moisture Content (%)
JS-25-1	0.41	11.54
JS-25-2	0.40	11.11
JS-25-3	0.43	10.81
JS-25-4	0.39	11.22
JS-25-5	0.41	10.89
JS-25-6	0.40	11.22
JS-25-7	0.39	11.22
JS-25-8	0.48	11.02
JS-25-9	0.42	11.43
JS-25-10	0.40	10.89

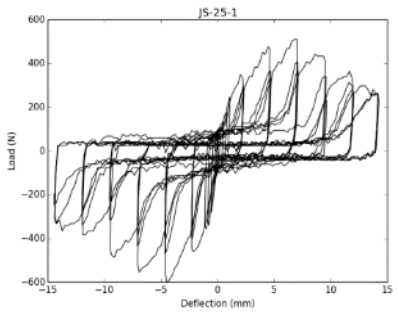

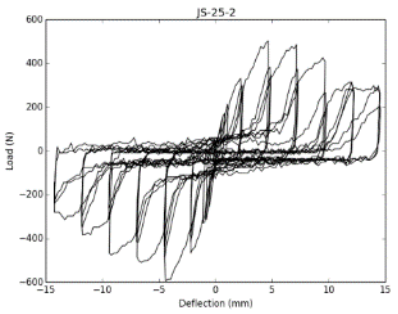

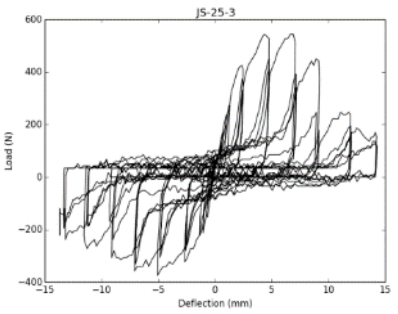

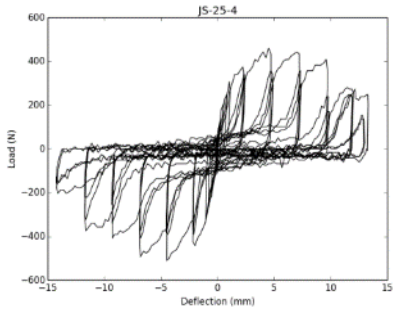

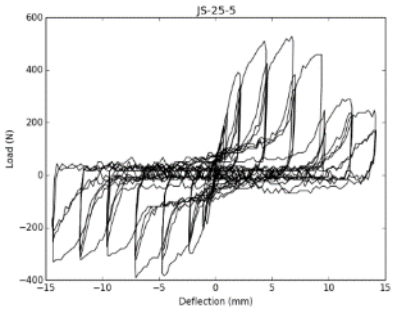

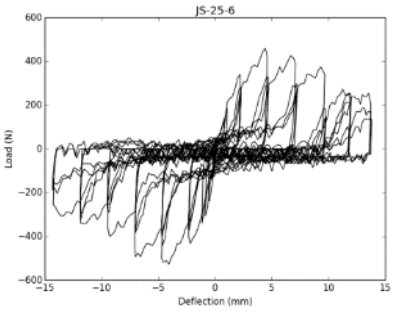

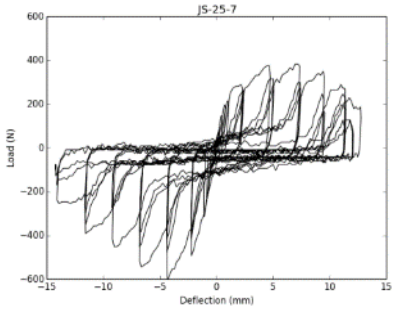

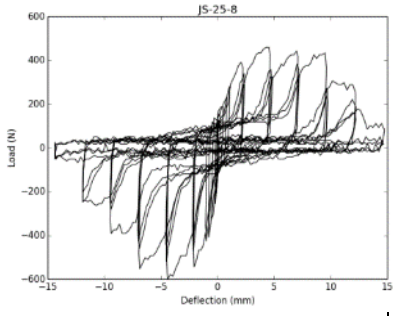

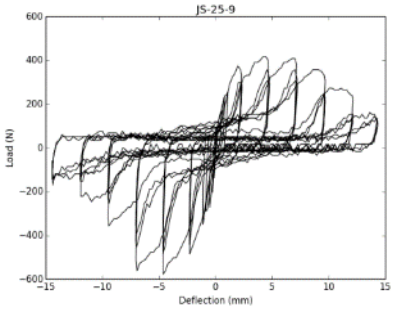

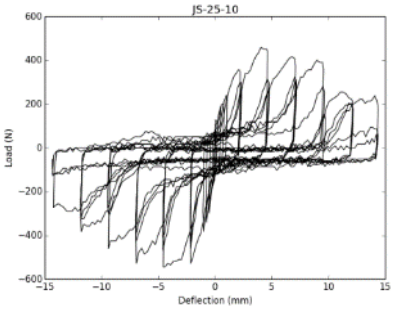

JS-#	Density (SG)	Moisture Content (%)
JS-26-1	0.42	13.77
JS-26-2	0.42	14.19
JS-26-3	0.43	14.19
JS-26-4	0.43	13.56
JS-26-5	0.45	14.36
JS-26-6	0.41	13.50
JS-26-7	0.41	13.45
JS-26-8	0.43	13.13
JS-26-9	0.42	13.83
JS-26-10	0.45	14.14

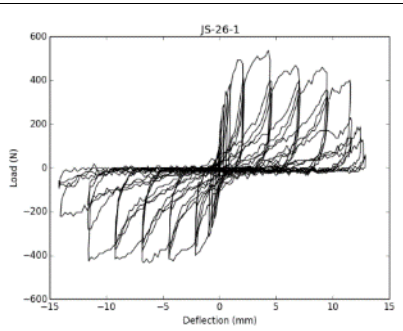

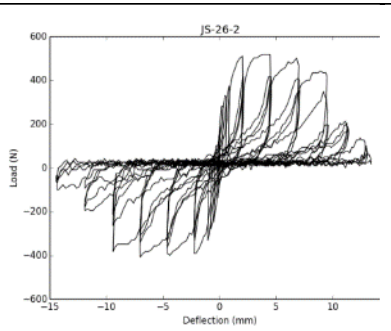

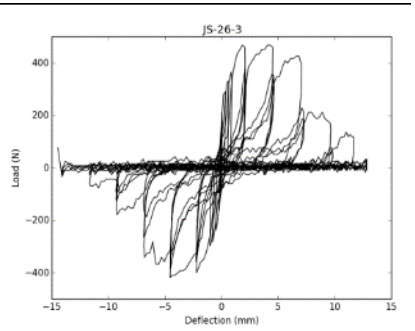

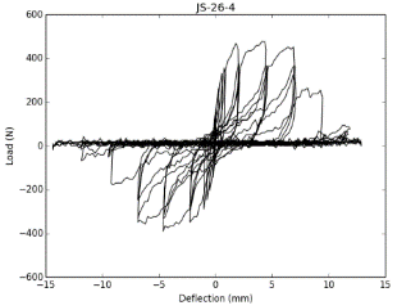

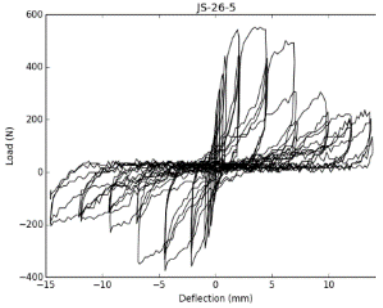

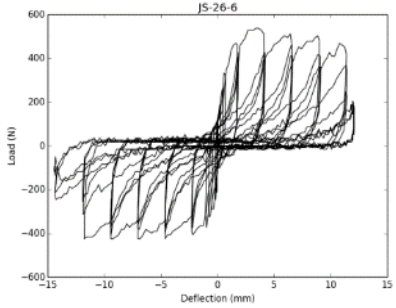

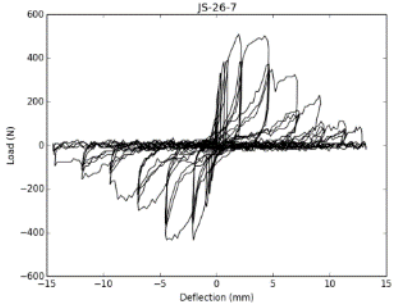

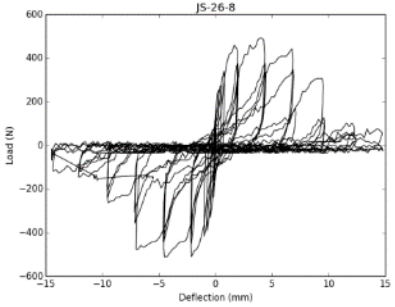

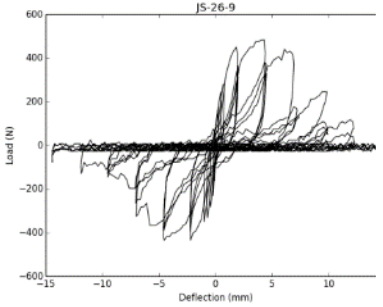

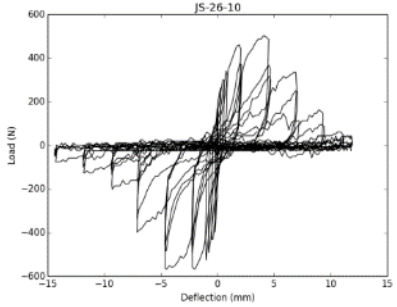

JS-#	Density (SG)	Moisture Content (%)
JS-27-1	0.40	12.67
JS-27-2	0.36	13.32
JS-27-3	0.40	12.81
JS-27-4	0.39	13.94
JS-27-5	0.45	12.17
JS-27-6	0.42	12.63
JS-27-7	0.37	14.21
JS-27-8	0.42	13.05
JS-27-9	0.42	13.66
JS-27-10	0.44	14.14

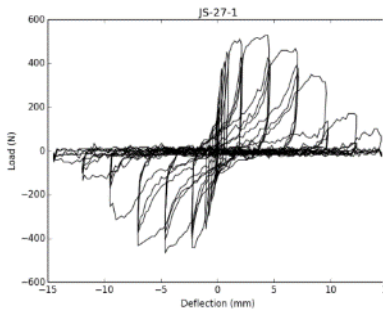

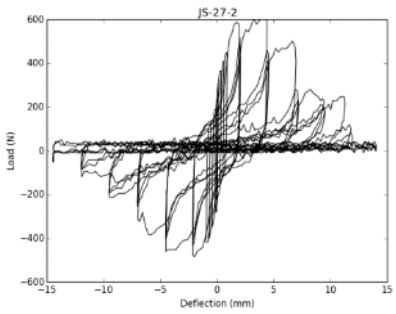

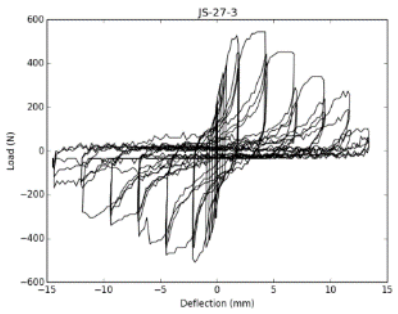

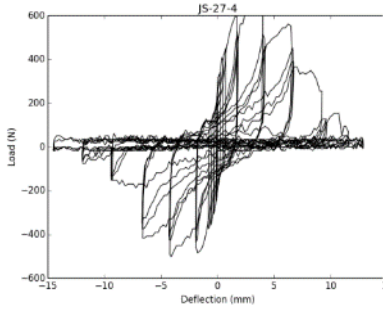

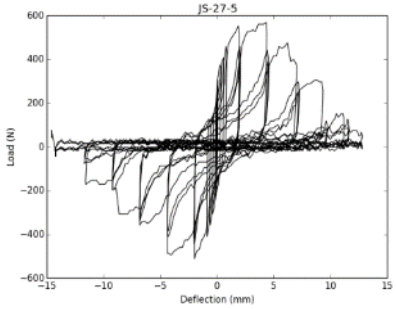

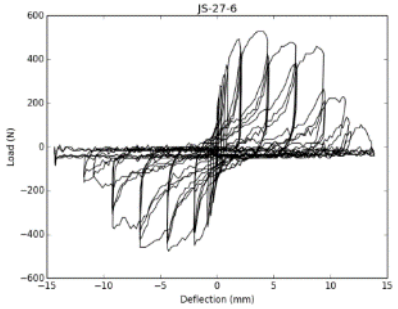

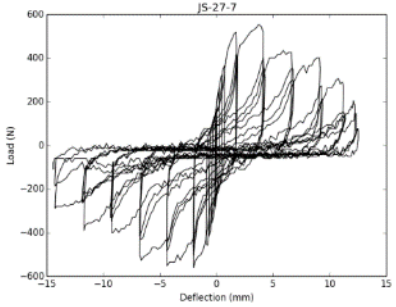

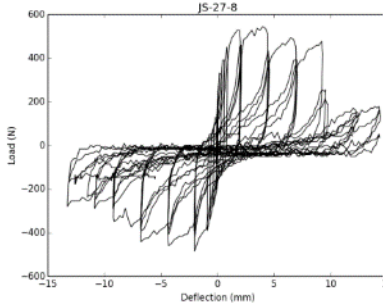

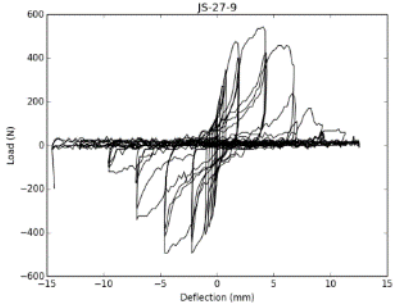

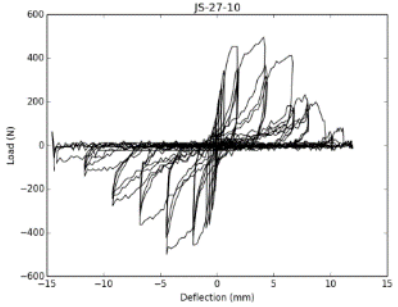

JS-#	Density (SG)	Moisture Content (%)
JS-28-1	0.42	12.76
JS-28-2	0.41	14.12
JS-28-3	0.42	13.71
JS-28-4	0.46	13.13
JS-28-5	0.46	14.78
JS-28-6	0.47	14.72
JS-28-7	0.46	14.09
JS-28-8	0.47	13.65
JS-28-9	0.41	14.09
JS-28-10	0.43	13.50

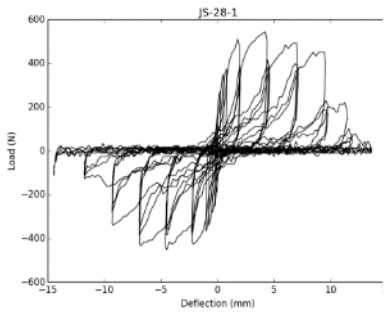

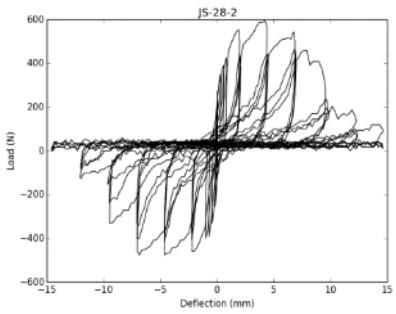

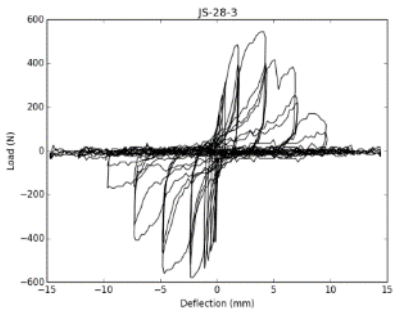

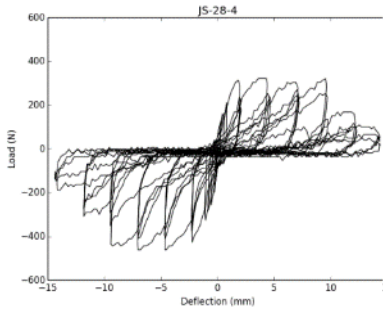

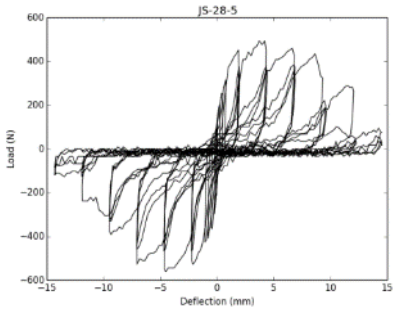

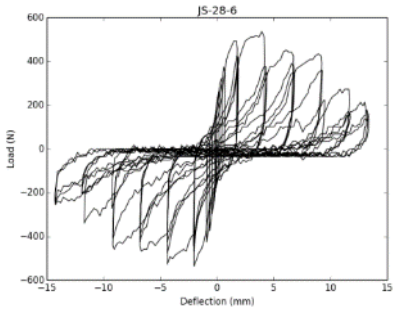

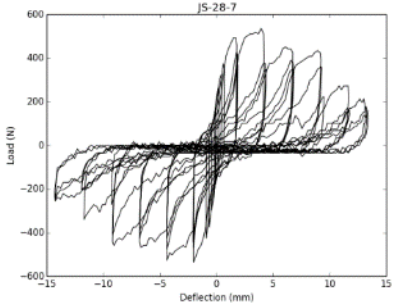

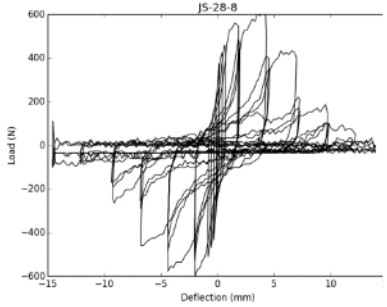

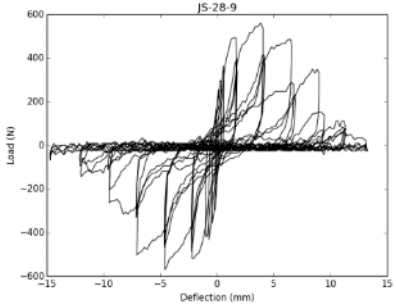

JS-#	Density (SG)	Moisture Content (%)
JS-30-1	0.41	8.03
JS-30-2	0.40	8.16
JS-30-3	0.41	5.45
JS-30-4	0.42	5.35
JS-30-5	0.43	8.10
JS-30-6	0.41	7.47
JS-30-7	0.41	8.0
JS-30-8	0.42	8.30
JS-30-9	0.42	5.36
JS-30-10	0.41	7.27